Vol. 182, April 30, 1986
Complete in one issue

ISSN 0003-2670

ANALYTICA CHIMICA ACTA

International journal devoted to all branches of analytical chemistry

ELSEVIER

ANALYTICA CHIMICA ACTA

International journal devoted to all branches of analytical chemistry
Revue internationale consacrée à tous les domaines de la chimie analytique
Internationale Zeitschrift für alle Gebiete der analytischen Chemie

PUBLICATION SCHEDULE FOR 1986

	J	F	M	A	M	J	J	A	S	O	N	D
Analytica Chimica Acta	179	180	181	182 183/1	183/2 184	185	186	187	188	189	190	191

Scope. *Analytica Chimica Acta* publishes original papers, short communications, and reviews dealing with ev aspect of modern chemical analysis both fundamental and applied.

Submission of Papers. Manuscripts (three copies) should be submitted as designated below for rapid and effici handling:

Papers from the Americas to: Professor Harry L. Pardue, Department of Chemistry, Purdue University, West Lafaye IN 47907, U.S.A.

Papers from all other countries to: Dr. A. M. G. Macdonald, Department of Chemistry, The University, P.O. Box 3 Birmingham B15 2TT, England. Papers dealing particularly with computer techniques to: Professor J. T. Cl Universität Bern, Pharmazeutisches Institut, Baltzerstrasse 5, CH-3012 Bern, Switzerland.

Submission of an article is understood to imply that the article is original and unpublished and is not being conside for publication elsewhere. Upon acceptance of an article by the journal, authors will be asked to transfer the copyri of the article to the publisher. This transfer will ensure the widest possible dissemination of information.

Information for Authors. Papers in English, French and German are published. There are no page charg Manuscripts should conform in layout and style to the papers published in this Volume. Authors should con Vol. 170 for detailed information. Reprints of this information are available from the Editors or from: Elsevier Editc Services Ltd., Mayfield House, 256 Banbury Road, Oxford OX2 7DH (Great Britain).

Reprints. Fifty reprints will be supplied free of charge. Additional reprints (minimum 100) can be ordered. An o form containing price quotations will be sent to the authors together with the proofs of their article.

Advertisements. Advertisement rates are available from the publisher.

Subscriptions. Subscriptions should be sent to: Elsevier Science Publishers B.V., Journals Department, P.O. I 211, 1000 AE Amsterdam, The Netherlands. Tel: 5803 911, Telex: 18582.

Publication. *Analytica Chimica Acta* appears in 13 volumes in 1986. The subscription for 1986 (Vols. 179–191 Dfl. 2730.00 plus Dfl. 312.00 (p.p.h.) (total approx. US $1192.94). All earlier volumes (Vols. 1–178) except Vols and 28 are available at Dfl. 231.00 (US $90.59), plus Dfl. 15.00 (US $5.88) p.p.h., per volume.

Our p.p.h. (postage, packing and handling) charge includes surface delivery of all issues, except to subscribers in U.S.A., Canada, Japan, Australia, New Zealand, P.R. China, India, Israel, South Africa, Malaysia, Thailand, Singap South Korea, Taiwan, Pakistan, Hong Kong, Brazil, Argentina and Mexico, who receive all issues by air deli (S.A.L. — Surface Air Lifted) at no extra cost. For the rest of the world, airmail and S.A.L. charges are available u request.

Claims for issues not received should be made within three months of publication of the issues. If not they canno honoured free of charge.

For further information, or a free sample copy of this or any other Elsevier Science Publishers journal, readers in U.S.A. and Canada can contact the following address: Elsevier Science Publishing Co. Inc., Journal Informa Center, 52 Vanderbilt Avenue, New York, NY 10017, U.S.A., Tel: (212) 916-1250.

0003-2670/86/$

Printed in The Netherlands

ANALYTICA CHIMICA ACTA
VOL. 182 (1986)

ANALYTICA CHIMICA ACTA

International journal devoted to all branches of analytical chemistry

ELSEVIER Amsterdam–Oxford–New York–Tokyo

Anal. Chim. Acta, Vol. 182 (1986)

0003-2670/86/$03

Printed in The Netherlands

Analytica Chimica Acta, 182 (1986) 1—16
Elsevier Science Publishers B.V., Amsterdam — Printed in The Netherlands

THE DETERMINATION OF FLUORIDE IN ENVIRONMENTALLY RELEVANT MATRICES

THE ANALYTICAL WORKING GROUP OF THE COMITÉ TECHNIQUE EUROPÉEN DU FLUOR*

(Received 3rd October 1985)

SUMMARY

This report covers analytical methods for the determination of total fluoride in gaseous emissions, rain water and aqueous effluents, vegetation, human urine, factory air and environmental air. All the methods are based on final measurement of fluoride by means of the fluoride ion-selective electrode. Interferences which cannot be eliminated by the masking power of the TISAB buffer solution are avoided by separation of fluoride by steam distillation. Decomposition methods are used for vegetation and for samples which may contain insolubles such as stack gases or aqueous effluents. Sampling of fluoride from air is done by alkaline absorption for the high concentration range (stack gases) and by filter methods for low fluoride concentrations, e.g., in factory and environmental air. Detection limits as low as 0.3 $\mu g\ m^{-3}$ fluoride can thus be achieved. The methods were established after the individual analytical procedures, common in the various member countries of CTEF, had been compared. Thus, the most practicable method was selected or an optimized version was designed for full testing. The accuracy of the different methods was verified by comparative tests.

Because of the environmental importance of fluoride, methods for its determination have become of widespread interest during recent years. Numerous publications have appeared concerning fluoride measurement, sampling of different materials and speciation of different types of fluoride. In particular, interest in speciation has produced many studies aimed at discriminating between gaseous and particulate fluoride and between soluble and insoluble particles. This interest arises from the diverse effects that different types of fluoride can have on vegetation, animals and men. Because

*Comité Technique Européen du Fluor (CTEF) is a committee of European producers of hydrogen fluoride and inorganic fluorides, and is organised as a sector group of the Conseil Européen des Fédération de l'Industrie Chimique de Bruxelles. The Analytical Working Group focuses on testing and selecting efficient and reliable sampling, and analytical procedures for plant effluents, atmosphere and foliage. The members of the Analytical Working Group are C. Harzdorf, N. E. Kinwel, L. Marangoni, J. W. Ogleby, J. Ravier, F. Roost and F. M. Zar Ayan.

Address for correspondence: B. Jensen, Sector Groups Department, Conseil Européen des Fédération de l'Industrie Chimique, Avenue Louise 250, Bte 72, B-1050 Bruxelles, Belgium.

0003-2670/86/$03.50

this field is still under discussion, the Analytical Working Group was asked only to deal with total fluoride in the first stage.

For total fluoride, various analytical methods, operated in the different countries or published in the literature, were compared by interlaboratory tests. The most effective procedure was selected and, after being verified by final comparative tests, is recommended as a CTEF method. In many cases, considerable refinements occurred during the course of establishing the methods.

The fluoride determination in all the methods follows similar general lines, and modifications are applied only if this is required by the particular matrix of the sample. This general principle comprises potentiometric determination, by means of the fluoride ion-selective electrode using a citrate buffer/sodium chloride mixture as the total ionic-strength adjustment buffer (TISAB). If this direct method fails to yield accurate results, owing to insoluble fluorides or interfering elements, an extended method including alkaline decomposition followed by steam distillation of hexafluorosilicic acid is applied prior to the potentiometric fluoride measurement. Sampling and sample pretreatment are adapted to the individual properties of the different types of sample. This field comprises absorption procedures for the different species of gas and the mode of disruption of organic matter.

In the following section, the general method for determining fluoride is first described. Subsequently, the different types of sample including particular analytical treatment, as well as results of interlaboratory tests, are presented in separate sections.

GENERAL METHODS FOR FLUORIDE DETERMINATION

Direct potentiometric determination

The fluoride ion-selective electrode is used throughout because of its favourable characteristics, e.g., superior selectivity, long dynamic range and ease of operation [1, 2]. The fluoride measurements are made in a mixture of the sample solution and TISAB solution; the latter eliminates the activity problem, adjusts the pH to an optimum value and complexes the interfering cations, such as iron(III) and aluminium, to a considerable extent [3]. The TISAB used here is 1 M in sodium chloride and 0.1 M in citrate buffer; the pH is 5.5. This solution was selected from a variety of different buffers because it provides optimum conditions regarding the response time, the masking capacity for interferents and the lifetime of the electrode. This decision resulted from the experience gained in several of the laboratories associated with the Analytical Working Group and from model tests, which were aimed in particular at the masking power of the TISAB solution.

Experimental

Reagents. All reagents should be of analytical-reagent grade and distilled water, or water of equivalent purity, must be used in the method.

TISAB solution. Sodium citrate dihydrate (29.4 g) and 58.5 g of sodium chloride are dissolved in ca. 900 ml of water; the pH is adjusted to 5.5 with ca. 6 M hydrochloric acid, and the solution is diluted to 1 l with water.

Standard sodium fluoride solution (1 ml = 500 μg F^-). Dried (120°C for 2 h) sodium fluoride (1.105 g) is dissolved in water and diluted to exactly 1 l. The solution should be stored in polypropylene containers and prepared every 14 days.

Apparatus. The equipment needed for potentiometric fluoride determination includes a fluoride ion-selective electrode, a reference electrode (e.g., saturated calomel electrode or silver/silver chloride electrode) and a pH/mV meter with a resolution of better than 0.5 mV. The measuring cell is made of borosilicate glass or polypropylene with a capacity of 100 ml and is fitted with a thermostatted jacket. The thermostatted bath must be capable of supplying water to the jacket of the cell at a pre-set temperature in the range 20—40°C to ±0.2°C. A magnetic stirrer is used.

Calibration procedure. Appropriate working standard fluoride solutions are prepared from the standard fluoride solution, covering the range 0.2—100 μg ml^{-1} fluoride. Standard working solution (20 ml) and 20 ml of TISAB solution are transferred to the dry measuring cell. The electrodes are inserted and the solution is stirred at a constant rate. The meter reading is taken after a constant value has been attained (drift <0.1 mV min^{-1}).

A calibration graph is constructed on semilogarithmic paper of at least 6 measuring points over the entire concentration range. Regular checking of the calibration graph is essential. The graph should be checked daily at one point to correct for the drift of the electrode and over the entire range weekly to correct for the response characteristic. A new calibration graph must be prepared for each new batch of TISAB solution.

Measurement procedure. A portion (20 ml) of sample solution, which has been adjusted to a pH in the range 3—6, and 20 ml of TISAB solution are transferred to the dry measuring cell. The electrodes are inserted, the solution is stirred at the same rate as for the calibration solutions, and the electrodes are allowed to attain a constant potential with a drift of <0.1 mV min^{-1}. The fluoride concentration of the sample solution is obtained from the calibration graph.

Determination in the presence of interferences

Interferences may be caused by the presence of insoluble fluorides or by the presence of high concentrations of fluoride-complexing elements. In such cases, an extended method is applied including alkaline decomposition and separation of fluoride by steam distillation [4, 5]. The fluoride content in the distillate is then determined by the measuring procedure described above.

If there is any doubt about the presence of interferents or insoluble fluorides in a particular type of sample, determinations should be made both by the direct and the extended method. If both procedures give the same results, the less time-consuming direct method is applicable. Otherwise, the extended method has to be applied.

Fluoride separation is most effective if fluoride is distilled from a mixture of perchloric and phosphoric acid. The latter is required to destroy fluoride compounds or complexes of polyvalent cations, such as aluminium, iron or titanium.

This extended procedure is predominantly relevant to stack gases, aqueous effluents and, with slight modifications, to vegetation. Interference from boron cannot be eliminated completely with the method. In this case, special treatment of the sample is required, but this is beyond the scope of the present study.

Experimental

Reagents. Sodium hydroxide (solid pellet form), perchloric acid (density 1.67 g ml^{-1}) and phosphoric acid (density 1.71 g ml^{-1}) are required.

Apparatus. A nickel dish (capacity ca. 500 ml) and a nickel crucible (capacity ca. 80 ml) are needed. The apparatus for steam distillation of fluoride is shown in Fig. 1. The contact thermometer regulates the power to the heating jacket under the distillation flask via a relay.

Procedure. The sample solution as specified in the individual methods or an appropriate volume of the thoroughly mixed sample, containing a minimum of 500 μg of fluoride, is transferred to the nickel dish and evaporated on a steam bath to a low volume. If the sample is not originally alkaline, sodium hydroxide solution must be added prior to evaporation until alkaline

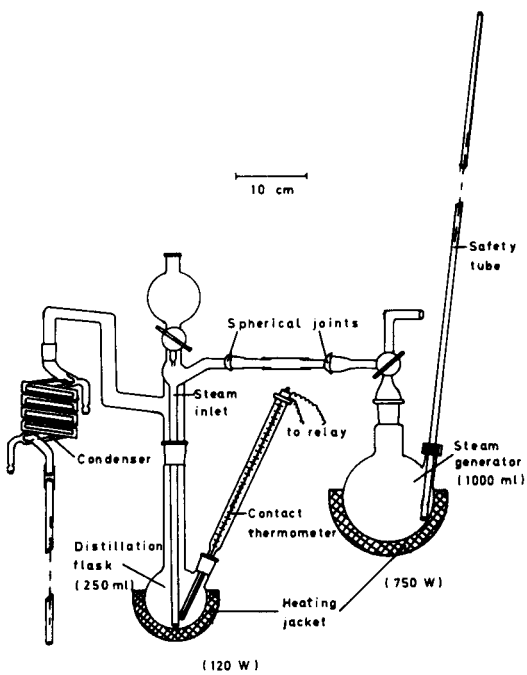

Fig. 1. Apparatus for fluoride distillation.

reaction is indicated. The residual solution in the dish is transferred quantitatively to the nickel crucible, using the minimum amount of water. Evaporation is then completed to dryness and 2 g of sodium hydroxide is added to the residue. The crucible is heated on a burner at dull red heat for about 10 min, until a clear melt is obtained. The crucible is then allowed to cool, the residue is treated with hot water and the contents of the crucible are transferred quantitatively into the distillation flask, taking care that the final volume is about 50 ml.

After assembly of the distillation apparatus, 35 ml of phosphoric and 35 ml of perchloric acid are added to the distillation flask and a 500-ml volumetric flask, containing 25 ml of water, is fitted to the outlet tube of the condenser with the end of the tube below the surface of the water. The contact thermometer is then set to 135°C and the heating jacket under the distillation flask is switched on. When the temperature reaches 135°C, steam is passed through the distillation mixture. The flow rate is regulated so as to obtain a distillation rate of 10 ml min^{-1}. The distillation is stopped when the volume of the distillate is approximately 450 ml. The volumetric flask is removed, the outlet tube of the condenser is rinsed with small volumes of water, and the solution in the flask is finally diluted to the mark.

The fluoride concentration of the distillate is then measured as described in the direct method.

GASEOUS EMISSIONS

Stack gases can consist of gaseous components, particles and droplets. The most crucial problem in the analysis is therefore the sampling step, because the inhomogeneous matrix presents difficulties in obtaining representative samples. This problem can be solved essentially by two means: isokinetic sampling and selection of an appropriate position for the probe.

Isokinetic sampling requires the measurement of the average flow velocity in the stack and calculation of the corresponding isokinetic aspirating rate in the sampling train. The latter must not exceed the limit of 12 l min^{-1} in order to ensure quantitative trapping of fluoride in the absorbing solutions. Consequently, the inner diameter of the probe has to be adapted adequately so as to achieve the required flow velocity at the orifice. Information is given later in this section to satisfy this requirement [6].

Proper positioning of the probe requires the selection of appropriate horizontal and vertical locations. For the horizontal location, the point of average flow velocity within the cross-section of the stack is chosen. For the vertical location, a minimum distance from any bends and constrictions in the stack has to be observed. Detailed recommendations are given to meet this prerequisite for accurate sampling in stacks. The sampling scheme and the accompanying measurements and calculations are presented both for circular and rectangular stacks.

Fluoride is trapped as usual in a train of Drechsel bottles, filled with sodium hydroxide solution. After being combined, the absorbing solutions

are prepared for fluoride determination by the direct potentiometric method or by the extended procedure including the decomposition and distillation step.

The method as specified is suitable for the determination of total fluoride in the concentration range 1—100 mg m^{-3} and is applicable to linear flow velocities in the stack in the range 1—30 m s^{-1}.

Experimental

Reagents. In addition to the reagents listed in the previous section, the following are required: sodium hydroxide solution (ca. 0.5 M), hydrochloric acid (density ca. 1.18 g ml^{-1}), hydrochloric acid (ca. 3 M) and sulphuric acid (density ca. 1.84 g ml^{-1}).

Apparatus. The sampling train is shown in Fig. 2. Sample probe A is a stainless steel tube, of the form and size shown in Fig. 2, fitted with electric heating tape controlled by an energy regulator. The probe is selected according to the range of stack gas velocity, as given in Table 1. The four Drechsel bottles (B, C, D, E) have spherical joints and capacity 250 ml and are made of borosilicate glass. Two absorbers (B and E) have open inlets and two absorbers (C and D) are equipped with frits (pore size 2). The gas meter (F), wet or dry, is fitted with a pressure gauge (I) and thermometer (H). A gas meter with an operating pressure gauge of ca. 25 cm of water from ambient should be suitable. For the gas pump (M), a membrane or vacuum pump capable of drawing air at a rate of up to 900 l h^{-1} is suitable. A flow control valve (G) is needed. Pyrex or plastic tube (L) connects the bottles to the gas meter. Flexible PTFE tubing (O) connects the probe outlet to the first Drechsel bottle. A pitot tube with inclined manometer is required.

Positioning of probe in a circular stack. The vertical position of the sample probe must be at least 8 stack diameters beyond any bend or constriction and 5 diameters from the exit. If the exit is less then 13 diameters from any constriction then the probe position is obtained from the following ratio: (distance to exit/distance to upstream bend) = 5/8.

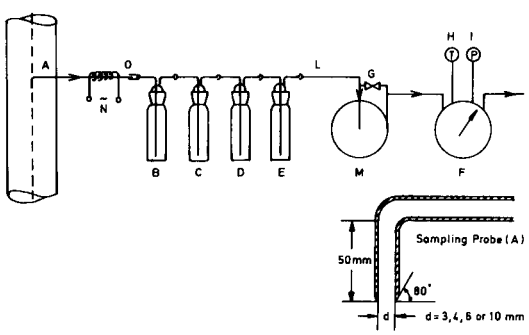

Fig. 2. Sampling train for emission measurements: A, sampling probe; B—E, absorbers; F, gas meter; G, regulation valve; H, thermometer; I, manometer; L, connecting tubes; M, gas pump; N, heater; O, flexible PTFE tube.

TABLE 1

Interdependence of gas velocity and probe diameter for isokinetic sampling

Range of linear velocity of stack gas (m s^{-1})		Internal diameter of probe (mm)
Minimum	Maximum	
16	30	3
7	16	4
2	7	6
1	2	10

To establish the horizontal position, the pressure drop is measured with the pitot tube and the linear flow velocity of the gas is calculated at 9 points as indicated in Fig. 3. The average flow velocity in m s^{-1} is then calculated from the following formula, using 8 of these measurements, but excluding the measurement at the centre: $(1/8)\ \Sigma_{i=1}^{i=8} V_i$ (in m s^{-1}). The velocities are plotted vs. the corresponding positions along one of the radii, including the measurement at the centre. From the resulting graph, the point of the average flow velocity ($\overline{V}$ m s^{-1}) is then determined. This is the point for the correct horizontal position of the probe.

Positioning of probe in a rectangular stack. The vertical position of the sample probe is established as for the circular stack. The equivalent diameter of the rectangular stack is calculated from 2 (Length × Width)/(Length + Width).

To establish the horizontal position, the pressure drop is measured and the linear flow velocity of the gas is calculated at the centres of 9 equal areas as shown in Fig. 4. The ratio of the length to the width of each area should be between 1 and 2. The average flow velocity (m s^{-1}) is again calculated from $(1/8)\ \Sigma_{i=1}^{i=8} V_i$. The pitot tube is then inserted into the stack and moved along a line parallel to one side and through the centre until the point is reached at which the gas velocity is $\overline{V}$ m s^{-1}. This is the point for correct horizontal position.

Isokinetic flow rate. The isokinetic flow rate, R, is calculated as follows: $R = 0.04712\ \overline{V}\ d^2$ l min^{-1}, where $\overline{V}$ is the average gas velocity (m s^{-1}) and d is the internal diameter of the probe (mm).

Sampling. The sample probe is installed as outlined above and the isokinetic flow rate is calculated. Portions (100 ml) of ca. 0.5 M sodium hydroxide solution are pipetted into absorbers B, C and D and a few drops of phenolphthalein indicator solution are added to each of them. Sulphuric acid (150 ml; d. 1.84 g ml^{-1}) is placed in bottle E. Each bottle is then weighed (total mass M_1).

The apparatus is then assembled, and the probe heating is switched on and adjusted to a temperature of 100—120°C. The pump is then started and the valve (G) is adjusted to give the calculated isokinetic aspirating rate through

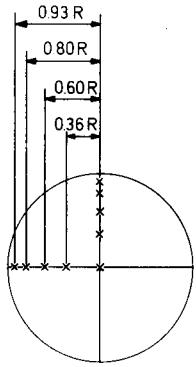

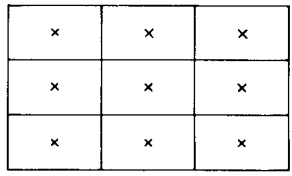

Fig. 3. Sampling scheme for a circular stack. Crosses denote points in cross-section at which gas velocity is measured. R is the radius of the stack.

Fig. 4. Sampling scheme for a rectangular stack. Crosses denote points in cross-section at which gas velocity is measured.

the sampling train. The pressure on the manometer (I) and the temperature on the thermometer (H) must be read.

After about 500 l of sample has been aspirated, the flow rate is reduced to a minimum value and the absorbers B, C, D and E are disconnected in that order. The volume of gas sampled is read from the gas meter and the absorbers are weighed to the nearest 0.1 g (total mass M_2).

Determination of fluoride. The contents of absorbers B—D are transferred quantitatively to a 500-ml volumetric flask and the resulting solution is neutralized with hydrochloric acid (ca. 3 M) to obtain a pH in the range 3—6 when checked with narrow-range indicator paper. This solution is ready for the direct potentiometric determination as specified above. It must be noted that if the pink colour has been discharged in all three absorbers, the sampling procedure must be repeated using a smaller volume of sample.

A blank must be determined by using the same procedure on a 30-ml aliquot of sodium hydroxide solution, neutralized with 3 M hydrochloric acid and diluted to a final volume of 50 ml.

If it is suspected or indicated that the sample contains particulate matter or interfering elements, the total fluoride method must be applied. In this case, the contents of the absorbers are transferred quantitatively to a 500-ml nickel dish and the extended procedure is continued. A blank is determined by following the complete procedure but omitting the sample.

Calculations

Sample gas volume. The volume of the sample gas in litres at STP from measurements on a wet gas meter is given by the formula:

$$Q = Z \times \frac{273}{273 + t} \times \frac{(A + P - C)}{760} + \frac{(M_2 - M_1)\,22.4}{18}$$

where Q is the volume of the sample gas (l) at STP, Z the volume of gas (l) given by the wet meter (F), T the temperature of the gas (°C), A the atmospheric pressure (mm Hg), P the pressure (mm Hg) of gas sample above atmospheric pressure as read on manometer I (if less than atmospheric pressure, P is negative), and C the vapour pressure of water (mm Hg) at temperature t°C; M_1 is the mass (g) of the absorption bottles B, C, D and E before absorption and M_2 the mass (g) of the absorption bottles B, C, D and E after absorption.

When a dry gas meter is used, a similar formula for the volume of sample gas in litres at STP applies, but the term C, the correction for water vapour is omitted.

The size of the correction to the gas volume because of condensed water will vary with the temperature and humidity of the stack gases. If initial measurements on a particular stack show this correction to be negligible, it can be omitted for later determinations. In such cases, there is no need to weigh the absorption bottles before and after the period of sampling, and absorption bottle E containing sulphuric acid can be omitted.

Fluoride content. The fluoride content of the gaseous emission samples (mg m^{-3}) at STP is given by $(A - B) \times 500/Q$, where A is the concentration of fluoride in the absorption solution (μg ml^{-1}), B is the concentration of fluoride in the blank, and Q is the volume of gas sample (l) at STP.

Comparative tests

To verify the method described, samples of different provenance were circulated for an interlaboratory test. It was not practicable to send out gas samples among the participating laboratories, thus sampling was done at the source as usual. The resulting absorption solutions were divided, taking care that no insolubles precipitated during division. The sub-samples were then distributed for analysis. The samples were analyzed by both the direct and the extended methods.

The results are listed in Table 2. The data show that no significant difference exists between the results of either method for the samples under test and that satisfactory agreement between the different laboratories could be achieved. Statistical treatment was not applied because of the lack of sufficient data.

AQUEOUS EFFLUENTS AND RAIN WATER

The determination of fluoride in water presents similar analytical aspects as the determination in absorption solutions obtained from gaseous emission measurements. Depending on the source of the samples, interference may be encountered owing to fluoride-complexing elements or particulate fluorides [7, 8]. This poses the problem of ensuring that the method is adequate and it is therefore indispensable to run initial tests by the direct and the extended method for every type of sample. According to the results, decisions can be made as to which method is to be chosen for routine purposes.

TABLE 2

Collaborative test on fluoride in absorption solutions sent to five laboratories

Sample	Fluoride found (mg l^{-1}) by 5 labs[a]									
	Direct method					Extended method				
	1	2	3	4	5	1	2	3	4	5
A	3.8	—	3.2	3.5	3.6	3.2	—	—	—	—
B	—	27	28	28	23	—	27	33	26	28
C	67	75	85	73	—	71	75	—	79	66
D	10.5	9.3	8.4	10.0	9.0	9.7	9.6	11.5	7.4	12.0
E	12.3	12.6	11.5	12.0	11.8	10.9	13.2	14.0	—	13.0
F	329	351	348	—	350	316	323	350	—	360

[a]All the numbers are the mean of duplicate determinations.

The method is suitable for the determination of total inorganic fluoride in water samples in the range 1—100 mg l^{-1} fluoride.

Experimental

Sampling. Samples are obtained either from special vessels for rain water, which may be adapted to the individual local conditions, or from the water pipes or the water reservoirs to be monitored. Sampling should be done during intensive mixing of the bulk sample and the volume should be big enough to yield a representative laboratory sample.

Determination of fluoride. In the direct method, a 20-ml portion of the sample is transferred to a 25-ml volumetric flask and, if necessary, the pH is adjusted to be within the range 3—6 with either 1 M hydrochloric acid or 1 M sodium hydroxide (narrow-range indicator paper). The solution is then diluted to the mark with water and the method is continued as specified in the section dealing with general methods.

In the extended method, a suitable volume of the thoroughly mixed sample containing a minimum of 500 μg of fluoride is pipetted into a nickel dish and treated as in the general extended method. A blank determination is run, following the entire procedure but omitting the sample.

Calculations are done as usual. The results must be corrected for the blank and for changes in concentration caused by distillation or dilution during pH adjustment.

Comparative test

Several samples of waste water were divided carefully so that equal, representative sub-samples were obtained. These were distributed to the participating laboratories and analyzed by the direct and extended methods.

The results, compiled in Table 3, show that sample E, and possibly sample C, contained insoluble fluorides or interfering elements, so that only the

TABLE 3

Collaborative test on fluoride in waste-water samples sent to five laboratories

Sample	Fluoride found (mg l^{-1}) by 5 labs									
	Direct method					Extended method				
	1	2	3	4	5	1	2	3	4	5
A	2.4	2.7	2.9	3.0	2.9	2.7	3.0	4.1	—	2.7
B	11.9	11.6	12.6	11.5	15.0	13.1	12.4	12.7	13.7	13.5
C	—	76	60	61	—	—	106	107	85	—
E	4.8	5.1	5.1	5.5	5.0	—	10.1	12.7	14.1	11.6
F	12.4	13.0	13.2	13.3	12.5	10.6	12.6	13.2	—	12.0

extended method yielded satisfactory results. The comparatively low precision of that category of data may be due to the difficulty of preparing rigorously equal sub-samples if particulate material is present. All the other samples under test yielded sufficiently concordant results whether the direct or the extended method was used.

VEGETATION

The most important aspect in the determination of fluoride in vegetation is the decomposition step and numerous publications have appeared in which the problem has been discussed and different decomposition techniques have been proposed [9—12]. The most important ones are acid digestion, oxygen combustion and dry ashing in combination with a fluoride-retaining agent. The participating laboratories of the Analytical Working Group conducted tests on these procedures, aimed in particular at the capability of the methods of covering a wide range of different types of sample. From this preliminary work, it became evident that most of the methods show limitations. In particular, samples with a high silica content can yield low results if a "mild" decomposition method such as acid digestion or oxygen combustion is applied.

Only dry ashing in the presence of magnesium acetate, followed by alkaline fusion of the residue and distillation of fluoride proved to be applicable to any type of sample. Consequently, this procedure was chosen as the general method for the fluoride determination in vegetation. The method is suitable for the determination of total inorganic fluoride in all types of herbage, cereals and in the leaves of trees and shrubs in the concentration range 20—5000 mg kg^{-1} in material dried at 60°C. No special pretreatment of the samples is recommended, e.g., washing, but extra precautions must be observed if the method is used for a project with a specific objective.

Experimental

Reagents. In addition to the reagents listed in the general section, a solution of magnesium acetate tetrahydrate (50 g l^{-1}) is needed.

Apparatus. Apart from the general equipment, the requirements are as follows: an electric oven (capable of maintaining 60 ± 0.5° C), borosilicate glass crystallizing dishes or polypropylene trays, nickel crucibles (capacity about 70 ml), and a knife mill, fitted with a 2-mm sieve.

Preparation of a test sample. A mass of 100—200 g of the fresh material is cut with scissors into pieces approximately 2 cm long and weighed. The sample is then spread over the surface of dish or tray and dried overnight at 60 ± 0.5° C. After cooling to room temperature, the sample is re-weighed and returned to the oven for a period of at least 2 h until a constant weight is obtained. The complete sample is then ground in the knife-mill and the resulting material is stored in a polyethylene sample bottle.

Procedure. A suitable test portion containing a minimum of 100 μg of fluoride is weighed into the nickel crucible. Magnesium acetate solution (25 ml) is added and the contents of the crucible, after careful mixing, are evaporated to dryness on an electric hotplate. The residue is then gently heated over a low flame until fumes cease to be evolved. Heating is then continued more strongly until all traces of carbon have burnt away. Any lumps formed must be broken up with the aid of a spatula to facilitate oxidation. The ignition is complete when a uniform, pale grey residue is obtained. During ignition, only dull red heat should be applied.

After addition of 5 g of sodium hydroxide, the residue is fused for 10 min. After cooling, the melt is dissolved in 20 ml of water and the contents of the crucible are transferred quantitatively to the distillation flask with small portions of water. The total volume in the flask must not exceed 50 ml. The distillation and final fluoride measurement are then done as specified in the general method. However, 50 ml of perchloric acid is used instead of a mixture of perchloric acid and phosphoric acid. The latter is not required because large amounts of fluoride-complexing elements are not to be expected in samples of vegetation.

Before the procedure is commenced, the distillation apparatus must be checked for an apparatus blank, which can result from memory effects. The blank determination is done with 50 ml of perchloric acid and the fluoride concentration in the distillate must not exceed 0.2 mg l^{-1}. Otherwise, blank distillations must be repeated until the given condition is satisfied. In addition to this preliminary blank test, a regular blank determination is needed in which the entire procedure is followed.

For calculation, adequate corrections for the blank and the change in volume during distillation must be applied.

Comparative test

Different types of vegetation, sampled in the vicinity of the plants of the participating companies, were distributed. The results given in Table 4 show good agreement.

TABLE 4

Collaborative test on fluroide in vegetation by five laboratories

Sample	Fluoride found (mg kg^{-1}) by 5 labs				
	1	2	3	4	5
Maize	—	624	570	576	—
Poplar leaves	46	—	53	—	47
Willow leaves	—	114	108	114	93
Shrub leaves	106	107	126	133	100
Oak leaves	301	347	362	364	351
Grass	—	66	67	—	63

HUMAN URINE

The determination of fluoride in urine is the least complex method in this series. No critical steps such as sample pretreatment or decomposition are encountered. The direct potentiometric method can be applied [13–15]. In preliminary tests, it was confirmed that no interference results from the composition of the matrix. These tests, aimed at establishing the recovery of fluoride, were first done with artificial urine spiked with known amounts of fluoride at the mg l^{-1} level. The recovery proved to be better than 94% in the range 0.2–5 mg l^{-1} fluoride. In addition, samples of normal urine were analyzed for their original fluoride content and analyzed again after being spiked with known amounts of standard fluoride solution. Again, these tests indicated satisfactory recoveries (better than 97%).

The method is suitable for the determination of fluoride in the range 0.2–20 mg l^{-1}.

Experimental

The direct potentiometric method is applied as described in the general section. The samples must be mixed carefully by shaking before an aliquot is taken for the determination. Only fresh samples (<1 day old) must be used because increasing amounts of precipitate may form during storage, thus introducing the risk of irreversible adsorption of fluoride.

For medical purposes, the fluoride concentration in mg l^{-1}, as obtained from the calibration graph, might have to be corrected to normal density or to normal creatinine level.

AIR

The fluoride determination in air is different from the other methods described in this report, as it is intended for very low concentrations at the $\mu g\ m^{-3}$ level. Consequently, trapping of fluoride in absorbing solutions is not suitable because of the inherent low sensitivity of such wet sampling methods.

Better results can be obtained with impregnated filters for trapping and subsequent extraction of fluoride into a small volume of TISAB solution for direct fluoride determination [8, 16, 17].

Preliminary tests were done along these lines and paper filters impregnated with sodium formate [16] were found to yield the best results with regard to absorption capacity and efficiency, tolerable flow rate and recovery of fluoride. Recoveries were checked with test gases produced by means of the permeation tube method [18]. The experiments proved a mean recovery of 98% at the 13 $\mu g\ m^{-3}$ fluoride level and of 96% at the 4 $\mu g\ m^{-3}$ level at an aspiration rate of 5 l min^{-1}.

The method is applicable for both normal and factory air. Only an adjustment in the sampling procedure is required, to take the difference in concentration into account. In the case of normal air, the method is designed for concentrations in excess of 0.3 $\mu g\ m^{-3}$ fluoride. Because of this low concentration level, a comparatively high aspiration rate (5 l min^{-1}) is applied and sampling times as long as 24 h may be required. In view of the resulting high linear flow velocities, two filters (each 47-mm diameter) in series are used to ensure complete absorption of fluoride.

In the case of factory air, it was decided to use the personal sampler system, which demands low sampling times and low aspiration rates, the latter because of the restricted performance of the light-weight pumps. Thus, small total amounts of fluoride have to be handled although the concentrations are on the mg m^{-3} level. Again, the filter method is suitable but the layout is different from that for normal air. Owing to the low aspiration rate of 0.5 l min^{-1} and so the low linear gas velocity, one filter is sufficient and the filter diameter can be smaller (25 mm). The method is designed for factory air with fluoride concentrations in the range 0.2—10 mg m^{-3}. If compounds which do not release all their fluoride by direct extraction with TISAB solution are suspected to be present, sodium hydroxide fusion must be applied in a preliminary step and a different citrate buffer solution is used.

The limits of interfering elements which can be tolerated with this procedure were estimated by model tests to be 100 μg of aluminium, 1000 μg of iron(III) and 1000 μg of calcium for a total amount of 19 μg of fluoride on the impregnated filter. This covers the range that is at all likely to be encountered in practice.

Experimental

Reagents. Apart from the reagents listed in the general section, a sodium formate solution (ca. 1 M) and a citrate buffer solution, free from sodium chloride, are needed. For the citrate buffer, 29.4 g of sodium citrate dihydrate is dissolved in ca. 900 ml of water, the pH is adjusted to 5.5 with hydrochloric acid and the solution is diluted to 1 l with water. (This special buffer solution is required only for the fluoride determination after alkaline fusion. It is used instead of the usual TISAB because in the given case the equivalent amount of sodium chloride is formed during neutralization of the melt.)

Impregnated paper filters are prepared by soaking filter paper (Whatman No. 4, trimmed to filters 47 mm or 25 mm in diameter) in ca. 1 M sodium formate and drying at room temperature in a fluoride-free atmosphere (e.g., vacuum dessicator); they are stored in a closed vessel until needed.

Apparatus. The sampling apparatus (Fig. 5) consists of the following parts. The sampling tube is made of polypropylene or PTFE. The filter holders are made of plastic, suitable for taking papers of 47- or 25-mm diameter as appropriate. For normal air, the gas pump, preceded in the system by a flow-control valve, must be capable of aspirating air at a rate of 300 l h^{-1}; the gas meter, wet or dry, is equipped with pressure gauge and thermometer. For factory air, the flow rate needed is only 30 l h^{-1}. It should be noted that the control valve and gas meter are not required for the personal samplers because the personal sampling pumps work at a fixed aspiration rate.

Plastic screw-capped bottles (ca. 100-ml capacity) and a mechanical shaker are also required.

Sampling. For normal air, an impregnated filter (47-mm diameter) is placed in each of two filter holders and the sampling train is assembled as shown in Fig. 5, using a minimum of tubing. A measured sample of air is drawn through the papers at a rate of 5 l min^{-1}. The total amount of fluoride collected must be minimally 5 μg. The sampling time must be adjusted accordingly.

For factory air, an impregnated filter (25-mm diameter) is placed in the filter holder of the personal monitor; the filter unit is attached to the pump and air is drawn through at a fixed rate of 0.5 l min^{-1} for a suitable time, but at least 20 min. The total amount of fluoride sampled must be at least 5 μg.

Direct potentiometric determination of fluoride after extraction. The filter(s) is removed from the filter holder(s) and placed in a 100-ml plastic bottle. After addition of 25 ml of conventional TISAB solution and 25 ml of water, the sealed bottle is shaken for 2 h in order to ensure complete extraction of fluoride and dissociation of any labile fluoride complexes present. The resulting suspension including the paper slurry is then poured into the measuring cell and the procedure is continued as in the general method. A blank determination with the impregnated filter papers is essential.

Potentiometric determination after decomposition. The paper filter(s) is removed from the filter holder(s) and placed in a nickel crucible together with 2 ml of water and 1 g of sodium hydroxide. The mixture is heated slowly to evaporate the water and the filter is burnt off. The residue is fused at dull

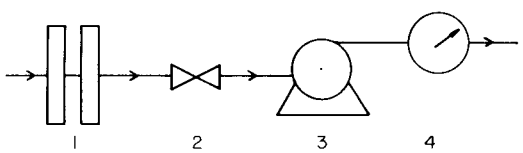

Fig. 5. Sampling train for the determination of fluoride in air: (1) filters and filter-holders; (2) flow control valve; (3) gas pump; (4) gas meter.

red heat for 20 min. After cooling, the melt is dissolved with 5 ml of water and the solution is transferred quantitatively to a 25-ml volumetric flask. The solution is neutralized with dilute hydrochloric acid (methyl orange indicator) and finally diluted to the mark with water. The contents of the flask are poured into the plastic bottle and the flask is rinsed in portions with a total volume of 25 ml of the citrate buffer solution, free from sodium chloride. The sealed bottle is shaken for 2 h to ensure decomplexation; the resulting solution is poured into the measuring cell and the procedure is continued as given for the general method.

A blank is determined with the impregnated filter papers and the reagents as described.

The results are expressed in $\mu g\ m^{-3}$ at STP after correction of the gas volume sampled as described under Calculations.

Comparative tests

Comparative tests were not done on account of the obvious impossibility of exchanging samples. The procedures described have given realistic results in the participating laboratories.

REFERENCES

1 M. S. Frant and J. W. Ross, Anal. Chem., 40 (1968) 1169.
2 R. Bock and S. Strecker, Z. Anal. Chem., 235 (1968) 322.
3 P. Kauranen, Anal. Lett., 10 (1977) 451.
4 H. H. Willard and O. B. Winter, Ind. Eng. Chem. Anal. Ed., 5 (1933) 7.
5 VDI Richtlinie No. 2452 (1963).
6 J. S. Jacobson and L. I. Heller, J. Air Pollut. Control Assoc., 26 (1976) 1065.
7 M. S. Frant and J. W. Ross, Science, 154 (1966) 1553.
8 J. S. Jacobson and L. H. Weinstein, J. Occup. Med., 19 (1977) 79.
9 M. Johnson, Fluoride, 9 (1976) 54.
10 A. E. Villa, Analyst (London), 104 (1979) 545.
11 W. Oelschläger and W. Wöhlbier, Forschungsbericht DFG, 14 (1968) 6.
12 J. A. Cooke, M. S. Johnson and A. W. Davison, Environ. Pollut., 11 (1976) 257.
13 J. D. Neefus, J. Cholak and B. E. Saltzman, Am. Ind. Hyg. Assoc. J., 31 (1970) 96.
14 J. Tusl, Anal. Chem., 44 (1972) 1693.
15 L. Singer, W. D. Armstrong and J. J. Vogel, J. Lab. Clin. Med., 74 (1969) 354.
16 C. Huygen, Anal. Chim. Acta, 29 (1963) 448.
17 L. H. Elfers and C. E. Decker, Anal. Chem., 40 (1968) 1658.
18 L. Kábrt, D. Chakraborti and L. Šucha, Scientific Papers of the Prague Institute of Chemical Technology H 15, (1980) 103.

Analytica Chimica Acta, 182 (1986) 17—31
Elsevier Science Publishers B.V., Amsterdam — Printed in The Netherlands

INTERLABORATORY COMPARISONS OF THE DETERMINATION OF pH IN POORLY BUFFERED FRESH WATERS

WILLIAM DAVISON

Freshwater Biological Association, The Ferry House, Ambleside, Cumbria LA22 0LP (Great Britain)

MICHAEL J. GARDNER

W.R.C. Environment, Medmenham, P.O. Box 16, Marlow, Bucks. SL7 2HD (Great Britain)

(Received 12th July 1985)

SUMMARY

Ten participants gathered at one location to compare measurements, made in the field and laboratory, of the pH of quiescent solutions of natural waters and dilute acids. The total error associated with a single routine measurement in the laboratory can be controlled to within ±0.2 pH, comprising a standard deviation of 0.05 pH and a bias of 0.1 pH. Inaccurate preparation of standard solutions is an appreciable source of bias. Larger errors observed for field measurements made with commercial equipment arise from poorly defined analytical procedures, the use of inappropriate electrodes, and probably dampness affecting the electronics. Stirring dilute solutions depresses the pH. This bias error, which is similar for all dilute solutions, depends on the type of liquid junction used in the reference electrode. Combination electrodes produce the largest stirring shifts (>0.2 pH) and separate electrodes, especially those with free-flowing junctions, the smallest. Correct choice of equipment and use of well-defined proven procedures are essential for the accurate and precise determination of pH.

Measurements of pH are so commonplace and apparently straightforward that they tend to be taken for granted. Simple, inexpensive equipment is routinely used to measure the pH of natural waters, which is usually in the range 4—10. However, recent work, associated with the phenomenon of acid rain, has shown that there can be considerable errors when pH is measured in solutions of low ionic strength [1—3]. Apparently the pH can be influenced dramatically by the type of liquid junction used as part of the reference electrode [4—6]. Although suggestions for new designs of liquid junction, based on the free diffusion of ions at a non-constrained interface, have emerged [7, 8], they are not as convenient as most commercial systems. The latter normally use a constraining element such as a ceramic frit, a sleeve or fibre wick to separate the bridge solution of the reference electrode from the measured solution. The rate of flow of bridge solution from this frit is important in determining the errors associated with the junction [6]. High flow rates minimize errors by preventing contamination effects and diffusion of the measured solution into the bridge solution.

0003-2670/86/$03.50

Stirring dilute solutions usually affects the pH [1], but there is little agreement on whether stirring should be recommended. Some argue [7, 9] that the glass electrode may produce errors in quiescent solutions, and others [2] that errors associated with the liquid junction are enhanced in stirred solutions. Because of this conflict, it has been suggested that ideally only electrode assemblies which do not show any appreciable stirring shift should be used [4].

The primary aim of this work was to assess precision and bias errors in routine determinations of pH, by comparing pH measurements made by different groups of scientists on samples of the same natural water. Previous attempts to circulate samples to individual laboratories had shown that sample instability could invalidate comparisons [10]. Therefore, it was arranged for representatives from ten different laboratories (Appendix 1) to meet to perform simultaneous measurements on freshly collected samples. Reasonable precautions (initial advice and checks on precision) were taken to avoid large errors or mistakes but no attempt was made to establish best possible controls by extending measurements and procedures to their limits. Measurements were made at a riverside and again on returning to a nearby (<5 miles) laboratory. This procedure was repeated over a two-day period at three different rivers. Dilute acids were also measured in the field and laboratory. They served as controls to assess pH changes associated with sample handling, sample instability and the performance of laboratory vs. field equipment. Precision tests were undertaken prior to the field exercise at the participants' home laboratory by making replicate measurements on acids and buffers over a ten-day period. This comprehensive series of tests provides new insight into the total analytical errors associated with the determination of pH.

EXPERIMENTAL

Equipment

Participants were provided with a set of recommendations concerning equipment and methodology which they were urged to adopt before embarking on the collaborative work. Most laboratory equipment conformed to the standards set by the recommendations, but few participants applied these test standards to the electrodes, usually combination electrodes, which they used for field measurements. The recommendations were as follows. "Use a conventional glass electrode and a separate calomel reference electrode filled with saturated potassium chloride solution, and having a liquid junction formed in a ceramic frit. Enhancement of the flow rate of the bridge solution by using a substantial (25—50 cm) head of electrolyte above the level of the sample is recommended but not obligatory. The reference electrode should be stored in saturated potassium chloride solution and the glass electrode in a buffer solution. The pH meter should discriminate to at least 0.01 pH regardless of whether measurements are made in the laboratory or in the

field. Replicate calibrations using at least two buffer solutions should agree to ±0.01 pH and the electrode slope should be within 2% of the theoretical value. Measurements made on the same air-equilibrated sample, under stirred and quiescent conditions, should be within 0.05 pH of one another."

The equipment used in laboratory and field tests is listed in Table 1.

Within-laboratory precision tests

In each of ten batches of analyses, each laboratory made duplicate determinations on the following solutions: (I) a buffer solution of pH 4.00; (II) 1.00×10^{-4} M hydrochloric acid or 0.50×10^{-4} M sulphuric acid; (III) either 1.00×10^{-5} or 3.00×10^{-5} M hydrochloric acid, or 0.50×10^{-5} or 1.50×10^{-5} M sulphuric acid; (IV) a sample of natural water of pH 4—6; (V) a sample of another natural water of pH 5—7.

Each batch was analysed on a separate day. The pH 4.00 buffer solution, which was treated as an "unknown", and the dilute acids were prepared freshly each day by each participant. Calibration was done each day with one independent pair of buffer solutions which were used throughout the tests.

Each laboratory provided their own water samples. Each natural water sample was collected in bulk and divided, soon after sampling, into twenty borosilicate glass bottles which were completely filled and stoppered. Each measurement was made on a sample from a freshly opened bottle, so avoiding pH drift caused by re-equilibration with the atmosphere. For each pH measurement the sample was stirred for 2 min by a magnetic stirrer. The stirrer was stopped and the pH recorded when the solution had remained quiescent for 2 min. This procedure provided, for each solution, twenty measurements. These could be treated by analysis of variance [11] to separate errors arising from within-day variations from those associated with day-to-day variations.

Inter-laboratory bias tests

All measurements were made during a two-day period, using the laboratory facilities of Trawsfynydd Power Station located in an upland area of mid-Wales. Three sampling locations were used, designated as rivers A, B and C. Measurements of electrical conductivity, total hardness and alkalinity (Table 2) showed that they were all soft waters.

Participants were requested to make the following measurements on each natural water and on samples of dilute acid with which they were supplied by the organisers: (a) measurements in the field with portable pH meters; (b) measurements in the laboratory with the equipment used in the precision test; and (c) measurements in the laboratory with the equipment used for field determinations. A different acid was used at each location and was designated by the location (A, B or C).

Electrodes were freshly calibrated for each replicate determination on each sample analysed. This involved one calibration routine, using pH 4 and

TABLE 1

Equipment used in the laboratory and in the field

Lab. no.	Laboratory			Field	
	pH meter	Glass electrode	Reference electrode	pH meter	Electrode
1	Philips PW 9409	Corning 311101	Corning 311602, unsealed, no remote reservoir	pHOX 42[a]	EIL combination
2	WRA CD390	Russell CE-7L	Combination electrode	pHOX Digimeter	pHOX combination
3	Orion 901	EIL 331032-100	Russell CR4/SA with removable 25-cm reservoir	Kent 3030	EIL combination
4	Radiometer PHM-84 + TTT-81 Digital Titrator	Radiometer G20401	Russell SRR2/7 with remote 30-cm reservoir	Gallenkamp pH stick	Combination
5	EIL 7065	Corning 311101	Corning 311602, unsealed, no remote reservoir	pHOX 42E	Corning combination
6	Orion 801A	Corning 311101	Corning 311602 with remote 40-cm reservoir	pHOX digital	pHOX combination
7	PHM 62	Russell SW-711	Russell SRR5/1 with remote 50-cm reservoir	Kane-May 7001[a]	Orion combination
8	EEL 12	Russell CWL-LCW	Combination Electrode	Jenway	Corning combination
9	Corning 110	Corning 311101	Calomel with remote 40-cm reservoir	WPA CD-390	as for lab.
10	Radiometer PHM-64	Corning 311101	Beckman 39416, unsealed	Orion 221	as for lab.

[a]Used temperature compensation. All other field measurements were made at river temperature.

TABLE 2

Characteristics of natural waters

River	Conductivity ($\mu S\ cm^{-1}$)	Hardness (mg $CaCO_3\ l^{-1}$)	Alkalinity (mg $CaCO_3\ l^{-1}$)	Mean pH[a]
A	35.6	17.5	<5	5.60
B[b]	35.0	15.0	<5	4.79
C	56.3	18.8	5	6.23

[a]Mean of measurements made in the laboratory. [b]Sample D collected from same location, on the second day.

7 calibration buffers supplied by the participant, per pair of determinations (i.e., river water and acid). Replicate measurements were made on portions of samples either freshly collected from the river or, in the laboratory, from freshly opened bottles. The pH values were recorded for quiescent solutions after appropriate equilibration of the electrodes, as described above.

In field and laboratory, three or four replicate determinations of the pH of the dilute acid and river sample were requested for each location. When the laboratory measurements on each acid and water pair were complete, four consecutive measurements were made on an unknown buffer solution which was supplied by the organisers. Four different unknown buffers were used, designated A—D, like the acid and water pairs.

For locations A and B (first day of tests), samples of dilute acid prepared in the laboratory by dilution of a stock solution of sulphuric acid, were taken to the riverbank sampling site in 500-ml borosilicate glass bottles. These bottles were used, after several rinses with the river water, for taking river water back to the laboratory. For location C, a bulk sample of acid was prepared and taken to the site in a large polyethylene container. The remaining acid, after measurement, was returned to the laboratory in the same container. A sample of River C was collected in bulk and returned to the laboratory in a similar container. River sample D, on which only laboratory determinations were made, was collected from River B on the second day.

All river samples were at 10 ± 2° C. Acid C was equilibrated to within 3° C of the river temperature before measurement. Most participants did the same for acids A and B and similarly equilibrated the buffers, but some used temperature compensation (Table 1). All laboratory measurements were made at 20 ± 2° C.

Determination of reference pH value

In an attempt to provide a value for the true pH, independent measurements were made in the laboratory at 20 ± 2° C with research equipment. A separate glass electrode, and a reference electrode which incorporated a free diffusion junction of the type previously described [8], were used. Such an electrode assembly should be free of the errors associated with constrained junctions used in commercial systems.

RESULTS AND DISCUSSION

Within-laboratory precision tests

Each laboratory conducted a prescribed series of precision tests which were used to identify problems prior to participation in the joint exercise at a single location. The results were treated by analysis of variance to obtain separate estimates of the random errors associated with measurements made within each day as opposed to those errors associated with day-to-day factors [11].

Day-to-day variations of <0.02 pH showed that replicate preparation of dilute acids and buffers was generally good. Except for two laboratories, which failed to prepare properly the solutions, the pH of the dilute acids was close to the value calculated from the concentration: it was assumed that the solution was in equilibrium with atmospheric carbon dioxide and corrections for activity coefficients were applied. Appreciable deviations (>0.05 pH) were usually restricted to stirred solutions. Unexpectedly, on two occasions buffers prepared from different sources differed by 0.1—0.2 pH, but generally they agreed to better than 0.05 pH.

Random errors associated with measurements made within each day were larger for natural waters than for buffers or dilute acids. There was also evidence for a progressive change in the pH of the natural waters from the first to the last day. Apparently, the samples of natural waters were unstable, the magnitude of the pH drift varying appreciably from bottle to bottle. With only one exception, the precision was worst for the natural water with the highest pH, irrespective of whether it was stirred or quiescent. Samples with a near-neutral pH may be intrinsically less stable or more difficult to measure.

An analysis of stirring shifts is given in Table 3. Where there was a significant change in pH, the value was lower in the stirred rather than the quiescent solution. Stirring shifts in the four dilute solutions, natural waters and acids were similar for a given laboratory. In contrast, all stirring shifts in buffer solutions were trivial. The size of the stirring shifts may be related to the electrode system used by the participating laboratories. Laboratories 3, 4, 6, 7 and 9, which used a separate glass electrode, and a calomel electrode with a pressurised head of potassium chloride, all found shifts of <0.03 pH. The stirring shift for those laboratories using separate glass and calomel electrodes without pressurised head (1, 5 and 10) was <0.07 pH. For laboratories 2 and 8, using combination electrodes, substantial shifts, in excess of 0.2 pH, were observed.

These results are consistent with those of other workers who have shown that stirring shifts are usually minimized when electrodes with free flowing junctions [4], or high fluxes of filling solution [6], are used. Brezinski [6] considered that stirring errors associated with low flow rates were caused by perturbation of diffusion profiles which extend from the junction into solution, introduction of surface charges within the pores of a partially clogged junction, and solution memory effects caused by inadequate flushing of the

TABLE 3

Difference between mean measured pH under quiescent and stirred conditions[a]

Lab.	Buffer I	Acid II	Acid III	Water IV	Water V	Mean shift[b]
1	0.001	0.074	0.086	0.063	0.039	0.065 ± 0.023
2	0.018	0.225	0.264	0.174	0.189	0.213 ± 0.047
3	0.007	0.034	0.026	0.020	0.026	0.026 ± 0.007
4	−0.006	0.004	0.008	0.009	0.002	0.006 ± 0.004
5	−0.001	0.057	0.067	0.054	0.047	0.056 ± 0.010
6	0.000	−0.002	0.001	−0.001	−0.003	−0.001 ± 0.002
7	0.011	0.018	0.024	0.027	0.017	0.021 ± 0.006
8	0.007	0.255	0.391	0.205	0.207	0.264 ± 0.103
9	0.002	0.002	0.006	0.006	0.005	0.005 ± 0.002
10	−0.003	−0.009	0.010	−0.007	−0.002	−0.002 ± 0.010

[a]Differences calculated from (quiescent − stirred) pH values. Stirred readings obtained after stirring sample for 2 min. Quiescent readings taken after stirring for 2 min followed by a further 2 min without stirring. [b]Mean stirring shift for dilute solutions II—V, with 90% confidence interval.

junction. Increasing the head of potassium chloride will increase the flow rate and reduce stirring shifts. Low-leakage ceramic frits, which are usually used in combination electrodes to avoid frequent replenishment of the filling solution, will tend to increase stirring shifts. The observations that measurements made on quiescent solutions produced results closest to the correct answer, and that the stirring errors were almost exclusively biased to lower pH, agree with other work [1, 4].

The results show that laboratories 2 and 8, and possibly 1 and 5, did not adequately test their electrodes, because the stirring shifts were sufficiently large to warrant rejection. These preliminary tests highlighted preparation errors which could be corrected prior to the main work. They also showed that stirring the solutions could bias the results and so all subsequent measurements were made on quiescent solutions.

Inter-laboratory bias tests

The maximum possible bias (m.p.b.) [12] for each replicate set of pH determinations was calculated by adding a precision error to the bias error, assessed as the difference between the measured mean and the true value. Thus, if the mean result of laboratory i, and its 90% confidence interval, are denoted by $xi + Li$, the value of the m.p.b. of laboratory i (95% confidence level) is calculated as $xi + Li - X$ if $xi > X$, or $xi - Li - X$ if $xi < X$, where X is the true pH value.

The original intention was to use the reference pH, measured with use of the free diffusion junction, as the best estimate of the true pH. The dilute acids were to corroborate this approach. However, inspection of the results (Tables 4—8) showed that, whereas the reference pH agreed with the assigned

TABLE 4

Means, with standard deviation (s.d.) and maximum possible bias (m.p.b.), of the pH of "unknown" buffer solutions

Lab. no.	Buffer A			Buffer B			Buffer C			Buffer D		
	Mean[a]	S.d.[a]	M.p.b.	Mean[a]	S.d.[a]	M.p.b.	Mean[b]	S.d.[b]	M.p.b.	Mean[a]	S.d.[a]	M.p.b.
1	4.023	0.006	0.024				6.883	0.005	—0.014	4.705	0.006	0.018
2	4.060	0.000	0.051	4.670	0.000	0.018	6.928	0.005	0.043			
3	4.061	0.004	0.059	4.703	0.002	0.054	6.862	0.004	—0.033	4.721	0.007	0.035
4	4.003	0.006	—0.015	4.650	0.000	—0.002	6.900	0.001	0.011	4.716	0.001	0.023
5	3.940	0.010	—0.086	4.587	0.012	—0.085	6.873	0.005	—0.024	4.613	0.010	—0.093
6	4.002	0.002	—0.010	4.649	0.004	—0.009	6.899	0.006	0.016	4.713	0.001	0.020
7	3.997	0.006	—0.022				6.898	0.005	0.013	4.698	0.005	0.009
8												
9	3.984	0.001	—0.026				6.889	0.001	—0.003			
10	3.970	0.000	—[c]				6.883	0.010	—0.019	4.730	0.000	—[c]
Mean[d]		4.009			4.652			6.890			4.694	
Assigned value		4.000			4.640			6.880			4.700	
Reference value[e]		4.010			4.648			6.895				

[a]For 3 results. [b]For 4 results. [c]Only 2 results reported; not included in mean of all laboratories. [d]Mean of results from all laboratories. [e]Reference value is the pH value measured in the laboratory with use of a free diffusion junction.

TABLE 5

Means, with standard deviation (s.d.) and maximum possible bias (m.p.b.), of the pH of "unknown" acid solutions measured in the field and laboratory on day 1
(Values for which m.p.b. exceeds 0.1 pH are asterisked.)

Lab. no.	Acid A, field			Acid A, laboratory			Acid B, field			Acid B, laboratory		
	Mean[a]	S.d.[a]	M.p.b.	Mean[a]	S.d.[a]	M.p.b.	Mean[b]	S.d.[b]	M.p.b.	Mean[b]	S.d.[b]	M.p.b.
1	4.433	0.115	0.347*	4.383	0.031	—0.078	4.433	0.058	0.142*	4.203	0.006	—0.078*
2	4.333	0.021	0.086	4.360	0.030	—0.101*	4.737	0.133	0.573*	4.177	0.015	—0.121*
3	4.500	0.100	0.388*	4.487	0.026	0.121*	4.683	0.076	0.423*	4.263	0.013	—0.030
4	3.553	0.216	—1.097*	4.387	0.012	—0.043	3.700	0.144	—0.936*	4.193	0.006	—0.088
5	4.083	0.126	—0.414*	4.323	0.015	—0.112*	3.350	0.200	—1.381*	4.560	0.020	0.323*
6	4.230	0.046	—0.131*	4.502	0.014	0.117*	4.553	0.031	0.215*	4.230	0.020	—0.074
7	4.507	0.012	0.244*	4.410	0.026	0.045	4.800	0.070	0.529*			
8	4.347	0.040	0.133*				4.517	0.040	0.195*			
9	4.390	0.026	0.152*	4.425	0.056	0.110*						
10	4.450	0.092	0.323*	4.450		—[c]	4.737	0.080	0.483			
Mean[d]		4.283			4.410			4.390			4.271	
Calculated value		4.255			4.255			4.520			4.520	
Reference value[e]					4.375						4.193	

Means, with standard deviation (s.d.) and maximum possible bias (m.p.b.), of the pH of natural waters measured in the field and laboratory on day 1
(Values for which m.p.b. exceeds 0.1 pH are asterisked.)

Lab. no.	River A, field			River A, laboratory			River B, field			River B, laboratory		
	Mean[a]	S.d.[a]	M.p.b.	Mean[a]	S.d.[a]	M.p.b.	Mean[b]	S.d.[b]	M.p.b.	Mean[b]	S.d.[b]	M.p.b.
1	5.867	0.058	0.570*	5.603	0.029	—0.049	4.733	0.058	0.172*	4.813	0.006	0.033
2	5.633	0.031	0.291*	5.537	0.021	—0.102*	4.767	0.012	0.127*	4.743	0.015	—0.073
3	5.700	0.173	0.600*	5.612	0.063	0.115*	4.775		—[c]	4.841	0.008	0.065
4	4.760	0.053	—0.725*	5.603	0.015	—0.026	5.383	0.516	1.603*	4.810	0.010	0.037
5	4.950	0.132	—0.670*	5.543	0.060	—0.163*	3.583	0.029	—1.125*	4.727	0.055	—0.157*
6	5.317	0.047	—0.158*	5.692	0.033	0.145*	4.710	0.017	0.080	4.807	0.013	0.038
7	5.820	0.020	0.459*	5.577	0.015	—0.053	4.970	0.020	0.345*			
8	4.573	0.006	—0.831*				4.367	0.025	—0.335*			
9	5.643	0.167	0.534*	5.662	0.023	0.097						
10	5.683	0.107	0.471*	5.735		—[c]	4.760	0.000	0.101*			
Mean[d]		5.395			5.604			4.659			4.790	
Reference value[e]		—			5.620			—			4.775	

[a—e]See footnotes to Table 4.

TABLE 7

Means, with standard deviation (s.d.) and maximum possible bias (m.p.b.), of the pH of Acids C and D. Acid C was measured in the field and in the laboratory
(Values for which m.p.b. exceeds 0.1 pH are asterisked.)

Lab. no.	Acid C, field			Acid C, laboratory			Acid C, laboratory[b]			Acid D, laboratory		
	Mean[a]	S.d.[a]	M.p.b.	Mean[a]	S.d.[a]	M.p.b.	Mean[a]	S.d.[a]	M.p.b.	Mean[a]	S.d.[a]	M.p.b.
1	4.650	0.058	0.122*	4.645	0.010	0.059	4.700	0.000	0.078	4.635	0.013	0.046
2	4.500	0.200	—0.331*	4.480	0.000	—0.118*	4.585	0.025	—0.067	—	—	—
3	4.713	0.048	0.173*	4.652	0.018	0.075	4.775	0.029	0.187*	4.635	0.012	0.044
4	4.565	0.019	—0.053	4.616	0.010	0.031	4.585	0.006	—0.044	4.594	0.002	—0.013
5	4.550	0.000	—0.046	4.615	0.042	0.067	4.513	0.048	—0.166*	4.590	0.018	—0.036
6	4.553	0.026	—0.074	4.627	0.006	0.036	4.473	0.022	—0.176*	4.591	0.005	—0.019
7	4.663	0.035	0.108*	4.508	0.085	—0.190*	4.635	0.010	0.024	4.583	0.013	—0.037
8	4.653	0.050	0.115*				4.700	0.044	0.129*			
9	4.538	0.023	—0.085	4.620	0.007	0.030	4.614	0.006	—0.015			
10	4.575	0.039	—0.066	4.618	0.010	0.031	4.645	0.006	0.029			
Mean[c]		4.596			4.598			4.622			4.605	
Calculated value		4.693			4.693			4.693			4.841	
Reference value[d]					4.904							

[a]For 4 results. [b]Laboratory determination with field equipment. [c]Mean of results from all laboratories. [d]Reference value is the pH value measured in the laboratory with use of a free diffusion junction.

TABLE 8

Means, with standard deviation (s.d.) and maximum possible bias (m.p.b.), of the pH of river samples C and D. River sample C was measured in the field and laboratory
(Values for which m.p.b. exceeds 0.1 pH are asterisked.)

Lab. no.	River C, Field			River C, laboratory			River C, laboratory[b]			River D, laboratory		
	Mean	S.d.[a]	M.p.b.	Mean	S.d.[a]	M.p.b.	Mean	S.d.[a]	M.p.b.	Mean	S.d.[a]	M.p.b.
1	6.238	0.048	0.111*	6.205	0.021	−0.052	6.275	0.050	0.186*	4.830	0.012	0.016
2	6.260	0.000	0.077	6.100	0.040	−0.179*	6.298	0.030	0.185*			
3	6.288	0.063	0.179*	6.277	0.036	0.087	6.350	0.058	0.270*	4.866	0.027	0.070
4	5.980	0.101	−0.322*	6.324	0.033	0.131*	6.200	0.016	0.072	4.840	0.004	0.018
5	6.038	0.025	−0.175	6.145	0.024	−0.115*	6.025	0.144	−0.293*	4.758	0.046	−0.124*
6	6.138	0.021	−0.070	6.226	0.008	−0.016	5.765	0.054	−0.447*	4.838	0.003	0.014
7	6.215	0.030	0.067	6.248	0.017	0.035	6.213	0.013	0.080	4.833	0.017	0.025
8	5.492	0.087	−0.793*				5.810	0.018	−0.359*			
9	6.253	0.029	0.104*	6.256	0.018	0.045	6.242	0.008	0.104*			
10	6.238	0.037	0.098	6.310	0.029	0.112*	6.300	0.037	0.196*			
Mean[c]		6.183			6.232			6.148			4.827	
Reference value[d]					6.294						4.841	

[a–d]See footnotes to Table 7.

value for the unknown buffers (Table 4), there was poor agreement with the calculated value for the dilute acids. Values obtained by using the free diffusion junction electrode for river samples (Tables 6 and 8) corresponded closely with the mean of the laboratory measurements, to within ±0.06 pH. Two of the three acids (Table 5) showed reasonable agreement between the mean and the reference value, but for Acid C (Table 7) there was a discrepancy of 0.3 pH. As the mean was not influenced by large errors from individual laboratories, it appears that the reference value is wrong. Although this was probably caused by human error (e.g., sample contamination or a wrongly labelled bottle), it cast sufficient doubt on the reference procedure to obviate its use as a true value in this instance. Instead, the mean result of all the laboratories was used (after outlier rejection) as the value against which to judge the bias of each laboratory. Alternative calculations, using reference values to assess bias for river samples, produced little difference in bias errors. One laboratory whose m.p.b. exceeded 0.1 pH, using the mean as the true value, had a m.p.b. <0.1 pH on using the reference value.

In contrast to the precision tests, the calculated pH values for the dilute acids (Tables 5 and 7) were unreliable. This may reflect the difficulty in preparing 40 l of dilute acid of exactly known concentration in an unfamiliar laboratory.

Measurements on buffer solutions achieved a good precision (standard deviation $\leqslant 0.012$). Although all bias errors were small (m.p.b. <0.1 pH), the pH measured by laboratory 5 was always lower than the mean of all laboratories by 0.018—0.081 (Table 4). The pH 4.00 calibration buffer used by laboratory 5 appears to be 0.07 pH too high. Laboratory 2 also displayed a smaller, but consistently positive bias. Evidently calibration errors cannot be ignored, even though they are usually of minor importance.

The precision of determinations made in the laboratory on river samples and dilute acids was generally good (Tables 5—8). Only on five occasions did the standard deviation exceed 0.05 pH, confirming the results from the precision tests that the larger random errors observed for natural waters which had been stored resulted from sample instability rather than the sub-sampling procedure. There were 18 instances when the m.p.b. exceeded ±0.1 pH, out of a possible 58 laboratory/solution combinations (Tables 5—8). Laboratories 2 and 5 accounted for 10 of these poor results. Laboratory 2 had a consistently negative bias while laboratory 3 had a smaller but consistently positive bias. There was no apparent improvement in performance as the tests progressed from samples A to D.

It is not possible unequivocally to relate the performance of participants to their equipment. Only laboratory 1 (separate conventional reference and glass electrodes) never exceeded a m.p.b. of ±0.1 pH, but the other laboratory (No. 5) using similar equipment performed worst. Laboratories 3, 4, 6, 7 and 9, which used pressurised reference systems, obtained m.p.b. values in excess of ±0.1 pH on only 7 out of a possible 34 occasions. However, this is not significantly ($p = 0.05$) better than the performance of the remaining laboratories.

Measurements made in the field were characterised by large random and systematic errors (Tables 5—8). Results for the second day (samples C) were appreciably better than for the first (samples A and B). Standard deviations and the m.p.b. were lower, possibly because the second day was dry whereas there was slight rain on the first day. Some laboratories reported evidence of instrument drift on the first day which probably arose from dampness lowering the input impedance; when some instruments were returned to a warm dry laboratory the drift was eliminated. Instrument malfunction would not explain the generally poor performance of participants on day 1. This is more likely to be due to operator error, because although all participants were experienced in the determination of pH, not all made measurements routinely in the field. The improvement in performance with increasing familiarity on the second day emphasises the need for a better defined analytical procedure.

The mean of the results from all participants can be used to assess differences between laboratory and field measurements (Table 9). There was excellent agreement between laboratory and field measurements for samples C, both river and dilute acid. The substantial differences observed for samples A and B therefore more likely reflect poor measurement procedure in the field rather than a genuine change in pH. Repeat measurements were made in the laboratory using the field equipment, but owing to a shortage of time only a few laboratories made measurements on samples A and B. Neither the mean of these measurements nor the determinations by individual participants (see Tables 7 and 8 for complete results for samples C) consistently agree with either the field or previous laboratory determinations. However, the differences between field and laboratory measurements made by using the same equipment, in theory indicative of sample instability, show a decrease in pH for river samples and an increase in pH for dilute acids. Evidently dilute acids are not ideal models for natural waters.

The mean value for river D agreed well with the mean of the laboratory determination of river B (Table 9). As these were sampled from the same site on consecutive days, it appears that the pH of this river remained constant and that the mean of all the measurements was repeatable on a day-to-day basis.

CONCLUSIONS

Interlaboratory testing at one site showed that standard deviations of laboratory measurements on dilute acids and natural waters were generally less than 0.05 pH and maximum possible bias errors were not usually larger than 0.1 pH. As 95% of all determinations will be within two standard deviations (s.d.) each side of the mean, the maximum error associated with a single measurement of pH will be ±(bias error + 2 s.d.) = ±0.2 pH. These results were obtained by laboratories which had been supplied with recommendations regarding equipment and procedures. Focussing of attention on

TABLE 9

Mean pH, and associated parameters, for the measurements by all laboratories on each sample

	A				B				C				D	
	River sample		Dilute acid		River sample		Dilute acid		River sample		Dilute acid		Laboratory	
	Determination		Determination		Determination		Determination		Determination		Determination			
	Field	Lab.	Field	Lab.	Field	Lab.	Field	Lab.	Field	Lab.	Field	Lab.	River	Acid
Mean pH[a]	5.39	5.60 (5.36)	4.28	4.41 (4.41)	4.66	4.79 (4.64)	4.39	4.27 (4.52)	6.18	6.23 (6.15)	4.60	4.60 (4.62)	4.83	4.60
Number of participating laboratories[b]	10	9(4)	10	9(3)	9	6(3)	9	6(3)	10	9(10)	10	9(10)	6	6
Range of mean results	1.3	0.19	0.96	0.18	1.8	0.12	1.4	0.38	0.80	0.22	0.21	0.17	0.10	0.05
Limits of range of mean results	4.57 −5.87	5.54 −5.73	3.55 −4.51	4.32 −4.50	3.58 −5.38	4.72 −4.84	3.35 −4.80	4.18 −4.56	5.49 −6.29	6.10 −6.32	4.50 −4.71	4.48 −4.65	4.76 −4.86	4.58 −4.63
No. of cases of mean bias >0.1 pH[c]	9	1	7	0	7	0	8	1	4	1	1	1	0	0
No. of cases of m.p.b. >0.1 units[d,e]	10	4*	9	5*	7*	1	9	1	6	4	5	2	1	0
No. of cases of s.d. >0.05[e,f]	4	0*	5	0*	1*	0	3	0	2	0	1	0	0	0

[a]Mean pH measured in the laboratory with the field equipment is given in parentheses. [b]This is the number of laboratories providing two or more replicate results for the samples concerned. For samples A and B (i.e., river and dilute acid), 3 replicate measurements were requested; for samples C and D, 4 replicate measurements were requested. The number of participating laboratories for laboratory measurements with field equipment is given in parentheses. [c]Calculated as the difference between the mean result of a single laboratory and the mean result of all laboratories. [d]Maximum possible bias (probability level = 0.05) is calculated by adding the 95% (single-sided) confidence interval to the mean bias. Maximum possible bias was not computed unless at least 3 results were reported for a given solution. [e]Asterisks indicate the number of cases from a maximum possible of 8 because one laboratory failed to provide three replicates. [f]Only standard deviations which are statistically significantly (F test, $p = 0.05$) greater than 0.05 pH units have been identified.

points of detail, and participation in a programme of testing, is sufficient to bring about improvements in previously prevailing analytical accuracy. Therefore, despite any problems caused by the unfamiliar circumstances of the bias tests, the estimate of a total error of ±0.2 pH is a reasonable assessment of the accuracy which might be achieved routinely when commercial equipment is used.

For field measurements, precision and bias errors were much worse, apparently because of increased operator error and poor equipment performance. Electrical equipment marketed specifically for field use can be prone to humidity problems, and the electrodes which are supplied are apparently selected because of their rugged construction rather than their proven performance. As sample instability is an established problem [10], high-quality field measurements are certainly desirable. In principle, the use in the field of laboratory-grade equipment and well defined analytical procedures should provide the necessary accuracy.

This work does not allow any single procedure to be identified which is clearly most suitable for the routine determination of the pH of natural waters. Considerable bias errors may be due to the preparation of standards, as well as inaccuracies associated with the actual measurement. Undoubtedly, care in the selection and initial testing of electrodes will improve the quality of results. Most important, however, is the unambiguous description of preparation and measurement procedures, and the adoption of routine analytical quality control. The quality of pH data, like those from any other analytical determination, will be greatly improved by strict adherence to a rigorously defined proven routine. Although implementing a programme of quality control will decrease errors, it will not ensure the accuracy of the determination. Comparison with a reference procedure incorporating a free diffusion junction may be a viable approach to the problem, as described in the I.U.P.A.C. recommendations for measurement of pH of fresh-water samples [13].

The authors thank all participants for freely giving their time, the Central Electricity Generating Board for providing laboratory facilities, Mick Burns for reference value measurements and Simon Blake for his assistance.

APPENDIX 1

List of Participants

Central Electricity Research Laboratories
Department of Agriculture and Fisheries for Scotland
Freshwater Biological Association
Forth River Purification Board
Grampian Regional Council
Northumbrian Water Authority
North West Water Authority
Solway River Purification Board

Water Research Centre
Welsh Water Authority

The sequence of participating laboratories in this list does not relate to the order of numbering of the laboratories in the tables.

REFERENCES

1 J. N. Galloway, B. J. Cosby and G. E. Likens, Limnol. Oceanogr., 24 (1979) 1161.
2 N. R. McQuaker, P. K. Kluckner and D. K. Sandberg, Environ. Sci. Technol., 17 (1983) 431.
3 W. F. Koch and G. Marinenko, in S. A. Campbell (Ed.), Sampling and Analysis of Rain, ASTM STP 823, 1983, pp. 10—17.
4 W. Davison and C. Woof, Anal. Chem., 57 (1985) 2567.
5 J. A. Illingworth, Biochem. J., 195 (1981) 259.
6 D. P. Brezinski, Analyst (London), 108 (1983) 425.
7 A. K. Covington, P. D. Whalley and W. Davison, Analyst (London), 108 (1983) 1528.
8 A. K. Covington, P. D. Whalley and W. Davison, Anal. Chim. Acta, 169 (1985) 221.
9 G. Mattock, pH Measurement and Titration, Heywood, London, 1961.
10 Analytical Quality Control (Harmonised Monitoring) Committee, Analyst (London), 109 (1984) 431.
11 A. L. Wilson, Talanta, 17 (1970) 31.
12 A. L. Wilson, Analyst (London), 104 (1979) 273.
13 A. K. Covington, P. D. Whalley and W. Davison, Pure Appl. Chem., 57 (1985) 877.

Analytica Chimica Acta, 182 (1986) 33—45
Elsevier Science Publishers B.V., Amsterdam — Printed in The Netherlands

ELIMINATION OF MAJOR MOLECULAR CHLORINE INTERFERENCE IN THE IODIMETRIC DETERMINATION OF SULPHUR IN SALINE SEDIMENTS

E. KISS

Research School of Earth Sciences, The Australian National University, G.P.O. Box 4, Canberra, A.C.T., 2601 (Australia)

(Received 15th August 1985)

SUMMARY

Free chlorine evolved during the high-frequency induction furnace combustion of saline sediments at >1500°C interfered very seriously in the iodimetric titration of liberated sulphur dioxide. Remedies based on absorption of chlorine on copper, antimony and other traps were only partly successful; copper was the most efficient but the loss of titratable sulphur was still very large. Sample desalination with refluxing anhydrous methanol in a Soxhlet extractor was the only method found to give satisfactory performance. This procedure was successful for a broad range of salinity values (reference sample mixed with sodium chloride in ratios of 0.09—1.6) without affecting the sulphur minerals present. The procedure showed excellent precision and good agreement with the "best" values available for the USGS MAG-1 Marine Mud (0.40% S) with a relative standard deviation of 1.29%. Iodimetric determination of sulphur in salt core samples (with the sediment in minor proportions) would also be possible.

Although the analytical chemistry of sulphur is extensive, only a few methods have been successful for geological materials. The most frequently used procedures which have gained a measure of importance in analytical geochemistry are various types of sample combustion (high-frequency induction or resistance heating), involving either iodimetric titration of absorbed sulphur dioxide [1, 2], or alkalimetric titration of the combustion gases collected in hydrogen peroxide [3]. Another application of the high-temperature combustion of siliceous materials (such as glasses) involves conductivity measurement of sulphur dioxide evolved [4].

In the iodimetric titration of sulphur dioxide, serious interference problems arise from the presence of chlorides and nitrates in some soils and sediments. Few workers have identified the mechanism of this interference, but several attempts have been made to overcome it by (i) precipitation of sulphate and complexiметric titration of excess of barium ions as recommended in a 1958 LECO procedure, and (ii) insertion of various types of halide absorbers [2, 3, 5] in the combustion line. Kaplan et al. [6], in studies of sulphur in marine sediments, found that the LECO iodimetric technique did not give reproducible results and much lower values were obtained than by

0003-2670/86/$03.50

wet combustion (bromine and aqua regia). These discrepancies were attributed to incomplete combustion of organic matter. Halide interference was also identified by Beesley and Chamberlain [4] because of the formation of hydrogen chloride in the pyrolysis/conductivity procedure employed, but Nebesar [1] and Pell et al. [5] referred to interference by halides which release iodine in the LECO iodimetric titrimetry, thus indicating the formation of free halogens.

The present study arose because of the poor reproducibility and low sulphur recovery by the LECO high-frequency combustion/iodimetric system (photometric titration) which was used for the analysis of lacustrine, restricted basin and marine sediments. The project, which was related to paleoclimatic investigations, required precise measurements of sulphur for temporal boundary estimations in the sediment record. In this paper, the gradual elucidation of the interference mechanism and the progressive evaluation of various remedial halide absorbers are described. This insight led to the realization that the iodimetric titration of sulphur only works for marine sediments if halides are removed first; molecular chlorine interferes catastrophically. Soxhlet extraction with methanol was the only method found to achieve satisfactory desalination and the results are excellent. Nitrate interference was not considered here.

In addition to such obvious factors as sulphur/chloride ratio, other typical problems encountered in the iodimetric determination of sulphur in sediments include seemingly unrelated parameters such as porosity variation, sulphur/organic carbon ratio and water salinity, ranging from fresh to hypersaline. For example, variations in the particle size and porosity of marine sediments have important bearing on the salinity distribution throughout the sample and also influence the degree of sample heterogeneity. The effect of these variables, therefore, makes it difficult to predict the exact level of interference even within the same core sample.

As far as the iodimetric technique is concerned, several workers have investigated the non-stoichiometric production of sulphur dioxide from soils and steel and in general, the adaptation of such systems as the LECO Sulphur Analyzer has been unsuccessful [3, 7], but the obvious advantage of rapidity and simplicity encouraged modifications to be made to procure a complete recovery of sulphur [3] in steel. However, in the present work it was found that if the conditions of combustion are maintained constant, it is not essential to obtain a 100% yield of the sulphur dioxide. The SO_2/SO_3 ratio was found to be constant for a very broad dynamic range (0.35—28% S) of sulphide standards and sulphates (gypsum and barite). This made the calibration of the potassium iodate titrant valid even when sulphide standards or high-purity barium sulphate were used interchangeably.

Other successful, but rather slow, procedures for the determination of sulphate, sulphide and total sulphur in soils and plant materials include spectrophotometry by the methylene blue method [8—11] or the coloured product formed between sulphur dioxide, pararosaniline and formaldehyde [12], x-ray fluorescence spectrometry [13, 14] and titrimetry [15].

PRELIMINARY INVESTIGATIONS

Mechanism of chlorine evolution and interference

Severe interferences were observed in the iodimetric titration of sulphur dioxide in the radiofrequency (r.f.) induction furnace during the combustion of chloride-bearing materials (e.g., marine muds and saline sediments) because of the production of free chlorine. The primary reaction, catalyzed by the release of chemically combined water, is likely to proceed according to the following steps at >1500° C:

$$\{[\text{Sediment}] + \text{NaCl}\} \rightarrow \{\text{Na}^+[\text{Sediment}]\} + \text{MeCl}_n + 1/2\text{Cl}_2\ (30\%) \qquad (1)$$

$$\text{SO}_2 + \text{Cl}_2 + \text{H}_2\text{O} \rightarrow \text{SO}_3 + 2\text{HCl} \qquad (2)$$

The generation of chlorine was confirmed by the familiar starch/iodine colour formed under the experimental conditions. Chlorine interference was very severe, especially for highly saline sediments containing minor to trace levels of sulphur. The interference involved not only gas-phase oxidation of SO_2 by co-generated chlorine but also oxidation of the iodide in the titration cell as the combustion gases were absorbed, often with evolution of iodine vapour. There were at least three reactions of chlorine with sulphur dioxide, which produced a complex interference pattern: (1) instant oxidation of SO_2 with Cl_2 during the evolution stage within the crucible at temperatures in excess of 1500° C; (2) gas-phase oxidation of SO_2 in the cooler zone during the transit interval; and (3) liberation of iodine in the titration cell by the remaining chlorine.

Modifications to avoid the interferences

Attempts to suppress chlorine formation (reaction 1) by adding a large excess of copper accelerator to the sample, thus removing chlorine formed at the combustion site, were unsuccessful because of the tendency to frequent blockage caused by large amounts of sublimed dust (copper[II] chloride). The composition of the accelerators was then modified by including vanadium pentoxide discs (as catalytic accelerators) or iron flakes with tin powder. Both of these produced an appreciable increase in the levels of chlorine and were therefore rejected in further experiments. An attempt to suppress reaction 2 by placing platinum gauze over the porous cover near the combustion zone was also unsuccessful.

Attention was then focussed on the gas-phase oxidation process in the cooler zone of the delivery tube. Various solid-state absorbents were tested for their ability to suppress or eliminate the influence of free chlorine on the titration. Proprietary F-Cl absorbents (LECO 769-608 antimony lumps) and self-indicating crystals (LECO 769-610) saturated rapidly and their application was therefore limited. Copper accelerator (LECO 501-263) was found to absorb chlorine very efficiently from the oxygen flow carrying both Cl_2 and SO_2 before it entered the photoelectric titration vessel. Copper lost its

fresh metallic lustre during chlorine absorption and thus acted as a self-indicating absorber. A smaller trap filled with proprietary crystals was also used to monitor leakage and saturation point from the copper trap. The chlorine production, measured gravimetrically, showed a yield of 29.3% from the available total chloride content. (The calculation was based on the weight-gain of a copper trap, connected in line with the delivery tube, after the combustion of six portions of sodium chloride totalling 0.64 g.) The balance remained trapped in the considerable amount of dust which consisted of NaCl, $CuCl_2$ and $FeCl_3$ sublimates.

In further experiments, the temporal production of chlorine was examined to see if the peak evolution of sulphur dioxide preceded the production of chlorine and so allow an almost acceptable recovery of sulphur. However, a 33% loss of sulphur occurred without the use of the copper trap. When combustion parameters including the quantity and/or type of accelerators were altered, the yield of SO_2 became too erratic to be useful. In these experiments, it was proved that chlorine evolution commences in the early stages and is produced throughout the entire combustion time, acting as a powerful gas-phase oxidant of the co-generated sulphur dioxide.

Other metal traps tested included aluminium foil, titanium sponge, and antimony lumps. Of these, only the antimony was effective in reducing the amount of chlorine in the oxygen carrier flow.

Quantitative studies of sulphur recovery

The preceding investigations suggested the need for more systematic and quantitative examination. In particular, a study was made of the gas-phase reaction mechanisms both within the immediate combustion environment and during the post-evolution stage. A sulphur reference sample (CRCP Molybdenum Ore PR-1, containing 0.79% S) of zero salinity was used as follows. Weighed samples (100–120 mg) were homogeneously mixed with known amounts of sodium chloride to yield increasing ratios of added NaCl/sample, equivalent to 2–59.5% NaCl content with combustion accelerators added (one copper ring and one scoop of copper metal and one scoop of iron flakes in that order) and the crucibles were covered with porous lids. The combustion was done in the usual manner (see below). The samples were subdivided into three groups. For group A, the combustion gases were absorbed directly in 1.5% hydrochloric acid for the simultaneous photoelectric titration. For group B (long-path gas-phase reaction), a trap containing 168 g of copper metal accelerator was inserted at a distance of 670 mm from the silica combustion tube; absorption and titration were the same as for group A. For group C (short-path gas-phase reaction), the procedure was as for group B except that a trap containing 180 g of copper metal was mounted directly on the top of the combustion tube as close to the induction zone as practicable (60 mm) followed by a small trap filled with F-Cl absorber (self-indicating crystals, LECO 769-610) for the detection of any chlorine leakage.

The results obtained in these experiments showed significantly diverse patterns and confirmed observations of extremely severe and irreversible chlorine interference. The effects of molecular chlorine on sulphur recovery are summarized in Fig. 1.

Direct absorption and titration of the combustion gases (Curve A, Fig. 1) produced highly unstable end-point responses. With no attempt made to absorb chlorine evolved, small amounts of chlorine from 2–12.6% NaCl admixtures competed with the iodate titrant and caused total loss of titratable sulphur at 12.6% NaCl. Even with 2% NaCl, the loss of sulphur was 12%. The initial darkening of the absorbent solution at the commencement of the burn showed chlorine to be co-generated with sulphur dioxide.

The combustion gases from saline samples passing through the large copper trap in group B experiments showed significant compositional changes compared to direct titration but the improvement in recovery of sulphur at high salinity levels was still inadequate (Fig. 1, Curve B). The results were inconclusive with the short-path trap (group C) because of the relatively large scatter of data points but the slight improvement in sulphur recovery indicated that the oxidation of sulphur dioxide was time-dependent (Fig. 1, Curve C).

In summary, the results showed that some useful improvements were achieved by post-evolution gas-phase absorption of molecular chlorine.

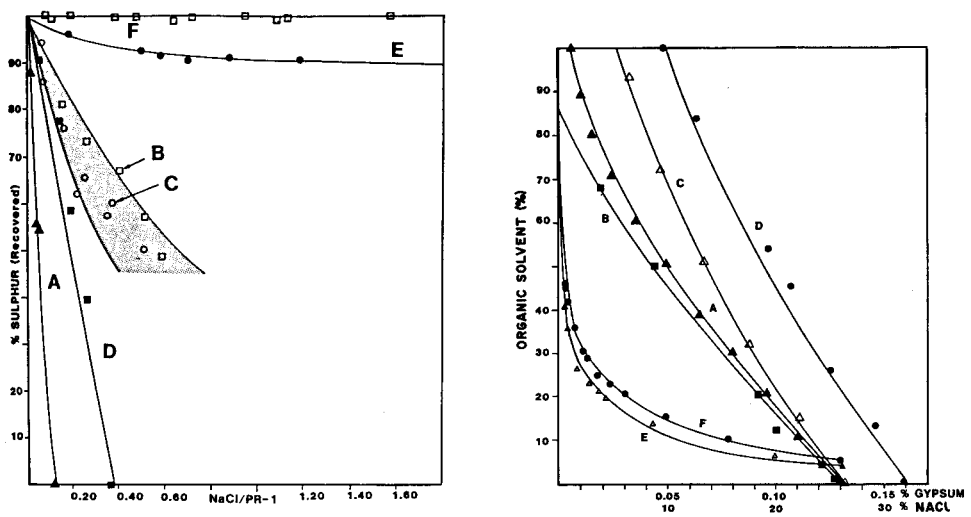

Fig. 1. Effect of molecular chlorine on the sulphur recovery in marine sediments by iodimetric titration. (A) Direct titration of combustion gases absorbed. (B and C) Copper traps (168 g and 180 g Cu at 670 mm and 60 mm from the combustion zone, respectively). (D) Methanol extraction and diffusive elimination of sodium chloride in porous filtering crucibles. (E) Selective extraction of halite with methanol (samples collected by filtration). (F) As for E, but samples Soxhlet-extracted in individual glass microfibre thimbles.

Fig. 2. Solubility of NaCl and gypsum in organic solvents (ternary systems). (A) NaCl/methanol/water; (B) NaCl/ethanol/water; (C) NaCl/ethylene glycol/water; (D) NaCl/glycerol/water; (E) gypsum/methanol/water; (F) gypsum/ethanol/water.

However, overall sulphur recovery (even after the total absorption of chlorine) was still very low, indicating that oxidation of SO_2 occurs inside the crucible at temperatures in excess of 1500°C. Because the possibilities were almost exhausted in these attempts to control the combustion chemistry, further efforts were made to remove high levels of salinity by sample pre-treatments.

It was envisaged that the salt content might be selectively leached with a suitable barium salt which would suppress the solubility of gypsum (main source of sulphur in sediments although pyrite and other sulphides may also be present in anoxic sediments) through the mass-ion effect and the formation of barium sulphate, which would remain adsorbed in the solid sediment particles. Aliquots of marine mud (USGS Marine Mud MAG-1) weighed into porous crucibles were leached by immersion in barium acetate solution. After the sample had been flooded by capillary action, the crucibles were drained. The treatment was repeated and the drained crucibles were dried at 110°C overnight. The end-point detection was then steady without any drift, showing the effective leaching of the sodium chloride. Unfortunately, however, the results were invariably low, typically yielding only one-third of expected sulphur. A likely explanation is that gypsum is appreciably soluble in barium acetate solution and the formation of a barium sulphate coating on the mud sample particles was too slow to prevent solubility loss of sulphate.

Sample pre-treatment

Sample pre-treatment aimed at the total extraction of chloride was examined in an attempt to remove chlorine interference. The relatively high solubility of some sulphur-bearing sediment constituents (e.g., gypsum) in aqueous leaching solutions precluded their use. Any desalination treatment therefore needed to be selective toward halite and related minerals only. Solubility data of sodium chloride and other alkali halides suggested favourably high values for alcohols, but other oxygen-containing solvents (ketones and ethers) would be less effective [16]. Solubilities of sodium chloride and calcium sulphate dihydrate were surveyed [17] in a wide range of binary, ternary and multicomponent organic solvent systems; the relevant relationships for sodium chloride and gypsum in some ternary compositions [17] are shown in Fig. 2. Glycerol and ethylene glycol appeared to be very effective in dissolving large amounts of sodium chloride but data for gypsum were lacking and it seemed probable that the solubility of gypsum would also be increased. Good agreement was found with the literature values of the solubility of sodium chloride in methanol and ethanol [16] using atomic absorption spectrometry to determine sodium in the saturated alcoholic solutions; methanol proved to be superior (14 200 mg l^{-1} NaCl) to ethanol (675 mg l^{-1} NaCl). Although solubilities are inversely related to temperature, extended refluxing in a Soxhlet extractor was successful in the desalination of the marine sediment MAG-1 without affecting gypsum or other sulphur-bearing constituents.

Three experimental procedures were used to test the effectiveness of methanol as a selective solvent: (1) elimination of chloride by diffusive

leaching in porous filtering crucibles from the pre-mixed samples of NaCl/molybdenum ore PR-1; (2) methanol leaching of NaCl/molybdenum ore PR-1 mixtures in closed centrifuge tubes, followed by collection on glass-fibre filter discs; and (3) Soxhlet extraction of the salt/PR-1 reference sample mixtures (mixing ratio: 0.1—1.2) in glass-fibre thimbles with methanol for several hours. The dried residues were analyzed for sulphur in the usual manner.

The efficiency of removing chlorine or chloride by various means is summarized in Fig. 1. It can be seen that the diffusive elimination of salt (curve D) in porous crucibles was extremely inefficient: the sulphur recovery was only marginally better than that with the direct titrations (curve A). For the other two sets of conditions, the methanol extraction of chloride was successful and the consistently high sulphur recoveries were independent of the chloride/sample ratios. The pre-treatment by methanol extraction ensured the highest recoveries and the observed end-points were stable and drift-free. Curves E and F highlight the manipulative difficulties in quantitative collection of solid particles from the filter assembly; losses in curve E tend towards a plateau within the mixing ratios (salt/PR-1) of 0.2—1.2, suggesting that only a simple mechanical loss is involved.

The individual self-cleaning action of glass-fibre thimble wadding in FEP-teflon filter sleeves (see below) (curve F) provided quantitative transference of the extracted sample, with all values of sulphur recovery approaching 100%. This procedure was therefore optimized for routine work. The recoveries of sulphur after desalination by methanol extraction are listed in Table 1.

TABLE 1

The efficiency of desalination by methanol extraction

NaCl/PR-1[a]	Sulphur (%)	Recovery (%)	NaCl/S[b]	Remarks
Nil	0.79	100.0	Nil	
Nil	0.790	100.0	Nil	
0.091	0.795	100.6	11.52	Soxhlet extraction (Duration 3 h)
0.118	0.778	98.6	14.94	
0.200	0.795	100.6	25.32	
0.391	0.788	99.7	49.49	
0.485	0.784	99.3	61.39	
0.632	0.779	98.6	80.00	
0.706	0.786	99.5	89.37	
0.947	0.790	100.0	119.87	Soxhlet extraction (Duration: 111/2 h)
0.991	0.780	98.7	125.44	
1.133	0.781	98.9	143.42	
1.571	0.790	100.0	198.86	

[a]Samples (100—150 mg) were premixed with pure sodium chloride in the appropriate ratios. Standard material used was CRCP Molybdenum Ore PR-1, containing 0.79% S.
[b]Ratio of NaCl to total sulphur calculated from the NaCl/sample pre-mix composition. ("Total sulphur" denotes the sum of sulphide-S and sulphate-S commonly found in sediments.)

Sulphur impurities in borosilicate glass micro-fibre extraction thimbles. The glass-fibre thimbles contained high levels of sulphate whereas various sizes of filter discs were at near blank level. The blank levels are listed in Table 2. This impurity is probably related to the inorganic binder used in manufacture. Aqueous leaching reduced blank levels to about a third, and soaking in dilute hydrochloric acid and rinsing with water produced blanks indistinguishable from combustion blanks. The small thimbles (9 × 40 mm) presented additional problems; poor mechanical strength, uneven wall thickness and loose fibre compression resulted in sample losses by leakage. This problem was overcome by the construction of FEP-teflon sleeves (see below) in which a 10-mm thimble base was cut and filled with shredded thimble glass fibres. This modification allowed extended Soxhlet extraction to be made without penetration of the sample particles through the filter wadding.

Scope and limitations. The proposed desalination procedure offers an effective sample pre-treatment for the interference-free iodimetric determination of sulphur. The solubility limitations of sodium chloride in anhydrous methanol extend the extraction time for quantitative treatment. However, eight individual samples can be extracted in a single Soxhlet extractor and assuming that safe operating conditions are maintained, overnight extraction in several extraction units will ensure rapid productivity. The special feature of the multi-extraction system is the lack of cross-contamination. This was achieved by careful height adjustment of the extraction thimbles preventing solvent flooding, by redistribution of the condensed solvent to the outside of the extraction basket thus avoiding direct impact on the sample, and by blanketing the powdered sample with a loose plug of fibre wadding (see below). This extraction technique allows iodimetric sulphur determinations

TABLE 2

Sulphur impurities in glass-fibre filters

Filter material	S found/unit (mg)	S found ($\mu g\ g^{-1}$)
Millipore filter disc, 24 mm	0.011	
Whatman filter disc, 4.25 cm	0.002	
Whatman filter disc, 5.5 cm	<0.002	
Extraction thimble, 10 × 50 mm[a]	2.96	1666
	3.36, 3.30	
Extraction thimble, 10 × 50 mm[a,b]	0.036, 0.054	
Extraction thimble, 9 × 40 mm[a]	0.256	1138
after soaking in water and decanting (3 times)	0.069	307
after leaching with 1:1 HCl and rinsing with water	<0.002	

[a]Schleicher and Schuell. [b]After Soxhlet extraction with water.

to be made in salt core samples which contain only a minor proportion of dispersed sediment.

EXPERIMENTAL

Reagents and apparatus

Starch/iodide solution. Dissolve 30 g of Vitex (modified starch; G.F.S. Chemical Co., Columbus, OH) in ca. 450 ml of cold water, add 15 g of potassium iodide and dilute to 500 ml. This solution has a long shelf-life if protected from light (with aluminium foil).

The absorbing solution was 1.5% (v/v) hydrochloric acid. Methanol was distilled in glass (Burdick & Jackson, Muskegon, MI).

Soxhlet extractor. A 1000-ml flask with a Quickfit cone 50/42 was used. The extraction basket was made from a 125-ml Nalgene teflon bottle by cutting off the upper section; all surfaces were perforated for maximal liquid flow-through. The basket accepted eight extraction sleeves for simultaneous extraction. The extraction thimble sleeves consisted of heat-shrinkable teflon tubing (10 mm diameter, 50 mm high). The base was tapered to hold the filter wadding by heat-shrinking the edge (ca. 1–2 mm) of the tube only. Individual sleeves were numbered for sample identification with a fine needle. The borosilicate glass-fibre thimbles were 603 g, 9 × 40 mm (Schleicher & Schuell).

LECO equipment. The materials used were from Laboratory Equipment Corporation (St. Joseph, MN): copper metal (501-263), copper rings (550-184), iron chip (501-077), vanadium pentoxide (Van-o-disc 761-933) and tin metal (501-076); F-Cl absorbers (769-608 and 769-610); combustion crucibles were of types porous filtering (528-030), solid (small; 528-018), solid (large; 528-038) with porous lids (528-042). Calibration standards contained 0.019% (501-503) and 0.027% (501-505) sulphur.

The dual-mode induction furnace model 523 and sulphur titrator model 518-000 (semi-automatic photoelectric titrator) were used. The titrator was modified by the addition of two Metrohm piston burettes containing potassium iodate titrants which were used interchangeably via teflon tubing (2 mm diameter) and a two-way stopcock connection (for one solution 1 ml $KIO_3 \approx 0.2$ mg S and for the other 1 ml $KIO_3 \approx 1.0$ mg S). This system allowed a very wide range of sulphur contents (2 mg kg^{-1}–55% S) to be handled.

Procedures

Soxhlet extraction. Prepare the borosilicate thimbles as follows. Immerse the thimbles in dilute (3 M) hydrochloric acid and soak for several hours. Decant and wash repeatedly with water until neutral. Dry the drained thimbles at 110° C overnight. Check the blank levels against the combustion blank (see below). Make smaller thimbles by cutting off a 10-mm closed (lower) section of the thimble and inserting it into a teflon sleeve. Tease out the remaining

upper portion of the extraction thimble to form a fibre pulp and store in ethanol if not needed immediately. Pack the fibre pulp into thimble base to yield a firm uniform packing.

Weigh 150—200 mg of finely powdered sediment sample directly into the extraction thimble sleeve; use polonium-210 static eliminator to prevent sample scatter. Place the loosely formed wadding over the sample. Transfer the eight teflon thimbles to the extraction basket and adjust the height in the Soxhlet extractor as necessary with suitable materials such as column packing rings. This will prevent solvent flooding over the top of the thimbles. Insert the extraction basket in the Soxhlet extractor containing ca. 800 ml of anhydrous methanol (with teflon boiling chips) in a 1-l flask and extract the sediment samples continuously for 4 h if salinity levels are expected to be <25% NaCl or up to 12 h for higher salt contents. To avoid splashing inside the thimbles causing uneven filling, divert condensed methanol droplets to the outside of the extraction basket by inserting teflon whiskers (fashioned from laboratory matting) in the condenser cone just above the extraction basket. Longer extraction times have no adverse effect provided that the sample particles are quantitatively retained on the fibre wadding. After an appropriate time, remove the extraction basket, drain the residual methanol from the thimbles and prepare combustion crucibles as follows. Place one disc of vanadium pentoxide catalytic accelerator into each crucible. Using a teflon rod, push out the filter wadding directly into the crucible. This operation is usually quantitative without any particles remaining in the teflon extraction sleeves after a single stroke; if not, use a small piece of fibre pulp (ethanolic) for particle collection. Press the wadding gently to occupy minimal space and dry the samples in a fume hood at 110° C overnight. Place another disc of vanadium pentoxide on top of the compressed thimble wadding and cover the crucible with a porous lid. Prepare at least two of each blank combustion charges as follows: place two discs of vanadium pentoxide in crucibles covered with porous lids for establishing combustion blanks, and one disc of vanadium pentoxide, glass fibre wadding and another disc in another set of crucibles with porous lids for determining chemical blanks.

Sample combustion. Fill the titration vessel to the mark (75 ml) with 1.5% (v/v) hydrochloric acid and add 5 ml of starch/iodide solution. Replace the glass wool trap in the delivery tube, set the microammeter reading of the photocell detector to a reference point by adding ca. 0.15 ml of potassium iodate titrant (1 ml $\approx$ 0.2 mg S), set the oxygen flow to 1.5 l min^{-1}, and commence a 6-min combustion cycle. Maintain the plate current at 400—450 mA while proceeding with the titration as usual. Coupling occurs almost immediately and vigorous evolution of SO_2 will occur within the first minute with only slight trailing observed after 3 min. Follow the procedure described by the manufacturer.

If the glass fibre thimbles have been purified adequately as recommended, the combustion and chemical blanks should be almost identical. Calibrate

the iodate titrant against an appropriate range of standards by burning blanks, samples and standards successively. Suitable standards include LECO 501-505 steel rings, CRCP Molybdenum Ore PR-1 and high-purity barium sulphate; the choice depends on the sulphur level expected. Calculate the sulphur concentration by the usual method. The value obtained for the USGS Marine Mud MAG-1 and some other reference samples are presented in Table 3.

CONCLUSIONS

The severe interference of free chlorine (derived from the induction furnace combustion of saline sediments) on the iodimetric titration of sulphur dioxide is caused by several reactions. It was found that the co-generation and temporal overlap of free chlorine and sulphur dioxide occur within the combustion zone at temperatures in excess of 1500°C. Contributions to the complexities of this interference mechanism arise from the occurrence of interaction within the induction zone, oxidation by chlorine in transit, and oxidation in the absorption/titration cell. Because of the severity of chlorine

TABLE 3

Determination of sulphur in saline sediments

Sample	Total S found (%)[a]	Other values	NaCl found (%)[b]	NaCl/S ratio	Remarks
USGS marine mud, MAG-1[c]	0.114 ± 0.029	0.43? [20, 21]	5.35 [18]	13.4	Direct measurement
	0.089 ± 16.5(4)	0.52 [22]	5.1 [19]		Barium acetate leach
	0.35 ± 13.4(3)	0.46 ± 0.06 [23]			LECO Cl-F absorbers
	0.32 ± 5.76(4)	0.39 [23]			Copper metal trap
	0.274 ± 7.13(4)				Diffusive leaching in methanol
	0.40 ± 1.29(14)				Soxhlet extraction (methanol)
NBS 1645 river sediment[d]	1.343 ± 4.56(6)	1.1	1.47 [18]	1.2	Direct measurement
	1.225 ± 2.99(8)				Soxhlet extraction (methanol)
NBS 1646 estuarine sediment[e]	0.939 ± 2.49(7)	0.96	2.58 [19]	2.8	Direct measurement
	0.927 ± 1.06(8)				Soxhlet extraction (methanol)

[a]Mean, with relative standard deviation; number in parentheses. [b]Soluble chloride was determined from the sediment suspension by potentiometry [18] or spectrophotometry [19]. [c]Fine grained gray-brown clayey mud from the Wilkinson Basin of the Gulf of Maine, from a depth of 282 m [22]. [d]This material was dredged from the bottom of the Indiana Harbor Canal. The major and trace element chemistry shows high levels of anthropogenic input (organic/industrial pollutants) compared to the average major river sediments. The lower sulphur value after methanol extraction may indicate the presence of organo-sulphur compounds in the 1.71 ± 0.26% oil and grease content reported. (NBS Certificate of Analysis, SRM 1645 River Sediment, Washington D.C. 20234, May, 1982). [e]This material was dredged from Chesapeake Bay. (NBS Certificate of Analysis, SRM 1646 Estuarine Sediment, Washington D.C. 20234, June, 1982).

interference, sulphur cannot be determined by this method at >12% salt content in marine sediments.

Various modifications relating to the sample combustion chemistry were ineffective and even metal traps for chlorine inserted at various distances from the induction zone were only partially successful in reducing the interference effects. Complete elimination of chlorine, so critical in iodimetric titration, could not be obtained by any treatment of the combustion gases.

The only effective treatment of marine sediments proved to be the removal of the halide. Selective extraction (Soxhlet extraction) with anhydrous methanol was found to be consistently effective over a very broad range. The desalination procedure was optimized for the removal of sodium chloride without solubility losses of the sulphur-bearing minerals in the sediment composition. With vanadium pentoxide incorporated in the catalytic combustion accelerator, the methanol-extracted saline materials yielded drift-free end-points. The results obtained for USGS MAG-1 Marine Mud reference material showed excellent precision and agreed well with the "best" published values of sulphur whereas direct (i.e., without sample pre-treatment) titrations produced values which were only one-third of accepted values with extremely poor reproducibility.

The author thanks Messrs. M. J. Head (Radiocarbon Dating Research Laboratory, R.S.Pac.S), B. Macdonald, J. M. Shelley for many stimulating discussions leading to the filter pad/extraction concept and Drs. J. R. Richards and T. Torgersen for critical comments on the manuscript.

REFERENCES

1 B. Nebesar, J. Chem. Educ., 48(12) (1971) A751.
2 C. B. Moore, C. F. Lewis, J. Cripe, F. M. Delles, W. R. Kelly and E. K. Gibson, Jr., Geochim. Cosmochim. Acta, Suppl. 3: Proc. Third Lunar Sci. Conf., 2 (1972) 2051.
3 T. S. Harrison and R. J. Spikings, Anal. Chim. Acta, 67 (1973) 145.
4 W. J. Beesley and B. R. Chamberlain, Talanta, 21 (1974) 318.
5 E. Pell, L. Machherndl and H. Malissa, Mikrochim. Acta, 4 (1963) 615.
6 I. R. Kaplan, K. O. Emery and S. C. Rittenberg, Geochim. Cosmochim. Acta, 27 (1963) 297.
7 M. A. Tabatabai and J. M. Bremner, Soil Sci. Soc. Am. Proc., 34 (1970) 417.
8 C. M. Johnson and H. Nishita, Anal. Chem., 24 (1952) 736.
9 P. L. Searle, Analyst (London), 93 (1968) 540.
10 M. A. Tabatabai and J. M. Bremner, Soil Sci. Soc. Am. Proc., 34 (1970) 62.
11 A. Steinbergs, O. Iismaa, J. R. Freney and N. J. Barrow, Anal. Chim. Acta, 27 (1962) 158.
12 C. Bloomfield, Analyst (London), 87 (1962) 586.
13 K. Norrish and J. T. Hutton, Div. Rep. Div. Soils, C.S.I.R.O., 1964, Aust. No. 3/64.
14 B. W. Chappell, Geology Department, Australian National University, personal communication, 1985.
15 D. S. Jenkinson, Analyst (London), 93 (1968) 535.
16 T. P. Whaley, in J. C. Bailar, Jr., H. J. Emeléus, R. Nyholm and A. F. Trotman-Dickenson (Eds.), Comprehensive Inorganic Chemistry, Vol. 1, Pergamon Press, Oxford, 1973, p. 406.

17 H. Stephen and T. Stephen, Solubilities of Inorganic and Organic Compounds, Vol. 1, Part 1, Macmillan, New York, 1983.
18 R. W. Freedman, Anal. Chim. Acta, 31 (1959) 214.
19 T. M. Florence and Y. J. Farrar, Anal. Chim. Acta, 54 (1971) 373.
20 S. Abbey, Geo. Surv. Can., paper 83-15 (1983).
21 S. Abbey, Geo. News., 6(1) (1982) 47.
22 F. T. Manheim, J. C. Hathaway, F. J. Flanagan and J. D. Fletcher, in F. J. Flanagan (Ed.), Geo. Surv. Prof. Paper, 840 (1976) 25.
23 E. S. Gladley and W. E. Goode, Geo. News., 5(1) (1981) 31.

Analytica Chimica Acta, 182 (1986) 47—59
Elsevier Science Publishers B.V., Amsterdam — Printed in The Netherlands

DETERMINATION OF METALS IN URINE BY DIRECT INJECTION OF SAMPLE, HIGH-PERFORMANCE LIQUID CHROMATOGRAPHY AND ELECTROCHEMICAL OR SPECTROPHOTOMETRIC DETECTION

A. M. BOND*, R. W. KNIGHT, J. B. REUST[a], D. J. TUCKER and G. G. WALLACE[b]

Division of Chemical and Physical Sciences, Deakin University, Waurn Ponds 3217, Victoria (Australia)

(Received 15th August 1985)

SUMMARY

A method for the rapid and simultaneous determination of copper, nickel and lead in urine is described. Direct injections of freshly acidified and filtered (0.45-μm) urine samples were made onto a reverse-phase separator column with a guard column for sample clean-up. By complexing the metals with a dithiocarbamate ligand included in the mobile phase, the metal complexes could be detected electrochemically (copper and nickel) or spectrophotometrically (copper, nickel and lead). The procedure is shown to provide a convenient method for the determination of copper and nickel at normal to occupationally exposed levels of urinary output (electrochemical detection) after direct injection of samples. Spectrophotometric detection methods were insufficiently sensitive for direct determinations of copper and nickel at some of the lower levels found in urine. The spectrophotometric detection of lead is subject to interference by u.v.-absorbing constituents present in urine and is restricted to detection of lead in persons over-exposed to lead, unless additional clean-up procedures are applied.

Urine, readily available and conveniently obtained, plays an important role in the clinical examination of the health status of humans [1]. Metals are found in all living organisms, and are excreted in urine, where they are available for detection. Some metals are essential to the health of humans whilst others may be toxic [2—5]. Urine provides information on the level and rate of toxic metal excretion [6, 7].

Many analytical techniques have been applied to trace metal determinations in urine. These include atomic absorption spectrometry (a.a.s.) [8—11], anodic stripping voltammetry (a.s.v.) [9, 12—15], mass spectrometry [16], x-ray spectrometry [17] and neutron activation analysis [18]. Spectrophotometric methods, predominantly based on dithizone complexation, have also been widely used. However, prior ashing of samples is required with most of these methods, which introduces a range of well known drawbacks [19]. The use of a.a.s. also generally requires sample pretreatment in the form of

---

Present addresses: [a]Analytical R & D, Sandoz Ltd., CH-4002 Basle, Switzerland. [b]University of Woolongong, New South Wales, Australia.

0003-2670/86/$03.50

digestion and/or liquid-liquid extraction to achieve adequate sensitivity and precision [20] although direct determination of some metals in urine by a.a.s. has been reported [19, 20]. Matrix effects in the more sensitive electrothermal a.a.s. methods tend to produce large non-atomic signals when untreated urine is used directly [21, 22] thereby limiting the usefulness of these methods. Much of the recent work for determination of metals in urine by electrochemical techniques has involved differential-pulse a.s.v. Whilst this is a very sensitive method, unexpected interferences from surface-active substances frequently present in urine mean that digestion or another form of separation is to be recommended for routine analysis [23, 24].

The above survey indicates that there is still a need for alternative, inexpensive and simple methods of determining metals in urine. Recently, Bond and Wallace [25, 26] have combined chromatographic methods with electrochemical and spectrophotometric detection as part of the development of microprocessor-based automated methods of simultaneously determining a range of metals, which may offer the prospect of a simple procedure. In this method, direct injection of a sample into a chromatographic system containing the dithiocarbamate ligand (DTC^-) in the running solvent is the first stage of the metal determination. The metal dithiocarbamate is formed after the sample injection and in a reaction coil. The metals are then separated as their dithiocarbamate complexes on a reverse-phase chromatographic column and finally determined by electrochemical and/or spectrophotometric monitoring.

Figure 1 schematically outlines the instrumental arrangement showing the various stages of the operation including sample pretreatment, formation of the complex, separation and detection. This paper describes the application of this system to the determination of copper, nickel and lead in urine.

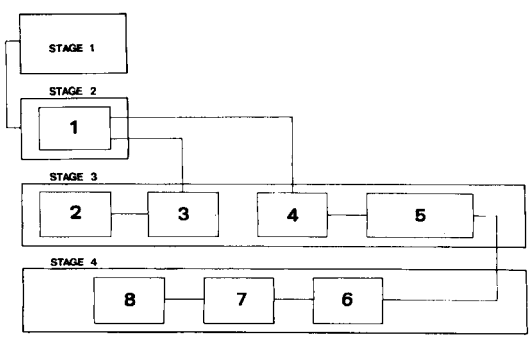

Fig. 1. Flow diagram of system for automated metal determination in urine. Stage 1, sample pretreatment; stage 2, complex formation; stage 3, separation; stage 4, detection. Components: (1) injection; (2) chromatographic solvent; (3) solvent delivery system; (4) guard column; (5) separation column; (6) u.v. detector; (7) electrochemical detector; (8) readout.

EXPERIMENTAL

Urine sample collection and qualitative tests

All urine was collected as random specimens by the clean-catch/midstream technique described by Schumann [27] and stored in urine containers supplied by Labco (Cheltenham, Victoria, Australia). Laboratory ware used for the collection, transfer and storage of urine was soaked for at least 24 h in 2 M nitric acid solution and rinsed thoroughly before use.

All urine samples were examined for their medical status as described elsewhere [24]. In vitro qualitative tests on urine for pH, protein, glucose, ketones, bilirubin, blood and urobilinogen were conducted on all urine samples using Multistix (Miles Laboratories, Elkhard, Indiana). The results obtained were in the normal range for all samples examined.

Instrumentation

Unless otherwise stated, all results were obtained using the experimental arrangement outlined in Fig. 1 and described in more detail elsewhere [25, 26].

Samples were injected by using a Rheodyne model 7126 sample injector in the manual mode with a 20-μl sample loop. All remaining liquid chromatographic equipment used was obtained from Waters Associates. The separation was done on a μBondapak C_{18} column (25 cm × 4.6 mm) using a model M6000A solvent delivery pump. The column was preceded by a guard column (25 mm × 4.0 mm) packed with Bondapak C_{18}/Corasil. A TL-4 amperometric flow-through thin-layer cell with glassy carbon working and auxiliary electrodes and an RE-1, Ag/AgCl (3 M NaCl) reference electrode from Bioanalytical Systems (West Lafayette, IN) were used for electrochemical detection. A variable-wavelength detector (model 450; Waters Associates) was used for spectrophotometric detection. Microprocessor-based systems for controlling the experimental arrangement have been described elsewhere [25, 28].

Reagents, standards and chromatographic solvents

All chemicals used were of analytical-grade purity unless otherwise stated. Organic solvents were of liquid-chromatography grade (Waters Associates). Acetate buffer was prepared as outlined by Vogel [29]. Ammonium pyrrolidinedithiocarbamate (Ajax Chemicals, Sydney, Australia) was recrystallized from ethanol prior to use. The urine standard, Ortho Control Urine II, was obtained from Ortho Diagnostic Systems (Raritan, New Jersey). All acids were AristaR grade (B.D.H., Poole, England) and metal standards of copper, nickel, cadmium, and lead were 1.000 g l^{-1} solutions (Fluka, Buchs, Switzerland).

Mixtures of acetonitrile and aqueous 0.02 M acetate buffer (pH 5.6), with 10^{-3} M sodium nitrate as supporting electrolyte, were used as the chromatographic solvents. Pyrrolidinedithiocarbamate (PDC^-) (10^{-4} M) was included in

these mixtures to effect metal complexation in the in situ mode [25, 26]. All chromatographic solvents were filtered through a Millipore membrane filter (0.45 μm) prior to use. Temperatures of (20.0 ± 0.5)° C were used in all determinations.

Procedures

Sample preparation methods. Samples were filtered through a 0.45-μm H.A. Millex single-use filter unit (Millipore) before injection.

Standard metal addition. To a known volume of urine, metal standard was added to provide a calculated concentration increase. After addition, the urine was gently mixed and allowed to stand for ten minutes before use.

Urine acidification. To a known volume of urine, concentrated hydrochloric acid was added until a pH of 2—3 was achieved.

Urine digestion. In method A, a conical flask containing 25.0 ml of urine and 5.0 ml of concentrated nitric acid was boiled to dryness. To the ash remaining, 3.0 ml of nitric acid was added and the sample was boiled again to dryness until a white ash remained. The white ash was then dissolved by addition of four drops of concentrated nitric acid and 1.0 ml of distilled water. This was quantitatively transferred to a 25.0-ml volumetric flask and made up to volume with acetate buffer (pH 5.6). The final solution was at pH 2—3.

Method B was the same as method A except that four drops of concentrated hydrochloric acid replaced concentrated nitric acid for dissolution of the remaining white ash.

Urine storage by freezing. Urine specimens were stored at −80° C. The samples were thawed over a period of 10—12 h at 2—6° C. Resulting sediment was dissolved by addition of hydrochloric acid followed by intermittent swirling for 30 min at room temperature.

Statistical analysis. Triplicate injections of each sample were made and the resultant peak heights were determined manually as specified by Johnson and Stevenson [30]. Unknown sample levels of metal were determined by standard addition and linear regression.

RESULTS AND DISCUSSION

Sample pretreatment

Sampling errors can arise in at least three areas: the taking of a truly representative sample, storage, and sample pretreatment. In physiological fluids such as urine, sampling is ideally done over a 24-h period to obtain a representative sample. In practice, this collection is quite cumbersome and the possible deterioration of certain constituents makes such specimens unattractive. The basic type of urine specimen used most frequently is a simple spot or random specimen [31]. Pretreatment of a urine sample will govern the use and decide the length and type of storage which can be applied to that sample. Analysis of untreated samples by different methods has been

investigated [19, 31—33] as well as pretreatments involving acidification, digestion, freeze-drying [23], freezing and dilution [34]. One aim in the development of a rapid method of determination is to minimize pretreatment. In the following sections, different forms of sample pretreatment are discussed. The choice of copper for initial investigations of metal determination in urine was based on the high stability of the copper pyrrolidinedithiocarbamate complex in chromatographic solvents and the very low levels of copper which can be detected [25, 26]. The detection limits [25, 26] are below the reported urinary copper levels of 17—60 $\mu g\ l^{-1}$ [6].

Comparison of untreated and acidified urine samples

Direct injections or injections of diluted solutions of urine into high-performance liquid chromatography (h.p.l.c.) systems with a guard column for sample clean-up, has been used by several workers [31—34]. The results obtained for copper response in fresh urine and fresh acidified urine using electrochemical (e.c.) and spectrophotometric (u.v.-visible) detection in a particular urine sample (No. 1) are shown in Table 1 and Fig. 2. For all samples examined, a positive response was observed for copper with a detection limit of about 20 $\mu g\ l^{-1}$. However, when constant-potential amperometry served as the detection method, the data were near the detection limit for some samples. A pulsed waveform in which the potential is periodically stepped from 0 to 0.6 V vs. Ag/AgCl could provide superior sensitivity for all samples examined as could external complex formation. These methods can be used for copper levels down to 2 $\mu g\ l^{-1}$. Spectrophotometric detection could not be used at these low levels. Graphs were constructed to establish

TABLE 1

Determination of copper in urine samples after different treatments, by the standard addition method[a]

Sample	Urine treatment[b]	Detection[c]	Copper concn. ($\mu g\ l^{-1}$)	Linear range[d] ($\mu g\ l^{-1}$)
1	None	E.c.	29.1 ± 1.5	10—320
1	None	Spect.	30.3 ± 2.2	10—635
1	Acidified	E.c.	43.1 ± 3.6	10—320
1	Acidified	Spect.	36.4 ± 3.2	10—635
1	Frozen (7d)	E.c.	41.2 ± 2.1	10—620
2	Acidified	E.c.	58.7 ± 3.8	10—600
2	Digested	E.c.	64.4 ± 3.6	10—600

[a]Chromatographic eluent: 70% CH_3CN, 30% aqueous buffer, 10^{-4} M PDC^-, 10^{-3} M $NaNO_3$. Flow rate 2 ml min^{-1}. Injection volume 20 μl. [b]Except where specified, fresh urine was used. Samples were acidified before digestion or freezing for 7 days. [c]E.c., electrochemical detection using glassy carbon electrode, with d.c. amperometry at 0.6 V vs. Ag/AgCl. Spect., spectrophotometric detection at 420 nm. [d]Linear regression fitted over this concentration range of standard additions with correlation coefficient 0.997 ± 0.002.

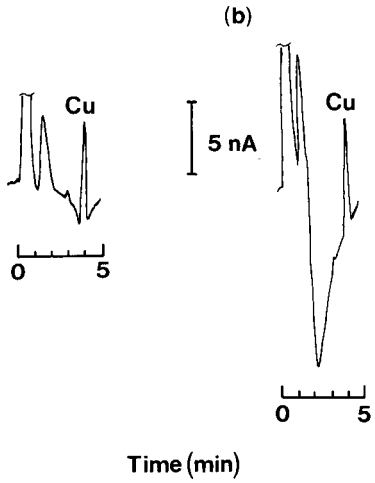

Fig. 2. Copper response for electrochemical detection: (a) fresh urine; (b) fresh acidified urine. Glassy carbon electrode used at an applied d.c. potential of +0.6 V vs. Ag/AgCl. Chromatographic solvent: 70% CH_3CN, 30% aqueous acetate buffer (pH 5.6), 10^{-4} M PDC^-, 10^{-3} M $NaNO_3$. Flow rate 2.0 ml min^{-1}.

the linear range of copper response on which linear regression could be based for determinations of copper levels in the original urine sample. Linearity was observed over a wide concentration range (Table 1). Levels of copper in sample 1 were found to be higher in fresh acidified urine (43.1 and 36.4 $\mu g\ l^{-1}$) than in fresh urine (29.1 and 30.3 $\mu g\ l^{-1}$) by electrochemical and u.v.-visible detection, respectively (Table 1). The variable background and response from sample to sample leads to the recommendation that the method of standard additions should be used for metal determinations.

Given the increased response for copper and other advantages produced y acidification, it would appear that sample pretreatment by acidification ould be preferable as a general procedure.

omparison of acidified and digested urine samples

The ability of the dithiocarbamate ligand to extract all the metal in ques-on from the urine sample to yield an accurate measurement, was of major nportance in considering this technique for quantitative analysis. Acidifica-on gave an increased value for the original unknown sample copper level. It as been reported that acidification can cause an undefined form of precipi-ıtion which produces lowered results in some methods of analysis [23]. igestion of urine destroys all the organic matrix, releasing any metal which ıay be irreversibly bound or in a form which inhibits its complexation. The ficiency of the PDC^- ligand in extracting copper from acidified urine was ıvestigated by comparison of copper response in fresh acidified urine with ıe response for digested fresh acidified urine. Many digestions require aborate equipment and considerable experience to perform [35]. In this ıvestigation, a simple wet digestion (method A, Experimental section)

which had been used successfully for urine pretreatment was investigated. This digestion was found to release an interferent which was detected by the amperometric method and had a retention volume similar to that of the copper complex. A simple modification to the digestion procedure was made (method B) and the desired response was achieved.

The results obtained for copper in these samples by electrochemical detection are also contained in Table 1. Levels of copper were found to be 64.4 $\mu g\ l^{-1}$ and 58.7 $\mu g\ l^{-1}$ in digested and undigested acidified urine, respectively. With the random and systematic errors involved, these results are regarded as being equivalent.

The efficiency of PDC^- in recovering metals added to fresh urine samples was investigated by Willis [19] for lead, nickel and some other metals. High recoveries for all metals examined after extraction into organic solvents were shown by flame a.a.s. Combining this information with the results obtained by comparison of digested with undigested urine for copper addition, the in situ method with PDC^- may be assumed to provide acceptable accuracy for the metals to be investigated (copper, nickel and lead).

Comparison of fresh acidified and frozen acidified urine samples

Often the immediate analysis of voided urine specimens is impossible because of variables outside the control of the operator. Simple acidification and refrigeration (0—6° C) only allows a maximum storage period of up to 48 h [27]. The suitability of freezing as a method of sample storage on acidified urine was investigated by comparison of copper response in fresh acidified urine with the response in the same samples after seven days of storage at —80° C. Identical samples of fresh acidified urine, as determined previously, were frozen and the results for copper by both methods of detection were compared, following the defined storage period. The level of copper after the storage period was determined electrochemically to be 41.2 $\mu g\ l^{-1}$, which is within experimental error of the value of 43.1 $\mu g\ l^{-1}$ obtained before storage (Table 1). When spectrophotometric detection was used, there was some interference in the copper response by absorbing constituents in the urine. The interference must have resulted from slight decomposition of the urine samples which was indicated by a darker colour, slight turbidity and increased odour after freezing. However, electrochemical detection does not suffer interference in this approach and the simultaneous use of both methods is advantageous because matrix effects do not operate equally with the different detection methods.

Multi-elemental analysis

The results obtained in the previous section demonstrate that the proposed method can be used to determine normal copper levels in urine if the samples are acidified. The application of this rapid method to nickel and lead was therefore investigated, with emphasis on the possibility of simultaneous detection.

Urinary nickel determination. The detection limits for copper and nickel have been reported by Bond and Wallace [25, 26]. Electrochemical detection is suitable for all but the lowest of normal urinary levels of nickel which have been reported to be in the range 2.3—85.0 $\mu g\ l^{-1}$ [6]. However, the spectrophotometric detection limit [25, 26] exceeds normal urinary nickel levels. Nickel exhibits similar electrochemical detection limits to copper and initial nickel determinations were done simultaneously with copper by applying a potential of +0.8 V vs. Ag/AgCl.

An example of the simultaneous electrochemical detection of copper and nickel in fresh acidified urine is shown in Fig. 3. This figure illustrates that adequate resolution of copper and nickel could be achieved and represents a sample at the limit of detection for both elements when d.c. amperometry is used for detection. Graphs were constructed to determine the linear ranges of copper and nickel response over which linear regression could be used for determination of copper and nickel levels in a particular urine sample (55.3 $\mu g\ l^{-1}$ and 56.0 $\mu g\ l^{-1}$, respectively). Linearity was observed for both elements over the range 10—600 $\mu g\ l^{-1}$ with a correlation coefficient of 0.997 ± 0.02. Figure 3 also shows that d.c. amperometric detection limits will barely be adequate for nickel in many samples and as was the case with the copper method, external complex formation or the pulse waveform should be attempted (0 to 0.8 V vs. Ag/AgCl) if the detection limit is inadequate.

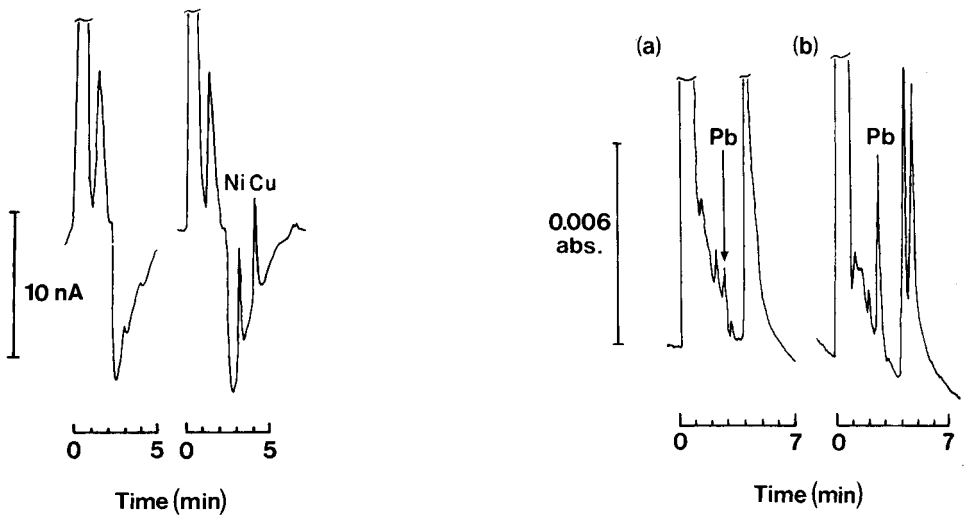

Fig. 3. Simultaneous determination of copper and nickel at the limit of detection (left-hand chromatogram) with d.c. amperometry in fresh acidified urine using electrochemical detection with a glassy carbon electrode at an applied potential of +0.8 V vs. Ag/AgCl. Other conditions as for Fig. 2. The right-hand chromatogram shows the result of standard additions of 600 and 600 $\mu g\ l^{-1}$ copper and nickel, respectively.

Fig. 4. Spectrophotometric detection (260 nm) of lead in fresh acidified urine by standard addition method: (a) sample; (b) standard addition of 500 $\mu g\ l^{-1}$. Chromatographic conditions as in Fig. 2.

Simultaneous determination of nickel and copper in fresh acidified urine is possible as a screening procedure on occupationally exposed individuals using the system described with direct injection and minimal sample clean-up.

Urinary lead determination. Bond and Wallace [26] found that the electrochemical and spectrophotometric detection limits for lead are 1 mg l^{-1} and 100 $\mu g\ l^{-1}$, respectively. These values were optimized for multi-element determinations and not for lead. The Health Commission of Victoria, Australia has published biological indices for urinary lead levels. The acceptable level for an unexposed person is less than 80 $\mu g\ l^{-1}$ and for an "occupationally exposed" person, 80—150 $\mu g\ l^{-1}$. Levels greater than 150 $\mu g\ l^{-1}$ are considered to be excessive. From the detection limits achieved by Bond and Wallace, only spectrophotometric detection would be sufficiently sensitive (at optimal wavelength) to detect lead levels of occupationally exposed persons. A standard addition of 500 $\mu g\ l^{-1}$ lead to fresh acidified urine with an unknown sample lead level was initially used to observe the lead response. The results obtained from u.v. detection are shown in Fig. 4. The lead response is observed against a variable u.v. absorbing background; absorbing constituents in urine have been reported by several workers [36—38]. The spectrophotometric detection of any metal in freshly acidified urine in the u.v. region is thus potentially subject to interference. Interferences in lead detection by u.v.-absorbing constituents is illustrated by Fig. 5, which shows lead detection in urine from three different donors after addition of 150 $\mu g\ l^{-1}$. The lead response in urine from donor 1 can be measured between two absorbing peaks. The lead response in urine from donor 2 can just be mea-

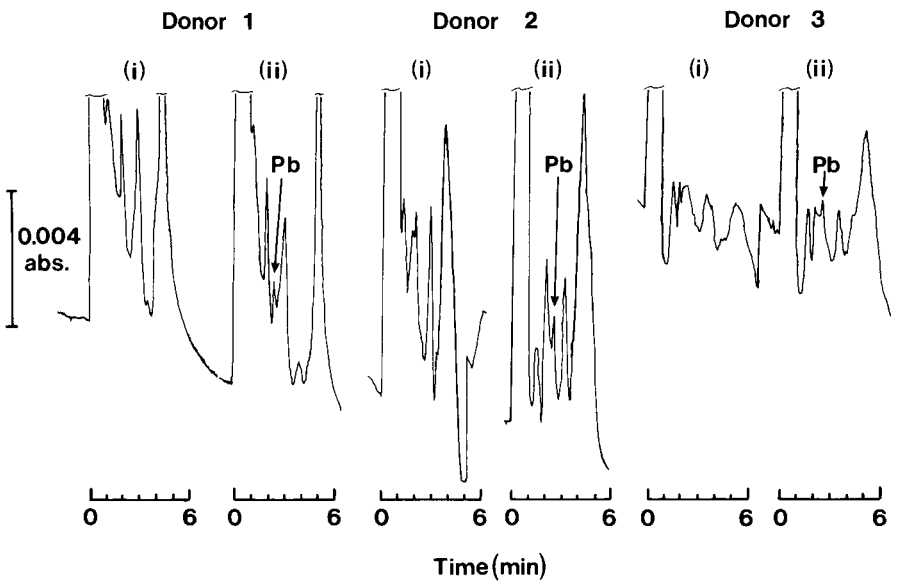

Fig. 5. Spectrophotometric detection (260 nm) of lead by the method of standard additions in three fresh acidified urine samples: (i) sample; (ii) sample with 150 $\mu g\ l^{-1}$ lead added. Chromatographic conditions as for Fig. 2.

sured on the side of an interfering peak. Interference from u.v.-absorbing background in urine from donor 3 makes the measurement of lead response impossible at the low levels required. The direct determination of lead in urine is therefore restricted to the excessive range.

The spectrophotometric detection of lead in freshly acidified urine under the same chromatographic conditions which proved successful for electrochemical detection of copper and nickel was investigated. The results obtained confirmed that successful lead detection is dependent on the nature of the urine specimen. The removal of the potential interfering constituents is required before a method of reliable lead detection can be reported at normal urinary levels. This may be achieved by using increased sample pretreatment, e.g., external complex formation and Sep-Pak preparation [39] or by a simple liquid-liquid extraction procedure [40].

Simultaneous determination of copper, nickel and lead. The simultaneous determination of copper, nickel and lead was possible in fresh acidified urine by means of electrochemical detection (0.8 V vs. Ag/AgCl) for copper and nickel and spectrophotometric detection (260 nm) for lead at levels where health problems may arise. Figure 6 shows an example of this on an occupationally exposed individual.

Comparison of copper, nickel and lead determinations in a standard urine sample with atomic absorption spectrometry. Copper, nickel and lead were determined simultaneously by the above procedure in a standard urine sample (Ortho Control Urine II). The copper and lead responses are shown in Fig. 7. The certificated values of copper and lead had been evaluated for the standard urine sample by interlaboratory a.a.s. experiments. The results obtained using electrochemical detection (Cu) and spectrophotometric detec-

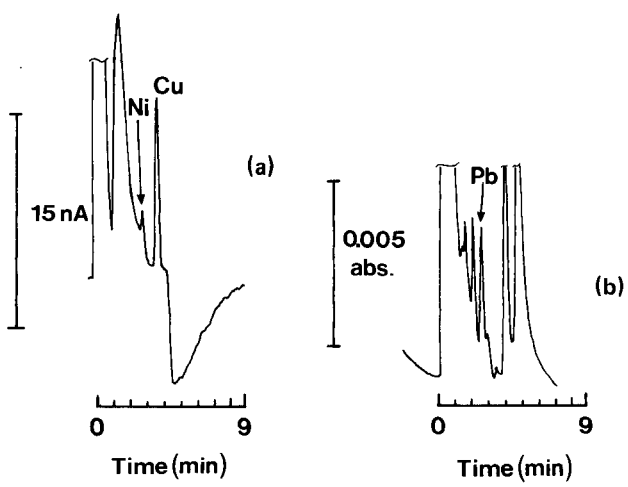

Fig. 6. Simultaneous determination of copper and nickel (electrochemical detection at glassy carbon electrode at 0.8 V vs. Ag/AgCl) and lead (spectrophotometric detection at 260 nm) in a freshly acidified sample. Chromatographic conditions as in Fig. 2.

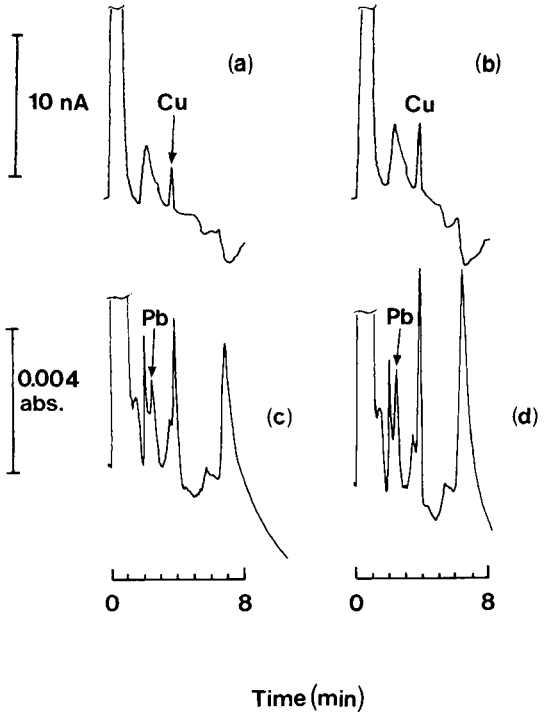

Fig. 7. Simultaneous determination of copper (electrochemical detection) and lead (spectrophotometric detection) in fresh acidified urine standard: (a) and (b) respectively refer to copper in urine, then standard addition of 100 $\mu g\ l^{-1}$; (c) and (d) are analogous experiments for lead. Conditions for (a) and (b) as for Fig. 2, (c) and (d) as for Fig. 4.

TABLE 2

The simultaneous determination of copper and lead in acidified urine standard[a] by electrochemical and spectrophotometric detection

Metal	Concentration ($\mu g\ l^{-1}$)		
	Certificated[a]	Calculated[b]	Detection
Copper	194 ± 55	204 ± 10	Electrochemical
Lead	100 ± 30	130 ± 10	Spectrophotometric

[a]Ortho control urine II (Lot. No. 095A01). [b]Values calculated by triplicate measurements of single standard addition (100 $\mu g\ l^{-1}$ copper and 100 $\mu g\ l^{-1}$ lead) in acidified standard urine.

tion (Pb) on the acidified standard urine samples are shown in Table 2 along with the certificated values. Agreement of data is satisfactory. Nickel data were not available for this standard. It should be noted that in this standard urine sample, the lead level is relatively high and is amenable to direct

spectrophotometric determination, unlike the case for normal lead urine levels where interference from background is expected unless clean-up procedures are applied.

This work was undertaken with financial support from the Ordnance Factory, Maribyrnong, Victoria, and the Australian Research Grants Scheme. The authors gratefully acknowledge this contribution. Ortho Control Urine II (Lot No. 095A01) was generously provided by H. W. Nürnberg, Jülich, West Germany. Discussions with and experimental assistance from V. Reust during this work were also highly valued.

REFERENCES

1 A. H. Free and H. M. Free, Urinalysis in Clinical Laboratory Practice, CRC Press, Ohio, 1976.
2 L. Friberg, G. F. Nordberg and V. B. Vouk (Eds.), Handbook on the Toxicity of Metals, Elsevier/North-Holland Biomedical Press, Amsterdam, 1979.
3 E. Berman, Toxic Metals and Their Analysis, Heyden, London, 1980.
4 A. McRae, L. Whelchel and H. Rowland (Eds.), Toxic Substance Control Source Book, Aspen, Maryland, 1978.
5 S. S. Brown (Ed.), Clinical Chemistry and Chemical Toxicology of Metals, Elsevier/North-Holland, New York, 1977.
6 G. V. Lyengar, W. E. Kollmer and J. M. Bowman, The Elemental Composition of Human Tissues and Body Fluids, Verlag Chemie, Weinheim, 1978.
7 C. Lenter (Ed.), Geigy Scientific Tables, CIBA-GEIGY, Basle, 1981.
8 F. Hofmann and M. Buechner, Z. Med. Laboratoriumsdiago., 18 (1977) 51.
9 A. A. Cernik, Proc. Anal. Div. Chem. Soc., 13 (1976) 227.
10 T. J. Kneip, Health Lab. Sci., 12 (1975) 379.
11 S. L. Gaffin and H. Hornung, Clin. Toxicol., 10 (1977) 543.
12 J. P. Franke and R. A. DeZeeum, J. Anal. Toxicol., 1 (1977) 291.
13 W. Lund and R. Erikson, Anal. Chim. Acta, 107 (1979) 37.
14 J. T. Kinard, Anal. Lett., 10 (1977) 1147.
15 T. R. Copeland, J. H. Christie, R. Osteryoung and R. K. Skogerboe, Anal. Chem., 45 (1973) 2171.
16 H, R. Schulten, B. Bohl, U. Bahr, R. Mueller and R. Palavinska, Int. J. Mass Spectrom. Ion Phys., 38 (1981) 281.
17 H. Kingston and P. H. Pella, Anal. Chem., 53 (1981) 223.
18 M. Molnar, T. Barna, A. Kovacs and T. Toth, Munkavedelem, 23 (1977) 34.
19 J. B. Willis, Anal. Chem., 34 (1962) 612.
20 NIOSH Manual of Analytical Methods, P8 CAM 208 and P8 CAM 262, (1981).
21 T. L. Ng, SNIC Bull., 4 (1976) 47.
22 B. Neidhart and C. Lippmann, Trace Element Anal. Chem. Med. Biol. Proc. Int. Workshop, 1980, p. 503.
23 J. Golimowski, P. Valenta, M. Stoeppler and H. W. Nuernberg, Talanta, 26 (1979) 649.
24 A. M. Bond and J. B. Reust, Anal. Chim. Acta, 162 (1984) 389.
25 A. M. Bond and G. G. Wallace, Anal. Chem., 55 (1983) 718.
26 A. M. Bond and G. G. Wallace, Anal. Chem., 56 (1984) 2085.
27 G. B. Schumann, Urine Sediment Examination, Waverly Press, Baltimore, 1980.
28 A. M. Bond, H. B. Greenhill, I. D. Heritage and J. B. Reust, Anal. Chim. Acta, 165 (1984) 209.
29 A. Vogel, A Textbook of Quantitative Inorganic Analysis, Longmans, London, 1968.

30 E. Johnson and R. Stevenson, Basic Liquid Chromatography, Varian Associates, California, 1978.
31 M. Goito, T. Nakamura and D. Ishii, J. Chromatogr., 226 (1981) 33.
32 K. Beschke, R. Jauch, W. Roth, A. Zimmer and F. W. Koss, GIT Labour-Med., 5 (1982) 357.
33 A. Von Hodenberg, W. Klemisch and K. O. Vollmer, Arzneimittel-Forschung, 27 (1977) 508.
34 L. A. Pachla and P. T. Kissinger, Anal. Chem., 48 (1976) 364.
35 T. T. Gorsuch, The Destruction of Organic Matter, Pergamon Press, Oxford, 1970.
36 S. Matsushita, Y. Tada and T. Ikushige, Toyota Soda. Kenkyu Hokoku, 24 (1980) 57.
37 H. Miygai, J. Miura and Y. Takata, Ganno. Shigetake, 25 (1979) 1617.
38 K. Seta, M. Washitake, T. Anmo, N. Takai and T. Okuyama, Bunseki Kagaku, 27 (1978) 73; J. Chromatogr., 181 (1980) 311.
39 A. M. Bond and G. G. Wallace, Anal. Chim. Acta, 164 (1984) 223.
40 A. M. Bond and D. E. Davey, unpublished work, Deakin University, 1985.

Analytica Chimica Acta, 182 (1986) 61—70
Elsevier Science Publishers B.V., Amsterdam — Printed in The Netherlands

POLYURETHANE FOAMS AS SELECTIVE SORBENTS FOR NOBLE METALS
Quantitative Extraction and Separation of Rhodium from Iridium in Hydrochloric Acid containing Tin(II) Chloride

LYNN JONES, IRIS NEL and KLAUS R. KOCH*

Department of Analytical Science, University of Cape Town, Rondebosch, Cape Town 7700 (South Africa)

(Received 30th September 1985)

SUMMARY

The distribution of rhodium(III) between polyether-type polyurethane foam and 0.5—5.0 mol dm^{-3} hydrochloric acid in the presence of small amounts of tin(II) chloride is described. The distribution of rhodium is affected by the extraction temperature, acid concentration and the Sn(II):Rh ratio. The capacity of the polyurethane foam for rhodium is in excess of 0.5 mmol g^{-1}. Rhodium is presumably sorbed in the form of a chloro(trichlorostannato)rhodium(III/I) complex anion. Iridium is not extracted by the foam under corresponding conditions and can be separated quantitatively from rhodium.

Polyurethane foams have become firmly established as convenient sorbents of a wide variety of inorganic and organic substances from solution [1—5]. There has been considerable recent interest in the extraction and separation of the platinum group metals by polyurethane foams [6—11]; Pd [7], Pt [8], Ru [9], Rh and Ir [10] and Os and Ru [11] can all be extracted by polyether-type polyurethane foams from aqueous solution containing excess of thiocyanate. The use of thiocyanate as the ligand to convert the precious metal into an extractable complex anion has some limitations. First, the method is not selective toward the platinum group metals because various transition metals are also extracted efficiently from thiocyanate medium [5]. Secondly, a thiocyanate-based extraction from highly acidic solutions is compromised to some extent by the formation of interfering thiocyanic acid and 5-amino-1,2,4-dithiazole-3-thione [8]. The extraction of platinum(II) from dilute hydrochloric acid solutions containing small amounts of tin(II) chloride by polyether-type polyurethane foams has been reported briefly [12, 13]. In this paper, the results of an examination of the extractability of rhodium chloride from 0.5—5.0 mol dm^{-3} hydrochloric acid containing tin(II) chloride by polyether-type polyurethane foams are described. The separation of rhodium from iridium appears to be feasible.

0003-2670/86/$03.50

EXPERIMENTAL

Materials and equipment

Commercially available, flexible, open-cell polyether-type polyurethane foam, reportedly prepared from Voranol CP3322 (Voranol is a trademark of the Dow Chemical Company; 100% polypropylene oxide glycol mixture; mean molecular mass 3400) and toluene diisocyanate (4:1 mixture of 2,4-TDI and 2,6-TDI), was carefully washed as recommended by Braun and Farag [1]. The foam was dried at 50°C prior to use. (Typical microanalytical data gave 61.3% C; 8.9% H and 4.9% N.)

Stock solutions of analytical-reagent grade rhodium(III) chloride trihydrate, potassium hexachloroiridate (Johnson Matthey) and tin(II) chloride dihydrate were freshly prepared, using nitrogen-purged solutions of hydrochloric acid (analytical-reagent grade) prepared with glass-distilled water. All solutions were used within 3—5 days of preparation and were stored under nitrogen as far as possible. Tin(II) chloride solutions were standardized by titration with standard potassium iodate solution.

Flame atomic absorption spectrometry (a.a.s.) was used to quantify rhodium and iridium (fuel-lean air/acetylene flame) and tin (fuel-rich air/acetylene flame). Interference effects in the a.a.s. were avoided by suitable matrix-matching. Lanthanum nitrate solution (0.2% w/v) was found to be a satisfactory releasing agent for rhodium and iridium. A Varian AA-6 spectrometer was used.

Extraction procedures

Batch metal-loading experiments were done under nitrogen at a chosen temperature controlled to ±0.1°C. Solutions containing the desired amounts of Rh/Ir, tin and hydrochloric acid were allowed to equilibrate for a definite time prior to addition of a weighed (80 ± 1 mg, unless otherwise stated) amount of clean foam which had been cut into small cubes (ca. 5 mm^3).

For dynamic loading experiments, a temperature-controlled glass cell was equipped with a peristaltic pump using wide bore (8 mm i.d.) tubing, to allow for the continuous recycling of solution and small blocks of foam. In this way rapid solution/foam contact was ensured. Aliquots (1.0 cm^3) were withdrawn from time to time for analysis. Typically, an initial solution volume of 100.0 cm^3 containing 50—75 $\mu g\ cm^{-3}$ rhodium was used from which not more than 12 × 1 cm^3 aliquots were withdrawn. Appropriate corrections were made for the metal content of the sample volume(s) that was (were) withdrawn when distribution coefficients were calculated.

In some extraction experiments, glass flasks sealed with rubber septa were shaken mechanically in a temperature-controlled water-bath. For these experiments, single blocks of polyurethane foam were wetted with ethanol and briefly dried between two sheets of filter paper, just prior to addition to the aqueous solution. This ensured rapid, uniform, contact between the foam and the aqueous phase. Aliquots of solution were examined only prior to

foam addition and after the desired contact time. The rhodium recovery and rhodium/iridium separations were studied in this manner.

The amount of precious metal (and tin) found on the foam was determined by dissolving the loaded foam in 10 cm^3 of concentrated nitric acid, boiling for 20 min to concentrate the volume to ca. 4 cm^3, adding 8 cm^3 of concentrated hydrochloric acid and further boiling for 15 min to dissolve any precipitate; the acid digest was then diluted to the required volume with distilled water after addition of lanthanum nitrate solution. This procedure ensured complete digestion of the loaded foam for subsequent a.a.s. Satisfactory material balance was achieved in this way.

The extent of metal sorption is described by the distribution coefficient, $D_m(M)$ = mass of M sorbed/dry mass of foam (M = Rh or Ir). For convenience, $D_m(M)$ can be converted to $D'_m(M)$, corresponding to the amount of metal M per unit mass of foam in mol kg^{-1} or mmol g^{-1}. The value of $D'_m(M)$ at a fixed temperature provides a convenient measure of the efficiency of sorption. The limiting value of $D'_m(M)$ is usually referred to as the (maximum) capacity, $C(M)$, of the foam. For the purposes of these experiments, mole ratios R_a and R_f are used; $R_a(M)$ corresponds to mole Sn(II)/mole M in the aqueous phase prior to foam addition, and $R_f(M)$ to mole Sn(total)/mole M found in the foam phase.

RESULTS AND DISCUSSION

Extraction of rhodium

Polyurethane foam does not extract a detectable quantity of rhodium when rhodium(III) chloride dissolved in 2 mol dm^{-3} hydrochloric acid is left in contact with the foam for several hours. Although the detailed nature of a rhodium(III) chloride solution in hydrochloric acid is highly complex, it is generally thought that at 2 mol dm^{-3} hydrochloric acid after suitable ageing, rhodium is fairly equally distributed between $RhCl_6^{3-}$ and $RhCl_5(H_2O)^{2-}$ [14]. In the presence of increasing quantities of tin(II) chloride (from $R_a(Rh) \geqslant 3$), however, significant amounts of rhodium are quite rapidly sorbed by the foam. This is clearly evident as the foam assumes the yellow colour from the yellow-orange aqueous phase. Presumably rhodium is sorbed in the form of well established, albeit incompletely characterized, chloro(trichlorostannato)-rhodium(III/I) complex anions. Analysis of the rhodium-loaded foam confirmed that significant quantities of tin are co-extracted with rhodium. Although Lo and Chow [15] have reported the sorption of tin chlorides by polyurethane foams, the published data pertain mainly to tin(IV) chloride. It was found here that if care is taken to exclude the possibility of tin(II) oxidation by atmospheric oxygen, then within experimental error (ca. 2%), essentially no tin is extracted at 1—2 mol dm^{-3} HCl, whereas with 3—4 mol dm^{-3} HCl, 6—6.4% of the total tin(II) chloride in solution is sorbed by the foam at 25°C.

Figure 1 shows the effect of temperature on the sorption of rhodium from

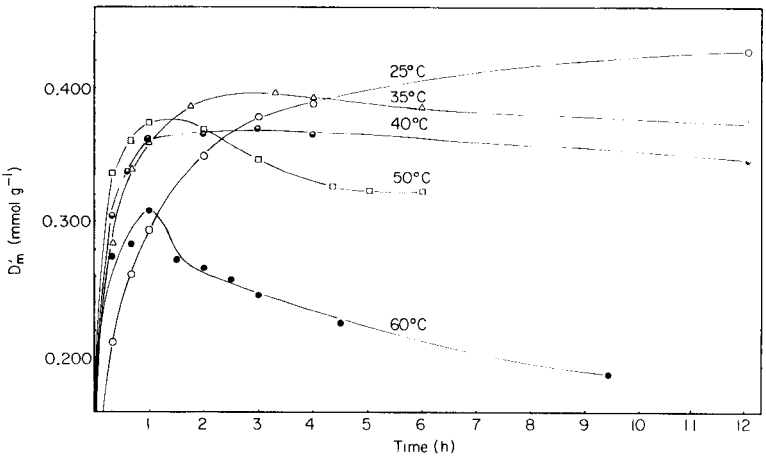

Fig. 1. The distribution of rhodium(III) chloride between polyurethane foam and solution in the presence of tin(II) chloride in 2.0 mol dm^{-3} HCl as a function of contact time at various temperatures. (R_a = 6; 80 mg of foam; 100 cm^3 of 7.3 × 10^{-4} mol dm^{-3} Rh.)

2 mol dm^{-3} hydrochloric acid in the presence of tin(II) chloride such that R_a(Rh) = 6 (solutions contained an excess of rhodium). Under these conditions, similar rates of rhodium sorption were obtained whether or not the solutions were allowed to equilibrate for 16 h prior to foam addition. Evidently then, the rate of sorption does not depend markedly on the rate at which the various equilibria concerning the chloro(trichlorostannato)rhodium(III) complexes are established [16]. Although these equilibria, and their kinetics, are incompletely understood, there is good evidence that the chloro(trichlorostannato)rhodium(III) anions are kinetically labile [16]. A 30-min pre-equilibration period (at the desired temperature) was therefore allowed prior to addition of the foam, unless otherwise stated. Figure 1 shows that the amount of rhodium sorbed depends markedly on the temperature, and that a higher temperature generally favours a lower D'_m(Rh) value. Furthermore at 50° and 60°C, the value of D'_m(Rh) decreases with time, while at 25°C, no satisfactory levelling off of D'_m(Rh) is observed within 12 h. Hence, an arbitrary choice of 40°C was used in subsequent experiments.

The effect of the relative concentration of tin(II) chloride on the extent of rhodium extraction can be seen from Fig. 2. It is clear from Fig. 2(a) that even at R_a = 3, a significant quantity of rhodium is sorbed after a foam/solution contact time of 1 h; the amount of rhodium sorbed under these conditions reaches a limiting value of 0.35 mmol g^{-1} after 6 h and remains essentially constant up to 20-h contact time. Increasing values of R_a result in a steady increase of rhodium sorbed (Fig. 2b). The maximum observed capacity of the foam with respect to rhodium is shown as a function of R_a, reaching C(Rh) = 0.51 mmol g^{-1} at R_a = 200. By monitoring simultaneously the amount of tin left in solution, it was possible to estimate the mole ratio Sn:Rh sorbed by the foam (R_f) at the various sampling times. Reliable esti-

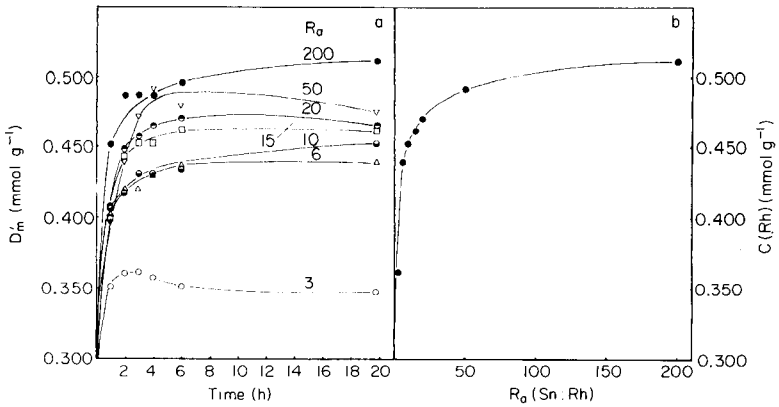

Fig. 2. The effect of R_a value on the distribution of rhodium between foam and 2.0 mol dm^{-3} HCl at 40°C. (80 mg of foam; 100 cm^3 of 7.3 × 10^{-4} mol dm^{-3} Rh; equilibration for 60 min before addition of foam.)

mates of the R_f value could only be obtained for solutions with initial $R_a < 20$. Table 1 shows the mean values of R_f (n = 6) obtained, reflecting the average number of moles of tin per mole of rhodium sorbed by the foam. Unfortunately, no clear trends were obtained although it seems reasonably certain that essentially all the tin sorbed is indeed associated with rhodium, because significant Sn(II) sorption could not be detected from 2 mol dm^{-3} hydrochloric acid in the absence of rhodium. The increase in standard deviation of the mean R_f value, as the tin concentration increases in the aqueous phase, may be largely due to the indirect measurement of tin sorbed by the foam. Thus it is reasonable to expect a larger error in the estimation of R_f, as the difference $[Sn]_o - [Sn]_t$ becomes smaller, because the initial concentration of tin, $[Sn]_o$, increases with R_a ($[Sn]_t$ is the tin(II) concentration at the sampling time t). This analysis indicates that a distribution of species is sorbed by the foam, rather than a single complex anion. Moriyama et al. [17] have shown, by means of ^{119}Sn-n.m.r. spectroscopy, that a distribution of species of the type $[Rh(SnCl_3)_nCl_{6-n}]^{3-}$ (n = 1—5) exists in 3 mol dm^{-3} hydrochloric acid as the value of R_a varies from 1 to 7. These authors further found that for $R_a > 6$, rhodium(III) is reduced by tin(II), with formation of a purple-red complex anion assigned as $[Rh(SnCl_3)_5]^{4-}$. It should be noted that no information about the rate of reduction of Rh(III) (nor its extent) at room temperature is available. Moriyama et al. pretreated all their solutions at about 100°C for 1 h prior to n.m.r.

TABLE 1

Mean Sn:Rh ratio on foam (R_f) calculated from $D'_m(Sn)/D'_m(Rh)$ for 6 determinations [T = 40°C, 2.0 mol dm^{-3} HCl, 80 mg of foam, 100 cm^3 of 7.3 × 10^{-4} mol dm^{-3} Rh(III)]

Nominal R_a	3	6	10	15	20
Mean R_f	3.6 ± 0.10	4.4 ± 0.26	3.6 ± 0.45	4.6 ± 0.47	4.5 ± 0.56

The liquid-liquid extraction of chloro(trichlorostannato)rhodium(III/I) complex anions by 4-methylpentan-2-one was examined by means of ^{119}Sn-n.m.r. and a distribution of species was found to persist in the organic phase [18]. It was also shown that a hydrido complex anion, $[RhH(SnCl_3)_4Cl]^{3-}$, is formed on extraction of rhodium(III) chloride in the presence of tin(II) from 2 mol dm^{-3} hydrochloric acid into 4-methylpentan-2-one [19]. Thus the detailed nature of the distribution of chloro(trichlorostannato)rhodium-(III/I) complex anions between the polyurethane foam and the aqueous phase remains unclear; the average number of tin atoms per rhodium atom of the sorbed complexes lies between 3 and 5, but it is impossible to decide whether Rh(III) or Rh(I) only, or a mixture of both, is involved.

The concentration of hydrochloric acid is expected to have a substantial influence on the distribution of rhodium between the foam and aqueous phase. Figure 3 shows the effect of the hydrochloric acid concentration on the R_f value and on C(Rh), the capacity of the foam, for a series of experiments for which R_a(Rh) = 10 at 40°C. Under these conditions, C(Rh) increases from a relatively low 0.36 mmol g^{-1} in 0.5 mol dm^{-3} HCl to a high value of 0.56 mmol g^{-1} in 5.0 mol dm^{-3} HCl. The dependence of D'_m(Rh) on the hydrochloric acid concentration is similar to the extractive behaviour of gallium [20], in which the amount of gallium (as $HGaCl_4$) sorbed by the polyurethane foam increases markedly as the hydrochloric acid concentration increases. This increase in gallium extraction has been ascribed, in part at least, to an increased number of "protonated ether sites in the polymer" [20]. A similar situation may be responsible for the trend observed in the case of the chloro(trichlorostannato)rhodium(I/III) complex anions.

The average number of tin atoms per rhodium atom extracted by the foam (R_f) decreases as the hydrochloric acid concentration increases (Fig. 3). This trend suggests that the expected mass-action effect (excluding any ionic strength effects), with increasing chloride ion concentration, is significant in the following equilibria (ignoring any possible Rh(I) species):

$$[RhCl_{6-n}(H_2O)_n]^{3-} + mSnCl_3^- \rightleftharpoons [RhCl_{6-n-m}(SnCl_3)_m]^{3-} + mCl^- + nH_2O$$

$$SnCl_2 + Cl^- \rightleftharpoons SnCl_3^-;\ SnCl_3^- + Cl^- \rightleftharpoons SnCl_4^{2-}$$

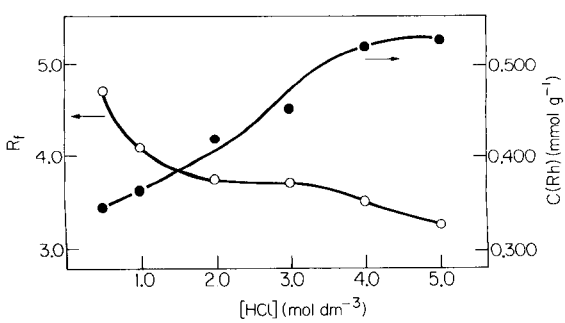

Fig. 3. The influence of hydrochloric acid concentration: (•) on the value of C(Rh); (○) on the R_f value. (40°C; R_a = 10; 80 mg of foam; 100 cm^3 of 7.3 × 10^{-4} mol dm^{-3} Rh.)

On the basis of published stability constant data [21], it was calculated that in 4.0 mol dm^{-3} hydrochloric acid, tin(II) is distributed approximately as 55% $SnCl_4^{2-}$, 32% $SnCl_3^-$, 12% $SnCl_2$ and 1% $SnCl^+$, while in 0.5 mol dm^{-3} hydrochloric acid the distribution is 30% $SnCl^+$, 53% $SnCl_2$, 12% $SnCl_3^-$ and 5% $SnCl_4^{2-}$. It seems likely, therefore, that the mass-action effect of chloride on the distribution of the chloro(trichlorostannato)rhodium(III/I) complex anions is significant, although no stability constant data are available.

Experiments to determine the effect of various concentrations of LiCl, NaCl and KCl on the extraction of rhodium by the foam yielded interesting results (Fig. 4). In one set of experiments, solutions were equilibrated for only 30 min prior to foam addition; in the other set, the aqueous phase was heated to 90°C for 1 h before the foam was added. Essentially similar trends were obtained; the distribution coefficients, D'_m(Rh) decreased in the order $H^+ > Li^+ > Na^+ > K^+$, with maximum capacity being reached after 6.25 h. A striking feature is that while the maximum capacities of the foam in the presence of H^+ only, H^+/Li^+ and H^+/Na^+ approach a similar value (0.43, 0.42 and 0.43 mmol g^{-1}, respectively), the presence of K^+ significantly decreases the maximum capacity of the foam (0.33 mmol g^{-1}).

Extensive studies aimed at elucidating the mechanism(s) by which hydrophobic anions are sorbed by polyurethane foams have suggested that several processes including adsorption, solvent extraction, anion exchange and complexation of metal species by the foam may be involved [3, 22]. Hamon et al. [22] showed that the sorption of $Co(SCN)_4^{2-}$ by polyether-type polyurethane foams depends markedly on the type (and radius) of the cation(s) concomitantly present in the aqueous solution, and presented convincing evidence for a cation-chelation mechanism of anion sorption. In this mechanism, the

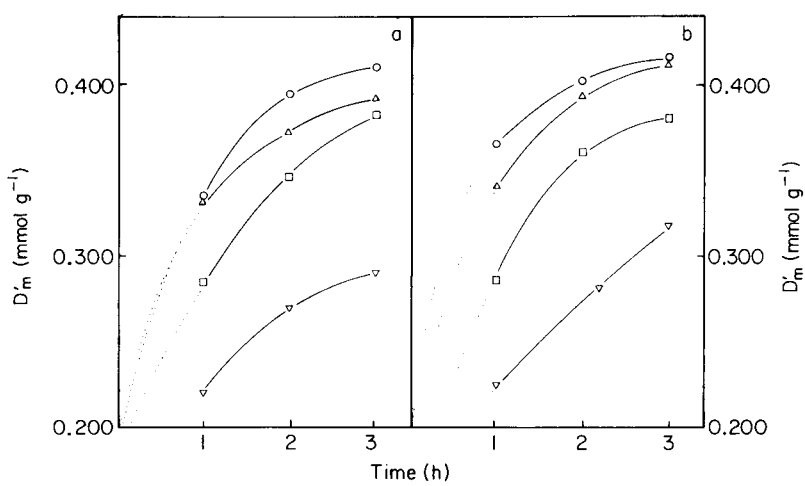

Fig. 4. The influence of alkali metal ions on the distribution of rhodium between foam and aqueous phase ($[Cl^-]$ = 2.0, $[H^+]$ = 1.0, $[M^+]$ = 1.0 mol dm^{-3} with $M^+ = H^+$, Li^+, Na^+ or K^+ at 40°C and R_a = 10). (a) Solution kept at 40°C for 30 min; (b) solution kept at 90°C for 60 min prior to foam addition. (▽) K^+; (□) Na^+; (△) Li^+; (○) H^+.

poly(alkeneoxy) chains of the polymer are envisaged as adopting helical conformations so allowing complex formation with appropriate simple cations. The anion in question is then extracted in association with these cationic "sites". The extraction efficiency for $Co(SCN)_4^{2-}$ [22], as well as other metal thiocyanates [7], from aqueous solution (pH 4—5) was found to follow the order $Li^+ < Na^+ < Cs^+ < Rb^+ < K^+ \leqslant NH_4^+$, with high concentrations of K^+ favouring efficient extraction in every case. This order is generally interpreted in terms of a predominating cation-chelation mechanism.

In the present study, the efficiency of rhodium extraction decreased with higher K^+ concentration. Analysis of the foam phase involved in the H^+/K^+ experiment showed that relatively large amounts of K^+ ions were co-extracted with rhodium (ca. 0.45 mmol $K^+ g^{-1}$). If it is assumed that rhodium is sorbed as a trivalent anion of the type $[Rh(SnCl_3)_nCl_{6-n}]^{3-}$ (n = 1—5), then the amount of K^+ found on the foam accounts for about 44% of the extracted rhodium. The balance of rhodium sorbed must then be associated with other cationic "sites" (if rhodium is extracted only as an anionic species). It is thus not unreasonable to suppose that rhodium is extracted as an acidic species, $H_3[Rh(SnCl_3)_nCl_{6-n}]$ (n = 1—5), analogous to the extraction of $HFeCl_4$ or $HGaCl_4$ as proposed by Gesser and co-workers [20, 23]. In view of the numerous nitrogen-containing linkages in the polymer [1], a degree of protonation of such moieties could result in a weak base anion-exchange mechanism. That increasing hydrochloric acid concentration results in larger D'_m(Rh) values (Fig. 3) is consistent with this view.

Separation of rhodium from iridium

The relatively high sorptive capacity of the polyurethane foam toward rhodium in the presence of tin(II) chloride prompted an examination of the selectivity of the foam toward rhodium in the presence of iridium in dilute hydrochloric acid. Initial experiments were aimed at establishing optimum conditions for the complete recovery of rhodium from solution. Typically, a 400-mg block of foam (representing a 3.3-fold excess at maximum capacity of about 0.4 mmol Rh g^{-1} of foam) previously wetted with a little ethanol, was added to 200 cm^3 of 2 mol dm^{-3} hydrochloric acid containing a known quantity of rhodium chloride (2.5—5.0 mg Rh) and the appropriate excess of tin(II) chloride. After vigorous mechanical shaking for a definite time, the loaded foam was removed, freed from excess solution, dissolved and analysed by a.a.s. Table 2 shows some results for rhodium recoveries, which were satisfactory within a reasonable time (0.5—1.5 h) provided that solutions containing sufficient tin(II) chloride were kept at 50°C for 3 h prior to addition of the foam.

Essentially quantitative separation of rhodium and iridium was achieved by selective sorption of the chloro(trichlorostannato)rhodium(III/I) complex anions by the polyurethane foam (Table 3). Under these conditions of sorption, no iridium could be detected on the foam. The mean mass of rhodium extracted by the foam represents 96 ± 2.8% of the total mass taken (Table 3).

TABLE 2

Recovery of rhodium (5.0 mg taken) after sorption on polyurethane foam

Rh found[a] (mg)		Recovery[b] (%)	Conditions[c]	
Solution	Foam		Shaking time (h)	Pre-treatment
0.5 ± 0.2	4.5 ± 0.2	100 ± 1.4	2.5	None
0.4[d]	4.8[d]	104	4.5	None
—	4.9 ± 0.1	99 ± 1.5	0.5	3 h, 50°C
—	5.1 ± 0.1	102 ± 2.4	1.5	3 h, 50°C

[a]Found by a.a.s. after decomposition of loaded foam with nitric acid. Mean of 4 determinations except where stated. [b]Total mass Rh found/mass Rh taken. [c]Loading at room temperature (20 ± 2°C); mass of foam 400 mg; volume of solution 200 cm^3; R_a = 50. [d]Mean of duplicates.

TABLE 3

Separation of rhodium (2.5 mg) from iridium (4.7 mg) under different conditions

Rhodium		Iridium		Conditions[d]	
Found[a] (mg)	%[b]	Found[c] (mg)	%[c]	Shaking time (h)	R_a[e]
2.4 ± 0.05	96	4.6 ± 0.1	98	1.5	15
2.4 ± 0.06 (10)	96	4.7 ± 0.2	100	1.5	20
2.3 ± 0.07 (4)	92	4.7 ± 0.1	100	1.5	25
2.4 ± 0.06 (6)	96	4.7 ± 0.2	100	1.5	50
2.5 ± 0.08 (4)	100	4.6 ± 0.1	98	3.0	50

[a]Found on foam (400-mg blocks); number of determinations in parentheses. [b]Mass of Rh on foam/mass of Rh taken. [c]Left in solution. [d]As in Table 2 with 3 h pre-equilibration at 50°C. [e]Sn(II): M mole ratio (M = Rh + Ir).

Analysis of the aqueous phases from the experiments listed in Table 3 for residual rhodium content showed that a mean of 50 μg Rh (n = 27) remained in solution; this amount accounts for at most 2% of the total mass of rhodium present. Given the method of quantifying rhodium, as well as the possibilities of mechanical losses and other experimental errors, a relative standard deviation of 2.5% is estimated for the determination of rhodium. Within this experimental error, the recoveries are satisfactory for both rhodium and iridium.

Although various iridium complexes involving the $SnCl_3^-$ moiety are known [24, 25], the reaction between iridium(IV) chloride and tin(II) chloride does not seem to have been examined in detail. This reaction is likely to involve a reduction of Ir(IV) to Ir(III), followed by complex formation involving $SnCl_3^-$. The complex formation is incomplete (and/or very slow) at room tempera-

ture, and prolonged heating at 100°C is required to produce, for example, $[(CH_3)_4N]_4[Ir_2Cl_2(SnCl_3)_4]$ [24]. In the present case, the failure to achieve any extraction of iridium by polyurethane foam is consistent with the view that substantial pre-treatment is necessary in order to produce appreciable quantities of (probably) extractable chloro(trichlorostannato)iridium(III) complex anions, analogous to the rhodium species. This difference in the behaviours of rhodium and iridium can be exploited conveniently to achieve excellent separation of these metals (Table 3). Further work is in progress to clarify mechanistic aspects of the sorption by the foam and to examine possible interferences in detail. Work done so far suggests that only platinum is likely to be co-extracted [12, 13] with rhodium under the conditions outlined above; Co, Ni, Mn, Cu, and Fe do not interfere at levels equimolar with rhodium, and up to 1 mol dm^{-3} sulphate or perchlorate and 0.1 mol dm^{-3} nitrate can be tolerated.

We are grateful to the University of Cape Town and the Council for Scientific and Industrial Research for generous financial assistance. One of us (I. N.) gratefully acknowledges an AECI Scholarship.

REFERENCES

1 T. Braun and A. B. Farag, Anal. Chim. Acta, 99 (1978) 1.
2 G. J. Moody and J. D. R. Thomas, Analyst (London), 104 (1979) 1.
3 G. J. Moody and J. D. R. Thomas, Chromatographic Separation and Extraction with Foamed Plastics and Rubbers, Chromatographic Science Series V21, M. Dekker, New York and Basel, 1982.
4 T. Braun, A. B. Farag and J. D. Navratil, Polyurethane Foam Sorbents in Separation Science, CRC Press, Florida, 1985.
5 T. Braun, Cellular Polymers, 3 (1984) 81.
6 A. Chow and R. A. Moore, Talanta, 27 (1980) 315.
7 A. Chow and S. J. Al-Bazi, Talanta, 29 (1982) 507; 30 (1983) 487.
8 A. Chow and S. J. Al-Bazi, Anal. Chem., 55 (1983) 1094.
9 A. Chow and S. J. Al-Bazi, Talanta, 31 (1984) 189.
10 A. Chow and S. J. Al-Bazi, Talanta, 31 (1984) 431.
11 A. Chow and S. J. Al-Bazi, Anal. Chim. Acta, 157 (1984) 83.
12 K. R. Koch and I. Nel, Analyst (London), 110 (1985) 217.
13 K. F. G. Brackenbury, M.Sc., Cape Town, 1985.
14 V. I. Shlenskaya, O. A. Efremenko, S. V. Oleinikova and I. P. Alimarin, Izv. Akad. Nauk SSSR, Ser. Khim., 8 (1969) 1643.
15 V. S. K. Lo and A. Chow, Talanta, 28 (1981) 157.
16 S. Iwasaki, T. Nagai, E. Miki, K. Mizumachi and T. Ishimori, Bull. Chem. Soc. Jpn., 57 (1984) 386.
17 H. Moriyama, T. Aoki, S. Shinoda and Y. Saito, J. Chem. Soc., Dalton Trans., (1981) 639.
18 K. R. Koch and J. M. Wyrley-Birch, unpublished results, 1984.
19 K. R. Koch and J. M. Wyrley-Birch, Inorg. Chim. Acta, 102 (1985) L5.
20 H. D. Gesser and G. A. Horsfall, J. Chim. Phys., 74(10) (1977) 1072.
21 A. E. Martell and R. M. Smith, Critical Stability Constants, Vol. 4, Plenum Press, New York, 1976, pp. 10 and 109.
22 R. F. Hamon, A. S. Khan and A. Chow, Talanta, 29 (1982) 313.
23 J. J. Oren, K. M. Gouch and H. D. Gesser, Can. J. Chem., 57 (1979) 2032.
24 J. F. Young, R. D. Gillard and G. Wilkinson, J. Chem. Soc., (1964) 5176.
25 O. M. Petrukhin, N. A. Borshch and Yu. A. Zolotov, Proc. Int. Solv. Extr. Conf., ISEC-80, Liege-Belgium, Vol. 3, 1980, p. 80.

Analytica Chimica Acta, 182 (1986) 71—81
Elsevier Science Publishers B.V., Amsterdam — Printed in The Netherlands

DYE-ASSISTED CHROMATOGRAPHIC DETERMINATION OF ALIPHATIC KETONES AND ESTERS WITH BRILLIANT GREEN

ANDRES TRUJILLO, SAM WOO KANG[a] and HENRY FREISER*

Strategic Metals Recovery Research Facility, Department of Chemistry, University of Arizona, Tucson, AZ 85721 (U.S.A.)

(Received 19th July 1985)

SUMMARY

Determinations of neutral nonchromophoric organic compounds by dye-assisted chromatography are extended to the determination of aliphatic ketones and esters by using reversed-phase conditions and a mobile phase containing Brilliant Green. Detection limits of 6—20 μg were obtained when a mobile phase containing 50% (v/v) methanol/water and 0.00010 M Brilliant Green was used with detection at 575 nm, and 0.5—2 μg with detection in the ultraviolet region. In the absence of dye the detection limits for several solutes were about four times higher than the corresponding values obtained with the dye. The dye was shown to form a dimer having a molar absorptivity two orders of magnitude smaller than that of the monomeric dye. Detection of non-chromophoric compounds is concluded to be due to the desorption of adsorbed dye by the analytes and the shift of the aggregation and hydration equilibria of the dye promoted by the organic solutes. The lowering of the capacity factors is interpreted in terms of the adsorption of dye by the column which reduces the hydrophobicity of the stationary phase.

The most widely used detectors in HPLC are photometers based on ultraviolet-visible absorption which are sensitive and selective enough for most purposes because solutes without an absorbing chromophore are undetected. Detection of ionic nonchromophoric analytes by reversed-phase HPLC with photometric detection has been illustrated by Eksborg et al. [1] using a mobile phase containing an ion-pairing reagent having a strong chromophore in the ultraviolet region. Other examples of the determination of ionizable nonchromophoric organic and inorganic species by ion-pair chromatography have appeared in the literature [2—4]. The mechanism of separations based on ion-pairing reagents is still in controversy [5—6].

DiNunzio and Freiser [7] extended the use of ion-pair chromatography to the visible range, using an aqueous Brilliant Green solution as the stationary phase and hexane/dichloromethane as the eluent in normal-phase chromatography. Separation and detection of several aliphatic acids under these conditions was done with high sensitivity using photometric detection at 630 nm. The discovery that neutral nonchromophoric analytes could be detected

[a]On study leave from Han Nam University, Taijun, Chungnam, Korea.

0003-2670/86/$03.50

down to microgram amounts by using reversed-phase HPLC and a mobile phase containing a dye salt promoted studies on its applicability to the detection of several families of compounds such as alcohols, sugars and organophosphorus compounds [8, 9].

In dye-assisted chromatography, a reversed-phase column is equilibrated with a mobile phase containing a dye salt. After equilibration, the same mobile phase is used in the elution of the compounds injected into the column. The amount of dye adsorbed by the column during the equilibration depends on factors such as the ionic strength of the solution, the concentration of dye and the concentration of organic modifier in the mobile phase. As in ion-pair chromatography [10], an increase in ionic strength or in dye concentration causes an increase in the amount of dye adsorbed by the column. Furthermore, an increase in the concentration of organic modifier in the mobile phase causes desorption of dye.

In this paper, it is demonstrated that separation and detection of poorly absorbing aliphatic ketones and esters can also be accomplished with the dye-assisted chromatographic technique. In addition, the chemistry of the dye was studied by spectrophotometric techniques in order to understand the role of the dye in the separation and detection of neutral species.

EXPERIMENTAL

Chemicals and apparatus

The ketones and esters used were obtained from several sources, and were used as received. Reagent-grade methanol and n-propanol (EM Science) were used without further purification. Distilled deionized water and methanol were degassed under vacuum. Brilliant Green bisulfate (Eastman) was used as received.

The modular chromatographic unit used consisted of an Altech pump (model 110A), a variable-wavelength detector (Schoeffel model SP-770 Spectroflow), and a 10-μl rotary valve injector (Spectra Physics, model SP-419-0410). A Varian Cary 219 u.v.-visible spectrophotometer digitally interfaced to an Apple II+ microcomputer was used for the measurement of the visible spectra of Brilliant Green solutions.

A stainless steel column (25 × 0.46-cm i.d.) slurry-packed with 5-μm particles of Spherisorb S5 ODS-2 was used. The average efficiency of the column was estimated to be 2300 plates for benzene, naphthalene and anthracene.

Procedure

The mobile phases consisted of mixtures of degassed methanol/water ranging from 10 to 50% (v/v) and containing either 1.0×10^{-4} M Brilliant Green or no dye at all. All mobile phases were filtered through a 0.45-μm Millipore filter before use. The pH of the mobile phases containing dye ranged from 4.2 to 4.4.

The column was thermostated at 30 ± 1°C with a water jacket and a Haake FE temperature controller. The average flow rate was maintained at 1.0 ml min^{-1}. Before the samples were injected, the column was equilibrated with the appropriate mobile phase. With dye-containing mobile phases, the equilibration was followed by measuring the absorbance of the eluent. Equilibration was achieved when the absorbance of the eluent was the same as that of the pure mobile phase.

Cleaning of the dye-saturated column and computation of the capacity factors, k', were done as reported previously [8].

The spectra of Brilliant Green solutions were recorded at 30°C in cells having path lengths of 0.1, 1.00, 5.00 and 10.00 cm. The solutions were left to equilibrate for 24 h before spectra were measured.

RESULTS AND DISCUSSION

Brilliant Green was used in the mobile phase because this dye had been found to be more sensitive than other dyes including methylene blue, Nile blue, or acridine orange. The nature of the dye is very important because only a few have been found to be useful in the determination of neutral species. Methylene blue and acridine orange are known to form aggregates in aqueous solution [11—13]. As a result of the aggregation reaction, solutions of those dyes deviate from Beer's law; the deviation is typically manifested as a decrease in the apparent molar absorptivity of the solution as the concentration of dye is increased.

In previous papers [8, 9], the effects of the dye on the retention and detection of neutral species were interpreted in terms of the formation of an adduct between the dye and the solutes; however, this theory must be revised in view of a recent report [14] on the aggregation of Brilliant Green. In addition to aggregation, Brilliant Green is known to undergo acid-base and hydration reactions typical of triphenylmethane dyes. Cigen and Ekstrom [15] and Fox et al. [16] have studied these reactions (Fig. 1) in great detail. Their results indicate that the predominant reaction at pH 4.5 is the hydration of the blue-green cation to form a colorless carbinol. Calculations indicate that in dilute dye solutions, 16% of the dye is present in the colorless carbinol form. The equilibria between the blue-green and carbinol forms can be shifted toward the blue-green form by lowering the activity of water, which is likely to occur during the elution of the neutral species because in the elution band, the concentration of organic species is considerably larger than in the rest of the mobile phase. Therefore, the absorbance of the band should be higher than that of the rest of the mobile phase.

Although the aggregation of Brilliant Green was studied by Vemulapalli and Gnanasambandan [14], they failed to consider the hydration of the dye and did not prove the formation of the dye dimers. Accordingly, the aggregation of Brilliant Green was re-examined at 30°C in order to establish the aggregation number and the aggregation constant of the dye.

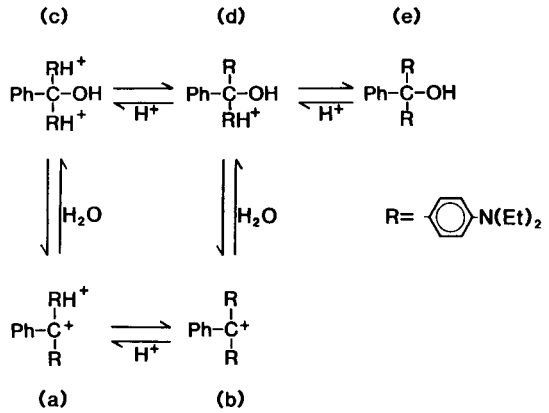

Fig. 1. Equilibrium reactions of Brilliant Green: (a) yellow form; (b) blue-green form; (c—e) colorless forms.

To study the aggregation of Brilliant Green, the visible spectra of several solutions (10^{-4}—10^{-7} M) of the dye were measured. In Fig. 2 the normalized spectra are shown to have maxima at 425 and 624 nm. It can be seen that as the concentration of dye is increased, the apparent molar absorptivity of the dye solution decreases. Because the wavelength of maximum absorbance remains independent of concentration, there is little possibility of having a tautomeric equilibrium; that type of reaction is likely to produce a a distinct wavelength shift when the composition of the solution is changed [17]. Thus, the change in apparent molar absorptivity is more likely to be due to the aggregation of the dye in which the aggregate has a smaller molar absorptivity than the monomer. A plot of log ϵ vs. $-\log C$, where ϵ is the apparent molar absorptivity of the solution and C is the analytical concentration of the dye, is shown in Fig. 3. The plot consists of two regions, one

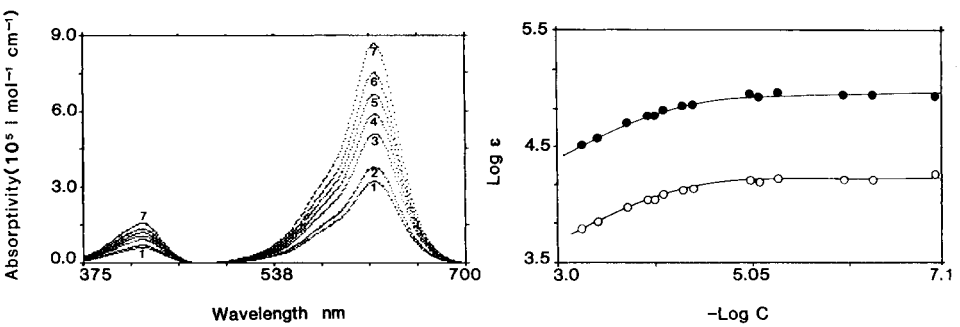

Fig. 2. Absorbance spectra of Brilliant Green solutions at 30.0°C. Concentration: (1) 565.0, (2) 327.0, (3) 188.0, (4) 113.0, (5) 75.3, (6) 37.7, (7) 5.53 (× 10^{-6} M).

Fig. 3. Logarithmic plot of the apparent molar absorptivity (l mol^{-1} cm^{-1}) with the molar concentration of Brilliant Green: (○) 425 nm; (●) 624 nm.

in which the apparent molar absorptivity changes with the concentration of dye and the other showing no dependence in the concentration of dye. The apparent molar absorptivity remains constant in dilute solution of dye because only monomer is present. Thus the apparent molar absorptivity corresponds to the molar absorptivity of the monomer which in this case is $(88.3 \pm 1.2) \times 10^3$ l mol^{-1} cm^{-1} at 624 nm and $(16.1 \pm 0.22) \times 10^4$ l mol^{-1} cm^{-1} at 425 nm. If the presence of colorless carbinol forms is considered, the corrected molar absorptivity of the monomer is 10.5×10^4 l mol^{-1} cm^{-1} at 624 nm. The presence of only two regions in Fig. 3 suggests that only two absorbing species are present at equilibrium, with one of them being the monomeric dye, D. Thus the aggregation equilibrium can be represented as $n\mathrm{D} \rightleftharpoons \mathrm{D}_n$, where n is the aggregation number and D_n is the aggregated dye.

To calculate the aggregation number and the aggregation constant, a suitable equation was derived, based on the mass-balance equation $C = [\mathrm{D}] + n[\mathrm{D}_n]$, where C is the total concentration of dye and [D] and $[\mathrm{D}_n]$ are the molar concentrations of the monomer and the aggregate dye, respectively. The overall equilibrium constant for the reaction is $K = [\mathrm{D}_n]/[\mathrm{D}]^n$ and the expression for the absorbance, A, of the solution per unit length is $A = \epsilon C = \epsilon_1[\mathrm{D}] + \epsilon_n[\mathrm{D}_n]$, where ϵ_1 and ϵ_n are the molar absorptivities of the monomer and aggregate, respectively. From these equations it is easily shown that

$$\log[(\epsilon - \epsilon_1 f_\mathrm{M})C] = n \log(Cf_\mathrm{M}) + \log(\epsilon_n K) \qquad (1)$$

where f_M is the fraction of dye present in the monomer form ($f_\mathrm{M} = [\mathrm{D}]/C$). The fraction was calculated from

$$f_\mathrm{M} = (\epsilon - \epsilon_1/n)/(\epsilon_1 - \epsilon_n/n) \qquad (2)$$

which was derived from the equation for absorbance, A.

From Eqn. 1, a plot of $\log(\epsilon - \epsilon_1 f_\mathrm{M})C$ (as y) vs. $\log(Cf_\mathrm{M})$ (as x) should be linear and have a slope equal to n and an intercept equal to $\log(\epsilon_n K)$. Because ϵ_n/n could not be evaluated by independent means, an iterative method was used in which the value of ϵ_n/n was varied over a wide range. At every value of ϵ_n/n, the corresponding values of $\log(\epsilon - \epsilon_1 f_\mathrm{M})C$ and $\log(Cf_\mathrm{M})$ were calculated and linear regression [18] was used to compute the standard error of the estimate (S_{yx}) and the correlation coefficient. The best value of ϵ_n/n was chosen as the one that yielded a straight line with the smallest value of S_{yx}^2 in the linear regression fit.

This iteration gave $\epsilon_n/n = 81 \pm 0.2$. From the linear regression, a correlation coefficient of 0.998 and $S_{yx}^2 = 3.22 \times 10^{-3}$ were obtained. The regression equation corresponding to Eqn. 1 is: $y = (2.01 \pm 0.05)x + (5.80 \pm 0.2)$. The linearity of the regression equation confirms the validity of Eqn. 1. A slope of two is indicative of the formation of a dimer, and from the y intercept, a dimerization constant $K = 10^{3.65 \pm 0.2}$ was obtained.

The observed molar absorptivity of the dimer ($\epsilon_2 = 162$ l mol^{-1} cm^{-1}) is considerably smaller than the corresponding value for the monomer. This

phenomenon has been observed with other dyes and has been explained in terms of the orientation of the two dye molecules in the dimer which effectively decreases the transition dipole moment of the dimer [19—22].

It is known [12, 13] that addition of organic solutes to solutions of dyes capable of undergoing aggregation reactions decreases the extent of the aggregation. Thus, the increase in the apparent molar absorptivity is caused by the shift in the dimerization equilibrium. In the case of Brilliant Green, it was decided to study the effect of methanol and propanol on the visible spectrum of an aqueous 1.0×10^{-4} M solution of the dye, which is 36% in the dimer form, to help explain the detection of neutral nonchromophoric analytes in the chromatographic experiments. The wavelength of maximum absorbance did not change appreciably (6 nm) with the concentration of alcohol indicating the absence of solvochromic effects [23]. Figure 4 shows a plot of the concentration of either methanol or propanol against the apparent molar absorptivity of the dye solution at 624 nm. When methanol is added to the dye solution, the value of ϵ increases linearly; addition of n-propanol causes a larger increase in ϵ which approaches a plateau at concentrations greater than 2 M n-propanol. The maximum apparent molar absorptivity observed in the presence of alcohols was 11.2×10^4 M^{-1} cm^{-1}, roughly 6% larger than the corrected molar absorptivity of the monomer. This change is too small to be considered significant because it may be due entirely to photometric errors and errors in the hydration constants used to correct ϵ_1.

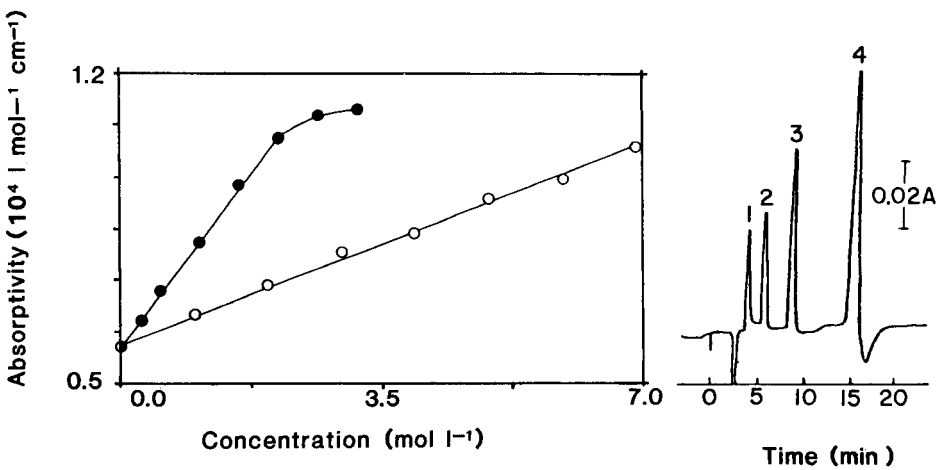

Fig. 4. Variation of the apparent molar absorptivity of Brilliant Green solutions (0.00010 M) at 624 nm as a function of alcohol concentration: (•) propanol; (○) methanol.

Fig. 5. Separation of ketones with Brilliant Green. Peaks: (1) methyl ethyl ketone; (2) methyl propyl ketone; (3) methyl isobutyl ketone; (4) methyl amyl ketone (100 μg each). Mobile phase: 0.00010 M Brilliant Green in 50% (v/v) methanol/water. Detection at 575 nm.

The increase in the apparent molar absorptivity of the dye in the presence of alcohols is more pronounced with n-propanol which is more hydrophobic than methanol. This result agrees with a report [22] that attributes the disaggregation of dyes by organic solutes to the disruption of the water structure around the aggregate. Thus the results observed can be explained in terms of the shift in the dimerization equilibria toward the formation of the highly absorbing monomer, and the shift in the hydration equilibria toward the formation of the colored ion, caused by the lowering of the dielectric constant.

In previous publications [8, 9], the detection and separation of non-chromophoric neutrals was attributed to the formation of an adduct between the organic solute and the dye; however, the above results indicate that the increase in absorbance caused by organic solutes is in a large part due to the shift of aggregation and hydration equilibria. If other reactions such as the formation of an adduct are taking place, their equilibrium constants are too small to cause a significant effect in the absorption spectrum of the dye.

Chromatography

In order to establish the optimal chromatographic conditions for the elution of the ketones and esters selected, the capacity factors, k', were studied using several mobile phases compositions containing methanol/water and 1.0×10^{-4} M Brilliant Green. Detection of both ketones and esters was done at 575 nm instead of 624 nm because the shorter wavelength was found to be more sensitive.

As can be seen in Table 1, k' values decrease with increasing concentration of methanol in the mobile phase and increase with increase in the hydrophobic character of the solute in accordance with the reversed-phase conditions. A typical chromatogram showing the separation of several ketones is shown in Fig. 5. A negative peak having a large retention time was observed when the concentration of methanol in the mobile phase exceeded 40% (v/v); this peak is due to the adsorption of additional dye necessary to compensate for the dye desorbed in the analyte band. At low methanol concentrations, no negative peaks were observed, probably because the fraction of dye desorbed by the analyte band is negligibly small compared with the amount of dye remaining in the column; thus the re-adsorption of dye is less noticeable.

To study the effects of the dye in the retention of the solutes, the capacity factors were measured using a cleaned column and several mobile phases containing methanol/water mixtures but no dye. As can be seen in Table 2, the same retention behavior as described above was observed, except that in the absence of dye, the capacity factors were larger than those observed under the corresponding conditions in the presence of dye. For all solvent compositions, a plot of the capacity factors obtained for both ketones and esters in the presence of dye, $k'_{(\mathrm{dye})}$, vs. the capacity factors obtained for the corresponding compounds in the absence of dye, $k'_{(\mathrm{no\ dye})}$, are linear and

TABLE 1

Capacity factors of esters and ketones in the presence of dye

Compound	Capacity factor, k'[a]				
	Methanol (% v/v)				
	10	20	30	40	50
Methyl acetate	1.01	0.87	0.84	0.65	0.44
Methyl propanoate	3.06	2.74	2.12	1.44	1.06
Ethyl acetate	2.59	2.53	1.94	1.38	1.02
Methyl butanoate	9.82	8.01	6.09	3.53	2.27
Propyl acetate	8.88	7.27	5.53	3.54	2.09
Methyl pentanoate	—	24.53	16.65	8.72	4.67
Ethyl butanoate	—	21.03	14.29	7.39	4.21
Methyl hexanoate	—	—	—	22.80	10.94
Propyl butanoate	—	—	—	18.52	9.12
Acetone	0.40	0.34	0.28	0.18	0.18
Methyl ethyl ketone	1.15	1.21	0.94	0.74	0.59
Methyl propyl ketone	4.01	3.47	2.76	2.13	1.24
Cyclohexanone	4.29	3.71	2.65	1.88	1.15
Methyl t-butyl ketone	9.65	8.82	5.94	3.94	2.18
Methyl isobutyl ketone	11.35	10.76	6.41	4.15	2.22
Methyl isoamyl ketone	—	—	19.23	10.06	4.76
Methyl amyl ketone	—	—	22.53	11.40	5.54
Ethyl butyl ketone	—	—	22.04	11.00	5.35

[a]Mobile phase: 1.0×10^{-4} M Brilliant Green in methanol/water mixtures. Detection at 575 nm; 100-μg samples.

have near-zero intercept (Table 3). The slopes of the plots decrease as the concentration of methanol in the mobile phase is increased. The decrease in the slopes suggests that as the amount of dye adsorbed on the column decreases (with increase in methanol concentration), the effect of the dye on the retention decreases and appears to become negligible at 50% methanol.

The systematic decrease in the capacity factors of the ketones and esters in the presence of Brilliant Green is analogous to the results described by Knox and Hartwick [6] in their study of reversed-phase ion-pair chromatography. These workers confirmed that the capacity factor for benzyl alcohol decreased in the presence of ion-pairing reagents in the mobile phase. The decrease in capacity factor was shown to vary linearly with the increase in surface concentration of the ion-pairing reagent. To explain those results, Knox and Hartwick [6] proposed that the adsorption of the ion-pairing reagent on the reversed-phase column increases the polarity of the column and therefore reduces the hydrophobic interactions between the solute and stationary phase. A more refined explanation for the phenomena, which takes account of the surface activity of the ion-pairing reagent, was proposed by Stranahan and Deming [5].

TABLE 2

Capacity factors of esters and ketones in the absence of dye

Compound	Capacity factor, k'[a]				
	Methanol (% v/v)				
	10	20	30	40	50
Methyl acetate	2.06	1.24	0.94	0.69	0.56
Methyl propanoate	8.18	4.47	2.53	1.82	1.09
Ethyl acetate	7.06	4.11	2.35	1.59	1.03
Methyl butanoate	26.85	12.88	7.06	4.06	2.38
Propyl acetate	24.51	12.41	6.65	3.88	2.18
Methyl pentanoate	—	—	19.47	9.86	5.18
Ethyl butanoate	—	—	17.71	8.81	4.63
Methyl hexanoate	—	—	—	25.71	11.65
Propyl butanoate	—	—	—	21.84	9.77
Acetone	1.18	0.72	0.41	0.29	0.27
Methyl ethyl ketone	3.08	2.00	1.12	0.76	0.62
Methyl propyl ketone	13.0	6.06	3.18	2.18	1.29
Cyclohexane	13.35	6.18	3.29	1.94	1.21
Methyl t-butyl ketone	32.53	15.47	7.41	4.03	2.26
Methyl isobutyl ketone	35.71	16.06	7.82	4.35	2.44
Methyl isoamyl ketone	—	—	21.90	10.48	5.12
Methyl amyl ketone	—	—	25.82	11.95	5.88
Ethyl butyl ketone	—	—	24.06	11.18	5.74

[a]Mobile phase: methanol/water mixtures containing no dye. Detection: esters at 210 nm and ketones at 280 nm. Samples: 100 μg.

Because Brilliant Green is strongly adsorbed by the stationary phase and is expected to be surface-active [24], the capacity factors of neutral species should be lowered in accordance with the results of Knox and Hartwick and the prediction of the model proposed by Stranahan and Deming.

The sensitivity of the method was investigated by preparing several calibration graphs. Each calibration graph was obtained by replicate injection

TABLE 3

Regression equations for plots of $k'_{(dye)}$ vs. $k'_{(no\ dye)}$[a]

Methanol (%)	Slope (SD)	Intercept (SD)	Correlation coefficient
10	3.09 (0.14)	−0.55 (0.90)	0.991
20	1.60 (0.06)	0.20 (0.32)	0.994
30	1.13 (0.02)	0.27 (0.18)	0.998
40	1.13 (0.02)	−0.15 (0.17)	0.998
50	1.07 (0.01)	0.01 (0.03)	0.999

[a]Same conditions as Table 5.

of 10-μl of a synthetic mixture of compounds found to be completely resolved, and by measuring the peak height of the eluted compounds. In Table 4, the linear regression equations for the calibration graphs are shown together with the range of concentrations used. The calibration graphs are linear and the slopes of the plots increase as the molecular weight of the solute increases. The dependence of the slope on the molecular weight of the solute is a consequence of the ability of the solute to shift the aggregation equilibrium toward the formation of the highly-absorbing dye cation.

In the presence of dye, the detection limits (S/N = 2) for ketones and esters were measured in both the visible and u.v. regions. The detection limits in the u.v. range are about an order of magnitude better than in the visible region (Table 5) because of the interaction of the solute with the dye and the contribution of the absorption by the carbonyl group in the solutes. The limits of detection obtained in the visible region decrease as the molecular weight of the analyte increases.

In the absence of dye, detection limits in the u.v. region for both ketones and esters were 2—5 μg, depending on the molecular weight of the solute. These detection limits are about four times higher than the values obtained under identical conditions in the presence of dye.

In conclusion, Brilliant Green cations were found to form dimers having apparent molar absorptivities far smaller than that of the blue-green monomer. The addition of organic solutes to solutions containing aggregated dye was found to promote the formation of the monomer. The more hydrophobic solutes were found to be more effective disaggregating agents. Detection of neutral nonchromophoric analytes in the presence of dye is possible because of the desorption of the dye by the analytes and the disaggregation of the dye promoted by the high concentration of organic compounds in the band containing the analyte.

TABLE 4

Calibration graphs (peak height vs. concentration) with Brilliant Green[a]

Compound	Linear regression parameters		
	Slope (SD)	Intercept (SD)	Range (μg)
Methyl ethyl ketone	0.23 (0.01)	−0.24 (0.14)	25—100
Methyl propyl ketone	0.36 (0.01)	0.51 (0.41)	20—150
Methyl isobutyl ketone	0.54 (0.01)	0.53 (0.36)	10—150
Methyl amyl ketone	0.86 (0.04)	−1.10 (0.69)	10—100
Methyl acetate	0.18 (0.004)	−0.13 (0.03)	25—200
Methyl propanoate	0.21 (0.003)	0.32 (0.06)	20—200
Methyl butanoate	0.30 (0.01)	0.39 (0.18)	10—150
Methyl pentanoate	0.50 (0.02)	0.90 (0.94)	10—100

[a]Mobile phase: 50% (v/v) methanol/water containing 1.0×10^{-4} M Brilliant Green. Detection at 575 nm. Peak heights are expressed as $10^{-3}\times$ absorbance; correlation coefficients are 0.996 to 0.999.

TABLE 5

Detection limits with Brilliant Green[a]

Compound	Detection limits (μg)	
	575 nm	U.v.[b]
Methyl ethyl ketone	20.4	0.7
Methyl propyl ketone	11.6	1.2
Methyl isobutyl ketone	7.7	1.7
Methyl amyl ketone	4.5	2.8
Methyl acetate	20.0	0.5
Methyl propanoate	14.1	0.6
Methyl butanoate	9.0	0.8
Methyl pentanoate	5.8	1.3

[a]Mobile phase: 50% methanol/water containing 1.0×10^{-4} M Brilliant Green. [b]Detection at 280 nm for ketones and 210 nm for esters.

This work was supported by a grant from the Office of Naval Research, No. N00014-81-K-0576.

REFERENCES

1 S. Eksborg, P. O. Lagerstom, R. Modin and G. Schill, J. Chromatogr., 83 (1973) 99.
2 M. Denkert, L. Hackzell, G. Schill and E. Sjogren, J. Chromatogr., 218 (1981) 31.
3 B. Sachok, S. N. Deming and B. A. Bidlingmeyer, J. Liq. Chromatogr., 5 (1982) 389.
4 W. E. Barber and P. W. Carr, J. Chromatogr., 260 (1983) 89.
5 J. J. Stranahan and S. N. Deming, Anal. Chem., 54 (1982) 2251.
6 J. H. Knox and R. A. Hartwick, J. Chromatogr., 204 (1981) 3.
7 J. DiNunzio and H. Freiser, Talanta, 26 (1979) 587.
8 T. Gnanasambandan and H. Freiser, Anal. Chem., 54 (1982) 1282; 54 (1982) 2379; 53 (1981) 909.
9 A. Trujillo, T. Gnanasambandan and H. Freiser, Anal. Chim. Acta, 162 (1984) 333.
10 R. H. A. Sorel and A. Hullshoff, in J. C. Giddings, E. Grushka, J. Cazes and P. R. Brown (Eds.), Advances in Chromatography, Vol. 21, M. Dekker, New York, pp. 87—129.
11 E. Rabinowitch and L. Epstein, J. Am. Chem. Soc., 63 (1941) 69.
12 V. Vitagliano, in E. Wyn-Jones and J. Gormally (Eds.), Aggregation Processes in Solution, Elsevier, Amsterdam, 1983, p. 271.
13 B. C. Burdett, in E. Wyn-Jones and J. Gormally (Eds.), Aggregation Processes in Solution, Elsevier, Amsterdam, 1983, p. 241.
14 G. K. Vemulapalli and T. Gnanasambandan, Anal. Chim. Acta, 164 (1984) 267.
15 R. Cigen and C. G. Ekstrom, Acta Chem. Scand., 17 (1963) 1843, 2083.
16 B. M. Fox, G. Hallas, J. D. Hepworth and D. Mason, J. Chem. Tech. Biotechnol., 30 (1980) 317.
17 D. E. Metzler, C. M. Harris, R. L. Reeves, W. H. Lawton and M. S. Maggio, Anal. Chem., 49 (1977) 864A.
18 D. M. Hirst, Mathematics for Chemists, Macmillan, London, 1976.
19 S. E. Sheppard and A. L. Geddes, J. Am. Chem. Soc., 66 (1944) 2003.
20 S. E. Sheppard, Rev. Mod. Phys., 14 (1942) 303.
21 W. West and S. Pearce, J. Phys. Chem., 69 (1965) 1894.
22 P. Mukerjee and A. K. Ghosh, J. Am. Chem. Soc., 92 (1970) 6419.
23 L. G. S. Brooker, A. C. Craig, D. W. Haseltine, P. W. Jenkings and L. L. Lincoln, J. Am. Chem. Soc., 87 (1965) 2443.
24 E. Heyman and A. Yoffe, Trans. Faraday Soc., 38 (1942) 408.

Analytica Chimica Acta, 182 (1986) 83—90
Elsevier Science Publishers B.V., Amsterdam — Printed in The Netherlands

AQUOCYANOCOBALT(III)-HEPTA(2-PHENYLETHYL)-COBYRINATE AS A CATIONIC CARRIER FOR NITRITE-SELECTIVE LIQUID-MEMBRANE ELECTRODES

RENÉ STEPÁNEK, BERNHARD KRÄUTLER*, PETER SCHULTHESS, BERNHARD LINDEMANN, DANIEL AMMANN and WILHELM SIMON*

Department of Organic Chemistry, Swiss Federal Institute of Technology (ETH), CH-8092 Zürich (Switzerland)

(Received 20th August 1985)

SUMMARY

The synthesis of aquocyanocobalt(III)-hepta(2-phenylethyl)-cobyrinate is described. It is a more lipophilic substitute for a previously reported nitrite-carrier. Membranes based on this more readily accessible cobyrinate exhibit selectivity coefficients for nitrite (K^{pot}) over nitrate and chloride of $10^{-4.2}$ and $10^{-4.6}$, respectively. Near-theoretical slopes were found for $10^{-4.5}$—$10^{-1.0}$ M nitrite. After contact of the sensor with flowing tap water for 35 days, no deterioration of the electrode characteristics was observed.

It has been shown recently [1, 2] that certain lipophilic derivatives of vitamin B_{12} (1, Fig. 1) exhibit considerable selectivity for nitrite when incorporated into solvent polymeric membranes. Such compounds can be used in analytically relevant sensors for nitrite [2]. Unfortunately, the nitrite carrier 1 is not easily synthesized [1]. In addition, it is desirable to have available an ion-selective component similar to 1 but with a higher lipophilicity. Because of the pronounced dependence of the electrode response on the carrier concentration in the membrane phase (see Fig. 6 [2]), a high partition coefficient of the ion-selective component between the sample and the membrane phase is essential for the type of carrier discussed, to ensure increased sensor lifetime. The lifetime is expected to be limited by a reduction in the slope of the electrode response at high activities of the primary ion (see Fig. 6 [2]). Here a convenient synthesis is reported for a considerably more lipophilic vitamin B_{12} derivative than 1 and its use in solvent polymeric membrane electrodes is described.

EXPERIMENTAL

Membranes and electrode system

The solvent polymeric membranes were prepared as described earlier [3] from 1% (w/w) carrier, 66% (w/w) of either bis(1-butylpentyl)adipate (BBPA; purum, 02150, Fluka, 9470 Buchs, Switzerland) or decane-1,10-diyl-

0003-2670/86/$03.50

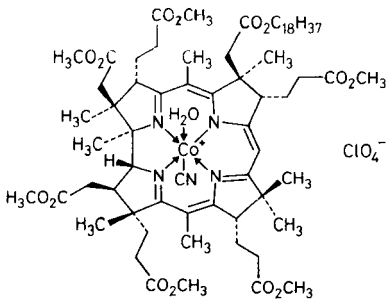

1a

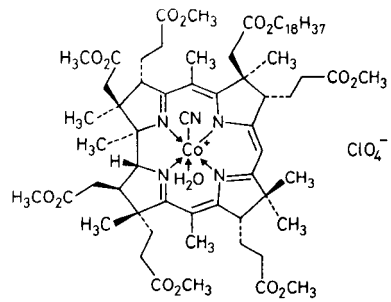

1b

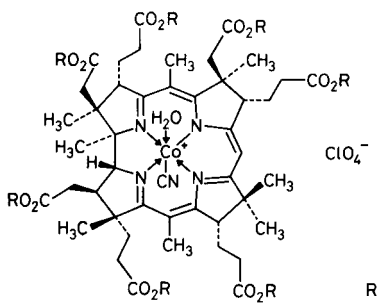

2a

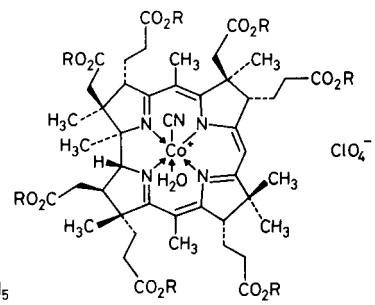

2b

Fig. 1. Structural formulae of the charged carriers used. The two coordination isomers (1a/1b) of aquocyano-Co(III)-a,b,d,e,f,g-hexamethyl-c-octadecyl cobyrinate perchlorate are available only as the mixture 1. Similarly, the two isomeric forms (2a/2b) of aquocyano-Co(III)-hepta(2-phenylethyl)cobyrinate perchlorate constitute the mixture 2.

diglutarate-bis-(1-butylpentylester) (ETH 469; p.a., 30585, Fluka) and 33% (w/w) poly(vinyl chloride) (PVC; high molecular weight, Fluka).

Cell assemblies of the following type were used: Hg; Hg_2Cl_2, KCl (satd.)|1 M LiOAc | sample solution || membrane || 0.01 M NaCl, 0.01 M $NaNO_2$, AgCl; Ag. The external reference electrode with a free-diffusion, free-flowing liquid junction which was used will be described elsewhere. The liquid membranes were mounted in Philips IS-561 electrode bodies (N.V. Philips' Gloeilampenfabrieken, Eindhoven, The Netherlands).

Procedures

E.m.f. measurements. For all e.m.f. measurements, double-distilled water (quartz equipment) and chemicals of puriss. or p.a. grade were used. The measuring equipment has been described with some comments on the necessary computations [2].

Separate solution method (s.s.m.) [4, 5]. The selectivity coefficients, log $K^{pot}_{Cl,X}$, were obtained in 0.1 M solutions of the corresponding sodium salts. The solutions were buffered with 0.01 M Tris and adjusted to pH 7.35 ± 0.05 with concentrated sulfuric acid.

Fixed interference method (f.i.m.) [4, 5]. The selectivity coefficients were graphically evaluated from the electrode functions of unbuffered sodium nitrite solutions containing 1 M concentrations of sodium chloride and sodium nitrate.

Practical response time [4, 5]. The electrode was conditioned in 40 ml of 3×10^{-3} M sodium nitrite for 3—5 min. The magnetic stirrer was then turned on (for about 2 s) and 1 ml of 0.3 M sodium nitrite was injected immediately (resulting in 1.024×10^{-2} M nitrite). E.m.f. values were measured at 160-ms intervals.

Drift [4, 5]. E.m.f. drift was examined by using a closed glass vessel with 0.1 M sodium nitrite at 24.5 ± 1°C. E.m.f. readings were taken at 15-min intervals. From a 70-h experiment, the second half yielded the results presented in this paper.

Lifetime. After the recording of a nitrite-electrode function, membranes based on 1 or 2 mounted in Philips IS-561 electrode bodies were subjected to a steady flow of regular Zurich tap water. After 35 days, the nitrite electrode function was re-examined.

Syntheses

Reagents. 2-Phenylethanol (Fluka, purum) was distilled. Potassium cyanide (Merck, p.a.) was used. *p*-Toluene sulfonic acid monohydrate (Fluka, puriss. p.a.) was dried by azeotropic removal of water from a benzene solution. Benzene, diethyl ether, hexane and chloroform were all from Fluka (puriss. p.a.). The chloroform was filtered through aluminum oxide (Woelm B, Akt. I). Thin-layer chromatography (t.l.c.) was done on plates coated with silica gel (Merck, Art. 5721). Trifluoroacetic acid (Fluka, purum) was redistilled. Methanol (Fluka, puriss.) was of u.v.-spectroscopic grade. Ethyl acetate, dichloromethane and acetone were of reagent grade.

Instruments. Perkin-Elmer PE-555 or Uvikon 810 u.v.-visible spectrophotometers were used; the data given below are λ_{max} in nanometer (log ϵ) and S indicates shoulder. For circular dichroism (CD) a Jobin-Yvon Mark III instrument was used; the wavelength of the extreme λ_m and of the zero passages λ_0 are given in nm (molar decadic circular dichroism, $\Delta\epsilon$). A Perkin-Elmer PE-125 infrared spectrometer was used with chloroform; relative intensities *s*, *m* and *w* denote strong, medium, and weak, respectively. A ^{1}H-n.m.r. Bruker WM-300 spectrometer was used ($CDCl_3$, 300.14 MHz, TMS internal reference, chemical shifts in ppm with δ(TMS) = 0, coupling constants J in Hz). The ^{13}C-n.m.r. spectrometer was a Bruker WM-300 model ($CDCl_3$, 75.47 MHz, TMS internal reference, chemical shifts in ppm with δ(TMS) = 0, multiplicities from the DEPT spectrum). For fast-atom-bombardment mass spectrometry (f.a.b.m.s.), a Kratos AEI MS-50 was fitted with the M-scan FAB-system (argon bombardment at 8—10 kV).

Dicyanocobalt(III)-hepta(2-phenylethyl)cobyrinate (3). A suspension of dicyanocobalt(III)-cobyrinate, as its heptapotassium salt 4 (55 mg, 43.5 μmol), in 8 ml of 2-phenylethanol was treated with a solution of 0.8 g of *p*-toluene sulfonic acid in 14 ml of dry benzene. Benzene was then distilled off, under reduced pressure, at 40°C and the resulting clear red solution was heated at 40°C under nitrogen for 3 days. The cold reaction mixture was diluted with 50 ml of dichloromethane and was neutralized by shaking with 100 ml of an ice-cold saturated aqueous solution of sodium hydrogencarbonate containing 0.5 g of potassium cyanide. The organic phase was filtered through a plug of dried cotton wool and the dichloromethane was distilled off. 2-Phenylethanol was removed under vacuum (10^{-3} Torr) at 40°C. The residue was purified by chromatography on three t.l.c. plates (first development with 1:4 acetone/hexane to wash off residual 2-phenylethanol; second development with 5:6 ethyl acetate/hexane plus 1% methanol containing 1% hydrocyanic acid). The nonpolar product fraction was eluted with 2:1 dichloromethane/methanol (1% HCN), and the solvents were removed under reduced pressure. The residue was taken up in ca. 50 ml of dichloromethane and shaken with ca. 100 ml of saturated aqueous sodium hydrogencarbonate (containing ca. 50 mg of potassium cyanide). The organic phase was filtered through a plug of cotton wool and dried (below 40°C in a rotary evaporator). The residue, uniform by t.l.c. (ethyl acetate/hexane/methanol + 1% HCN, 200:100:3; R_f = 0.43), was then dissolved in diethyl ether and precipitated by addition of hexane. The product 3 was obtained as 71 mg of a violet powder (ca. 41.2 μmol; 95% yield) after drying (room temperature, ca. 10^{-3} Torr, ca. 16 h).

The following spectral data were obtained. Ultraviolet-visible (methanol + 0.05% HCN; $c = 2.698 \times 10^{-5}$ mol l^{-1}): 251 S (3.91), 257 S (3.87), 265 S (3.89), 268 S (3.91), 277 (4.04), 310 (3.99), 353 S (4.18), 369 (4.50), 419 (3.40), 512 S (3.75), 544 (3.95), 583 (4.04). Circular dichroism (methanol + 0.05% HCN; $c = 2.698 \times 10^{-5}$ mol l^{-1}): 246 S (−12.8), 253 (−15.8), 266 S (−3.52), 277 (−3.15), 309 (−13.0), 325 (−7.97), 347 (−12.8), 367 (−8.90), 396 (22.1), 427 (13.2), 494 (−0.59), 536 (−0.39), 577 (0.46), 582 (−1.22), 605 (0.45), λ_0 at 375, 467, 546, 595 nm. Infrared (4%): 3080 w, 3060 w, 3010 m, 2980 m, 2120 w, 1727 s, 1602 w, 1579 s, 1498 s, 1468 m, 1454 m, 1400 m, 1391 m, 1365 m, 1351 m, 1104 m, 1087 m, 1048 m, 1030 m, 1010 m, 1000 m. ^{1}H-n.m.r.: 1.13, 1.17, 1.18, 1.32, 1.39, 1.44 (6 s, 6 CH_3), 1.53 (s, H_2O), 2.08, 2.16, [2 s, 2 CH_3, C(5)—CH_3, C(15)—CH_3] superimposed by 1.0—2.8 (m, total ca. 51 H); 2.80—3.04 (m, ca. 16 H); 3.38 [m, 1 H, HC(8)]; 3.68—3.80 [m, 2 H, HC(19) and HC(3)]; 4.15—4.52 (m, 14 H); 5.52 [s, 1 H, HC(10)]; 7.05—7.36 (m, including $CHCl_3$ ca. 50 H). Fast-atom-bombardment m.s.: 1721 (32, M^+ + 1), 1720 (39, M^+), 1719 (36), 1718 (14); 1696 (29), 1695 (57, M^+ + 1—CN), 1694 (100, M^+—CN), 1693 (82), 1692 (29); 1669 (23, M^+ + 1—2CN), 1668 (21), 1667 (25); 1655 (17); 1641 (15); etc. ^{13}C-n.m.r. ($CDCl_3$): 15.1, 15.7, 16.6, 18.4, 19.1, 19.8, 21.9 (7 q, 7 CH_3); 24.9, 25.8, 26.4, 30.0 (4 t, 4 C); 30.9 (q, CH_3); 31.1, 31.4, 31.9, 32.7, 33.9, 34.8, 34.96 (triple intensity), 35.03 (triple intensity) (8 t, 12 C); 39.2

[d, C(18)]; 41.2, 42.3 [2 t, C(2'), C(7')]; 45.6, 47.0, 48.6 [3 s, C(2), C(7), C(12)]; 53.6, 54.0, 56.6 [3 d, C(3), C(8), C(13)]; 58.2 (s, C(17)]; 64.8, 64.9, 65.0 (double intensity), 65.05, 65.11, 65.5 (6 t, 7 C); 74.7 [d, C(19)]; 82.4 [s, C(1)]; 91.2 [d, C(10)]; 102.1, 103.4 [2 s, C(5), C(15)]; 126.4 (double intensity), 126.5 (double intensity), 126.6 (double intensity), 126.7 (4 d, 7 C); 128.37 (sixfold intensity), 128.45 (eightfold intensity), 128.5 (fourfold intensity), 128.8 (tenfold intensity) (4 d, 28 C); 130.1, 130.4 (2 s, 2 CN); 137.3 (double intensity), 137.5, 137.6 (double intensity), 137.7 (double intensity) (4 s, 7 C); 163.37, 163.42 [2 s, C(6), C(14)]; 170.3, 171.0, 171.2, 171.3, 172.0, 172.2, 172.7, 173.0, 175.0, 175.5, 176.0 (11 s, 11 C).

Aquocyanocobalt(III)-hepta(2-phenylethyl)cobyrinate perchlorate (2). A solution of 3 (36.6 mg, 21.3 μmol) in 3 ml of chloroform under nitrogen was treated with 5 μl of trifluoroacetic acid and the reaction mixture was stirred at room temperature for 10 min. The volume of the red solution of the product was reduced by half by evaporation (room temperature, 10^{-3} Torr) and then diluted to its original volume with fresh chloroform. The volume of the solution was again reduced by evaporation of solvent as before, then diluted with 50 ml of dichloromethane and shaken vigorously with ca. 50 ml of aqueous 1 M sodium phosphate buffer (pH 3.1), containing ca. 800 mg of sodium perchlorate. A colour change from red to orange was observed. The organic phase was filtered through a plug of cotton wool and the solvent was stripped off (rotary evaporator at room temperature). The red residue was dissolved in dichloromethane and was precipitated by addition of hexane. After drying the precipitate (10^{-3} Torr, room temperature, ca. 16 h), compound 2 was obtained as a brick-red powder (37.6 mg, 98%). In t.l.c. (2:1 ethyl acetate/hexane) R_f was 0.59 (on $NaClO_4$-impregnated plates). The following spectral data were obtained. Ultraviolet-visible (methanol, $c = 3.004 \times 10^{-5}$ mol l^{-1}): 248 S (4.24), 252 S (4.21), 254 S (4.18), 258 S (4.15), 264 S (4.10), 268 S (4.08), 274 (4.08), 321 S (4.10), 353 (4.40), 385 S (3.75), 402 (3.73), 459 S (3.82), 490 (3.93), 522 (3.89), 586 S (2.78). Infrared (4%): 3080 w, 3060 w, 3020 m, 2955 m, 2133 w, 1727 s, 1601 w, 1578 s, 1495 s, 1469 m, 1452 m, 1415 w, 1390 m, 1348 m, 1302 m, 1284 m, 1144 s, 1085 m, 1048 m, 1017 m, 997 m, 901 w. ^{1}H-n.m.r.: 1.13, 1.23, 1.25, 1.27, 1.31, 1.41, 1.47, 1.54, 1.64, 1.65 (b, superimposed by signal from H_2O), 2.197, 2.20, 2.27, 2.30 (14 s) superimposed by 1.1—2.8 m, in total ca. 52 H; 2.80—3.06 (m, 15 H, 7 CH_2-phenyl and 1 H?); 3.22—3.38 (m, 1 H); 3.65—3.80 (m, 1 H); 3.99 (d, J = 10, ca. 1 H); 4.07 (d, J = 11, ca. 1 H): 4.14—4.56 (m, 14 H, 7 CH_2-OCO and 2 H) 6.31, 6.38 (2 s, 1 H); 7.08—7.38 (m, including $CHCl_3$, 37 H) (the spectrum indicates a ca. 2:1 mixture of the stereoisomeric forms **2a/2b**).

RESULTS AND DISCUSSION

Synthesis of compound 2

The lipophilic cationic carrier aquocyanocobalt(III)-hepta(2-phenylethyl)-cobyrinate perchlorate, **2**, is available as a (ca. 2:1) mixture of the stereoisomers **2a**/**2b**. It was synthesized via the dicyanocobalt(III)-hepta(2-phenylethyl)cobyrinate, **3**: *p*-toluene sulfonic acid catalyzed esterification of the dicyanocobalt(III)-cobyrinate, **4** [6—8] (used as its heptapotassium salt) with 2-phenylethanol and work up with addition of potassium cyanide gave **3** in ca. 95% yield. Treatment of a solution of **3** in chloroform with trifluoroacetic acid converted **3** to a mixture of the stereoisomeric aquocyanocobalt-(III)-cobyrinates **2a**/**2b** in practically quantitative yield. Compound **4** is readily produced by acid- [6, 7] or base-catalyzed [8] hydrolysis of the ester functions of dicyanocobalt(III)-heptamethylcobyrinate **5** ("cobester" [9, 10]), which in turn is available in crystalline form by methanolysis of vitamin B_{12} [9, 10]. The seemingly simpler synthetic approaches to **2** by direct acid-catalyzed esterification of vitamin B_{12} [9, 10] or by acid-catalyzed transesterification of **5** with 2-phenylethanol proved unsuitable, because there the formation of **3** was accompanied by sizable fractions of epimers [7].

Characteristics of the membranes

A comparison of the selectivities of membranes based on the new lipophilic carrier **2** with the previously described ionophore **1** is shown in Fig. 2. As expected, the selectivities are almost identical. The very high selectivities for nitrite over nitrate and chloride are further illustrated in Fig. 3. As a consequence of these high selectivities, the detection limit for nitrite is at about $10^{-4.6}$ M even in the presence of a background of 1 M sodium chloride (Fig. 3).

The observed slopes of the electrode response were -56.9 ± 1.3 mV ($10^{-4.5}$—$10^{-1.0}$ M, $n = 7$) and -57.3 ± 1.7 mV ($10^{-4.5}$—$10^{-1.0}$ M, $n = 7$) (theoretical: -58.2 mV) for pure sodium nitrite solutions (Fig. 4, right-hand side). With a background of 1 M sodium chloride, the slope was reduced to -53.0 ± 1.8 mV ($10^{-4.5}$—$10^{-1.5}$ M, $n = 6$) and for 1 M sodium nitrate to -54.2 ± 2.0 mV ($10^{-4.0}$—10^{-1} M, $n = 5$) (see Fig. 3).

The response times observed for a stepwise change in the nitrite concentration from 3×10^{-3} M to 10^{-2} M were 0.9 ± 0.3 s ($n = 5$) and 3.9 ± 1.3 s ($n = 5$) for $t_{90\%}$ and $t_{1\,mV}$, respectively. Membrane resistances obtained were in the order of 50 MΩ, which corresponds to specific resistances of about 1.2 GΩ cm (20°C).

In 10^{-2} M sodium nitrite, an e.m.f. drift of the cell assembly of $<5\ \mu V\ h^{-1}$ was observed over a period of 35 h at 24.5 ± 1°C. The standard deviation of a single determination was $\pm 40\ \mu V$ ($n = 140$).

Figure 4 corroborates the increased lifetime of sensors based on compound **2** compared to those containing compound **1**. For a further improvement of the sensor lifetime, the more lipophilic plasticizer ETH 469 was

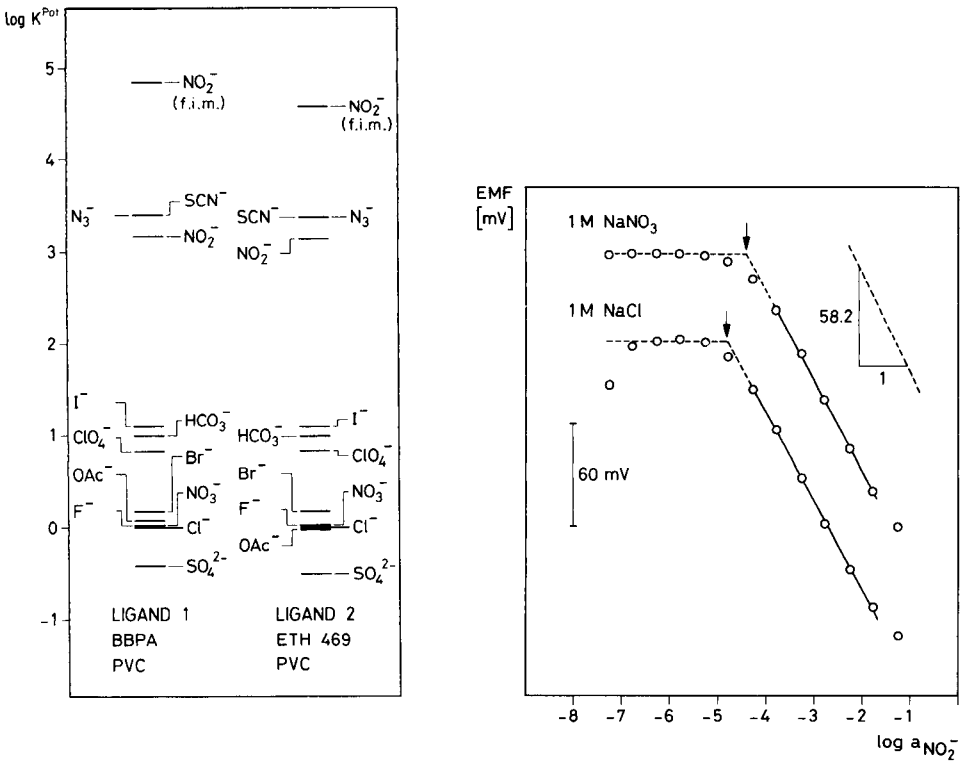

Fig. 2. Selectivity coefficients, log $K^{pot}_{Cl,X}$, for a solvent polymeric membrane based on ligand 1 with BBPA are compared to those of a membrane based on 2 with ETH 469 as plasticizer (both in PVC). Except where specified, the separate solutions method was used [4, 5].

Fig. 3. E.m.f. response of a liquid-membrane electrode cell based on carrier 2 (ETH 469, PVC) to varying activities of nitrite in the presence of 1 M $NaNO_3$ or 1 M NaCl (unbuffered solutions). The arrows indicate the detection limit for the primary ion in the presence of the interfering ion. The selectivity factors obtained are log $K^{pot}_{NO_2,NO_3} = -4.2$ and log $K^{pot}_{NO_2,Cl} = -4.6$.

used. After 35 days of continuous contact of the membranes with flowing Zurich tap water, the slope of the electrode response of sensors with 2 remained unchanged at high sample activities. Membranes with 1, however, exhibited a significant reduction in slope.

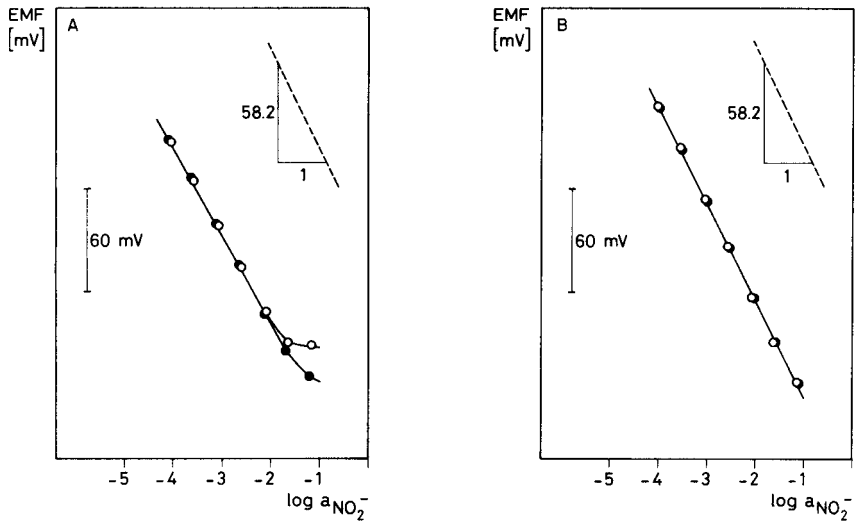

Fig. 4. E.m.f. response of liquid membrane electrodes: (A) ligand **1**, BBPA, PVC; (B) ligand **2**, ETH 469, PVC. (•) Shortly after preparation; (○) after a 35-day immersion in a steady flow of tap water. At high nitrite activities, the electrode based on **1** shows a significant decrease in the slope of the electrode response whereas the slope obtained by the electrode based on **2** remains virtually unchanged.

We thank Prof. Dr. A. Eschenmoser for support of this work, S. Blume for help with the preparative work, and Dr. J. Meili for measuring the f.a.b. mass spectrum. We acknowledge financial support from the Swiss National Science Foundation, from Corning Ltd., Sudbury (to P. S.), and from ETH-Z (to B. K. and D. A.).

REFERENCES

1 P. Schulthess, D. Ammann, W. Simon, C. Caderas, R. Stepánek and B. Kräutler, Helv. Chim. Acta, 67 (1984) 1026.
2 P. Schulthess, D. Ammann, B. Kräutler, C. Caderas, R. Stepánek and W. Simon, Anal. Chem., 57 (1985) 1397.
3 P. Anker, E. Wieland, D. Amman, R. E. Dohner, R. Asper and W. Simon, Anal. Chem., 53 (1981) 1970.
4 G. G. Guilbault, R. A. Durst, M. S. Frant, H. Freiser, E. H. Hansen, T. S. Light, E. Pungor, G. Rechnitz, N. M. Rice, T. J. Rohm, W. Simon and J. D. R. Thomas, Pure Appl. Chem., 48 (1976) 127.
5 G. G. Guilbault, R. A. Durst, M. S. Frant, H. Freiser, E. H. Hansen, T. S. Light, G. J. Moody, E. Pungor, G. Rechnitz, N. M. Rice, T. J. Rohm, J. Růžička, W. Simon and J. D. R. Thomas, IUPAC Inf. Bull., (1978) 70.
6 G. Bartels and A. Eschenmoser, unpublished work.
7 R. Stepánek, dissertation, ETH Zürich, 1986.
8 C. Nussbaumer, Dissertation No. 7623, ETH Zürich, 1984.
9 R. Keese, L. Werthemann and A. Eschenmoser, unpublished work.
10 L. Werthemann, Dissertation No. 4097, ETH Zürich, 1968.

Analytica Chimica Acta, 182 (1986) 91—101
Elsevier Science Publishers B.V., Amsterdam — Printed in The Netherlands

ION-SELECTIVE ELECTRODES BASED ON SIDEROPHORES: SALICYLATE RESPONSE OF A FERRIMYCOBACTIN MEMBRANE

DEREK MIDGLEY

Central Electricity Research Laboratories, Kelvin Avenue, Leatherhead, Surrey KT22 7SE (Great Britain)

(Received 22nd August 1985)

SUMMARY

Siderophores are compounds which transport iron across cell membranes; mycobactins are hydrophobic siderophores and were expected to be suitable for inclusion in the organic membrane phase of a liquid ion-exchange electrode responsive to iron(III) ions. In practice, no iron(III) response was obtained from mycobactin membranes (in a variety of solvents), but they did respond to salicylate ion with a sensitivity of 27—29 mV/decade over the range 2×10^{-3}—3×10^{-2} mol l^{-1} at pH 7. The effects of pH and interference by other anions are described and the possible mechanisms of the electrode are discussed. The selectivity of the electrode for salicylate is better than that of quaternary ammonium liquid ion-exchange electrodes.

Siderophores are compounds which facilitate the transport of iron across cell membranes [1, 2]. This study was started as an investigation of their potential as the active components of liquid ion-exchange electrodes for iron(III). No practical electrode for the measurement of iron(III) activity has so far been developed, although such an electrode would be of use in corrosion studies and in environmental, medical and physiological applications. Mycobactins [3] form the most promising class of siderophores for these purposes because they are hydrophobic and would not leach out of the organic phase of the liquid ion-exchange electrode.

The electrodes prepared showed none of the iron(III) response expected, but were sensitive to salicylate (with exceptionally high selectivity). This finding suggests that mycobactins alone are not sufficient to account for microbial iron transport; enzymatic processes have also been implicated [3].

Theory

The e.m.f. of the cell incorporating one of the membrane electrodes under study is given by

$$E = E^0_{Ag/AgCl} - k \log [Cl^-]' + S \log [X]/[X]' - E_{ref} + E_j \quad (1)$$

where $E^0_{Ag/AgCl}$ is the standard potential of the silver/silver chloride reference electrode inside the membrane electrode, $k = RT \ln (10)/F$ is the Nernst

slope factor, $[Cl^-]'$ is the chloride activity of the inner filling solution of the electrode, [X] and [X]′ are the activities of the transported ion X outside and inside the electrode, S is the slope factor for the membrane electrode, E_{ref} is the potential of the external reference electrode and E_j is the liquid junction potential. In practice, $[Cl^-]'$ and [X]′ are kept constant and conditions are arranged such that E_j varies less than the precision of measurement. When constant terms are collected into a single constant, E^0, Eqn. 1 is simplified to

$$E = E^0 + S \log [X] \quad (2)$$

Ideally, $S = k/z$ where z is the charge (with sign) on X, but with real membranes S is usually slightly smaller than predicted.

EXPERIMENTAL

Apparatus

The e.m.f.'s were measured with a digital pH meter reading to 0.1 mV and were displayed on a chart recorder. Solutions were stirred magnetically and were kept at 25°C by means of a thermocirculator connected to the water jacket of the test cell.

The membrane electrodes were made from Orion series 92 electrode bodies filled with appropriate aqueous and organic phases. The external reference electrode was a Corning, model 476029, silver/silver chloride electrode with a 4 mol l^{-1} potassium chloride filling solution and a ceramic frit junction.

Reagents and solutions

Reagents were of analytical-reagent grade (BDH) unless otherwise specified.

Electrode membranes. Ferrimycobactin S, was extracted from *Mycobacterium smegmatis* at the Department of Biochemistry, University of Hull, and was dissolved in either decan-1-ol, diphenyl ether or dinonyl phthalate (all BDH laboratory-reagent grade). The solution contained 1.0 ± 0.1% ferrimycobactin by weight, which was safely below the saturated concentration at room temperature. The solvents have been widely used in other liquid ion-exchange electrodes because they are hydrophobic, viscous and involatile.

Electrode filling solutions. During the experiments directed at determining the iron(III) response and the first studies of the salicylate response, the filling solution consisted of a 0.02 mol l^{-1} solution of iron(III) chloride buffered at pH 4. For most of the salicylate studies, the filling solution contained 0.05 mol l^{-1} sodium salicylate, pH 4 acetate or pH 7 Tris buffer, and 0.15 mol l^{-1} sodium chloride.

Buffer solutions. Buffer pH 7.0 was prepared from 6.05 g of tris(hydroxymethyl)aminomethane and 46.5 ml of 1 mol l^{-1} nitric or hydrochloric acid made up to 1 l [4]. A second pH 7.0 buffer (used in only one trial) was prepared from 5.96 g of *N*-2-hydroxyethylpiperazine-*N*′-2-ethanesulphonic acid (HEPES) and 5.5 ml of 1 mol l^{-1} sodium hydroxide solution made up to

500 ml [4]. The pH 8.0 buffer was prepared from 6.05 g of tris(hydroxymethyl)aminomethane and 14.6 ml of 2 mol l^{-1} hydrochloric acid made up to 1 l [4]. The pH 4.0 buffer was prepared from 161.2 g of anhydrous acetic acid and 49.5 g of sodium acetate dissolved in water and made up to 1 l; this stock solution was diluted twentyfold for use with the electrodes. Nitric acid (10^{-3} mol l^{-1}) was prepared by dilution of ConVol reagent (BDH). The pH 9.2 buffer was 0.01 mol l^{-1} sodium tetraborate. A pH 5.35 buffer was prepared by adding sodium hydroxide to the pH 4 buffer until the desired pH was attained.

Standard solutions. All the stock standard solutions listed below (0.1 mol l^{-1} except where stated otherwise) contained one of the buffers at the same concentration as above. More dilute standards were prepared by dilution of the stock solution with the appropriate buffer solution. The stock solutions prepared contained iron(III) chloride (0.02 mol l^{-1}), or iron(III) nitrate; sodium salicylate; citric acid monohydrate (pH 4) or trisodium citrate dihydrate (pH 7); malonic acid (pH 4) or malonic acid/0.2 ml l^{-1} sodium hydroxide (pH 7); tartaric acid (pH 4); maleic acid (pH 4) or maleic acid/0.18 mol l^{-1} sodium hydroxide (pH 7); dipotassium EDTA (pH 4) or dipotassium EDTA/0.1 mol l^{-1} sodium hydroxide (pH 7); potassium hydrogenphthalate (pH 4) or potassium hydrogenphthalate/0.1 mol l^{-1} tris(hydroxymethyl)aminomethane (pH 7); resorcinol; catechol; potassium thiocyanate; sodium sulphite (pH 7); 5-sulphosalicylic acid/0.1 mol l^{-1} sodium hydroxide (pH 7); sodium oxalate (pH 7) or oxalic acid/0.15 mol l^{-1} tris(hydroxymethyl)-aminomethane (pH 4); 4-hydroxybenzoic acid/0.1 mol l^{-1} sodium hydroxide (pH 7); 3-hydroxybenzoic acid/0.1 mol l^{-1} tris(hydroxymethyl)aminomethane; sodium 4-aminosalicylate (pH 7); sodium sulphate; potassium dihydrogenphosphate (pH 4) or 0.05 mol l^{-1} potassium dihydrogenphosphate/0.05 mol l^{-1} disodium hydrogenphosphate (pH 7). Malonic acid, maleic acid, catechol, and 4- and 3-hydroxybenzoic acid were general-purpose reagents.

RESULTS

Electrodes with diphenyl ether as solvent gave noisy signals which sometimes had excursions of 5—10 min duration imposed on them. Work with these electrodes never proceeded beyond preliminary investigations and none of the results reported below was obtained with them. With dinonyl phthalate and decan-1-ol solvents, the signals were much less noisy and no excursions were observed. These two solvents appeared to be equally satisfactory and no distinction is normally made below between results obtained using different solvents.

Iron response

None of the electrodes responded directly to iron(III) ion. In microbial systems, iron transport is assisted by the release of compounds of indeterminate structure known as exochelins, which form complexes with the iron.

Salicylate can fulfil the same role in synthetic culture media [5] and the response of the electrode to iron(III) in the presence of salicylate was investigated. With an excess of iron and a constant iron/salicylate ratio, virtually no response was obtained. With an excess of salicylate and a constant iron/salicylate ratio, the e.m.f. decreased in an approximately Nernstian manner, implying that the electrode responded to a negatively charged species, whether a salicylatoiron(III) complex or salicylate itself. With a constant concentration of salicylate in large excess over a variable iron(III) concentration, hardly any response was evident. The electrode, therefore, appeared to be responding to salicylate and not to a complex, and this response is investigated further below.

Salicylate response

Sensitivity. Calibrations at different pH values are shown in Fig. 1 for an electrode in which decan-1-ol served as the solvent. The best sensitivity was obtained at pH 7, where the linear part of the calibration had a gradient of −28.9 mV per decade, which is almost equal to the Nernstian slope for a doubly-charged anion. Electrodes with dinonyl phthalate as solvent were studied less extensively, but the best slopes, about −30 mV per decade, were obtained at pH 4.

Selectivity. The substances listed in Table 1 were tested in the range 1×10^{-3}–1.3×10^{-2} mol l^{-1}. Only in the cases of phthalate and maleate at pH 4, and then only for the electrode with dinonyl phthalate, were the responses approximately Nernstian. The other non-zero responses had a more or less linear dependence on concentration (Fig. 2) but in some cases (e.g., thiocyanate at pH 7) the responses were not truly linear or log-linear. For the sake of comparison, Table 1 shows these doubtful values in parentheses.

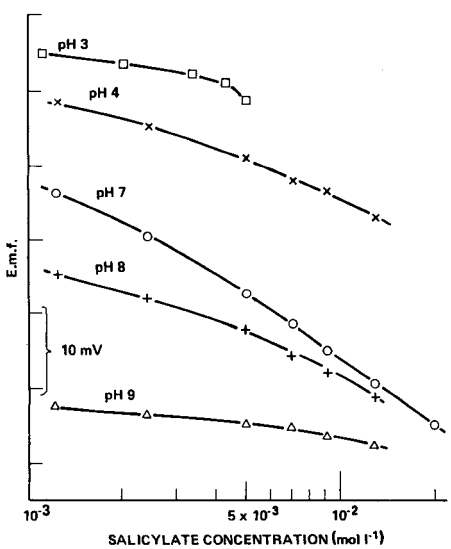

Fig. 1. Calibration curves at different pH values with decan-1-ol as solvent.

TABLE 1

Interferences[a]

Substance	Response at pH 4		Response at pH 7	
	mV/decade	mV/mmol l^{-1}	mV/decade	mV/mmol l^{-1}
Phthalate	27[b]	—	0	0
	(10[c])	0.76[c]		
5-Sulphosalicylate	—	—	0	0
4-Aminosalicylate	—	—	0	0
3-Hydroxybenzoate	—	—	(3—5)	0.18
4-Hydroxybenzoate	—	—	0	0
Catechol	—	—	(6—9)	0.3
Resorcinol	(4)	(0.35)	(3)	0.13
EDTA[d]	0	0	0	0
Tartrate	0	0	—	—
Maleate	(20[b])	(0.7[b])	0	0
	(5[c])	(0.25[c])	—	—
Thiocyanate	(10)	0.64	(10—15)	(1—34)
Sulphite	—	—	(2)	0.21

[a]Tested in the range 1.0×10^{-3}—1.3×10^{-2} mol l^{-1}. Parentheses indicate results where the linear or the log linear relationship is only approximate. [b]Dinonyl phthalate solvent. [c]Decan-1-ol solvent. [d]There was also no response at either pH to citrate, oxalate, malonate, phosphate or sulphate.

Linear non-Nernstian responses are common at the lower end of electrode response ranges [6] and it is not surprising that responses to interfering substances should take the same course.

The results show that when salicylate is further substituted with a charged group, the response is lost; neither 4-aminosalicylate nor 5-sulphosalicylate gave a response. The ability of salicylate to chelate iron(III) is presumably of importance, as there was no response to a non-chelating isomer (4-hydroxybenzoate). Other common chelating agents, such as EDTA and hydroxycarboxylic acids, showed no response, but phthalate and maleate interfered, as did the strongly complexing thiocyanate.

In aqueous solution, the interfering and non-interfering substances form iron(III) complexes of the same order of stability. The non-interfering substances, however, have more polar groups such as hydroxyl, carboxyl or sulphonate than can participate in chelation; the presence of such polar groups does not favour extraction into the organic phase and makes transport across the membrane less likely. Brown and Ratledge [7] demonstrated great differences between salicylate and 4-aminosalicylate in iron transport in mycobacteria. The chelating groups in phthalate and maleate are arranged almost identically, but phthalate had a greater interfering effect. The presence of the benzene ring in the phthalate structure should increase the tendency to dissolve in non-polar solvents.

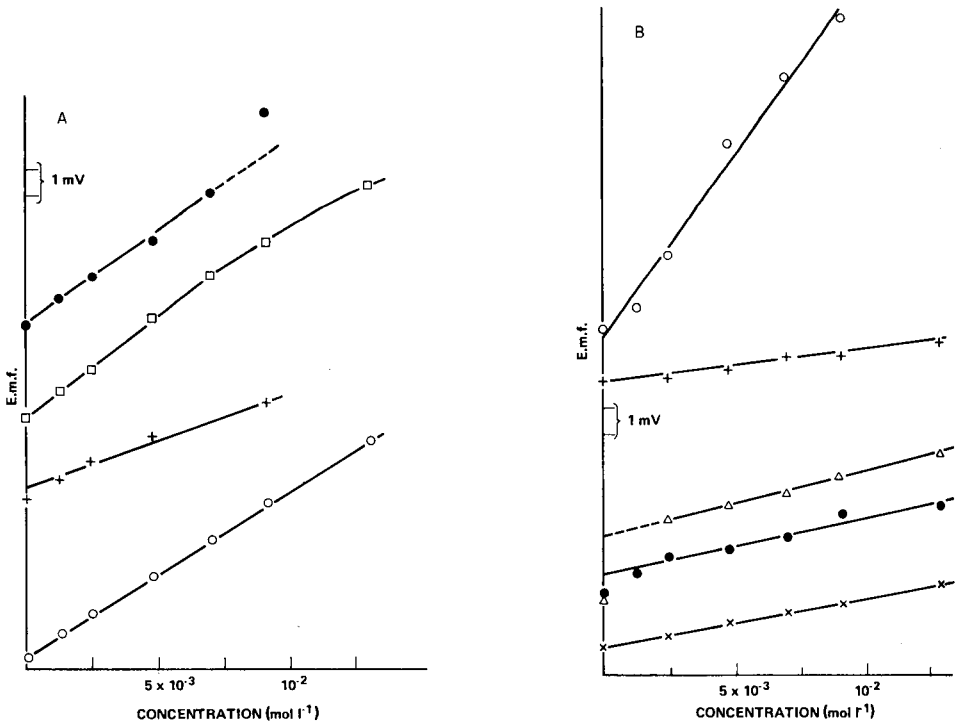

Fig. 2. Interferences. (A) At pH 4: (○) thiocyanate; (+) resorcinol; (□) phthalate; (●) maleate. (B) At pH 7: (○) thiocyanate; (+) resorcinol; (△) catechol; (●) sulphite; (×) 3-hydroxybenzoate.

The interference tests imply that a response is obtained only when the ligand can enter the organic phase, i.e., it does not arise indirectly by extraction of iron(III) from the membrane. It also follows that the ferrimycobactin complex is directly involved in the response mechanism, because there was no response to 4-hydroxybenzoate. It is also notable that phthalate and maleate did not interfere at pH 7, when both groups in each ligand would be fully ionised; this implies that only singly-charged hydrogenphthalate and hydrogenmaleate ions can be extracted from aqueous solution, i.e., when these ligands most resemble salicylate. Thiocyanate is in ionic form at both pH 4 and pH 7, and little difference was observed in its interference at the two pH values. Similarly, little difference was observed for resorcinol, which is non-ionic at both pH values.

The selectivity of the electrode for salicylate is emphasised by the small degree of interference from catechol. In aqueous solution [8, 9], catechol complexes are stronger than those of salicylate, and catechol itself seems as likely as salicylic acid to be taken up by an organic phase. On the grounds of stereochemistry, it is not surprising that resorcinol interferes less than catechol, because hydroxyl groups in the 1- and 3- positions are badly placed for

chelation. The small response to 3-hydroxybenzoate, compared with no response to 4-hydroxybenzoate, shows, however, that when the second substituent group is in the 3-position it has some power to produce a response.

Effect of pH. The effect of pH on the sensitivity is shown in Fig. 1. Because the electrodes appear to be responding to the doubly-charged salicylate species, the e.m.f. at a particular total concentration of salicylate would be expected to vary in proportion to the logarithm of the concentration of the doubly-charged ion. Table 2 shows the rounded distribution of salicylate species at different values of pH. The e.m.f. would ideally be expected to vary as shown in column 5 (neglecting changes in activity coefficients and liquid junction potentials) or, with allowance for the lower slope factors evident from Fig. 1, as shown in column 6. The observed changes at 9.1×10^{-3} mol l^{-1} are considerably smaller, implying that some different or additional mechanism is involved. The interference tests suggested that only singly-charged ions could be extracted.

Standard potential. Substituting in Eqn. 1 gives a predicted standard potential of about 230 mV in the pH 7 buffer medium. The value calculated from observed e.m.f.s was within ±20 mV of that predicted. The standard potential tended to decrease with time, at about 5 mV/day for the first day or two after a new filling solution was injected and thereafter at about 1 mV/day. When the filling solution was replaced, the old solution had acquired a red colour, implying that iron had been extracted from the membrane and formed complexes in the solution. This would reduce the free salicylate concentration inside the electrode and so decrease the standard potential, in accordance with the trend observed.

Response time. Figure 3 shows the response of the electrode to additions of sodium salicylate. The response is complete in about 2 min. When concentrations were decreased by about 50% by diluting the salicylate solution with more buffer solution, the response was complete within 30 s.

TABLE 2

Effect of pH on salicylate speciation and e.m.f.

pH	Proportion (%) of total salicylate			E.m.f. change[a]		
	$[H_2Sal]$	$[HSal^-]$	$[Sal^{2-}]$	Predicted[b]		Observed[c]
				Ideal	Observed	
3	50	50	5×10^{-9}	120	95	≈80
4	7.3	93	10^{-7}	90	58	17
5.35	0.35	99.6	2×10^{-6}	50	23	14
7	10^{-2}	100	10^{-4}	0	0	0
8	10^{-3}	100	10^{-3}	−30	−22	−15
9.2	10^{-4}	100	10^{-2}	−65	−52	−35

[a]With respect to pH 7 (Tris). [b]Predicted from ideal slope (taken as 30 mV/decade) and the observed slope (Fig. 1). [c]At 9.1×10^{-3} mol l^{-1}.

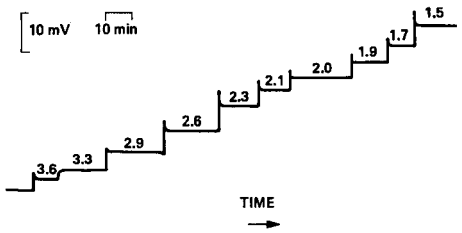

Fig. 3. Response to increased salicylate concentration; the numbers above the curves give −log [salicylate] in mol l^{-1}.

DISCUSSION

Electrode response

Ratledge and Marshall [5] showed that the uptake of iron by mycobacteria could be followed on a timescale measured in tens of seconds and that enzymatic processes were highly unlikely to be involved in the transfer of iron from the surrounding medium to the cell wall. Both these facts suggested that an ion-selective electrode should be practicable. The lack of response to iron is more likely to arise from the difficulty of removing iron from the ferrimycobactin complex. Ratledge and Marshall [5] suggested that, in the living cell, the release of iron involved an NADH-linked reductase that reduced iron(III) to iron(II) in the complex. The weakly bound iron(II) could then be removed easily from the complex. Such a mechanism would be difficult to achieve in an ion-selective electrode.

Ratledge and Winder [10] observed the accumulation of salicylic acid, but not other phenolic acids or phenols, by iron-deficient mycobacteria. Brown and Ratledge [7] demonstrated that salicylic acid was assimilated much more than 4-aminosalicylic acid by cells in iron-deficient media, that no uptake of salicylate occurred with iron-sufficient cells and that uptake of 4-aminosalicylic acid was the same in iron-sufficient and iron-deficient media. The mechanism of uptake was thus different for the two acids and this is interesting in view of the complete lack of response of the present electrode to 4-aminosalicylate. Parallels between the behaviour of membranes in ion-selective electrodes and those in living cells should, however, not be drawn too closely.

Electrode mechanism

The effect of pH indicates that the doubly-charged salicylate ion, $C_7H_4O_3^{2-}$, is not involved in the mechanism and that an alternative explanation is required for the sensitivity of about 30 mV per decade. The simplest is that the e.m.f. is a function of the square root of the concentration of singly-charged salicylate ion, $C_7H_5O_3^-$. Schemes based on this assumption are discussed below.

The anion sensitivity of the electrode requires that the membrane contains a relatively immobile cationic species [11]. Candidates for this species include

a protonated ferrimycobactin complex or a cation (other than a proton) extracted from the aqueous test and filling solutions. In the following treatments, L^- represents the salicylate ion $C_7H_5O_3^-$, M represents mycobactin, and activity coefficients have been omitted for convenience (in the aqueous phase they are kept constant by the concentration of background electrolyte). Because of the observed selectivity of the electrode for salicylate, it is assumed that it exists in the organic phase mainly as the complex $FeML^-$, which has the dissociation constant, $K_D = [L^-][FeM]/[FeML^-]$.

Mechanism (i): Mycobactin acts as hydrogen ion carrier. The equilibrium

$$L^-(aq) + H^+(aq) + 2FeM(org) \rightleftharpoons FeMH^+(org) + FeML^-(org)$$

has the equilibrium constant

$$K_A = [FeMH^+]_{org}[FeML^-]_{org}/[FeM]^2_{org}[L^-]_{aq}[H^+]_{aq} \quad (3)$$

Electroneutrality demands that $[FeMH^+]_{org} = [FeML^-]_{org} + [L^-]_{org}$ but because of the assumption that $[FeML^-]_{org}$ is the predominant form of salicylate in the membrane, the approximation $[FeMH^+]_{org} \approx [FeML^-]_{org}$ is valid. As the inner surface of the membrane can be considered to be in a constant state, the boundary potential may be written

$$E_B = E^0 - k \log ([L^-]_{aq}/[L^-]_{org}) \quad (4)$$

where k is the Nernst slope factor (theoretically 59.16 mV/decade at 25° C) and E^0 includes constant terms from the inner (reference) surface of the membrane.

Combining Eqns. 3 and 4 with the expression for K_D gives

$$E_B = E^0 + k \log \{[L^-]_{aq}[FeM]_{org}/K_D(K_A[FeM]^2_{org}[L^-]_{aq}[H^+]_{aq})^{1/2}\}$$

$$= E^0 + k \log K_D K_A^{1/2} + (k/2) \log [H^+]_{aq} - (k/2) \log [L^-]_{aq} \quad (5)$$

At a given pH in the aqueous phase, therefore, Eqn. 5 predicts that the electrode should have a sensitivity of about −30 mV per decade to salicylate, which is much as observed. It also predicts, however, a −30 mV/pH response, which is twice that observed, and that at a given pH the e.m.f. should be independent of the composition of the buffer controlling the pH, except for changes in activity coefficients. Changing from pH 7 Tris to pH 7 HEPES buffer, however, produced a shift of −20 mV.

Although this mechanism predicts the response of the electrode to salicylate at pH 7, it fails to account for the effects of pH and the nature of the buffer.

Mechanism (ii): Hydrogen ion carrier extracted. The equilibrium in this case is

$$L^-_{(aq)} + CH^+_{(aq)} + FeM_{(org)} \rightleftharpoons FeML^-_{(org)} + CH^+_{(org)}$$

and the equilibrium constant

$$K_B = [FeML^-]_{org}[CH^+]_{org}/[FeM]_{org}[CH^+]_{aq}[L^-]_{aq} \quad (6)$$

where C represents the hydrogen ion carrier (presumably the base of the buffer added to the aqueous phase). Electroneutrality requires that $[FeML^-]_{org} \cong [CH^+]_{org}$ (assuming that $[FeML^-]_{org} \gg [L^-]_{org}$). Equation 4 and the expression for K_D are still valid in this case. Combining these equations with Eqn. 6 therefore gives

$$E_B = E^0 - k \log \{[L^-]_{aq}[FeM]_{org}/K_D(K_B[FeM]_{org}[CH^+]_{aq}[L^-]_{aq})^{1/2}\}$$
$$= E^0 + k \log K_D K_B^{1/2} - (k/2) \log [FeM]_{org} + (k/2) \log [CH^+]$$
$$- (k/2) \log [L^-]_{aq} \quad (7)$$

In the organic phase, $[FeM] \gg [FeML^-]$ and [FeM] can be regarded as being constant. Collecting constant terms and expanding $[CH^+]_{aq}$ by use of its association constant, K_H, gives

$$E_M = E^{0''} + (k/2) \log K_H + (k/2) \log [C]_{aq} - (k/2)\,pH - (k/2) \log [L^-]_{aq} \quad (8)$$

Equation 8 shows the same dependence on log $[L^-]_{aq}$ and pH as Eqn. 4 but also brings in a dependence on the concentration and nature (through the term log K_H) of the carrier. The nature of the carrier also influences Eqn. 8 through the unknown constant K_B, which is included in the $E^{0''}$ term. This scheme, therefore, contains the possibility of explaining the 20-mV difference between measurements in HEPES and Tris buffers at pH 7.

According to Eqn. 8, halving $[C]_{aq}$ at constant pH and $[L^-]_{aq}$ should have produced a shift of −8.7 mV; the observed shift with Tris buffer was −2 mV at pH 7. Also according to Eqn. 8, changing from pH 7 Tris buffer to pH 8 Tris buffer at constant $[L^-]_{aq}$ and constant $[C]_{aq} + [CH^+]_{aq}$ should have produced a shift of −6 mV instead of the observed −15 mV. The requirement that the cation in the organic phase be relatively immobile may mean, however, that true equilibrium was not reached before measurements were made.

This mechanism explains the slope factor for the salicylate response at pH 7 and introduces terms which predict that the buffer composition (at a given pH) will have an effect, but it still fails to account quantitatively for the effects of pH and buffer composition. In the case of the nitric acid, acetate or borax buffers, it is difficult to see what species might carry the hydrogen ion across the interface in the form CH^+ and the electrode may be reaching some limiting response which would account for the low sensitivities in these media (Fig. 1).

Comparison with other salicylate-selective electrodes

Liquid ion-exchange electrodes for salicylate have been reported previously: in all cases they were based on a tetra-alkylammonium exchanger. Coetzee and Freiser [12] and James et al. [13] used trioctylmethylammonium salicylate in decan-1-ol in, respectively, liquid and coated wire forms. The useful range extended down only to 10^{-3} mol l^{-1} and the selectivity was poor, e.g., the selectivity coefficients for 3-hydroxybenzoate were 0.13—0.22 and for nitrate up to 0.42. Choi and Fung [14] obtained better results with this

exchanger in dibutyl phthalate solvent: the useful range reached 4×10^{-5} mol l^{-1} and the selectivity was improved, e.g., for 3-hydroxybenzoate the selectivity coefficient was 0.05. Haynes and Wagenknecht [15] used tetraheptylammonium salicylate in decan-1-ol, which gave a working range of $1—10^{-4}$ mol l^{-1}, but the electrode was approximately equally selective to other aromatic anions such as benzoate and 4-hydroxybenzoate. Mitsana-Papazoglou et al. [16] tested a variety of exchangers and solvents: the best combination was tetraoctylammonium salicylate in *p*-nitrocymene, which gave a Nernstian response down to 2×10^{-5} mol l^{-1}. All the electrodes had approximately the Nernstian response expected for a singly-charged ion (—53 to —60 mV/decade). Haynes and Wagenknecht [15] used their electrode to monitor the concentration of unreduced salicylic acid during the electrolytic production of salicylaldehyde and a miniature PVC membrane version was used in studies of respiring cells [17]. Choi and Fung [14] analysed aspirin tablets (after hydrolysis). Compared with these electrodes, the siderophore-based electrode has a lower sensitivity (ca. —27 mV/decade) but better selectivity, especially towards other aromatic anions.

I wish to thank Professor Colin Ratledge of the University of Hull for the gift of mycobactin S. This work was carried out at the Central Electricity Research Laboratories and is published by permission of the Central Electricity Generating Board.

REFERENCES

1 J. B. Neilands, in W. F. Anderson and M. C. Hiller (Eds.), Development of Iron Chelators for Clinical Use, U.S. Dept. of Health, Education and Welfare, Publication No. (NIH) 76-994 (1975), p. 5.
2 J. B. Neilands, Ann. Rev. Biochem., 50 (1981) 715.
3 C. Ratledge, in C. Ratledge and J. Stanford (Eds.), The Biology of the Mycobacteria, Vol. 1, Academic Press, London, 1982, p. 186.
4 D. D. Perrin and B. Dempsey, Buffers for pH and Metal Ion Control, Chapman and Hall, London, 1974.
5 C. Ratledge and B. J. Marshall, Biochim. Biophys. Acta, 279 (1972) 58.
6 D. Midgley, Ion-Selective Electrode Rev., 3 (1981) 43.
7 K. A. Brown and C. Ratledge, Biochim. Biophys. Acta, 385 (1975) 207.
8 A. E. Martell and L. G. Sillén, Stability Constants, Special Publication No. 17, The Chemical Society, London, 1964; Stability Constants Supplement No. 1, Special Publication No. 25, Chemical Society, London, 1971.
9 D. D. Perrin, Stability Constants of Metal-Ion Complexes. Part B. Organic Ligands. Pergamon, Oxford, 1979.
10 C. Ratledge and F. G. Winder, Biochem. J., 84 (1962) 501.
11 W. E. Morf, The Principles of Ion-Selective Electrodes and of Membrane Transport, Elsevier, Amsterdam, 1981, p. 274.
12 C. J. Coetzee and H. Freiser, Anal. Chem., 41 (1969) 1128.
13 H. James, G. Carmack and H. Freiser, Anal. Chem., 44 (1972) 856.
14 K. K. Choi and K. W. Fung, Anal. Chim. Acta, 138 (1982) 385.
15 W. M. Haynes and J. H. Wagenknecht, Anal. Lett., 4 (1971) 491.
16 A. Mitsana-Papazoglou, E. P. Diamandis and T. P. Hadjiioannou, Anal. Chim. Acta, 159 (1984) 393.
17 R. W. Hendler, H. S. Oruganti, R. I. Shrager, D. C. Songco and W. S. Friauf, Rev. Sci. Instrum., 54 (1983) 1749.

Analytica Chimica Acta, 182 (1986) 103—112
Elsevier Science Publishers B.V., Amsterdam — Printed in The Netherlands

MEDIATED AMPEROMETRIC BIOSENSORS FOR D-GALACTOSE, GLYCOLATE AND L-AMINO ACIDS BASED ON A FERROCENE-MODIFIED CARBON PASTE ELECTRODE

JONATHAN M. DICKS, WILLIAM J. ASTON[a], GRAHAM DAVIS[b] and ANTHONY P. F. TURNER*

Bioelectronics Division, Biotechnology Centre, Cranfield Institute of Technology, Cranfield, Bedfordshire, MK43 0AL (Great Britain)

(Received 15th October 1985)

SUMMARY

Direct-current cyclic voltammetry is used to investigate the suitability of a ferrocene derivative as a mediator with galactose, glycolate and L-amino acid oxidases. The three enzymes coupled catalytically to ferrocene monocarboxylic acid exhibiting homogeneous second-order rate constants in the range 0.4×10^5 to 8.5×10^5 l mol^{-1} s^{-1}. Enzyme electrodes which responded to D-galactose, glycolate or L-amino acids were constructed. The appropriate oxidase was retained behind a dialysis membrane at a carbon paste electrode containing the poorly soluble derivative 1,1'-dimethylferrocene. All the electrodes responded rapidly to millimolar concentrations of their respective substrates producing 95% of the steady-state current response in <2 min. This general method of biosensor construction should be widely applicable to oxidases and other oxidoreductase enzymes.

A new approach to the construction of amperometric biosensors with the ferricinium ion as a mediator has been described in previous reports from this laboratory [1—3]. The significant advantages offered by the use of ferrocene-modified carbon electrodes over alternative enzyme electrodes have been discussed [4—6] and the possibility of exploiting a range of oxidoreductase enzymes in this manner has been indicated. In this paper, three novel enzyme electrodes are examined in which oxygen, the natural electron acceptor for oxidases, is replaced by the ferricinium ion. The extension of the original work on glucose oxidase [2] to other oxidases suggests that the technique is generally applicable to this class of enzyme. In addition, the three new analytical probes for glycolate, galactose and L-amino acids that are characterized here may be developed and applied to clinical and biotechnological monitoring.

During the photorespiration of plant tissues (i.e., the rapid evolution of

---

Present addresses: [a]Genetics International (UK) Inc., Abingdon, Oxon, OX1 1RL, Great Britain. [b]The Medical School, University of Newcastle-upon-Tyne, Newcastle-upon-Tyne, NE2 4HH, Great Britain.

0003-2670/86/$03.50

carbon dioxide under illumination), biochemical reactions occur in association with the synthesis and metabolism of glycolic acid [7, 8]. Fluctuations in the glycolate pool can be affected by illumination intensity, atmospheric oxygen and carbon dioxide levels and temperature [9, 10]. Monitoring of photorespiratory activity usually involved assaying carbon dioxide evolution with an infrared gas analyser. Drawbacks associated with these assay procedures included insensitivity to rapid variations in carbon dioxide levels and anomalous measurement of activity resulting from plant structure, such as the diffusion gradient of carbon dioxide through the plant, the refixation of previously photorespired carbon dioxide and changes in stomatal diameter affecting the release of carbon dioxide. Measuring photorespiration in algae and submerged aquatic plants is subject to even greater discrepancies than for land plants because the diffusion of carbon dioxide in water is several orders of magnitude slower than in air. A ^{14}C-assay has been applied to monitor photorespiration, but it still suffers from the drawbacks of the normal carbon dioxide assay [11].

The spectrophotometric determination of glycolic acid up to 0.1 mg ml^{-1} was described by Calkins in 1943 [12] and is still widely applied. Although the common organic acids do not interfere, the assay is very slow and continuous on-line fermentation monitoring of algae and cyanobacteria, which have been reported to excrete millimolar concentrations of glycolate into the media [9, 10], would prove to be impractical.

Galactose and lactose are important substrates in fermentation and food production with possible implications in clinical medicine. Previously, galactose, lactose and galactoside concentrations have been determined by using a coupled spectrophotometric assay based on galactose oxidase (EC 1.1.3.9) from *Dactylium dendroides* and a horseradish peroxidase/chromogen system [13, 14]. The chromogens used such as *o*-dianisidine [13, 14], *o*-cresol [15], benzidine [16] and *o*-tolidine [17, 18] have several disadvantages. Exact estimation of the molar absorptivity of the chromogen obtained in the peroxidase reaction is difficult (several values can be found in the literature) and consequently, enzyme activities are usually recorded in arbitrary units involving absorbance rather than in moles of substrate oxidised. In addition, the chromogen often inhibits galactose oxidase, is sensitive to light or sulphyldryl reagents, tends to precipitate, requires organic solvents, is affected by pH or is a suspected carcinogen. The horseradish peroxidase used in the chromogenic system can have an activating effect on the galactose oxidase [19—22]. Alternative assays for galactose oxidase activity include fluorimetry [23], manometry [24, 25], coulometry [26] and polarography [19, 27, 28]. Amperometric enzyme electrodes incorporating immobilised galactose oxidase have been reported [29—31]. These biosensors rely on the monitoring of oxidised species, such as hydrogen peroxide, produced during the enzymatic reaction.

The rapid assay of amino acids is critical in a variety of fermentation processes because they are a major product and, in many cases, also an important

medium constituent. Clinical applications include the monitoring of various metabolic disorders, such as diabetes [32]. Several L-amino acid biosensors have been reported. These have involved detection of either ammonia released by L-amino acid oxidase (EC 1.4.3.2), with an ammonium ion-sensitive electrode [33—36], or hydrogen peroxide by amperometric means [37, 38]. The potentiometric methods are significantly affected by interferences from singly-charged cations (Na^+, K^+, H^+).

EXPERIMENTAL

Chemicals

Glycolate oxidase (EC 1.1.3.1, from *Spinacea oleracea*), galactose oxidase (EC 1.1.3.9 type V, from *Dactylium dendroides*) and L-amino acid oxidase (EC 1.4.3.2 type V, from *Crotalus adamenteus* venom) were obtained from the Sigma Chemical Co. Ferrocene monocarboxylic acid was from Sigma and 1,1'-dimethylferrocene was from Polysciences (Warrington, PA). All other chemicals and biochemicals were of analytical grade and were supplied by BDH, Sigma and Aldrich.

Direct-current cyclic voltammetry

Experiments were done in a glass cell with two compartments, the working compartment having a volume of 1 cm^3. The electrodes used were a 4-mm diameter, pyrolytic graphite disc working electrode and a 1-cm^2 platinum-gauze counter electrode. A saturated calomel electrode (SCE) was used as reference, separated from the working compartment by a Luggin capillary. Potentials relating to cyclic voltammetry experiments refer to the SCE. Prior to use, the working electrode was cleaned with an alumina/water paste (particle size 0.3 μm). The auxiliary electrode was cleaned by cycling between −0.1 V and +1.1 V in 1 M sulphuric acid until a consistent cyclic voltammogram was obtained, and then washed thoroughly with deionised water. Voltammograms were obtained by using a potentiostat (Oxford Electrodes, Garsington, Oxford) and were recorded on a JJ PL1000 XY/t recorder (J. J. Lloyd Instruments Ltd., Warsash, Southampton).

The supporting electrolyte consisted of 50 mM buffer salts, either phosphate, Tris-HCl or borate depending on the required pH, and was 0.1 M in potassium chloride. Ferrocene monocarboxylic acid was used at 0.2 mM. The substrates, sodium glycolate, L-leucine and D(+)-galactose (allowed to stand at room temperature for 2 h to allow complete mutarotation), were used at 50 mM. Temperature control within the cell was maintained to within ±0.5°C with a water-jacket fed from a thermostat bath (Model FE, Grant Instruments, Barrington, Cambridge). The temperatures maintained in the cell were 25°C for glycolate oxidase [39] and galactose oxidase [40] and 37°C for L-amino acid oxidase [41]. All solutions were first deoxygenated thoroughly by passing nitrogen. Cyclic voltammograms were recorded at scan rates of 1 to 100 mV s^{-1} over the potential range 0—400 mV. Scans were initiated at 0 V and the first scan was recorded.

Construction and testing of enzyme probes

A 5-mm platinum disc (0.025 mm thick) was attached to a copper wire with conducting thermosetting silver epoxy resin and secured inside a 6-mm diameter glass tube with Araldite epoxy resin so as to form a 2-mm deep well in the top of the tube. The well was packed with a mixture of 1,1′-dimethylferrocene and synthetic graphite powder (BDH Chemicals) blended to a paste with Spectrosol-grade liquid paraffin (BDH Chemicals). The stock paste contained 125 mg of 1,1′-dimethylferrocene, 2.5 g of graphite and 1.5 ml of liquid paraffin [1, 3]. The enzyme was made up in 50 mM buffer to a concentration of 50 mg ml^{-1} and 20 μl of this solution was pipetted onto the paste and covered with a 5-mm circle of absorbent paper tissue. A polycarbonate membrane (20-mm diameter, 30-nm pore size (Nuclepore)) was placed over the end of the electrode so as to exclude any air, and was secured with a rubber O-ring.

The electrochemical cell used to test the enzyme probes had a working volume of 5 ml and was operated in a two-electrode mode with a 40 × 5 mm Ag/AgCl reference electrode. Probes were equilibrated at an operating voltage of 220 mV (vs. Ag/AgCl) in electrolyte buffer for 1 h prior to calibration. The electrolyte composition and temperatures were the same as those used for the cyclic voltammetry studies. Portions of substrate solution were added to the cell and mixed thoroughly throughout the experiment with a magnetic stirrer.

Programmable testing. A four-channel programmable interface package [5] designed in association with Artek (Lavendon, Bucks.) connected to a BBC microcomputer model B (Acorn, Cambridge) was used to test the probes. The interface provided 12-bit software control of the voltage applied concurrently to four enzyme electrodes and allowed the amperometric response of each to be continuously recorded. The program was written principally in BBC BASIC.

Enzyme activity/pH profiles

The 0.10 M buffers used were sodium phosphate (pH 6.0—8.0), Tris-HCl (pH 8.0—9.5) and borate (pH 9.5—10.5). Cyclic voltammetry was normally done at the pH optimum for the natural redox couple of the enzyme; for glycolate oxidase this was pH 8.3 [39] and for L-amino acid oxidase it was pH 7.8 [41]. In the presence of ferrocene monocarboxylic acid, the pH optimum of galactose oxidase shifted to pH 9.0. At the pH optimum for the reaction with oxygen (pH 6.5), galactose oxidase did not give a cyclic voltammogram indicative of a catalytically coupled reaction. Kinetic constants for galactose oxidase were measured at pH 9.0. Enzyme probes were tested at the pH optimum for their reaction with oxygen in all three cases.

Separation techniques

High-performance gel-filtration chromatography. For gel filtration of the three enzymes, a Varian 5000 liquid chromatograph was used with an LKB

Ultropak TSK-G-3000-SW (7.5 × 600 mm) column. The carrier solution contained sodium phosphate buffer (0.10 M, pH 7.0) and 0.10 M sodium chloride. The sample (1 ml containing 20—100 mg of protein) in the sodium phosphate buffer was injected onto the column and eluted at 0.5 ml min^{-1} and 28 atmospheres pressure. The eluted protein was monitored spectrophotometrically at 280 nm. The molecular weight markers used were: α-lactalbumin (m.w. 14 200), bovine erythrocyte carbonic anhydrase (29 000), chicken egg albumin (45 000), bovine serum albumin (monomer 66 000, dimer 132 000), and jack bean urease (dimer 240 000, tetramer 480 000).

SDS/polyacrylamide gel electrophoresis. Electrophoresis was done in 12% (w/v) acrylamide gels using the discontinuous buffer system of Laemmli [42]. The following proteins were used as molecular weight markers: α-lactalbumin (m.w. 14 200), soybean trypsin inhibitor (20 100), PMFS-treated trypsinogen (24 000), bovine erythrocyte carbonic anhydrase (29 000), rabbit muscle glyceraldehyde-3-phosphate dehydrogenase (36 000), egg albumin (45 000), and bovine albumin (66 000). The gels were analysed for protein bands by staining with coomassie brilliant blue R250 and monitoring the absorbance at 650 nm on a Beckman DU8 spectrophotometer gel-scanning system.

RESULTS AND DISCUSSION

Estimation of purity and molecular weight of the enzymes

The purity of the respective enzyme as a percentage of the total protein was determined by gel-filtration chromatography and polyacrylamide gel electrophoresis. Estimation of the enzyme monomeric molecular weight by electrophoresis and the molecular weights reported by other workers allowed an approximate value for enzyme molarity to be calculated (Table 1).

TABLE 1

Monomeric molecular weights of the enzymes determined by SDS/polyacrylamide gel electrophoresis and gel-filtration chromatography, and the estimated purity of the enzyme preparations

Enzyme	Enzyme purity (% of total protein)		Monomeric molecular weight	
	Electrophoresis	Gel filtration	Electrophoresis	Literature value
Glycolate oxidase	38	45	39 600	37 000 [43]
L-Amino acid oxidase	42	52	60 000	61 600 [44]
Galactose oxidase	41	—[a]	68 000	68 000 [40]

[a]Not determined.

The enzyme/mediator catalytically-coupled reactions

Direct-current cyclic voltammetry showed that addition of glycolate oxidase to ferrocene monocarboxylic acid and glycolate altered the reversible Nernstian behaviour of the ferrocene at a pyrolytic graphite electrode. The enzyme induced an increase in the oxidation current and concomitant lowering of the reduction current. This phenomenon was most apparent at slower scan rates (Fig. 1). This observation is indicative of the enzyme-dependent catalytic re-reduction of ferricinium ion produced at oxidising potentials [2].

The theory of stationary electrode voltammetry developed by Nicholson and Shain [45] can be used to analyze a catalytically-coupled reaction. The reaction scheme can be described as: $R - e^- \rightleftharpoons O$; $Z + O \xrightarrow{k_f} R$, where R and O refer to the respective reduced and oxidized forms of the species, Z is the reduced enzyme, and $k_f (= k[Z])$ is the pseudo-first-order rate constant. If the experimentally derived parameter i_K/i_D, the ratio of the kinetically-controlled current (in the presence of the enzyme) to the diffusion-controlled current (in the absence of the enzyme), is equated to the kinetic parameter $(k_f/a)^{1/2}$, a value of k_f/a for each enzyme concentration can be derived (where $a = nFv/RT$, v being the scan rate in V s^{-1}). A plot of k_f/a vs. $1/v$ at each enzyme concentration under pseudo-first-order conditions should be linear, with a slope of RTk_f/nF. This procedure allows a pseudo-first-order rate constant to be obtained independent of scan rate. A plot of k_f vs. enzyme concentration is also linear with a slope equal to the second-order homogeneous rate constant k_s for the reaction between ferricinium monocarboxylic acid and the enzyme. Rate constants for the enzymes used in this work were

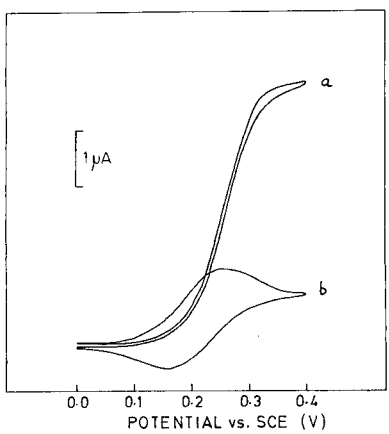

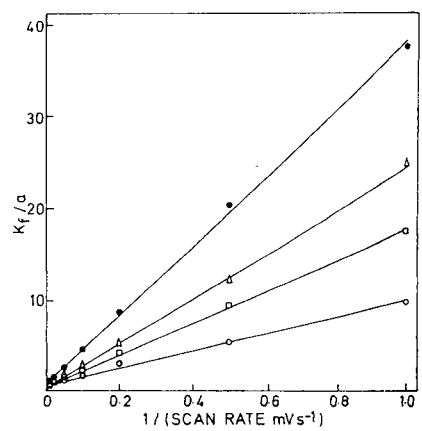

Fig. 1. Cyclic voltammograms of ferrocene monocarboxylic acid (0.2 mM) at pH 8.3 and 25°C (scan rate 1 mV s^{-1}): (a) in the presence of 50 mM glycolate with 12.1 μM glycolate oxidase; (b) in the presence of 50 mM glycolate only.

Fig. 2. Kinetic parameter K_f/a as a function of $1/v$ for the interaction between ferrocene monocarboxylic acid and glycolate oxidase at the following enzyme concentrations: (○) 1.61; (□) 3.78; (△) 6.27; (●) 12.1 μM. Cyclic voltammetry was done at pH 8.3 and 25°C.

determined by the above method, with the enzyme concentration expressed in terms of mol l^{-1}.

Ferricinium ion as an oxidant for glycolate oxidase, L-amino acid oxidase and galactose oxidase

The cyclic voltammograms produced by ferrocene monocarboxylic acid showed no indication of being affected by the sole addition of either of the three enzymes or their respective substrates. Galactose oxidase did not detectably couple catalytically with ferrocene monocarboxylic acid at the pH optimum for its natural co-substrate oxygen and so a pH profile for this enzyme was constructed. This profile showed an optimum for use with ferrocene monocarboxylic acid of pH 9.0, hence all cyclic voltammetric studies with this enzyme were done at this pH at 25°C.

In Fig. 2 the data are plotted for a series of glycolate oxidase concentrations as k_f/a vs. $1/v$. Values for the calculated pseudo-first-order and second-order homogeneous rate constants are presented in Fig. 3 and Table 2, respectively. The results show that all three enzymes couple catalytically to ferrocene monocarboxylic acid in free solution. Whilst galactose oxidase was not at the pH optimum exhibited in the presence of its natural redox acceptor, all the enzymes exhibited k_s values for the interaction between enzyme and mediator in the range 0.4×10^5—8.5×10^5 l mol^{-1} s^{-1}. The rates of these fast catalytic reactions are suitable for biosensor applications.

Enzyme electrode calibration

Ferrocenes meet many of the criteria required of a mediator [4—6]; the oxidised form of 1,1'-dimethylferrocene is stable at pH 7.0 and its reduced

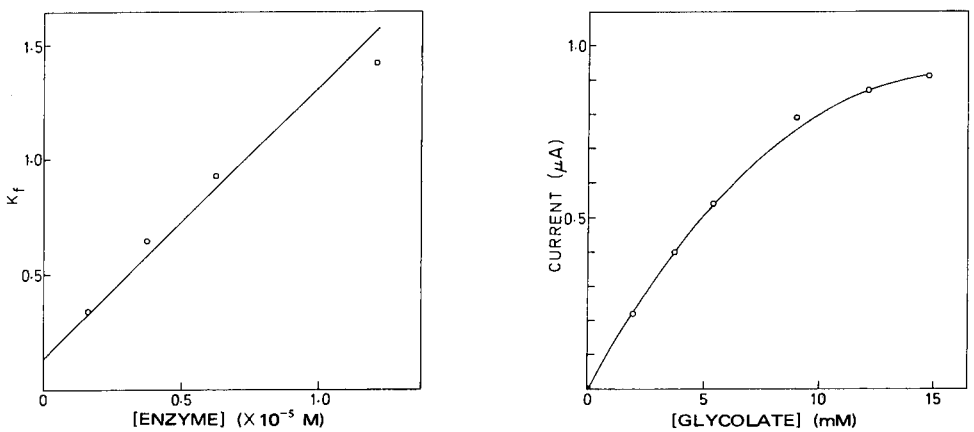

Fig. 3. Pseudo-first-order rate constant K_f as a function of glycolate oxidase concentration for the interaction between ferrocene monocarboxylic and acid and glycolate oxidase. Cyclic voltammetry was done at pH 8.3 and 25°C.

Fig. 4. Typical calibration curve for the glycolate oxidase/1,1'-dimethylferrocene electrode. Steady-state currents were measured at 220 mV vs. Ag/AgCl, pH 8.3 and 25°C.

TABLE 2

Homogeneous second-order rate constants (k_s) for the interaction between enzyme and ferrocene monocarboxylic acid, determined by cyclic voltammetry

Enzyme	k_s ($l\ mol^{-1}\ s^{-1}$)	Temp. (°C)	pH
Glycolate oxidase	1.15×10^5	25	8.3
L-Amino acid oxidase	0.40×10^5	37	7.8
Galactose oxidase	8.5×10^5	25	9.0

form is relatively insoluble in aqueous solution, which aids its entrapment in a sensor configuration. The oxidation potential of 1,1′-dimethylferrocene is low enough to decrease interferences from other reduced substances and the compound gave the most effective oxidation of glucose via glucose oxidase at physiological pH [2]. Therefore, 1,1′-dimethylferrocene was chosen as the mediator for the enzyme electrode construction.

A typical calibration curve for a glycolate oxidase enzyme electrode is presented in Fig. 4 and apparent K_m values for all the enzyme electrodes are presented in Table 3. The latter derived from Eadie-Hofstee plots (current/[S] vs. current where [S] is the substrate concentration). All the electrodes tested gave 95% of the total current response in under 2 min. Steady-state currents were measured at an applied potential of 220 mV (vs. Ag/AgCl).

The enzyme sensors utilising 1,1′-dimethylferrocene showed a response to their substrate at the pH optimum of the enzyme. However, the apparent Michaelis constant (K_m) values derived for the sensors are higher than would be normally found for the enzyme in free solution, because the membrane trapping the enzyme produces conditions limited by diffusion of the substrate. Reproducibility from electrode to electrode and general electrode performance may be improved by using a covalently immobilized enzyme [2]. It is clear, however, that the principles applied to the construction of previous sensors [1—3] may be used to harness other oxidases that will utilise artificial electron acceptors, and allow the construction of a range of sensors capable of continuous operation. Further work is in progress to establish the practical usefulness of these probes in real analytical situations.

TABLE 3

Apparent Michaelis constant (K_m) values for the interaction between enzyme and 1,1′-dimethylferrocene in an enzyme/carbon paste electrode configuration

Enzyme probe	K_m (mM)	Temp. (°C)	pH
Glycolate oxidase	13.1	25	8.3
L-Amino acid oxidase	16.5	37	7.8
Galactose oxidase	14.5	25	6.5

This work was first presented at the Second Conference for Analytical Science (Analyticon 84) held at the Barbican Centre, London, September, 1984. A. P. F. Turner is a Senior Fellow of the British Diabetic Association and J. M. Dicks holds a SERC Studentship. G. Davis and W. J. Aston thank Genetics International for financial support. The authors are grateful to Professor I. J. Higgins and Dr. M. Cardosi for helpful advice.

REFERENCES

1 W. J. Aston, R. E. Ashby, I. J. Higgins, L. D. L. Scott and A. P. F. Turner, in M. J. Allen and P. N. R. Usherwood (Eds.), Charge and Field Effects in Biosystems, Abacus, Tunbridge Wells, 1984, p. 491.
2 A. E. G. Cass, G. Davis, G. D. Francis, H. A. O. Hill, W. J. Aston, I. J. Higgins, E. V. Plotkin, L. D. L. Scott and A. P. F. Turner, Anal. Chem., 56 (1984) 667.
3 A. P. F. Turner, W. J. Aston, I. J. Higgins, J. M. Bell, J. Colby, G. Davis and H. A. O. Hill, Anal. Chim. Acta, 163 (1984) 161.
4 W. J. Aston and A. P. F. Turner, in G. E. Russel (Ed.), Biotechnology and Genetic Engineering Reviews, Vol. 1, Intercept, Newcastle Upon Tyne, 1984, p. 89.
5 A. P. F. Turner, in The World Biotech Report, 1985 Vol. 1: Europe, Online, Northwood, 1985, p. 181.
6 I. J. Higgins, M. F. Cardosi and A. P. F. Turner, in NATO ASI Series (Life Sciences), Plenum, New York, 1985, in press.
7 I. Zelitch and S. Ochoa, J. Biol. Chem., 201 (1953) 707.
8 I. Zelitch, J. Biol. Chem., 201 (1953) 719.
9 R. K. Ingle and B. Coleman, Planta, 128 (1976) 217.
10 M. Larsson, C. Larsson and R. Ullrich, Plant Physiol., 70 (1982) 1637.
11 I. Zelitch, in A. S. Pietro (Ed.), Methods in Enzymology, Vol. 69, Part C, Academic Press, New York, 1980, p. 453.
12 V. P. Calkins, Ind. Eng. Chem. Anal. Ed., 15 (1943) 762.
13 G. Avigad, C. Asensio, D. Amaral and B. L. Horecker, Biochem. Biophys. Res. Commun., 6 (1961) 474.
14 G. Avigad, D. Amaral, C. Asensio and B. L. Horecker, J. Biol. Chem., 237 (1962) 2736.
15 W. Fisher and Z. Zapf, Hoppe-Seyler's Z. Physiol. Chem., 337 (1964) 186.
16 H. Roth, S. Segal and D. Bertoli, Anal. Biochem., 10 (1965) 32.
17 H. Forster and M. Haslbeck, Z. Klin. Chem. Klin. Biochem., 5 (1967) 198.
18 R. A. Schlegel, C. M. Gerbeck and R. Montgomery, Carbohydr. Res., 7 (1968) 193.
19 L. Cleveland, R. E. Coffman, P. Coon and L. Davis, Biochemistry, 14 (1975) 1108.
20 L. D. Kwiatowski and D. J. Kosman, Biochem. Biophys. Res. Commun., 53 (1973) 715.
21 G. A. Hamilton, R. L. Libby and C. R. Harzell, Biochem. Biophys. Res. Commun., 55 (1973) 333.
22 J. Olsen, PhD Thesis, University of Maryland; Diss. Abstr. Int. B, 37 (1977) 3934.
23 G. G. Guilbault, P. J. Brignac and M. Juneau, Anal. Chem., 40 (1968) 1256.
24 J. A. D. Cooper, W. Smith, M. Bacila and H. Medina, J. Biol. Chem., 234 (1959) 445.
25 G. A. Hamilton, J. DeJersey and P. K. Adolf, in T. King, H. S. Mason and M. Morrison (Eds.), Oxidases and Related Redox Systems, Vol. 1, University Press, Baltimore, MD, 1973, p. 103.
26 C. D. McGlothlin and W. C. Purdy, Anal. Chim. Acta, 88 (1977) 33.
27 D. Amaral and M. Bacila, Arq. Biologia Technol., 12 (1967) 179.
28 G. T. Zancan and D. Amaral, Biochim. Biophys. Acta, 198 (1970) 146.
29 F. Lang, E. Gstrein, J. Geibel, W. Rehwald, H. Völkl and H. Oberleithner, Bioelectrochem. Bioenergetics, 11 (1983) 365.

30 J. M. Johnson, H. B. Halsall and W. R. Heineman, Anal. Chem., 54 (1982) 1377.
31 H. L. Pardue and C. S. Frings, J. Electroanal. Chem., 7 (1964) 398.
32 A. P. F. Turner and J. C. Pickup, Biosensors, 1 (1985) 85.
33 G. G. Guilbault and E. Hrabankova, Anal. Lett., 3 (1970) 53.
34 G. G. Guilbault and E. Hrabankova, Anal. Chem., 42 (1970) 1779.
35 G. Johansson, K. Edström and L. Ögren, Anal. Chim. Acta, 85 (1976) 55.
36 R. M. Ianniello and A. M. Yacynych, Anal. Chim. Acta, 131 (1981) 123.
37 G. G. Guilbault and G. J. Lubrano, Anal. Chim. Acta, 69 (1974) 183.
38 R. M. Ianniello and A. M. Yacynych, Anal. Chem., 53 (1981) 2090.
39 A. L. Baker and N. E. Tolbert, Methods Enzym., 9 (1966) 338.
40 M. J. Ettinger and D. J. Kosman, in T. G. Spiro (Ed.), Metal Ions in Biology, Vol. 3, Copper Proteins, Wiley, New York, 1981, p. 219.
41 D. Wellner and A. Meister, J. Biol. Chem., 235 (1960) 2013.
42 U. K. Laemmli, Nature (London), 277 (1970) 680.
43 Y. Lindqvist and C. I. Brändén, J. Biol. Chem., 254 (1979) 7403.
44 T. P. Singer and E. B. Kearney, Arch. Biochem. Biophys., 29 (1950) 190.
45 R. S. Nicholson and I. Shain, Anal. Chem., 36 (1964) 706.

Analytica Chimica Acta, 182 (1986) 113—122
Elsevier Science Publishers B.V., Amsterdam — Printed in The Netherlands

COMPARISON OF MICROBIAL SENSORS BASED ON AMPEROMETRIC AND POTENTIOMETRIC ELECTRODES

MARCO MASCINI*

Dipartimento di Scienze e Tecnologie Chimiche, II Universita di Roma Tor Vergata, 00173 Roma (Italy)

ADRIANA MEMOLI

Istituto di Chimica Farmaceutica e Tossicologica, I Universita di Roma La Sapienza, Roma (Italy)

(Received 6th September 1985)

SUMMARY

Microbial sensors based on oxygen and carbon dioxide electrodes coupled with immobilized *Saccharomyces* are compared for measurements of glucose and other carbohydrates. With the oxygen sensor, the yeast works under aerobic conditions but anaerobically with the carbon dioxide sensor. The two metabolisms of the same strain make little difference to the lifetimes (>15 days), selectivities and response rates (5—10 min) of the sensors. The effects of pH are very different owing to the pH sensitivity of the carbon dioxide sensor. The viable concentration ranges overlap; the oxygen-based sensor is more useful for low concentrations of glucose (0.01—1 mmol l^{-1}) while the carbon dioxide-based sensor is better suited for 1—10 mmol l^{-1}. With the oxygen-based sensor, the response time is governed by the rate of metabolism; with the carbon dioxide-based sensor, the response time of the potentiometric carbon dioxide electrode is the rate determining step.

Several microbial sensors have been described in recent years [1—10]. A bacteria or yeast is coupled with some electrometric device, usually an amperometric oxygen electrode [1—5] or a potentiometric ammonia or carbon dioxide sensor [6—10]. The features of the two types are quite different because the amperometric devices have a linear response and the measurement of oxygen is limited by the oxygen concentration in the buffer regulated by the oxygen partial pressure in the air, whereas the carbon dioxide sensor is a logarithmic device for which the sensitivity in aqueous solutions is limited by the partial pressure of carbon dioxide in air and by the pH of the sample solution [11]. It seemed worthwhile to compare the analytical features of a single microbial strain which can be coupled directly with both types of sensor to obtain information on the practical application of the class of electrochemical devices generally called "microbial sensors".

Saccharomyces cerevisiae was used; this well known yeast strain has been fully characterized [12]. Its metabolism has been studied extensively [13]; glucose (and other carbohydrates and some amino acids) are transported

0003-2670/86/$03.50

across the plasma membrane of the yeast cell and it is metabolized through a glycolytic cycle. In anaerobic conditions, the final step of this cycle is the production of ethanol; in aerobic conditions the final pathway is Krebs (citric acid, TCA) cycle which needs oxygen for the processes of oxidative phosphorylation. Both processes develop carbon dioxide. Coupling this yeast with an oxygen or carbon dioxide sensor is straightforward and the assembled microbial electrode responds to glucose (and some other organic compounds) by decreasing the oxygen concentration or by increasing the production of carbon dioxide. The behaviour of the two sorts of sensor was compared in terms of analytical features such as calibration curves, sensitivity, selectivity, pH effect, response time and lifetime.

EXPERIMENTAL

Apparatus and reagents

An Orion Research Model 97-08 oxygen electrode was used, attached to a Radiometer pHM-64 meter and an Omniscribe recorder (Houston Instruments). The gas-permeable membranes were polypropylene and the internal solution was 0.1 mol l^{-1} potassium chloride. For calibration of the oxygen sensor, the meter reading was set to 10.0 (in the pH scale) with the sensor in aerated buffer without living cells; in this way, a decrease of 1 in the pH scale on the meter corresponds to a decrease of 10% of the saturation level. The carbon dioxide sensor was obtained from Radiometer (model pCO_2 E-5036-0) and the gas-permeable membranes were teflon (D-602); the internal solution was 0.01 mol l^{-1} sodium hydrogen carbonate/0.1 mol l^{-1} potassium chloride.

Measurements were made in a cell thermostated at 30 ± 0.2°C unless specified otherwise.

Suspensions of cells were measured by turbidimetry with a Beckman Model DB-G spectrophotometer (1-cm silica cells).

All chemicals used were of reagent grade. Solutions were prepared with distilled-deionized water.

Culture and immobilization of the micro-organisms

The yeast strains were obtained from bakeries or from the American Testing Culture Collection (ATCC 2814). The strain was cultured under aerobic conditions in Petri dishes in Sabourand dextrose/agar at 27°C for 48 h. The cells were washed several times with distilled water until the oxygen content of a 0.25% (w/v) suspension was stable, to ensure that all nutrients had been washed out. Such a suspension diluted tenfold had an absorbance of 0.35 at 562 nm. A portion (6 ml) of the undiluted suspension was placed dropwise on a porous acetylcellulose membrane (type GA, 0.45-μm pore size, 25-mm diameter; Metricel, Gelman, Ann Arbor, MI) under moderate vacuum. The membrane with adsorbed micro-organisms was dried and stored in a refrigerator.

Assembly of the microbial sensors and procedure

The assembly of the probe is summarized in Fig. 1. Small disks (7-mm diameter) were cut from a 25-mm diameter porous membrane and used for both types of probe. The immobilized micro-organism was coupled with the electrode by holding the porous membrane against the gas-permeable membrane by means of a dialysis membrane and a rubber ring. The treated side of the porous membrane faced the gas-permeable membrane. The structure of both the probes was such that the lower part with gas-permeable membrane could be unscrewed for storage in a refrigerator between experiments.

The assembly of the immobilized micro-organism membrane makes it possible to renew the external dialysis membrane if any microbial hydrolytic effect alters the response time characteristics.

For testing the probes, 20 ml of phosphate buffer (0.1 mol l^{-1}, pH 6.8 unless otherwise specified) was placed in a thermostated cell at 30°C under constant and moderate magnetic stirring, and aliquots of a standard solution of the substance being tested were added. The phosphate buffer solution was saturated with air before testing was started.

RESULTS AND DISCUSSION

Response time

Figure 2 shows typical response curves of the electrodes coupled with immobilized *Saccharomyces cerevisiae*. With the oxygen electrode (Fig. 2a),

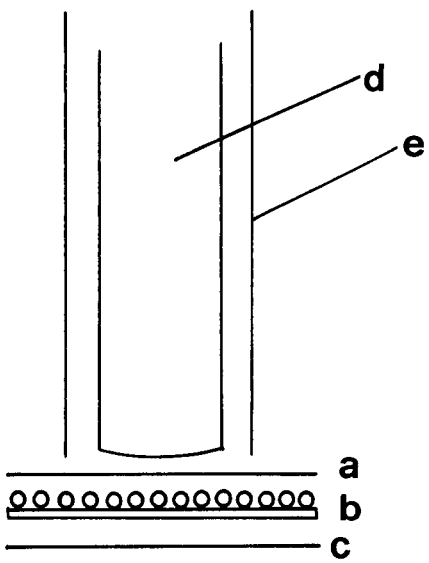

Fig. 1. The assembled microbial electrode: (a) gas-permeable membrane; (b) cellulose acetate membrane with immobilized cells on the internal side; (c) dialysis (cellulose) membrane; (d) internal element sensor (pH or oxygen electrode); (e) external case of the sensor to which the gas-permeable membrane and dialysis membrane are fixed with a rubber O-ring.

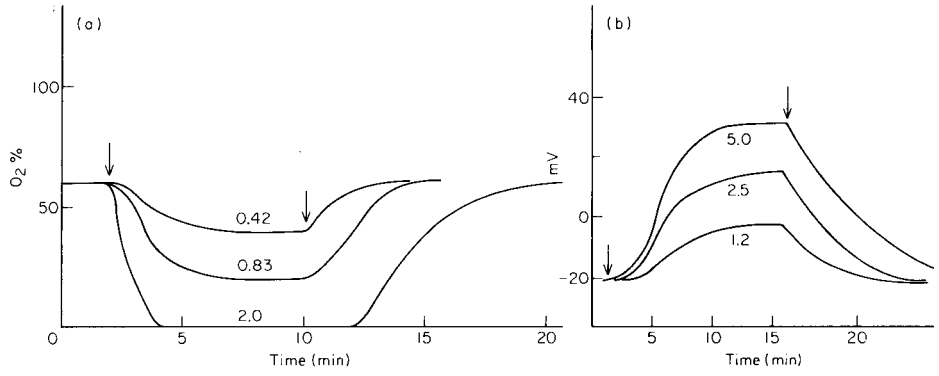

Fig. 2. Response curves of the microbial sensors. (a) Coupling with the oxygen sensor: the arrows indicate the introduction of the glucose into phosphate buffer pH 6.8 (0.01 mol l^{-1}) and then washing with buffer. (b) Coupling with the carbon dioxide sensor: the arrows indicate the introduction of glucose into phthalate buffer pH 5.0 (0.1 mol l^{-1}) and then washing to restore the initial value. The numbers correspond to the final concentration of glucose (mmol l^{-1}).

the current at zero time obtained with buffer solution is smaller than the current obtained without immobilized cells and shows the endogenous respiration level of the immobilized micro-organism. This difference decreases with time, indicating the lifetime of the strain, and thus acting as a measure of the activity of the sensor. This difference cannot be too great because of the subsequent reaction with oxygen of glucose. It was established during the testing that the difference between the oxygen in aerated buffer with and without the microbial membrane should not be higher than 60% or less than 10%. When the glucose solution was injected into the cell, the assimilation process began and consumption of oxygen occurred, causing a decrease in the current. In a few minutes, a new stable value of current was obtained.

With the carbon dioxide sensor (Fig. 2b), the initial value corresponds to an endogenous carbon dioxide level because of the respiration rate of the yeast. This value was in the range 0.2—0.5 mmol l^{-1} of hydrogen carbonate and, as for the oxygen sensor, it can be considered a measure of the activity of the cells. The value decreases with the lifetime of the assembled sensor, but it is much less sensitive than the oxygen measurement.

The response times of the microbial sensors are rather high in comparison with the response time of an oxygen electrode, which must be due to the microbial metabolism. However, the response time of a carbon dioxide electrode in a sample which is at pH 5—7 is of the same order of magnitude. Thus the cell sensors assembled with the carbon dioxide probe are slower than the oxygen-based sensors.

Calibration curves

Figure 3 shows typical calibration curves for both the glucose sensors. The linear range of concentration with the oxygen-coupled sensor is 0.05—0.7 mmol l^{-1} with a typical correlation coefficient (r) of 0.992. The higher limit of the glucose concentration can be compared with the oxygen concentration of 0.24 mmol l^{-1} at 30°C. Half of this oxygen is consumed by the microbe metabolism; at zero glucose concentration, the percentage of available oxygen was about the half of the dissolved oxygen (100%). Then the stoichiometric ratio between the glucose added and oxygen consumed is 7:1; this is a variable ratio depending on the lifetime of the organisms and becomes higher when they are exhausted.

In Fig. 3(b) the calibration curves for the carbon dioxide-coupled sensor are compared with the response to hydrogen carbonate under the same conditions. The response of cells electrode is a function of the buffer concentration; if the buffer is 0.1 mol l^{-1}, the stoichiometric ratio between glucose and carbon dioxide in the linear range is almost 1:1, but if the buffer is 0.01 mol l^{-1}, the ratio becomes 1:2. In the latter case, the response tends to be super-Nernstian, which can be explained by a change of pH in the layer surrounding the cells next to the gas-permeable membrane. The ionic strength also influences the endogenous level of carbon dioxide, which is higher in the 0.01 mol l^{-1} buffer. The linear range of concentration (mV vs. log concentration) in the 0.1 mol l^{-1} phosphate medium with the carbon dioxide-coupled sensor is 1—15 mmol l^{-1} with a typical slope of 60 mV/decade and a correlation coefficient of 0.996.

Comparison between the two concentration ranges shows that the carbon dioxide-coupled sensor works in a range tenfold higher than the oxygen-coupled sensor. With the latter, the oxygen in solution is completely consumed at the limiting value and the metabolism of the cells becomes anaerobic.

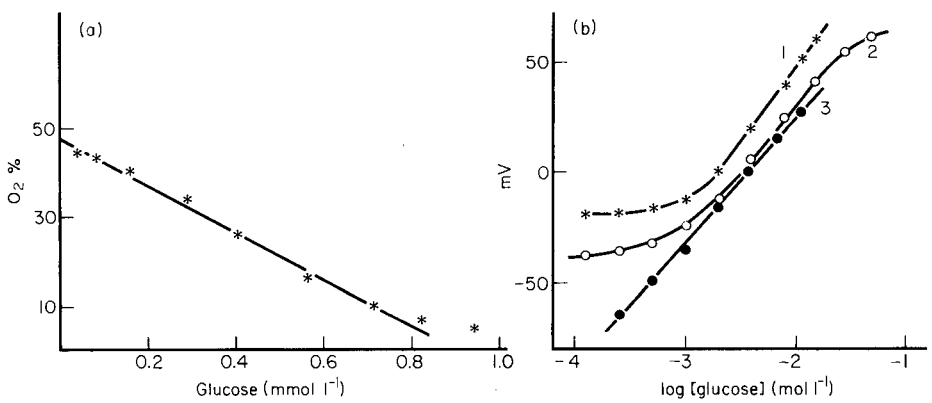

Fig. 3. Calibration curves for glucose. (a) With the oxygen-coupled sensor in phosphate buffer (0.01 mol l^{-1}, pH 6.8). (b) With the carbon dioxide sensor: (1) 0.01 mol l^{-1} phosphate buffer pH 6.8; (2) 0.1 mol l^{-1} phosphate buffer pH 6.8; (3) curve for hydrogen carbonate in 0.1 mol l^{-1} phosphate buffer shown for comparison.

The limited sensitivity of the carbon dioxide-coupled sensor can be attributed to the pH values of the samples and to the endogenous level of carbon dioxide. The range can be extended slightly by using a diluted internal solution of sodium hydrogen carbonate (0.001 mol l^{-1}) [11], but the response time is then even longer. From the sensitivity point of view, the oxygen electrode gives a linear relationship between concentration and current and so provides constant sensitivity in the linear range; 0.02 mmol l^{-1} is the standard deviation. With the carbon dioxide electrode, the relationship is logarithmic, i.e., the sensitivity to glucose varies, and the standard deviation is typically 4% over the entire concentration range.

Effects of pH and temperature

Figures 4 and 5 illustrate the effect of pH on the calibration plots of the two types of sensor. The oxygen and the carbon dioxide electrodes themselves behave differently in that the response of the former is unaffected by the pH of the solution whereas the response characteristics of the latter vary in the same range [11]. Figure 4(a) shows the calibration plots obtained for glucose at different pH and Fig. 4(b) shows the variation of oxygen concentration after addition of glucose (0.3 mmol l^{-1} in the final solution) as a function of pH. Figure 5 shows the calibration plots for glucose with the carbon dioxide-coupled sensor as a function of pH (the ionic strength of the buffers was 0.1 mol l^{-1} in all cases) as well as the endogenous value without glucose added and the value (mV) for a given glucose concentration (2.4 mmol l^{-1}) as function of pH.

There is a large variation of potential and slopes depending on the pH of

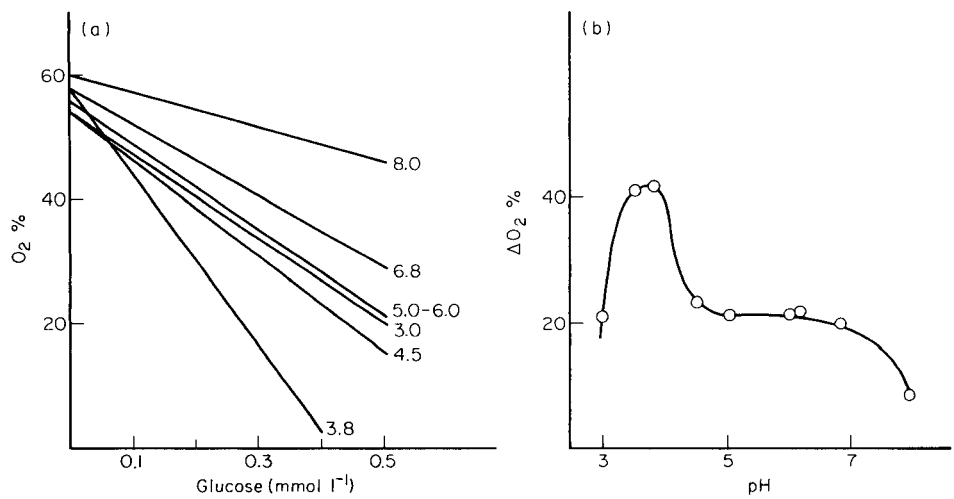

Fig. 4. Effect of pH with the oxygen-coupled sensor: (a) glucose calibration curves at the pH values indicated (0.01 mol l^{-1} phosphate buffer for pH 6.0—8.0 and 0.01 mol l^{-1} phthalate buffer for pH 3.0—6.0); (b) variation of % oxygen on addition of glucose to a final concentration of 0.3 mmol l^{-1}.

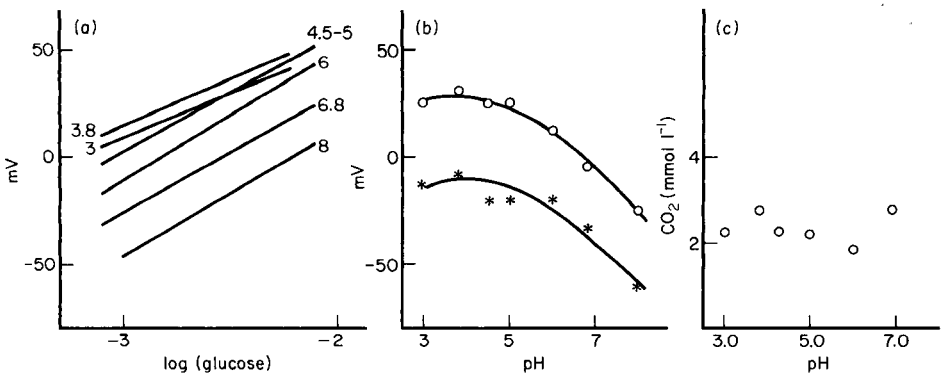

Fig. 5. Effect of pH with the carbon dioxide-coupled sensor: (a) glucose calibration curves at the pH values indicated; (b) endogenous values (lower curve) and mV values (upper curve) corresponding to an addition of glucose to give a final concentration of 2.4 mmol l^{-1} as a function of pH; (c) carbon dioxide concentration as a function of pH on addition of glucose to give a final concentration of 2.4 mmol l^{-1}. Buffers as for Fig. 4, but 0.1 mol l^{-1} concentration.

the buffers. Stable values can be obtained at pH 8.0 in phosphate buffer; at this pH, however, the addition of hydrogen carbonate does not result in a good response with a carbon dioxide-linked electrode. In this case, it seems likely that the pH of the layer containing the cell slurry is less than 8.0 because of carbon dioxide production and that this explains the Nernstian response at the high pH. Figure 5(c) shows the amount of carbon dioxide produced for the same glucose concentration as in Fig. 5(b) (2.4 mmol l^{-1}); the concentration of carbon dioxide was evaluated from a set of calibration curves for the carbon dioxide electrode at different pH values. It can be seen that the amount of carbon dioxide produced is almost the same, in the range 2—3 mmol l^{-1}, i.e., the ratio between the glucose added and the carbon dioxide produced at the surface of the electrode is about 1:1 at all pH values.

The curve for the oxygen-coupled sensor (Fig. 4b) can be considered representative of the aerobic metabolism of the yeast; it has a narrow maximum value around pH 3.5—4.0 [12]. The curve for the carbon dioxide sensor (Fig. 5b) is a mixed response of the anaerobic metabolism of the yeast and the response of the carbon dioxide sensor; therefore, the increase of potential in the lower pH range is not due to increased microbial activity but to a shift in the equilibrium between hydrogen carbonate and carbon dioxide. Figure 5(c) should be the response of the cells to pH variations in anaerobic conditions, but there is some doubt because the pH given on the abscissa corresponds to the pH of the bulk solution which is not necessarily the pH of the layer of solution around the slurry of cells. Experiments in which the cells were dispersed in the solution showed that carbon dioxide produced at pH >6.0 does not exhibit a Nernstian slope (50 mV/decade) and at pH >7.5 the sensor is unable to detect any production of carbon dioxide.

Temperature has a slight influence on both the aerobic and anaerobic activity. In the range 20—40°C, there was a small change of about 10% of the oxygen consumed or the carbon dioxide produced, such as has been described in the literature [14].

Selectivity of the sensors

The selectivity of the microbial sensors is summarized in Fig. 6. As is well known, the selectivity of these cells is not high, generally speaking. In the present case, the pattern of selectivity in the two metabolisms was found to be practically the same. Lactose is not assimilated by the strain and is not detected by either sensor. Maltose and fructose consume oxygen linearly with increasing concentration but the calibration plots are flatter than that for glucose. Sucrose has a calibration plot steeper than that for glucose (Fig. 6a). With the oxygen sensor, the selectivity can be calculated as the ratio of the slopes of the different compounds to the slope of the glucose calibration curve. The following pattern was found: sucrose 1.6, fructose 0.75, maltose 0.6.

In the anaerobic metabolism (Fig. 6b), maltose gives a very insensitive response (probably because of a very long time of assimilation) while sucrose and fructose provide the same slope as glucose, though the response to fructose is shifted somewhat. The ratio of fructose added to carbon dioxide produced is 1:1, whereas the ratio between glucose or sucrose and carbon dioxide produced is 1:2. However, it is well known that yeasts can utilize several oligosaccharides after adaptation [13]. Therefore the selectivity factor can vary according to the culture media, to the storage and to the environmental condition of the strain.

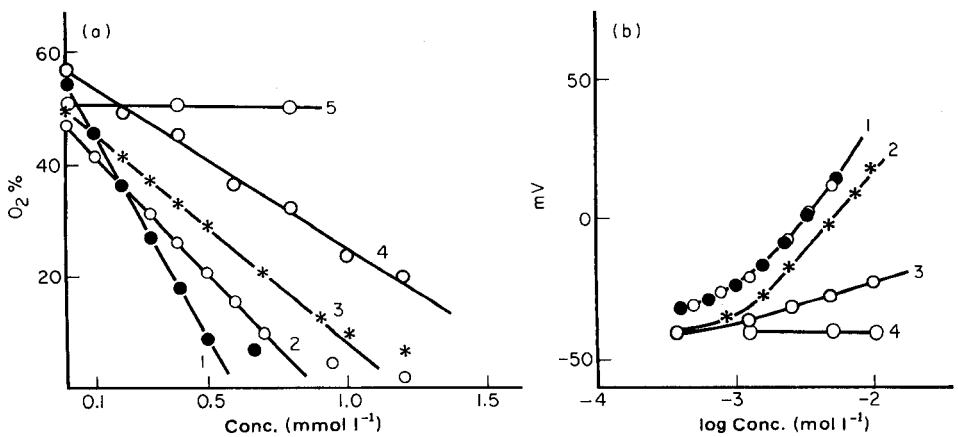

Fig. 6. Selectivity of the glucose microbial sensors (0.1 mol l^{-1} phosphate buffer pH 6.8). The equations of the lines are given (x = mmol l^{-1}, y = % O, and r = correlation coefficient). (a) The oxygen-coupled sensor: (1) sucrose, $y = 53 - 88.5x$, $r = 0.996$; (2) glucose, $y = 47 - 53.5x$, $r = 0.992$; (3) fructose, $y = 50 - 40.9x$, $r = 0.997$; (4) maltose, $y = 57 - 31.7x$, $r = 0.989$; (5) lactose. (b) The carbon dioxide-coupled sensor: (1) glucose (○) and sucrose (●); (2) fructose; (3) maltose; (4) lactose.

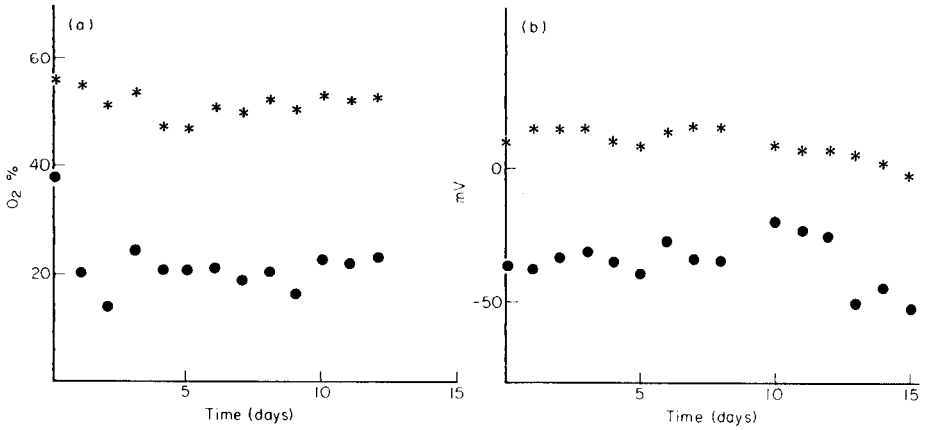

Fig. 7. Lifetime of the microbial sensors. (a) The oxygen-coupled sensor: the upper plot is the level of oxygen without glucose; the lower plot corresponds to a final glucose concentration of 0.5 mmol l^{-1}. (b) The carbon dioxide-coupled sensor: the upper plot is the response to a final 2.5 mmol l^{-1} glucose concentration; the lower plot shows the endogenous level of carbon dioxide in the buffer. In all cases, 0.01 mol l^{-1} phosphate buffer pH 6.8 is used.

Lifetimes of the assembled microbial sensors

Figure 7 shows the stability of the two assembled sensors. Figure 7(a) includes the features of the oxygen-coupled probe, giving the endogenous level of oxygen and the response to a given addition of glucose. Small fluctuations of 10—20% were observed during two weeks of continuous operation. Figure 7(b) summarizes the same features, giving the endogenous level of CO_2 and the response to a given glucose concentration during the same period. While the endogenous level is more variable, because of the small carbon dioxide concentration, the value corresponding to a given glucose concentration is remarkably stable during this time. The lifetime is also dependent on the use of the sensor and can roughly be estimated as a month of continuous operation.

REFERENCES

1 I. Karube and S. Suzuki, Ion Select. Electr. Rev., 6 (1984) 15.
2 C. R. Lowe, Biosensors, 1 (1985) 3.
3 D. Kirstein, L. Kirstein and F. Scheller, Biosensors, 1 (1985) 131.
4 I. Karube, T. Nakahara, T. Matsunaga and S. Suzuki, Anal. Chem., 54 (1982) 1725.
5 B. J. Vincke, M. J. Devleeschouwer and G. J. Patriarche, Anal. Lett., 18 (1985) 593.
6 G. A. Rechnitz, Anal. Chem., 54 (1982) 1194A.
7 G. A. Rechnitz, R. K. Kobos, S. J. Riechel and C. R. Gebauer, Anal. Chim. Acta, 94 (1977) 357.
8 M. Mascini and G. A. Rechnitz, Anal. Chim. Acta, 116 (1980) 169.
9 D. L. Simpson and R. K. Kobos, Anal. Chem., 55 (1984) 1974.
10 R. K. Kobos, in H. Freiser (Ed.), Ion Selective Electrodes in Analytical Chemistry, Plenum Press, New York, 1980, Vol. 2, p. 1.

11 E. H. Hansen and N. R. Larsen, Anal. Chim. Acta, 78 (1975) 459.
12 S. Burrows, in A. H. Rose and J. S. Harrison (Eds.), The Yeasts, Academic Press, London, 1970, Vol. 3, p. 349.
13 A. Sols, C. Gancedo and G. Dela Fuente, in A. H. Rose and J. S. Harrison (Eds.), The Yeasts, Academic Press, London, 1971, Vol. 2, p. 119.
14 J. L. Stokes, in A. H. Rose and J. S. Harrison (Eds.), The Yeasts, Academic Press, London, 1971, Vol. 2, p. 119.

Analytica Chimica Acta, 182 (1986) 123—131
Elsevier Science Publishers B.V., Amsterdam — Printed in The Netherlands

DETERMINATION OF HYDROGEN CYANIDE IN AIR USING MASS AMPLIFICATION BY HEAVY LIGAND REPLACEMENT ON A COATED QUARTZ PIEZOELECTRIC CRYSTAL

J. F. ALDER*, A. E. BENTLEY and P. K. P. DREW

Department of Instrumentation and Analytical Science, University of Manchester Institute of Science and Technology, P.O. Box 88, Manchester M60 1QD (Great Britain)

(Received 28th September 1985)

SUMMARY

Piezoelectric crystals coated with bis(pentan-2,4-dionato)nickel are used to detect the presence of hydrogen cyanide in the range 13—93 ppm (10^{-6} mol mol^{-1}). The displacement of the heavy ligand pentan-2,4-dione by a light molecule (HCN) yields an increase in sensitivity, compared to simple absorption of the analyte (i.e., mass amplification). A continuous flow system is used at relative humidities of 40—92%. The lifetime of such a device is limited by hydrolysis. Reproducibility from coated-crystal to coated-crystal is poor, probably owing to inconsistencies in coating techniques.

The determination of gaseous hydrogen cyanide is important because of the possibility of its accidental release within chemical plants and electroplating works. Its toxic dangers are well known and the threshold limit value is 10 ppm. Piezoelectric crystals have been used for hydrogen cyanide measurements in solution by Nomura and Hattari [1, 2] but there are no reports of their use for hydrogen cyanide in gaseous systems. Coated piezoelectric sensors [3] make use of a coating material that sorbs the gas of interest by physisorption or chemisorption. Because sensitivity is a function of mass change, one limiting factor is the molecular weight of the sorbed molecule, which for hydrogen cyanide is small. However if, as demonstrated here, a small molecule displaces a larger molecule from the coating the overall mass change may be greater than the mass of the original small molecule. This may be termed "mass amplification". This concept has not been applied to piezoelectric crystal detectors before.

If the heavy displaced ligand is to leave, it must be carried off in the air stream passing over the crystal. Therefore the reaction can be considered irreversible, which has several consequences. First, the frequency change is positive (mass is lost), rather than as usual negative change which may offer some discrimination against interferents or dust settling on the crystal. Second, the coating material is consumed on reaction, so that the sensor is a "one-shot" device if exposed to hydrogen cyanide, but will have a long life if it is not. Replacement costs are small when set against the personnel and

0003-2670/86/$03.50

equipment risks involved in accidental hydrogen cyanide release. Third, in contrast to conventional practice, the reaction does not proceed to an equilibrium, thus the usual sensitivity factor reported in terms of Hz ppm^{-1} is inapplicable and a rate-dependent quantity (Hz min^{-1} ppm^{-1}) must be used to describe the detector behaviour.

One suitable group of coating materials that had previously been identified [4] from infrared absorption studies as reacting with gaseous hydrogen cyanide at 80% relative humidity (r.h.) and ambient temperatures is the transition metal β-diketonates, particularly bis(pentan-2,4-dionato)nickel(II), $Ni(acac)_2$. Infrared absorption spectra of this compound before and after exposure to hydrogen cyanide are shown in Fig. 1. The complex structure from the pentan-2,4-dione disappears and a line at 2170 cm^{-1} believed to be a C≡N stretch, appears. This evidence supports the overall reaction

$$Ni(acac)_2 + 2HCN = Ni(CN)_2 + 2H(acac)$$

As the pentan-2,4-dione is volatile and completely evaporates in a stream of air, there is a net loss of 146 Dalton per hydrogen cyanide molecule sorbed, which is a fractional mass change of 57%. Uncertainties in the hydration states of both nickel species make this only an estimate and the overall fractional frequency changes when the reaction is allowed to go to completion was measured to be ca. 35%.

EXPERIMENTAL

All transition metal β-diketonates, unless otherwise specified, were from Aldrich and were used as received. Tris(pentan-2,4-dionato)cobalt(III) was prepared as described by Bryant and Fernelius [5].

The gas rig used is shown in Fig. 2. A stream of humidified air (ca. 50% r.h.) from a cylinder is passed at around 760 cm^3 min^{-1} through two flow cells formed from B29 sockets with inlets through a "dog leg" in the top to aid mixing. This flow is made up from 700 cm^3 min^{-1} from a humidifier and 60 cm^3 min^{-1} of air (dried over granular phosphorus pentoxide) to which hydrogen cyanide can be added. Addition is made from a flow stream of

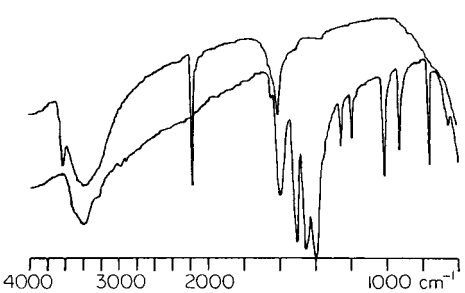

Fig. 1. Infrared absorption spectra of bis(pentan-2,4-dionato)nickel film before and after 1-h exposure to 250 ppm HCN at 80% r.h.

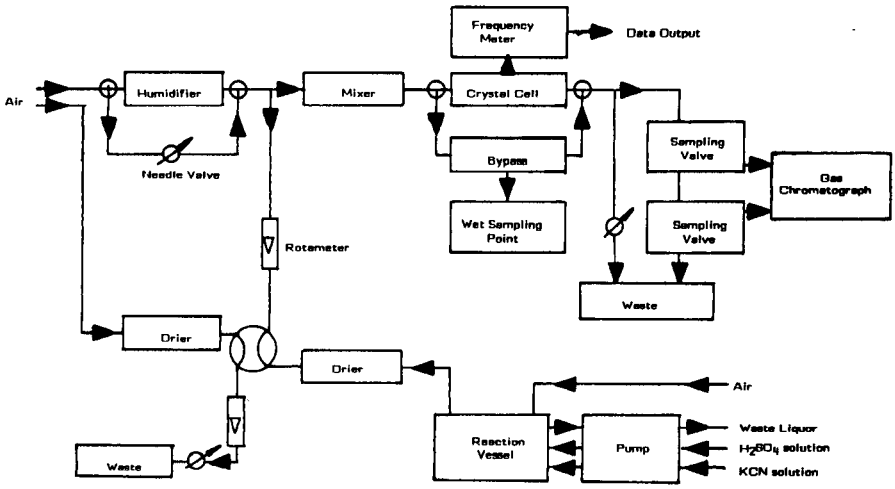

Fig. 2. Constant-humidity hydrogen cyanide exposure rig for coated-crystal testing.

hydrogen cyanide via a four-way tap. This arrangement ensures that the cyanide concentration may be changed rapidly between 0 and 100 ppm without affecting the relative humidity.

Hydrogen cyanide-containing atmospheres were generated by bubbling air through a multi-necked reaction vessel into which (1 + 9) sulphuric acid and 0.5% (w/v) potassium cyanide solution were pumped continuously using a peristaltic pump (Watson Marlow, Falmouth, Cornwall). The waste was continuously removed to maintain a constant solution volume and concentration. All waste lines were vented into absorption towers of modified charcoal (Type 1100; Sutcliffe Speakman, Leigh, England) to trap the hydrogen cyanide, before bubbling through an indicator comprising a saturated solution of ammoniacal copper nitrate, which turns green when the charcoal towers become exhausted, and into a fume cupboard. (Unimpregnated charcoal is unsuitable for trapping hydrogen cyanide.)

Hydrogen cyanide was determined with a gas chromatograph (Model 437A, Packard-Becker, Delft, The Netherlands) with a flame ionisation detector (FID), a 2-m Porapak-QS column at 120°C and a 1-ml automatic gas sampling valve programmed to sample every 5 min. The FID was calibrated originally by means of the colour reaction between hydrogen cyanide and alkaline picric acid; the method was similar to that described by Fischer and Brown [6]. In later experiments, cyanide-containing gas was bubbled through 50 ml of 0.1 M sodium hydroxide for a few minutes to obtain a solution in the range 2—20 $\mu g\ ml^{-1}$ cyanide, which was determined with a cyanide electrode (Model 940600, Orion, Cambridge, MA) by reference to a calibration curve produced daily.

Humidity was determined by using a second matched Porapak-QS column and a thermal conductivity detector. The latter was calibrated by collection of water from the airstream over granular phosphorus pentoxide.

The crystal units were 14.9-MHz AT-cut bulk quartz piezoelectric resonators (Quartz Crystal Co., New Malden, Surrey) with gold electrodes. A Pierce-type oscillator was used, based on a design by Frerking [7] buffered by an r.f. amplifier (560C; R.S. Components, London) configured as a 50-ohm line driver (data sheet R/4591; R.S. Components). Output from both oscillators was monitored on two separate 120-MHz frequency meters (PM6671, Pye-Unicam, Cambridge) each fitted with a PM9695 digital-to-analogue converter (DAC) and the output voltages were displayed on a two-pen chart recorder.

As it is the rate of change of the oscillator frequency with time that is related to cyanide concentration, the voltage from each DAC was passed to the AD ports of a microcomputer (BBC Model B). The present value was subtracted from the previous value and the difference (dF) plotted against time. It must be emphasised that the two crystals allow parallel testing of coatings and are not being used to correct each other for temperature variations.

Coatings were applied with a fresh cotton wool bud (Q-tips) from a methanolic solution. The coated crystals were allowed to dry before being smeared to produce a more uniform coating and to remove any loosely held particles. This method was found to be the best over several years work in this laboratory. The amount of coating can be quantified approximately by measuring the frequency change on coating, through Sauerbrey's equation [8], because the actual mass change (ca. 3 μg) would be difficult to measure precisely.

RESULTS AND DISCUSSION

Experiments were made by placing a freshly coated crystal in a cyanide-free air stream. Inititally, the frequency rose rapidly as any remaining solvent evaporated and the coating came to equilibrium with the rig atmosphere. The four-way tap was then switched to introduce the air stream containing hydrogen cyanide. There was sometimes a small (<5 Hz) frequency change on re-equilibration followed by a continuous increase in frequency. The rate of this change decreased with time but could not be fitted well to any particular rate law. After 10 min the flow was switched back to clean air. In earlier work, where the coated crystal was first equilibrated with dry air, an initial rapid decrease in frequency occurred, which was presumably due to water uptake. This was followed by a gain in frequency, the rate of gain of which passed through a maximum. Examples of both behaviour with time are shown in Fig. 3, which illustrates the importance of ensuring that the introduction of hydrogen cyanide is not accompanied by a simultaneous change in humidity. A blank experiment was also done to detect the occurrence of hydrolysis or evaporation by simply leaving the coated crystal in the clean air stream for the same time period.

If the reaction is allowed to go to completion (i.e., the frequency stabilises), the difference between the final and initial frequencies can be noted to estimate the fractional mass change of the complete reaction.

The maximum rate of frequency change increases with the amount of

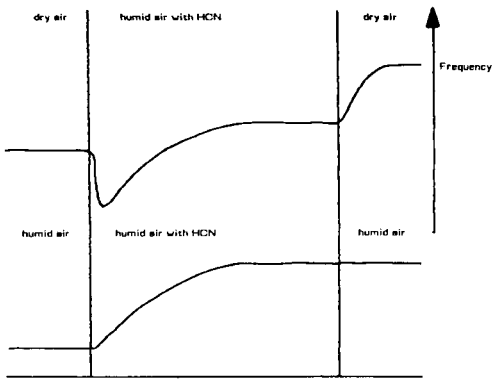

Fig. 3. Response of coated crystal to humid air containing hydrogen cyanide with respect to the responses in dry and humid air without hydrogen cyanide.

coating (Fig. 4). However, this occurs at switchover, at the same time as any re-equilibration or pressure pulses, which may introduce uncertainty into the measurement. To allow time for the system to equilibrate, the data in Fig. 4 were taken 5 min after switchover. A similar effect occurs in the absence of hydrogen cyanide at a much slower rate, as shown in Fig. 5, undoubtedly because of hydrolysis of the coating with loss of pentan-2,4-dione. These data

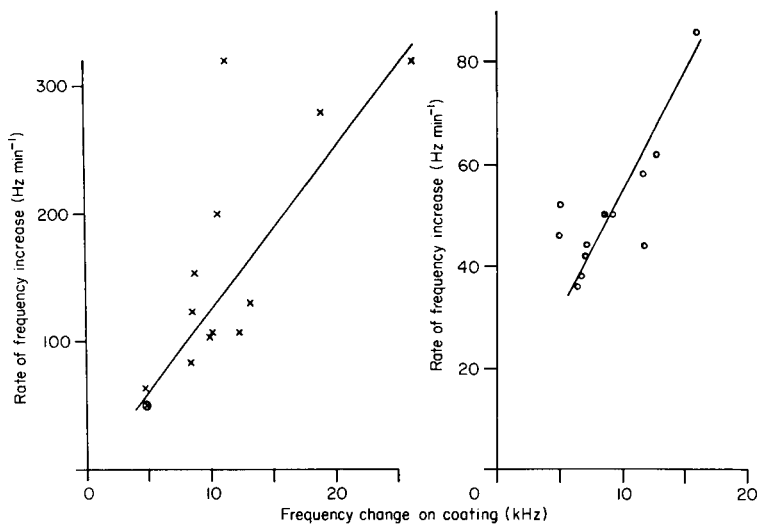

Fig. 4. Response of a crystal coated with bis(pentan-2,4-dionato)nickel at 24.4—25.6°C, 86—89% r.h. to 40—42 ppm hydrogen cyanide, showing dependence on coating frequency change. (The area covered is ca. 2×10^{-5} m^2; from the Sauerbrey equation [8] the frequency change corresponds to ca. 0.4 μg kHz^{-1}.) The rate of frequency increase was measured after 5 min.

Fig. 5. Response of a crystal coated with bis(pentan-2,4-dionato)cobalt at 24—25°C; 85—87% r.h. for various amounts of coating. Frequency increase measured after 5 min.

suggest that in experiments to examine the dependence on any other parameter, either the amount of coating must remain constant or the response rates must be linearly normalised, to take into account the change in coating mass, provided that the mass is small. The latter course was chosen in this work because the method of coating used was incapable of high reproducibility, even with long practice.

Other transition metal complexes with pentan-2,4-dione were evaluated as potential coating materials. The results are shown in Table 1. The use of the same coating technique for each compound caused greater variation in the amount of coating deposited between compounds than for the same compound.

Reaction rates with hydrogen cyanide were found to decrease in the order $Co(II)(acac)_2$, $Ni(II)(acac)_2$, $Cu(II)(acac)_2 \gg Co(III)(acac)_3 > Pd(II)(acac)_2$, as did the rates of hydrolysis in wet air in the absence of hydrogen cyanide (Table 1C). All the complexes except that of palladium are octahedral and the metal is fully coordinated with pentan-2,4-dione and water so that any exchange or displacement must require a dissociative step. Pearson and Moore [9] proposed an S_N1 mechanism. The process probably involves an inner coordination sphere exchange of ligands. Published data [10] show the rate for cobalt(III) ligand exchange to be at least 10^9 times slower than for the other three metal ions. In the doubly chelated species [Ni(II), Co(II), Cu(II)], the two apical positions are occupied by more labile solvent or adduct molecules.

Kinetic data reported by Pearson and Moore [9] suggest that loss of pentan-2,4-dione in aqueous solution occurs in two stages. The first ligand is lost by a rapid unspecified process to yield $Ni(H_2O)_4(acac)$. The second is lost by a slower process. One end of the remaining chelating ligand detaches and is either protonated (and remains unattached to the metal) or recombines with the metal. A suitable anion (X) can replace one of the complexed water molecules to give $Ni(CN)(H_2O)_3(acac)$ in which the metal chelate bonding is destabilised so that there is less chance that the partially dissociated ligand will rebond to the metal.

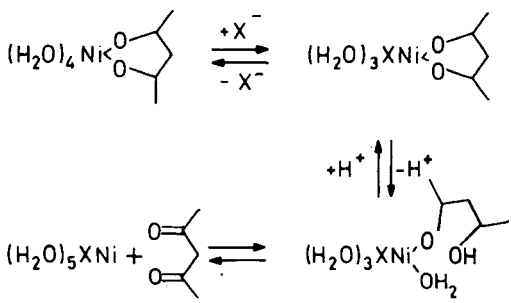

This means that the extra stability arising from chelation is decreased, and loss of pentan-2,4-dione by evaporation into the air stream becomes more probable (i.e., faster). This mechanism suggests that the presence of acid will catalyse the hydrolysis, so some mixed coatings were prepared by the addition

TABLE 1

Comparison of responses of crystals coated with pentan-2,4-dione complexes of different transition metals

Metal ion	Frequency change on coating (kHz)	Rate of change (Hz min^{-1})[a]		HCN conc. (ppm)	H_2O conc. (mg l^{-1})	R.h. (%)	Temp. (°C)
		Initially	After 5 min				
A. Reaction with HCN at moderate humidity							
Pd(II)	1.74	0 (0)	0 (0)	100	12.0	54	24.0
	3.11	0 (0)	0 (0)				
Co(III)	7.87	<1 (0)	<1 (0)	85	13.0	61	23.2
	8.12	0 (0)	0 (0)				
Cu(II)	3.16	24 (44)	17 (54)	103	12.2	55	24.0
	4.71	30 (64)	21 (45)				
Ni(II)	9.68	9 (9)	5.5 (6)	96	12.6	60	21.9
	11.21	7 (6)	5.5 (5)				
Co(II)	10.96	58 (48)	45 (38)	90	12.5	62	22.4
	21.93	66 (30)	66 (30)				
B. Reaction with HCN at high humidity							
Pd(II)	3.14	0 (0)	0 (0)	42	17.5	78	24.1
	3.18	0 (0)	0 (0)				
Co(III)	5.04	6 (12)	2 (4)	44	17.7	78	24.2
	5.57	8 (14)	4 (7)				
Cu(II)	2.33	42 (180)	15 (64)	44	17.8	79	24.2
	2.93	50 (170)	17 (58)				
Ni(II)	4.31	60 (139)	41 (95)	43	17.6	78	24.2
	5.21	76 (146)	42 (81)				
Co(II)	5.10	108 (212)	84 (164)	43	18.1	79	24.4
	6.53	100 (153)	84 (129)				
C. Reaction in absence of HCN							
Co(III)	1.60	−4 (−25)	−2 (−13)	0	19.5	83	24.9
	1.89	2.5 (13)	0 (0)				
Cu(II)	2.70	16 (59)	10 (37)	0	19.2	82	24.8
	4.01	26 (65)	13 (32)				
Ni(II)	5.82	22 (38)	11 (19)	0	19.2	82	24.8
	8.12	36 (44)	17 (21)				
Co(II)	6.21	60 (97)	32 (52)	0	18.9	83	24.4
	6.08	86 (141)	42 (69)				

[a]Numbers in parentheses give the rate of change normalised to a 10-kHz frequency change on coating.

of acids and bases. Triethylenediamine, acridine, benzoic acid and the free ligand pentan-2,4-dione, however, gave no significant change in hydrolysis rate. Dibutylamine appeared to increase the rate, but this was probably due to bleeding of dibutylamine from the crystal.

Substitution of other ligands in nickel complexes, including dibenzoylmethane, dipivaloylmethane, formate and acetate, gave no improvement in selectivity towards hydrogen cyanide.

The unreactivity of the cobalt(III) complex could be ascribed to the well-known kinetic inertness of such complexes, as well as the blockage of its apical positions by the third chelating ligand. The planar palladium(II) complex appeared to be inert, although it has been reported to undergo nucleophilic substitution by an S_N2 process [11]. It had been expected that such a second-row transition metal would have more affinity for a "soft" ligand such as cyanide rather than the "hard" water.

Figure 6 shows a calibration graph for hydrogen cyanide obtained by use of the nickel complex at high humidity. The response flattens out at concentrations above 35 ppm. Because water is involved in the hydrogen cyanide/coating reaction, the effect of humidity was investigated in both the presence and absence of hydrogen cyanide. Results are shown in Fig. 7 for the effect of relative humidity. The very slight response to water at low humidities contrasts with the rapid rise in response with increasing humidity, presumably because of adsorbed water coverage; such water could be available to solvate and stabilise the dissociating transition state and hence increase the reaction rate. The presence of hydrogen cyanide significantly increases the rate of loss of ligand, as shown in Table 1 (A and B), but the shape of the rate of loss vs. relative humidity response is very similar, as would be expected from the

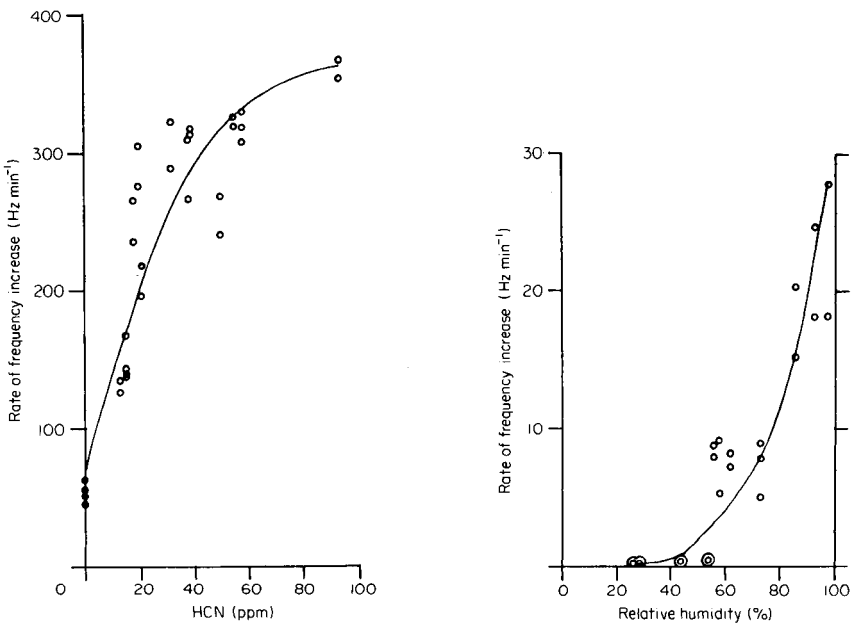

Fig. 6. Response to hydrogen cyanide concentration normalised to 10-kHz frequency change on coating with bis(pentan-2,4-dionato)nickel (24.7—25.8°C, 87—92% r.h.) Frequency increase measured after 5 min.

Fig. 7. Rate of frequency change vs. relative humidity for a $Ni(acac)_2$-coated crystal at 24.2—26.1°C, normalised to a 7-kHz frequency change on coating. Frequency increase measured after 5 min.

above mechanism. At high humidity the device will have a lifetime of only a few hours.

This work illustrates some of the advantages and disadvantages of using irreversible reactions as the basis of coated piezoelectric crystal sensors. Frequency changes are large (kHz) and easily measured because the whole mass of coating reacts; for reversible coating reactions, which are confined to the surface, the total frequency response is typically less than 200 Hz, and the effects of temperature, ageing and co-adsorbed water, dependent on atmospheric humidity, combine to degrade the precision. Unfortunately, as the present coating is consumed on exposure, testing prior to use is (partially at least) destructive and successful exploitation will require a far higher repeatability of sensor-coating technique and behaviour. This deficiency is demonstrated by the poor reproducibility of responses from one coated-crystal to another. Comparative data are lacking because most workers only report data on a single coated crystal rather than between units or successive coating applications. An exception is the work of Kindlund and Lundstrom [12], who used different amounts of a liquid silicone oil coating for the determination of halothane and found scattering for very small amounts (<1 kHz change on coating). They attributed this to the formation of islands of silicone oil on an uncoated electrode. In this work, the coating is solid and is laid down rapidly on solvent evaporation. It appears optically flat and no features can be discerned under an optical microscope (although that may be due to its transparency). Differences in reactivity could arise from variations in true surface area and varying proportions of crystalline and amorphous material.

If a second crystal sensitive only to water, or a commercial humidity sensor, were used to monitor the water concentration, then the humidity dependence of the response could be corrected for by solving the appropriate equations with a microcomputer as has been previously demonstrated [13]. The effect of temperature has yet to be investigated but as a rate-determining quantity it will amost certainly require further compensation. Even if a reversible reaction is used, both parameters will still require monitoring and a correction must be applied to the response.

REFERENCES

1 T. Nomura and O. Hattari, Anal. Chim. Acta, 115 (1980) 323.
2 T. Nomura, Anal. Chim. Acta, 124 (1981) 81.
3 J. F. Alder and J. J. McCallum, Analyst (London), 108 (1983) 1169.
4 A. E. Bentley, MSc Thesis, UMIST, University of Manchester, 1983.
5 B. E. Bryant and W. C. Fernelius, Inorg. Synth., 5 (1957) 188.
6 F. B. Fischer and J. S. Brown, Anal. Chem., 24 (1952) 1440.
7 M. E. Frerking, Crystal Oscillator Design and Temperature Compensation, Van Nostrand-Reinhold, New York, 1978, p. 69.
8 G. Z. Sauerbrey, Z. Phys., 155 (1959) 206.
9 R. G. Pearson and J. W. Moore, Inorg. Chem., 5 (1966) 1523.
10 F. A. Cotton and G. Wilkinson, Advanced Inorganic Chemistry, 4th edn., Wiley-Interscience, New York, 1980, p. 1188.
11 R. G. Pearson and D. A. Johnson, J. Am. Chem. Soc., 86 (1964) 3983.
12 A. Kindlund and I. Lundstrom, Sensors and Actuators, 3 (1982/3) 63.
13 P. R. Fielden, J. F. Alder, J. J. McCallum and T. Stanios, Anal. Chim. Acta, 162 (1984) 85.

Analytica Chimica Acta, 182 (1986) 133—145
Elsevier Science Publishers B.V., Amsterdam — Printed in The Netherlands

FACTORS AFFECTING THE PRECISIONS OF ANALYSES, BY POTENTIOMETRIC TITRIMETRY, OF SOLUTIONS CONTAINING TWO WEAK ACIDS

MARIA BETTI, PAOLO PAPOFF and LOUIS MEITES*[a]

C.N.R. Istituto di Chimica Analitica Strumentale, Dipartimento di Chimica e Chimica Industriale dell'Università, Via Risorgimento, 35, 56100 Pisa (Italy)

(Received 7th August 1985)

SUMMARY

This paper deals with potentiometric titrations in which mixtures of two monobasic weak acids are titrated with a strong base, and in which weighted non-linear regression analysis is used to find the concentrations and values of pK_a for both acids. The precisions of the resulting values of the concentrations depend on the difference between the values of pK_a, on the ratio of the initial concentrations, and on the standard errors of measurement of both the pH and the volume of base. For any given values of the ratio of concentrations and the standard errors of measurement, the precision with which the concentration of the stronger acid can be evaluated is, in general, poorest when the difference between the pK_a values (Δ) is approximately 1.5, and improves if Δ is either larger or smaller than that value. Even if Δ is as small as 0.1, the precision that is attainable is very much better than it is generally believed to be. Surprisingly, there are conditions under which the concentrations of both acids can be determined with fair precision even though titrimetric data will not reveal that two acids are present in the sample.

More than 60 years have elapsed since the pioneering work of Kolthoff and others [1] first showed that potentiometric acid-base titrations are capable of yielding better accuracy and precision than visual ones. Their superiority is particularly marked in analyzing mixtures of acids, for it is much easier to identify and locate two or more points of maximum slope on a potentiometric titration curve than to make a rational selection of indicators for a visual titration.

In this paper, the titration of a mixture of two weak monobasic acids HA_1 and HA_2 is considered. The former is arbitrarily taken to be the stronger. The solvent is assumed to be water, and the titrant to be a c_b M solution of a strong base. The classically optimum situation is that in which two requirements are fulfilled. One is that the value of pK_{a2} must be considerably smaller than that of $p(K_w/c_b)$, where K_{a2} is the former or conditional dissociation

[a]Permanent address: Department of Chemistry, George Mason University, 4400 University Drive, Fairfax, VA 22030, U.S.A.

0003-2670/86/$03.50

constant of the weaker acid under the experimental conditions employed and is equal to $[H^+][A_2^-]/[HA_2]$, while K_w is the ion-concentration product $[H^+][OH^-]$ under the same conditions. The value of $p(K_w/c_b)$ is equal to the value of the pcH ($= -\log_{10}[H^+]$) that is approached as the volume of reagent increases without limit, and corresponds to the horizontal asymptote of the titration curve. If this requirement is not satisfied, the conditional equilibrium constant of the reaction $HA_2 + OH^- = A_2^- + H_2O$ can have only a fairly small value, the slope of the titration curve cannot become very large in the vicinity of the second equivalence point, and the corresponding point of maximum slope cannot be very precisely located. The second requirement is that the value of pK_{a1} must be considerably smaller than that of pK_{a2}, where pK_{a1} is the conditional dissociation constant of the stronger acid. If this requirement is not satisfied, the reaction $A_1^- + HA_2 = HA_1 + A_2^-$ can occur to an appreciable extent, the two stages of neutralization overlap, the slope of the titration curve is relatively small in the vicinity of the first equivalence point (which corresponds to the neutralization of the HA_1), and the corresponding point of maximum slope cannot be very precisely located. To satisfy both these requirements, if the concentration of each acid and of the base is in the neighborhood of 0.1 M, pK_{a2} should not exceed about 8, and the difference Δ ($= pK_{a2} - pK_{a1}$) between the values of pK_a for the two acids should not be smaller than about 5.

Titrations can be, and in modern practice frequently are, made with systems that do not fulfill these rather restrictive requirements, but failure to fulfill them always entails some loss of precision. Decreasing $p(K_w/c_b)$ decreases the precision with which the sum of the two concentrations can be found, decreasing Δ decreases the precision with which the concentration of the stronger acid can be found, and decreasing either of these quantities decreases the precision with which the concentration of the weaker acid can be found.

The familiar conclusions thus summarized reflect the traditional identification of end-points in potentiometric titrimetry with points of maximum slope on the corresponding titration curves. More recently, it has been shown that this is neither necessary nor advantageous, for two reasons. One is that a substantial error may be incurred in attempting to locate a point of maximum slope, especially when the slope does not vary greatly in the vicinity of the end-point; the other is that points of maximum slope almost never coincide with the equivalence points that they are taken to represent. An alternative was first proposed by Ingman et al. [2], who were able to achieve reasonable accuracy and precision in determining the concentrations of both acetic acid and propionic acid in mixtures of the two, even though the values of pK_a are so nearly equal (they differ by only 0.12) that there could not have been a point of maximum slope near the first equivalence point. Barry and Meites [3], who titrated acetate ion with hydrochloric acid at very low concentrations, secured accuracies and precisions that were between one and a half and two orders of magnitude better than could have been obtained by

locating points of maximum slope, and were even able to conduct successful titrations of solutions so dilute that there were no points of inflection on the titration curves.

These things were made possible by using non-linear regression analysis to find the best values of the parameters appearing in the theoretical equation for the titration curve by fitting the experimental data to that equation. New techniques for handling data, including deviation-pattern recognition [4] and automatic classification [5], may serve ultimately as the bases of automatic procedures for finding the number and identifying the natures (strong; weak; mono-, di-, or tri-basic [6]; slightly soluble, etc.) of the acids present in a mixture [7]. Experimental titrations always involve random errors of measurement of both the pH and the volume of reagent, and the effects of these on the theoretically attainable precisions of the concentrations and pK_a values obtained by weighted non-linear regression analysis have been studied for titrations of solutions containing a strong acid [8] or a single monobasic weak acid [9]. This paper presents the results of an investigation of the precisions of the parameters that characterize the titration of a mixture of two monobasic weak acids.

THEORY AND PROCEDURE

The fundamental equation for the titration of such a mixture may be written in the form

$$[H^+] - [OH^-] = \{K_{a1}/(K_{a1} + [H^+]) + xK_{a2}/(K_{a2} + [H^+]) - f\}c_1^0/(1 + rf) \quad (1)$$

where K_{a1} and K_{a2} are the conditional dissociation constants of the two acids as defined above, c_1^0 is the initial formal or analytical concentration of the stronger acid, and x is the ratio of concentrations given by $x = c_2^0/c_1^0$. Here c_2^0 is the initial formal or analytical concentration of the weaker acid, and f is the titration parameter defined by $f = V_b c_b/V_a^0 c_1^0$. In this equation, V_b is the total volume of base that has been added at any point, c_b is the concentration of the base, V_a^0 is the initial volume of the mixture being titrated, and r is the dilution parameter [10] defined by $r = c_1^0/c_b$. According to these definitions, f is equal to 1 at the first equivalence point and to $(1 + x)$ at the second.

For each desired combination of these parameters, the theoretical coordinates of 30 points along a titration curve were computed from Eqn. 1. The contemplated operation of an "intelligent" autotitrator [7] was simulated by distributing these points in the following way. The first point always corresponded to $f = 0$ (the start of the titration), and the value of f at each subsequent point was obtained by adding an increment Δf to the last preceding value. The algorithm employed to generate the values of Δf was

(1) if $2 < N < 5$, $\Delta f = 0.02$

(2) if $N > 5$, $\Delta f = |1 - f|/2$

where N is the ordinal number of the point being generated and f denotes the value at the $(N-1)$th point. As the first equivalence point was approached, the second of these equations yielded progressively smaller values of Δf, but any value below 0.01 was discarded and replaced by 0.01. When f had increased above 1.05, further values of Δf were generated by the equation

(3) if $f > 1.05$, $\Delta f = |(1 + x) - f|/2$

again with 0.01 as a lower limit. With $x = 1$ this yielded a set of points for which the successive values of f, rounded off to the nearest 0.001 unit, were 0, 0.02, 0.04, 0.06, 0.08, 0.54, 0.77, 0.885, 0.943, 0.972, 0.986, 0.996, 1.006, 1.016, 1.026, 1.036, 1.046, 1.056, 1.528, 1.764, 1.882, 1.941, 1.971, 1.985, 1.995, 2.005, 2.015, 2.025, 2.038, and 2.057. A human chemist conducting the same titration might well attempt to secure points distributed in a generally similar way.

The value of $[H^+]$ at each point was obtained by solving Eqn. 1, using a Newton-Raphson procedure that was terminated when two successive approximations differed by 0.001% or less, and was then converted into a value of the pH. In making this conversion, the value of the apparent single-ion activity coefficient y_{H^+} was assumed to be 1, so that

$$pH = -\log_{10} (y_{H^+}[H^+]) = pcH \qquad (2)$$

Since y_{H^+} is taken to be a constant, experiments based on the results of these calculations must of course be conducted in such a way as to minimize or eliminate its variation. Adding a swamping concentration of a neutral electrolyte will serve that purpose and will also minimize variations of the liquid-junction potential, the value of which does not appear explicitly in these equations but does affect that of y_{H^+}.

The resulting data pairs were combined with a general program (VARPWR) for estimating the variances of the parameters in weighted non-linear regression analysis [11]. That program differs from one previously described [12] in that it includes provision for errors in measurements of the independent variable as well as the dependent one. It applies an increment equal to $4\,\sigma_{pH}$, where σ_{pH} is the value assigned to the standard error of a measurement of pH, to the pH value for each point in turn. For each of the perturbed sets of data thus produced, it finds the best values of the various parameters V_i by weighted non-linear regression, stores the resulting values of $\Delta V_i/\Delta pH$ as estimators of the partial derivatives $\partial V_i/\partial pH$ at the point under consideration, restores the pH value that was altered, and goes on to the next point. After effecting the fit and restoring the original pH value for the last point, it obtains estimates of the derivatives $\partial V_i/\partial V_b$, where V_b is the volume of base, in a similar way. Finally it combines the values of the derivatives to yield estimates of the variances of the parameters. Much computation is required, and the calculation of $[H^+]$ from Eqn. 1 at each point is fairly lengthy. It was therefore impractical to perform the calculations except with single-precision arithmetic, and the values of the variances are considered to have uncertainties in the order of ±5–10%.

In weighted regression, one must minimize the quantity Q defined by the equation

$$Q = \sum (\mathrm{pH_{meas}} - \mathrm{pH_{calc}})^2 / [\sigma_{V_b}{}^2 (\mathrm{dpH/d}V_b)^2 + \sigma_{\mathrm{pH}}^2]^2 \qquad (3)$$

To obtain the necessary expression for $\mathrm{dpH/d}V_b$, Eqn. 1 was solved for f in accordance with Bishop's demonstration [13] that titration-curve equations are generally linear with respect to f regardless of their degree with respect to $[H^+]$. An expression for $\mathrm{d}f/\mathrm{d}[H^+]$ was easily obtained, and was combined with the chain-rule expression

$$\mathrm{dpH/d}V_b = (\mathrm{dpH/dpc_H})\,(\mathrm{dpc_H/d}[H^+])\,(\mathrm{d}f/\mathrm{d}V_b)/(\mathrm{d}f/\mathrm{d}[H^+]) \qquad (4)$$

to give

$$\mathrm{dpH/d}V_b = 0.434294\, c_b < \{r([H^+] - K_w/[H^+]) + c_1^0\}^2/V_a^0(c_1^0)[H^+] >$$
$$< \{r([H^+] - K_w/[H^+]) + c_1^0\}\{K_{a1}/(K_{a1} + [H^+])^2 + xK_{a2}/(K_{a2} + [H^+])^2\}$$
$$+ \{1 + K_w/[H^+]\}\{1 + r[K_{a1}/(K_{a1} + [H^+]) + xK_{a1}/(K_{a2} + [H^+])]\} > \qquad (5)$$

which was used in computing each value of the denominator of Eqn. 2.

In synthesizing the "data", it was always assumed that $V_a^0 = 25$ cm^3, that both c_1^0 and c_b were equal to 0.1 M, that $K_w = 1 \times 10^{-14}$ mol^2 dm^{-6}, and that $y_{H^+} = 1$. The values of pK_{a1} were varied from 3 to 6; those of Δ were varied from 0.1 to 7; those of x were varied from 0.0316 to 1; and those of σ_{pH} and σ_{V_b} were usually taken to be 0.001 pH and 0.01 cm^3, respectively. These standard errors of measurement are slightly, but in modern practice not excessively, optimistic, and it is shown below how changes of their values affect the standard errors of the parameters. The computations were performed by a Radio Shack TRS-80 Model II microcomputer in single-precision FORTRAN.

RESULTS AND DISCUSSION

These equations contain six parameters: c_1^0, c_2^0, pK_{a1}, pK_{a2}, pK_w, and y_{H^+}. The couplings among them are so strong, and the error surface is so flat, that the fits are unduly slow and poorly convergent. Much better behavior was obtained on reformulating the parameters as c_1^0, x, $p(K_{a1}y_{H^+})$, $p(K_{a2}y_{H^+})$, $p(K_w y_{H^+})$, and y_{H^+}. Because the standard error of $K_w y_{H^+}$ would be of little interest in any practical application, only the standard errors of the other five parameters are given in the Tables that follow. Those of c_1^0, x, and y_{H^+} are relative standard errors and are expressed as percentages; those of $p(K_{a1}y_{H^+})$ and $p(K_{a2}y_{H^+})$ are the absolute standard errors of these dimensionless quantities.

Table 1 shows the general behaviors of these standard errors. The relative standard error of c_1^0 increases slowly from 0.015% for large values of Δ to a maximum value of 0.035% for $\Delta = 2$ (Table 1, part A). This would be expected on the basis of traditional methods of interpreting titration curves.

TABLE 1

Standard errors of the parameters for $pK_{a_1} = 4$, 5 or 6, given $c_1^0 = 0.1$ M, $x = 1$, $pK_w = 14$, $y_{H^+} = 1$, $\sigma_{pH} = 0.001$, and $\sigma_{V_b} = 0.01$ cm³ ($F = 1$, $G/F = 10$)

Δ	pK_{a_2}	Absolute or relative standard errors				
		c_1^0	x	$p(K_{a_1} y_{H^+})$	$p(K_{a_2} y_{H^+})$	y_{H^+}
A. For $pK_{a_1} = 4$						
7	11	0.015%	0.12%	0.00084	0.0017	1.07%
6	10	0.015%	0.060%	0.00084	0.0014	1.07%
5	9	0.015%	0.036%	0.00085	0.00100	1.07%
4	8	0.016%	0.035%	0.00086	0.00093	1.08%
3	7	0.019%	0.039%	0.00091	0.00092	1.09%
2	6	0.035%	0.073%	0.0012	0.00092	1.16%
1.5	5.5	0.022%	0.051%	0.00086	0.00084	1.07%
1	5	0.017%	0.030%	0.0011	0.0010	1.04%
0.5	4.5	0.014%	0.026%	0.0019	0.0018	0.97%
0.3	4.3	0.019%	0.039%	0.0030	0.0028	0.96%
0.1	4.1	0.0053%	0.0071%	0.0025	0.0022	0.75%
B. For $pK_{a_1} = 5$						
6	11	0.015%	0.14%	0.00082	0.0020	4.19%
5	10	0.015%	0.060%	0.00081	0.0013	4.21%
4	9	0.015%	0.036%	0.00083	0.0010	4.22%
3	8	0.018%	0.039%	0.00088	0.00092	4.22%
2	7	0.032%	0.069%	0.00107	0.00092	4.24%
1.5	6.5	0.010%	0.028%	0.00075	0.00081	4.12%
1	6	0.0035%	0.016%	0.00102	0.00102	3.96%
0.5	5.5	0.0080%	0.013%	0.0018	0.0018	3.55%
0.3	5.3	0.010%	0.020%	0.0031	0.0029	3.32%
0.1	5.1	0.0089%	0.0076%	0.0052	0.0050	2.88%
C. For $pK_{a_1} = 6$						
5	11	0.016%	0.12%	0.00083	0.0017	24.5%
4	10	0.016%	0.059%	0.00084	0.0014	24.2%
3	9	0.019%	0.040%	0.00087	0.0010	24.4%
2	8	0.030%	0.066%	0.00105	0.00091	24.2%
1.5	7.5	0.0076%	0.027%	0.00078	0.00082	23.6%
1	7	0.0073%	0.011%	0.00100	0.00099	22.2%
0.5	6.5	0.0055%	0.012%	0.00196	0.0019	18.8%
0.3	6.3	0.0093%	0.012%	0.0029	0.0027	16.6%
0.1	6.1	0.0060%	0.0073%	0.0040	0.0035	14.2%

However, decreasing Δ below 2 improves the relative precision of c_1^0, and does so to such an extent that it should actually be possible to obtain better precision in determining one acid for which $pK_a = 4.0$ in the presence of another for which $pK_a = 4.1$ than could be obtained if the second acid were much weaker.

The reason why this conclusion is surprising is that our ideas about the precisions with which titrations can be made have been overwhelmingly

influenced by the behaviors of the slopes of titration curves. Of course, a point of maximum slope is better defined, and can be located more precisely, if the variations of slope are large than if they are small. When the data are interpreted by non-linear regression analysis, however, the locations and even the existence of points of maximum slope are irrelevant. A much more important consideration is that the form of the weighting factor (the denominator of the righthand side of Eqn. 3) is such that points close to a point of maximum slope exert very little influence on the results. The data-acquisition schedule used in this work yields a number of points in the vicinity of the first equivalence point. If Δ is large, those points have little weight, but decreasing Δ decreases the slope in that region, renders those points more influential, and tends to improve the precision. Another reason why the precision of c_1^0 improves as Δ becomes very small is that the presence of the weaker acid then has substantial effects on the pH values at and near the very start of the titration, even though points in this region would be ignored in locating the end-points in the customary way.

The relative precision of x varies in a more complex way because it involves the relative precisions of both c_1^0 and c_2^0. It is poor if $\Delta = 7$, improves rapidly as Δ decreases to 5, and in a general way follows the variations of the relative precision of c_1^0 if Δ is less than about 5. If Δ is very small, and if the standard errors of measurement have the values assumed here, it should be possible to determine both constituents of an equimolar mixture with precisions of a few hundredths or thousandths of a per cent.

Although there are minor irregularities reflecting complexities that do not seem to require discussion, the general behaviors of the precisions of $p(K_{a1}y_{H^+})$, $p(K_{a2}y_{H^+})$, and y_{H^+} can be summarized much more briefly. If Δ exceeds about 3, the precision of $p(K_{a1}y_{H^+})$ is high and is independent of Δ because it is insensitive to the points at $f > 1$. As Δ decreases below 3, those points exert more influence on the value of that quantity, and its precision becomes steadily poorer. The precision of $p(K_{a2}y_{H^+})$ is best if Δ is approximately 1.5—2, and becomes slowly worse as Δ increases above that value or decreases below it. The relative precision of y_{H^+} changes very little with Δ but is slightly worse for values of Δ in the neighborhood of 1.5—2 than for either larger or smaller values. Generally similar patterns of behavior will be evident in all the Tables that follow.

The effect of pK_{a1} on the precisions of all these quantities is illustrated by Table 1. The general trends, for any one value of Δ, are that the relative precisions of c_1^0 and x are almost independent of pK_{a1} if Δ is large but are slightly improved by increasing pK_{a1} if Δ is small; that the absolute precisions of $p(K_{a1}y_{H^+})$ and $p(K_{a2}y_{H^+})$ are independent of pK_{a1}, regardless of the value of Δ; and that the relative precision of y_{H^+} rapidly becomes worse as pK_{a1} increases. As was noted in the preceding paragraph, if $pK_{a1} = 4$ there is a small maximum in the relative standard error of y_{H^+}, but that maximum is only barely detectable if $pK_{a1} = 5$ and is entirely absent if $pK_{a1} = 6$.

Table 2 shows the effects of x. Part A of Table 2, for which $x = 1$, may be

TABLE 2

Standard errors of the parameters for different values of x (= 1, 0.3162, 0.1, 0.03162), given c_1^0 = 0.1 M, pK_{a1} = 3, pK_w = 14, y_{H^+} = 1, σ_{pH} = 0.001, and σ_{V_b} = 0.01 cm³ (F = 1, G/F = 10)

Δ	pK_{a2}	Absolute or relative standard errors				
		c_1^0	x	$p(K_{a1}y_{H^+})$	$p(K_{a2}y_{H^+})$	y_{H^+}
A. For x = *1*						
7	10	0.015%	0.059%	0.00096	0.0014	0.447%
6	9	0.014%	0.035%	0.00092	0.00099	0.445%
5	8	0.015%	0.034%	0.00094	0.00090	0.446%
4	7	0.016%	0.033%	0.00096	0.00090	0.449%
3	6	0.019%	0.040%	0.00101	0.00092	0.456%
2	5	0.036%	0.075%	0.0014	0.00091	0.517%
1.5	4.5	0.0064%	0.018%	0.00092	0.00085	0.489%
1	4	0.0052%	0.011%	0.0012	0.0010	0.457%
0.5	3.5	0.0037%	0.012%	0.0022	0.0020	0.433%
0.3	3.3	0.0046%	0.010%	0.0035	0.0030	0.419%
0.1	3.1	0.0051%	0.0076%	0.0016	0.0010	0.327%
B. For x = *0.3162*						
7	10	0.017%	0.106%	0.00095	0.0025	0.448%
6	9	0.017%	0.089%	0.00095	0.0021	0.445%
5	8	0.017%	0.088%	0.00097	0.0020	0.448%
4	7	0.018%	0.090%	0.00099	0.0021	0.457%
3	6	0.023%	0.098%	0.00106	0.0022	0.464%
2	5	0.055%	0.252%	0.0015	0.0025	0.519%
1.5	4.5	0.064%	0.297%	0.0014	0.0024	0.492%
1	4	0.0067%	0.073%	0.0012	0.0020	0.477%
0.5	3.5	0.0049%	0.058%	0.0020	0.0041	0.479%
0.3	3.3	0.0041%	0.053%	0.0034	0.0076	0.57%
0.1	3.1	0.0029%	0.043%	0.0049	0.013	0.65%
C. For x = *0.1*						
7	10	0.018%	0.30%	0.00098	0.0054	0.451%
6	9	0.018%	0.27%	0.00098	0.0048	0.454%
5	8	0.018%	0.26%	0.00097	0.0049	0.450%
4	7	0.019%	0.27%	0.00099	0.0050	0.451%
3	6	0.025%	0.32%	0.00107	0.0055	0.464%
2	5	0.050%	0.60%	0.0013	0.0058	0.488%
1.5	4.5	0.050%	0.59%	0.0014	0.0051	0.504%
1	4	0.0021%	0.26%	0.0012	0.0058	0.481%
0.5	3.5	0.0054%	0.28%	0.0020	0.013	0.58%
0.3	3.3	0.0099%	0.31%	0.0029	0.023	0.65%
0.1	3.1	0.0106%	0.32%	0.0074	0.067	0.71%
D. For x = *0.03162*						
7	10	0.018%	0.94%	0.00099	0.0195	0.449%
6	9	0.018%	0.84%	0.00099	0.0194	0.456%
5	8	0.018%	0.81%	0.00099	0.0190	0.456%
4	7	0.020%	0.86%	0.00101	0.0193	0.459%
3	6	0.026%	1.00%	0.0011	0.0194	0.471%
2	5	0.061%	2.1%	0.0014	0.021	0.51%
1.5	4.5	0.11%	3.7%	0.0018	0.020	0.55%
1	4	0.0045%	4.7%	0.0012	0.018	0.48%
0.5	3.5	0.0025%	5.0%	0.0020	0.043	0.60%
0.3	3.3	0.0048%	5.8%	0.0031	0.076	0.66%
0.1	3.1	0.0043%	6.0%	0.0058	0.170	0.54%

compared with Table 1. It exhibits the general features described above, with some slight modifications that reflect the further decrease of pK_{a1}. Because the data-acquisition schedule yields fewer and fewer data points between the two equivalence points as x decreases, the chief effects of decreasing x are to worsen the precisions of both x and $p(K_{a2}y_{H^+})$. For the same reason, these fits are less well-conditioned, and irregularities are more prominent, especially at the lowest values of Δ, than they are for most of the other conditions studied. Consequently, it is not easy to discern trends in the behaviors of the other parameters, although it does appear that the maximum value of the relative standard error of c_1^0 becomes more marked and moves toward lower values of Δ as x decreases.

The significance of these results in practical titrimetry can be most easily appreciated by inspecting Fig. 1, which shows the portion of the titration curve that includes the first equivalence point for the titration corresponding to the last line of Table 2 for $x = 1$. The curve is almost perfectly linear in this region, and the existence of the equivalence point at $f = 1$ would be impossible to discern. In a prior investigation [14] of the conditions that must be satisfied to permit detecting the presence of both acids on the basis of titrimetric data, the data-acquisition schedule was assumed to be different from the one employed here, the standard error of

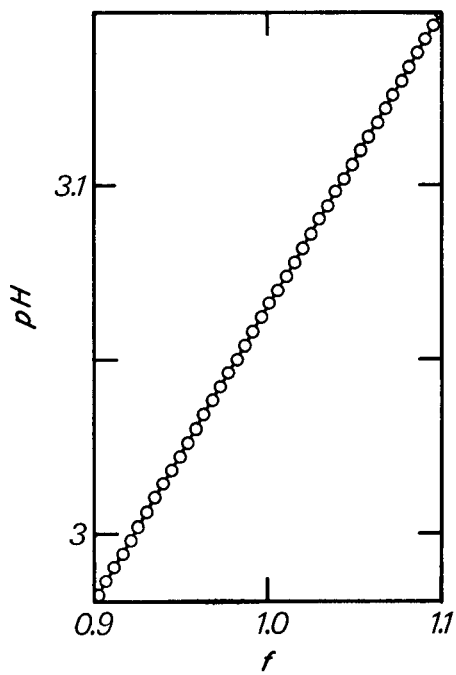

Fig. 1. The variation of pH with f in the vicinity of the first equivalence point on the titration curve for the titration, with 0.1 M base, of a mixture containing 0.1 M HA_1 ($pK_{a1} = 3$) and 0.1 M HA_2 ($pK_{a2} = 3.1$). The apparent single-ion activity coefficient of hydrogen ion, y_{H^+}, is assumed to be equal to 1.

measurement of the pH was assumed to be 0.002 rather than 0.001 pH as is assumed here, and the standard error of measurement of the volume of reagent was tacitly assumed to be zero. It was concluded that a difference of 0.1 between the values of pK_a for two weak acids does not suffice to ensure that the presence of both can be detected even if their concentrations are equal, and that the limit of detection corresponds, for example, to $\Delta = 0.349$ if $x = 0.03$. From the equations given earlier [14], it can be calculated that the limit of detection for that value of x would correspond to $\Delta = 0.236$ if σ_{pH} were equal to 0.001 and x were equal to 0.03162. The difference between the two data-acquisition schedules probably has only a small effect, and the limit of detection will certainly be higher if σ_{V_b} is finite. It can be concluded that, although titrimetric data of this precision will not reveal the presence of two acids in a mixture for which $\Delta = 0.1$ and $x = 0.03162$, they should make it possible to determine the concentrations of both with fair precision if other information is available to show that there are two acids in the mixture. In other words, titrimetry should permit the determination of both acids even though it does not permit the detection of both under the same conditions. There seems to have been no prior demonstration of the possibility of determining a substance under conditions so unfavorable that its presence cannot be detected.

All of the foregoing results correspond to $\sigma_{pH} = 0.001$ and to $\sigma_{V_b} = 0.01$ cm^3. These have the orders of magnitude that are appropriate to careful work with modern apparatus, but are unlikely to be identical with the values that characterize any particular practical titration. To permit prediction of what the standard errors of the parameters will be for any other combination of the standard errors of measurement, it is convenient to rewrite the familiar equation

$$\sigma_{V_i} = [\sigma_{pH}^2(\partial V_i/\partial pH)^2 + \sigma_{V_b}^2(\partial V_i/\partial V_b)^2]^{1/2} \tag{6}$$

in the form

$$\sigma_{V_i} = F[(\partial V_i/\partial pH)^2 + (G/F)^2(\partial V_i/\partial V_b)^2]^{1/2} = F\sigma^*_{V_i} \tag{7}$$

where $F = \sigma_{pH}/0.001$, $G/F = (\sigma_{V_b}/\sigma_{pH})(25/V_b^*)$, and $\sigma^*_{V_i}$ is defined as the quantity within square brackets in Eqn. 7. Tables 1 and 2 give values of $\sigma^*_{V_i}$ (or, for some parameters, of $\sigma^*_{V_i}/V_i$) for $F = 1$ and $G/F = 10$. In these equations, V_i denotes the ith parameter while V_b is the total volume of base added at any point and V_b^* is the volume of base added at the first equivalence point, so that $V_b^* = V_a^0 c_i^0/c_b$. The factor $(25/V_b^*)$ appears in the expression for G/F because a standard error of 0.001 cm^3 in the measurement of volume will have approximately the same effects on the standard errors of the parameters if $V_b^* = 2.5$ cm^3 as one of 0.01 cm^3 does if $V_b^* = 25$ cm^3. This is not quite exact because the effects of dilution will be slightly different, but it cannot be substantially erroneous unless r is very large.

As long as G/F is constant, the standard errors of the parameters are proportional to F. Under the conditions that correspond to the first line of

TABLE 3

Standard errors of the parameters as G/F increases from 0.01 to 100, given c_1^0 = 0.03162 M, x = 1, pK_{a1} = 3, pK_w = 14, y_{H^+} = 1 and σ_{pH} = 0.001

Δ	pK_{a2}	Absolute or relative standard errors				
		c_1^0	x	$p(K_{a1}y_{H^+})$	$p(K_{a2}y_{H^+})$	y_{H^+}
A. For σ_{V_b} = 0.000 01 cm³ (F = 1, G/F = 0.01)						
7	10	0.00085%	0.035%	0.00045	0.00053	0.24%
6	9	0.00096%	0.0068%	0.00045	0.00042	0.24%
5	8	0.0015%	0.0034%	0.00048	0.00038	0.25%
4	7	0.0030%	0.0060%	0.00063	0.00034	0.28%
3	6	0.00039%	0.0012%	0.00049	0.00035	0.25%
2	5	0.00011%	0.00082%	0.00056	0.00039	0.26%
1.5	4.5	0.00021%	0.00075%	0.00063	0.00043	0.27%
1	4	0.00027%	0.00065%	0.00078	0.00051	0.28%
0.5	3.5	0.00040%	0.00093%	0.0014	0.00097	0.31%
0.3	3.3	0.00021%	0.00058%	0.0018	0.0013	0.27%
0.1	3.1	0.00030%	0.00087%	0.00078	0.00032	0.21%
B. For σ_{V_b} = 0.000 1 cm³ (F = 1, G/F = 0.1)						
7	10	0.00099%	0.030%	0.00046	0.00054	0.28%
6	9	0.00105%	0.0065%	0.00047	0.00043	0.28%
5	8	0.0015%	0.0036%	0.00050	0.00038	0.28%
4	7	0.0033%	0.0067%	0.00060	0.00033	0.29%
3	6	0.00053%	0.0012%	0.00050	0.00037	0.28%
2	5	0.00045%	0.0012%	0.00057	0.00040	0.29%
1.5	4.5	0.00019%	0.0010%	0.00064	0.00044	0.30%
1	4	0.00038%	0.00085%	0.00080	0.00053	0.32%
0.5	3.5	0.00043%	0.00098%	0.0013	0.00093	0.33%
0.3	3.3	0.00052%	0.0014%	0.0020	0.0016	0.34%
0.1	3.1	0.00018%	0.00065%	0.0034	0.00030	0.28%
C. For σ_{V_b} = 0.001 cm³ (F = 1, G/F = 1)						
7	10	0.0026%	0.027%	0.00053	0.00063	0.30%
6	9	0.0025%	0.0074%	0.00052	0.00052	0.29%
5	8	0.0027%	0.0063%	0.00053	0.00042	0.29%
4	7	0.0032%	0.0068%	0.00061	0.00031	0.30%
3	6	0.0043%	0.0090%	0.00066	0.00049	0.31%
2	5	0.0016%	0.0034%	0.00062	0.00047	0.31%
1.5	4.5	0.0011%	0.0030%	0.00072	0.00049	0.32%
1	4	0.00096%	0.0029%	0.00089	0.00062	0.34%
0.5	3.5	0.00071%	0.0019%	0.0016	0.0012	0.37%
0.3	3.3	0.00084%	0.0025%	0.0022	0.0017	0.34%
0.1	3.1	0.00024%	0.0058%	0.0023	0.0017	0.28%
D. For σ_{V_b} = 0.1 cm³ (F = 1, G/F = 100)						
7	10	0.28%	0.66%	0.0081	0.0096	3.5%
6	9	0.27%	0.56%	0.0078	0.0073	3.4%
5	8	0.22%	0.49%	0.0072	0.0070	3.3%
4	7	0.19%	0.41%	0.0067	0.0075	3.3%
3	6	0.19%	0.37%	0.0069	0.0083	3.3%
2	5	0.34%	0.68%	0.0085	0.0086	3.4%
1.5	4.5	0.76%	1.58%	0.013	0.0095	3.9%
1	4	0.12%	0.28%	0.0068	0.0080	3.1%
0.5	3.5	0.10%	0.19%	0.012	0.0013	3.1%
0.3	3.3	0.093%	0.20%	0.022	0.0022	3.0%
0.1	3.1	0.068%	0.21%	0.040	0.0037	2.8%

Table 2, for example, the relative standard error of c_1^0 is 0.015% if σ_{pH} = 0.001 (so that F = 1) and σ_{V_b} = 0.01 cm^3 (so that, since V_b^* = 25 cm^3, G/F = 10). If σ_{pH} and σ_{V_b} were equal to 0.005 and 0.05 cm^3, respectively, one would have F = 5 and G/F = 10. Because the latter is unchanged, the relative standard error of c_1^0 would be just five times the value given above, or 0.075%.

Table 3 and Table 2 (part A) show how the values of the $\sigma_{V_i}^*$ vary as G/F increases from 0.01 to 100 by successive factors of 10. As would be expected, their variations are small if G/F is small, although the relative standard errors of c_1^0 and x are not quite independent of G/F even if that quantity is as small as 0.1. The variations become much larger if G/F exceeds 1, and the standard errors of all the parameters must approach proportionality to G/F as that quantity becomes very large.

From these tables it is possible to estimate the standard errors of the parameters for any combination of values of F and G/F. Suppose, for example, that the titration corresponding to the first line of Table 2 is conducted in such a way that σ_{pH} = 0.005 and σ_{V_b} = 0.02 cm^3, so that F = 5 and G/F = 4. If F = 1 and G/F = 1, the first line of Table 3C gives the relative standard error of c_1^0 as 0.0026%; if F = 1 and G/F = 10, the first line of Table 2A gives the relative standard error of c_1^0 as 0.015%. Semilogarithmic interpolation, which though surely not exact is probably accurate enough for any practical purpose, indicates that the relative standard error of c_1^0 will be about 3 times as large with G/F = 4 as with G/F = 1, or say 0.0075% with F = 1, and hence about 0.038% with F = 5.

Conclusions

Although the numerical values given in this paper depend on the data-acquisition schedule on which they are based, generally similar behavior will probably be obtained with any other schedule that seems to be reasonably well adapted to the demands of the problem. It can be concluded that, in general, changes of the experimental variables and conditions affect the precisions of the parameters in ways that are very different if the parameters are evaluated by non-linear regression analysis from the ways in which such changes affect precisions in interpretations of titration-curve data by classical techniques. It can also be concluded that non-linear regression analysis should permit two weak acids of nearly equal strengths to be determined far more precisely than has heretofore been thought possible.

This work was aided by the generous support of the Consiglio Nazionale delle Richerche, to which the senior author (L. M.) is indebted for a visiting fellowship during the summer of 1985.

REFERENCES

1 See, for example, I. M. Kolthoff and N. H. Furman, Potentiometric Titrations, 2nd edn., Wiley, New York, 1931.

2 F. Ingman, A. Johansson, S. Johansson and R. Karlson, Anal. Chim. Acta, 64 (1973) 113.
3 D. M. Barry and L. Meites, Anal. Chim. Acta, 68 (1974) 435.
4 L. Lampugnani and L. Meites, Anal. Chem., 45 (1973) 1317.
5 L. Meites, CRC Crit. Rev. Anal. Chem., 8 (1979) 1.
6 B. H. Campbell and L. Meites, Talanta, 21 (1974) 393.
7 H. C. Smit, L. Meites and G. Kateman, work in progress.
8 H. C. Smit, L. Meites and G. Kateman, Anal. Chim. Acta, 153 (1983) 121.
9 G. Kateman, H. C. Smit and L. Meites, Anal. Chim. Acta, 152 (1983) 61.
10 L. Meites and J. A. Goldman, Anal. Chim. Acta, 29 (1963) 472.
11 L. Meites, The General Non-Linear Regression Program CFT4A, The George Mason Institute, Fairfax, VA, 1985.
12 L. Meites, Anal. Chim. Acta, 74 (1975) 177.
13 E. Bishop, Anal. Chim. Acta, 22 (1960) 101.
14 L. Meites, Anal. Lett., 15(A5) (1982) 507.

Analytica Chimica Acta, 182 (1986) 147—155
Elsevier Science Publishers B.V., Amsterdam — Printed in The Netherlands

STRIPPING VOLTAMMETRY OF MANGANESE BASED ON CHELATE ADSORPTION AT THE HANGING MERCURY DROP ELECTRODE

JOSEPH WANG* and JAWAD S. MAHMOUD

Department of Chemistry, New Mexico State University, Las Cruces, NM 88003 (U.S.A.)

(Received 18th April 1985)

SUMMARY

A novel electrochemical stripping approach for the trace measurement of manganese is presented. The metal chelate with eriochrome black T is adsorbed on a hanging mercury drop electrode, and the subsequent reduction current of the accumulated chelate is measured by voltammetry. Adsorptive preconcentration for 5 min results in a detection limit of 6×10^{-10} M (32 ng l^{-1}). Cyclic voltammetry is used to characterize the redox and interfacial processes. Optimal experimental conditions include a 0.02 M piperazine-*N*,*N*'-bis(2-ethanesulfonic acid) solution (pH 12) containing 1×10^{-6} M eriochrome black T, a preconcentration potential of —0.80 V, and a linear potential scan. The response is linear up to 2.9×10^{-7} M, and the relative standard deviation at 1.8×10^{-7} M is 1.5%. The effects of possible interferences from metal ions or organic surfactants are evaluated.

Recent environmental and biochemical studies have revealed the need for improved methods capable of measuring trace and ultratrace levels of manganese. Atomic absorption of neutron activation measurements at these levels usually require laborious enrichment steps, e.g., extraction or coprecipitation. The utility of stripping analysis, the most sensitive electroanalytical technique, for this purpose has been examined in several studies [1—5]. Conventional stripping measurements of manganese(II), based on electrolytic preconcentration as the metal at the mercury film electrode, allow measurements of nanomolar levels in various natural waters [2, 3]. However, such measurements suffer from problems caused by large hydrogen evolution background, low solubility of manganese in mercury, irreversible redox process, and formation of various intermetallic compounds. Cathodic stripping procedures, based on anodic preconcentration as hydrated manganese dioxide have also been reported [4, 5].

The present paper describes an extremely sensitive and simple stripping procedure for trace measurements of manganese, in which preconcentration is achieved by adsorption of the manganese/eriochrome black T chelate on the hanging mercury drop electrode. Adsorptive stripping voltammetry has been shown recently to be an effective alternative to conventional stripping analysis with electrolytic deposition [6]. This approach is based on the formation of an appropriate surface-active complex or chelate of the metal ion, its controlled interfacial accumulation on the electrode surface, and the

0003-2670/86/$03.50

voltammetric quantification of the surface-bound species, usually by a negative-going potential scan. As a result, low concentrations of nickel [7], cobalt [8], aluminum [9], lanthanides [10], copper [11], uranium [12] and vanadium [13] have been measured in the presence of various complexing ligands. The results of a detailed investigation into the optimal experimental conditions for the trace measurements of manganese, in the presence of the azo dye eriochrome black T are reported below.

EXPERIMENTAL

Apparatus and reagents

The equipment used to obtain the voltammograms, a PAR 264 voltammetric analyzer with a PAR 303 static mercury drop electrode, was described in detail before [9, 10]. All solutions were prepared from double-distilled water. A 1000 mg l^{-1} manganese stock solution (atomic absorption standard; Aldrich) was used, and diluted as required for standard additions. A 10^{-4} M stock solution of eriochrome black T (Fisher) was prepared daily. Supporting electrolyte was 0.02 M PIPES [piperazine-*N*,*N*′-bis(2-ethanesulfonic acid), disodium salt monohydrate; Aldrich], adjusted to pH 12 with sodium hydroxide.

Procedure

The supporting electrolyte solution (10 ml), containing 1×10^{-6} M eriochrome black T, was pipetted into the cell, and purged with nitrogen for 8 min. The preconcentration potential (usually −0.80 V) was applied to a fresh mercury drop while the solution was stirred. After the preconcentration period, the stirring was stopped, and after 15 s the voltammogram was recorded by applying a negative-going linear scan; the scan was terminated at −1.30 V. After background stripping voltammograms had been obtained, aliquots of the manganese standards were introduced. Throughout this operation, nitrogen was passed over the solution surface. All data were obtained at room temperature.

RESULTS AND DISCUSSION

Figure 1 shows linear scan voltammograms for 10 μg l^{-1} (1.8×10^{-7} M) manganese(II) in the presence of eriochrome black T and solochrome violet RS obtained with and without preconcentration. The interfacial accumulation of the corresponding metal chelates, i.e., increased surface concentrations, is clearly indicated from the substantial increase of the peak current at −0.98 V; peak current enhancements of 9 and 10 are obtained with eriochrome black T and solochrome violet RS, respectively. The formation of the polarographically-active chelate of manganese with solochrome violet RS has been reported [14], but no such data are available regarding the corresponding behavior of the eriochrome black T/manganese chelate. The

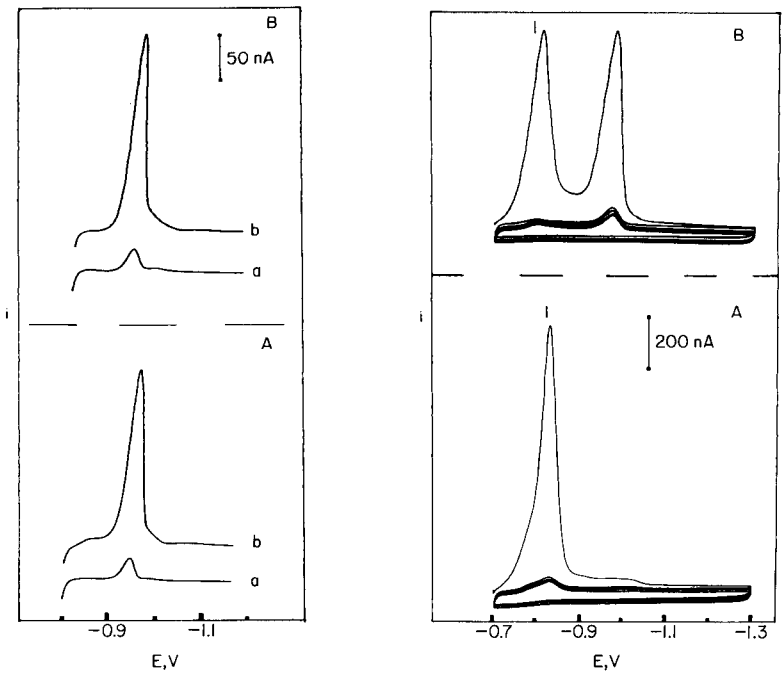

Fig. 1. Linear-scan voltammograms for 10 $\mu g\ l^{-1}$ manganese(II): (A) in the presence of 1×10^{-6} M eriochrome black T; (B) in the presence of solochrome violet RS. Preconcentration at −0.80 V for (a) 0 s and (b) 45 s, at 400 rpm stirring. Scan rate, 50 mV s^{-1}. Supporting electrolyte, 0.02 M PIPES (pH 12).

Fig. 2. Repetitive cyclic voltammograms obtained after 60-s stirring at −0.70 V: (A) 2×10^{-6} M eriochrome black T; (B) as (A) but after addition of 40 $\mu g\ l^{-1}$ manganese(II). Scan rate and electrolyte, as in Fig. 1.

distinct reduction wave of the solochrome violet RS chelate at the dropping mercury electrode, coupled with the surface-active properties of the chelate, allowed measurements of mg l^{-1} concentrations of manganese [14]. As shown in Fig. 1, the use of the hanging mercury drop electrode permits convenient quantification at the $\mu g\ l^{-1}$ level, as the adsorptive accumulation proceeds over significantly longer time scales than those allowed at the dropping electrode. Similar improvements, based on the formation and adsorption of chelates with solochrome violet RS, have been illustrated recently in measurements of aluminum [9]. The data of Fig. 1 indicate that both dyes offer similar sensitivity. However, measurements with eriochrome black T are less susceptible to interferences from other metal ions; hence, this ligand was used throughout this study.

The spontaneous accumulation can be verified and evaluated by using cyclic voltammetry. Figure 2A shows repetitive cyclic voltammograms for 2×10^{-6} M eriochrome black T obtained following 1-min stirring at −0.70 V.

The first scan (designated as 1) exhibits a large cathodic peak at —0.82 V related to reduction of the adsorbed dye. No peak is observed in the anodic branch. Subsequent scans yield substantially smaller cathodic peaks, indicating rapid desorption of the reduced dye from the surface. When the same experiment was repeated in the presence of 40 μg l^{-1} manganese (Fig. 2B), an additional peak, related to reduction of the adsorbed chelate, is observed in the cathodic branch of the first scan (E_p = —0.99 V). The significantly smaller peaks observed in the subsequent scans indicate desorption of the product from the surface. When a potential of —0.80 V was applied during the stirring period, only a single cathodic peak (not shown) related to the adsorbed chelate was observed.

The surface coverage can be measured from the quantity of charge consumed by the surface process during the cyclic voltammetric experiment. With 40 μg l^{-1} manganese, 2 × 10^{-6} M eriochrome black T and stirring at —0.80 V, maximum adsorption density was observed after a 3-min accumulation. The maximum charge, obtained by integrating the reduction current, was found to be 1.28 μC. This amount is equivalent to an adsorbed layer of 2.1 × 10^{-10} mol cm^{-2}. The area occupied by a chelate molecule cannot be estimated because the data indicated co-adsorption of the free dye. The peak current for the adsorbed chelate at saturation is proportional to the potential scan rate (v). A plot of log i_p vs. log v was linear, with a slope of 0.88 over the 20—200 mV s^{-1} range.

The dependence of the adsorptive stripping peak current on the preconcentration time was evaluated for 5 μg l^{-1} manganese. The stripping peak increased linearly with preconcentration time at first and then levelled off at times longer than 3 min. Least-squares treatment of the linear range yielded the equation i(nA) = (2.33 ± 0.05) t(s) + 20.4 ± 6.4 nA with r = 0.998 and S_{yx} = 6.90. Because the peak current depends on the amount of chelate adsorbed; full surface coverage is approached for times longer than 3 min. Obviously, different time profiles would be obtained under different experimental conditions (e.g., rate of mass-transport, bulk concentration) affecting the amount adsorbed. Overall, convenient measurement of manganese at the 0.5- and 10-μg l^{-1} levels is feasible after preconcentration for 300 and 20 s, respectively.

The pH of the solution affects the height and potential of the manganese chelate stripping peak (Fig. 3). The pH was varied by adding dilute hydrochloric acid or sodium hydroxide. The largest peak height is obtained at pH 12.5 (curve a). This pH also yields the largest peak current enhancement (6-fold at 30 s), as compared to other solutions for which the enhancement ranges from 3 to 5. The peak potential becomes more negative as the pH increases (curve b), shifting 8 mV between pH 10.5 and pH 12.5. Subsequent experiments involved solutions with pH 12.0, which yielded the best signal/background characteristics. The use of other alkaline solutions, e.g., borate buffer or ammonium chloride, yielded inferior results compared to PIPES. Heating the solution to 40°C or 80°C during chelate formation

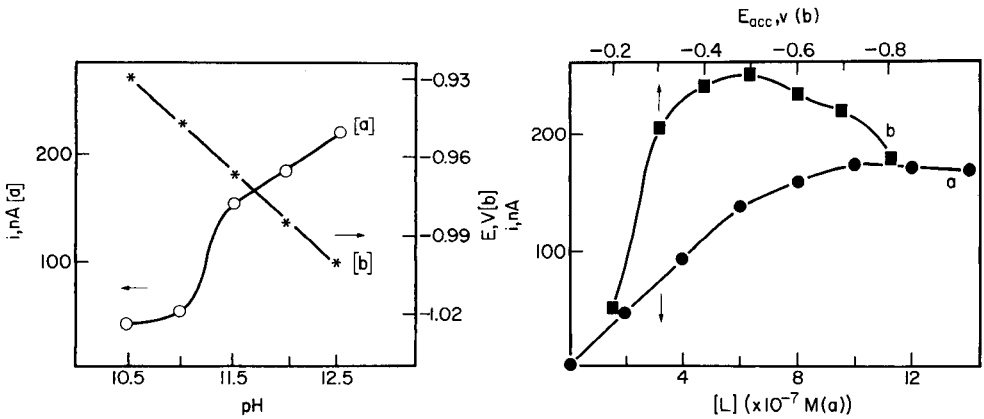

Fig. 3. Effect of the solution pH on the peak current (a) and potential (b) of the manganese/eriochrome black T chelate. Conditions as in Fig. 1A, except that 30-s preconcentration was used.

Fig. 4. Effect of ligand concentration (a) and preconcentration potential (b) on the stripping peak current. Preconcentration for 60 s. Other conditions as in Fig. 1A.

resulted in responses similar to those obtained at room temperature; the latter was used throughout.

The concentration of eriochrome black T has a pronounced effect on the adsorptive stripping response. The stripping peak for 10 $\mu g\, l^{-1}$ manganese was measured in the presence of various concentrations of the dye; the results are presented in Fig. 4 (curve a). The peak height increases in a linear fashion with the dye concentration to 8×10^{-7} M, after which it remains constant. The chelate peak depends on the molar ratio, [dye]/[Mn(II)]. The change of the dye concentration did not affect the shape of the stripping peak. Subsequent trace and ultratrace measurements were done in solutions containing 1.0×10^{-6} M eriochrome black T.

The effect of the preconcentration potential on the peak current was evaluated over the —0.2 to —0.8 V range (Fig. 4, curve b). The largest peak is observed for potentials at —0.5 V. A gradual decrease (up to 30%) in the chelate peak was observed on changing the preconcentration potential from —0.50 V to —0.80 V. Nevertheless, best results, based on the overall signal-to-background characteristics, were obtained at a preconcentration potential of —0.80 V. At this point, the peak is not affected by the baseline current associated with the preceding dye peak (in contrast to the response obtained at more positive potentials). Accordingly, this potential was used for all further work, despite the reduction in the chelate peak. Mass-transport during the preconcentration step also affects the manganese/eriochrome black T stripping peak. For example, a stirring rate of 400 rpm resulted in a 3.8-fold enhancement of the response, compared to that obtained in a

quiescent solution (8 μg l^{-1} manganese, 1-min preconcentration). Such mass-transport control indicates a fast rate of chelate adsorption.

The linear-scan stripping mode yielded slightly better signal-to-background characteristics than the differential pulse waveform. While similar response characteristics were observed for these waveforms without preconcentration, a smaller peak current enhancement coupled with increased background current characterized the differential pulse scan following the accumulation. As a result of its response characteristics and its speed advantage, the linear-scan mode was used throughout this study. Stripping peak half-widths of 38 and 50 mV were obtained in the linear-scan and differential-pulse modes, respectively.

Analytical utility

The effective preconcentration associated with the adsorption process results in extremely low detection limits. Figure 5 shows linear-scan voltammograms for 1.0 μg l^{-1} (1.8×10^{-8} M) manganese after preconcentration for 1 and 5 min. A detection limit near 32 ng l^{-1} (6×10^{-10} M) is estimated based on the signal-to-noise characteristics (S/N = 2) of the data for 5 min preconcentration. This concentration corresponds to 320 pg in the 10 ml of

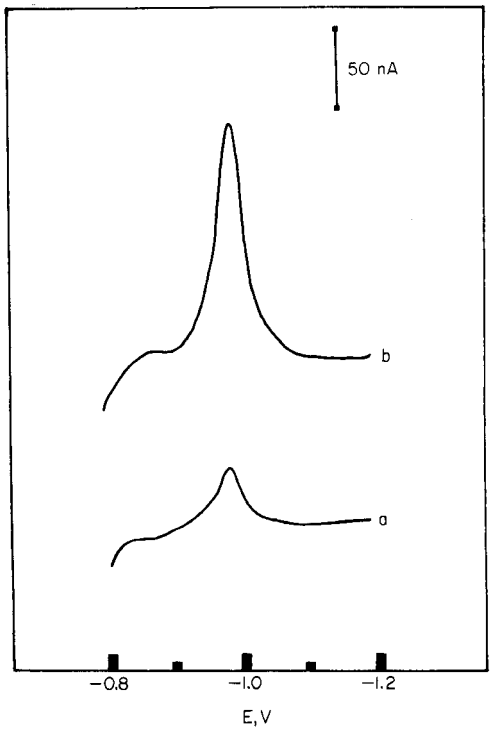

Fig. 5. Linear scan voltammograms for 1.0 μg l^{-1} manganese after preconcentration for: (a) 60 s; (b) 300 s. Other conditions as in Fig. 1A.

solution used. Such a detection limit is similar to those obtained in conventional stripping voltammetry with electrolytic deposition.

At the 1—10 $\mu g\ l^{-1}$ level, significantly shorter preconcentration times suffice. Figure 6 illustrates the response for successive standard additions of 2 $\mu g\ l^{-1}$ (3.6×10^{-8} M) manganese, using 30-s preconcentration. Well-defined stripping peaks are observed. In contrast, the conventional voltammetric response, without preconcentration, does not permit convenient quantification (dotted lines). The five measurements shown in Fig. 6 were part of a series of ten concentration increments. Deviations from linearity were observed for concentrations higher than 16 $\mu g\ l^{-1}$ (2.9×10^{-7} M). Such curvature is consistent with a process that is limited by adsorption of the analyte; above a certain level, the surface becomes saturated with the adsorbed chelate. Least-squares treatment of the linear portion (2—16 $\mu g\ l^{-1}$) yielded a slope of 19.85 ± 0.38 nA l μg^{-1}, an intercept of −2.98 ± 3.41 nA, and a correlation coefficient of 0.999. The direct response (without preconcentration) yielded a slope of 2.27 ± 0.05 nA l μg^{-1}, an intercept of 4.87 ± 0.62 nA, and a correlation coefficient of 0.998. The linear range depends on the operational parameters affecting the surface coverage. For example, with 90-s preconcentration, the calibration plot levelled off above 8 $\mu g\ l^{-1}$ (not shown; slope of the linear portion, 49.32 ± 1.89 nA l μg^{-1}; intercept, −8.83 ± 8.16 nA; correlation coefficient, 0.999). Accordingly, the linear range can be extended by using lower rates of mass-transport, shorter preconcentration times or sample dilution. However, this is not essential as direct voltammetric measurements of the chelate can be used for manganese concentrations higher than 10 $\mu g\ l^{-1}$. In contrast, at the 0.1—1 $\mu g\ l^{-1}$ level, only the adsorptive approach offers the desired sensitivity. When the method of standard additions is used for quantification, three additions are necessary to ensure that the measured current varies linearly with concentration. Conventional stripping measurements of manganese, based on electrolytic preconcentration, suffer also from a limited linear range [2, 3].

The precision was evaluated from eight repetitive measurements of a 10 $\mu g\ l^{-1}$ manganese solution (conditions as in Fig. 1, except that the preconcentration time was 30 s). The mean peak current was 175.6 nA with a

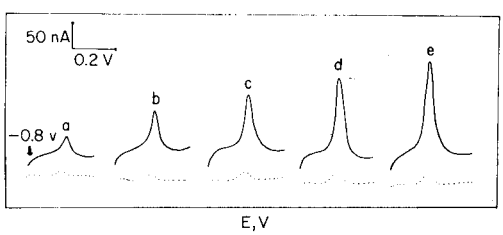

Fig. 6. Stripping voltammograms obtained with increasing manganese concentration in steps of 2 $\mu g\ l^{-1}$ (a—e). Preconcentration for 30 s. Other conditions as in Fig. 1A. The dotted lines represent the response without preconcentration.

range of 172.5—181.6 nA and a relative standard deviation of 1.5%. These data indicate reproducible accumulation of the metal chelate on the mercury surface.

The major sources of interferences are likely to be organic surfactants that compete with the chelate on the surface sites, and coexisting metal ions that form reducible and adsorbable chelates with eriochrome black T. The effects of various surfactants and metals on the 10 $\mu g\ l^{-1}$ manganese response were investigated for 60-s preconcentration. The manganese peak was not affected by an addition of 100 $\mu g\ l^{-1}$ gelatin; further additions up to 500 and 1000 $\mu g\ l^{-1}$ resulted in 30% and 70% depressions of the peak, respectively. Humic acid at 100, 500 and 1000 $\mu g\ l^{-1}$ resulted in 0%, 12% and 36% depressions of the initial peak, respectively. The manganese peak height diminished strongly in the presence of Triton X-100; 17% and 31% diminutions were observed after additions of 100 and 500 $\mu g\ l^{-1}$ of this non-ionic surfactant. Destruction of organic surfactants by ultraviolet irradiation is recommended for samples suspected to contain relatively high levels of these materials [13]. Measurements of 10 $\mu g\ l^{-1}$ manganese were not affected by the addition of 10 $\mu g\ l^{-1}$ Mg(II), Bi(III), Se(IV), Sn(IV), Pb(II), Hg(II) and In(III); 5%, 10%, 11% and 12% depressions of the peak height were observed after additions of 10 $\mu g\ l^{-1}$ Ti(IV), Fe(III), Ni(II) and Cu(II), respectively. Similar addition of Zn(II) yielded 8% enhancement. No change in the peak for 10 $\mu g\ l^{-1}$ manganese was observed on additions of 50 $\mu g\ l^{-1}$ Se(IV), Bi(III), Pb(II), Sn(IV) and Hg(II); 50 $\mu g\ l^{-1}$ In(III), Mg(II), Cu(II), Zn(II), Ca(II), Ti(IV), Fe(III) and Ni(II) resulted in 15, 16, 20, 21, 21, 21, 35 and 35% diminutions of the 10 $\mu g\ l^{-1}$ manganese peak, respectively; 50 $\mu g\ l^{-1}$ Zn(II) enhanced the peak by 20%. An appropriate separation or masking step would be required in the presence of elevated levels of these ions. Conventional stripping measurements of manganese (based on electrolytic deposition) suffer from severe intermetallic interferences when metals such as copper, nickel, cobalt or chromium are present [2]. Work in this laboratory is in progress toward the development of new adsorptive stripping procedures for other metal ions, for which conventional stripping measurement is difficult.

This work was supported by the National Institutes of Health under Grant No. GM30913-02.

REFERENCES

1 D. Monnier, E. Martin and W. Haerdi, Anal. Chim. Acta, 34 (1966) 346.
2 J. O'Halloran, Anal. Chim. Acta, 140 (1982) 51.
3 H. Eskilsson and D. R. Turner, Anal. Chim. Acta, 161 (1984) 293.
4 Kh. Z. Brainina, Zh. Anal. Khim., 19 (1964) 810.
5 A. Trojánek and F. Opekar, Anal. Chim. Acta, 126 (1981) 15.
6 J. Wang, Am. Lab., 17(5) (1985) 41.
7 A. Braun and M. Metzger, Fresenius Z. Anal. Chem., 318 (1984) 321.

8 A. Meyer and R. Neeb, Fresenius Z. Anal. Chem., 315 (1983) 118.
9 J. Wang, P. A. M. Farias and J. S. Mahmoud, Anal. Chim. Acta, 172 (1985) 57.
10 J. Wang, P. A. M. Farias and J. S. Mahmoud, Anal. Chim. Acta, 171 (1985) 215.
11 C. M. G. van den Berg, Anal. Chim. Acta, 164 (1984) 195.
12 C. M. G. van den Berg and Z. Q. Huang, Anal. Chim. Acta, 164 (1984) 209.
13 C. M. G. van den Berg and Z. Q. Huang, Anal. Chem., 56 (1984) 2383.
14 S. M. Palmer and G. F. Reynolds, Fresenius Z. Anal. Chem., 216 (1966) 202.

Analytica Chimica Acta, 182 (1986) 157—162
Elsevier Science Publishers B.V., Amsterdam — Printed in The Netherlands

SPECTROPHOTOMETRIC DETERMINATION OF SILVER WITH 4-(3,5-DIBROMO-2-PYRIDYLAZO)-*N*,*N*-DIETHYLANILINE IN THE PRESENCE OF SODIUM DODECYLSULFATE

K. OHSHITA

Laboratory of Chemistry, Daido Institute of Technology, Minami-ku, Nagoya (Japan)

H. WADA* and G. NAKAGAWA

Laboratory of Analytical Chemistry, Nagoya Institute of Technology, Showa-ku, Nagoya (Japan)

(Received 12th April 1985)

SUMMARY

The bidentate ligands, 4-(3,5-dibromo-2-pyridylazo)-*N*,*N*-diethylaniline (3,5-diBr-PAEA) and 4-(3,5-dibromo-2-pyridylazo)-*N*-ethyl-*N*-(3-sulfopropyl)aniline (3,5-diBr-PAESA) react with silver(I) ion to form the AgL_2 chelate in the presence of anionic or nonionic surfactant. The molar absorptivity at 600 nm is 80 000 l mol^{-1} cm^{-1} in 0.1% sodium dodecylsulfate solution. Optimum conditions for the spectrophotometric determination of silver in the range 0.1—1.0 mg l^{-1} with 3,5-diBr-PAEA are reported. A flow-injection procedure is also presented.

Recently, it was reported that 2-(3,5-dibromo-2-pyridylazo)-5-diethylaminophenol (3,5-diBr-PADAP) reacts only slightly with silver ion in aqueous solution, but on the addition of sodium dodecylsulfate (SDS) the absorbance is increased dramatically [1]. Generally, silver(I) complexes have a linear or a tetrahedral structure, thus it seems highly unlikely that 3,5-diBr-PADAP coordinates with silver ion as a terdentate ligand. It seemed worthwhile, therefore, to examine the chelate formation of silver ion with bidentate or monodentate pyridylazo compounds, which should be more selective for silver than the terdentate reagents.

In a previous study [2], several bidentate reagents were synthesized, and copper(II) ion was found to react very sensitively to form a CuL_2 chelate with 4-(3,5-dibromo-2-pyridylazo)diethylaniline (3,5-diBr-PAEA) and 4-(3,5-dibromo-2-pyridylazo)-*N*-ethyl-*N*-(3-sulfopropyl)aniline (3,5-diBr-PAESA) in the presence of anionic surfactants such as SDS. In the present study, the reactions of silver ion with some bidentate or monodentate pyridylazo derivatives in the presence of surfactant were examined. Silver ion forms a stable chelate (AgL_2) with 3,5-diBr-PAEA in the presence of SDS. The reaction provides a very sensitive spectrophotometric determination of silver.

0003-2670/86/$03.50

EXPERIMENTAL

Reagents and apparatus

Silver(I) solution was prepared by dissolving silver (99.99% purity) in nitric acid, boiling out nitrogen oxides and diluting the solution appropriately. All the other reagents used were the same as those described earlier [2]. The water used was redistilled from a hard-glass vessel.

A Union Giken SM-401 spectrophotometer and a Hitachi-Horiba Model F-7 pH meter were used. The home-made flow-injection manifold is shown in Fig. 1. The components were as described earlier [2].

Procedures

Recommended procedure for the batch method. The sample solution containing less than 25 μg of silver ion is placed in a 25-ml volumetric flask, and 2.5 ml of 10^{-2} M EDTA, 2.5 ml of 1% (w/v) SDS solution, 1 ml of 2 M acetic acid/sodium acetate buffer (pH 5.5) and 1 ml of 10^{-3} M 3,5-diBr-PAEA in ethanol are added. The mixture is diluted to the mark with water and mixed well. After 10 min at room temperature, the absorbance is measured at 600 nm against the reagent blank.

Recommended procedure for flow-injection analysis. The reagent stream (R) contains 5×10^{-5} M 3,5-diBr-PAEA, 5% (v/v) ethanol and 0.4% (w/v) SDS. The carrier stream (B) contains 0.1 M acetic acid/sodium acetate buffer (pH 5.5) and 10^{-3} M EDTA. Each is pumped at 0.8 ml min^{-1}. The sample (40 μl) is injected into the buffer stream via a rotary valve with an appropriate loop. Sample and reagent are mixed in the 300-cm coil and the absorbance is measured at 600 nm.

Pretreatment for the waste fixing solutions. A sample containing less than 25 μg of silver is placed in a 50-ml beaker, and 5 drops of 30% hydrogen peroxide, 1 ml of nitric acid (1 + 1) and 1 ml of sulfuric acid (1 + 1) are added. The mixture is heated to fuming, and heating is continued for 2–3 min. After the solution has cooled to room temperature, 1 ml of nitric acid (1 + 1) is added and the beaker wall is rinsed carefully with about 5 ml of water. The solution is warmed to dissolve any residue, and then transferred to a 25-ml volumetric flask. After addition of 1 ml of 5% (w/v) potassium

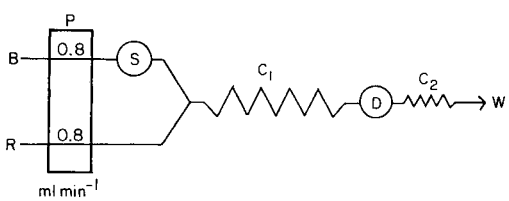

Fig. 1. Flow diagram: P, peristaltic pump; S, sample injector (40 μl); C_1, mixing coil (300 cm, 0.5 mm i.d.); C_2, back-pressure coil (50 cm, 0.25 mm i.d.); D, spectrophotometer (600 nm) with flow cell (10 μl); B, acetate buffer (0.1 M, pH 5.5) containing EDTA (10^{-3} M); R, 3,5-diBr-PAEA (5×10^{-5} M) containing ethanol and SDS.

citrate solution and a drop of phenolphthalein solution, the mixture is neutralized with 4 M sodium hydroxide (to pink), adjusted back to colorless with nitric acid (1 + 5), and finally diluted to the mark.

RESULTS AND DISCUSSION

Reaction with silver ion

In aqueous or aqueous-ethanol solution, silver ion reacted slightly with the terdentate and bidentate reagents synthesized in the previous work [2]. With 3,5-diBr-PADAP, 2-(3,5-dibromo-2-pyridylazo)-5-[*N*-ethyl-*N*-(3-sulfopropyl)-amino]phenol (3,5-diBr-PAESPAP), 2-(5-bromo-2-pyridylazo)-5-diethylaminophenol (5-Br-PADAP), 3,5-diBr-PAEA and 3,5-diBr-PAESA, the absorbances of the chelates formed were enhanced dramatically by the addition of nonionic or especially anionic surfactant. The molar absorptivities (1 mol^{-1} cm^{-1}) in 0.1% SDS solution are 77 000, 60 000, 60 000, 80 000 and 80 000, respectively [2]. A bathochromic shift was observed on the addition of surfactant, as can be seen in Fig. 2 for the absorption spectra of the silver/3,5-diBr-PAEA chelate. In contrast to these reagents, 4-(2-pyridylazo)anilines and 2-(2-pyridylazo)-5-dialkylaminophenols, which have no bromine in the

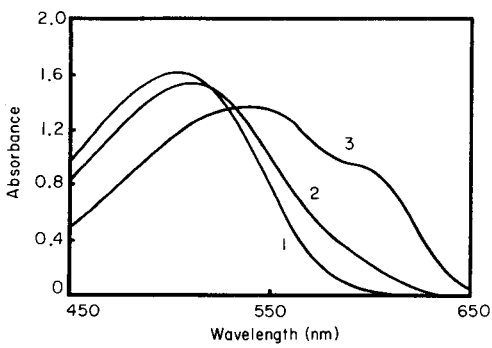

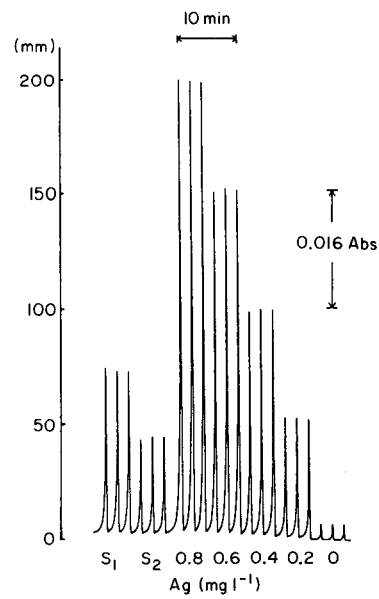

Fig. 2. Absorption spectra of 3,5-diBr-PAEA (4×10^{-5} M) and its silver(I) (10^{-5} M) chelate: (1) 3,5-diBr-PAEA in aqueous 40% (v/v) ethanol or 0.1% (w/v) SDS solution; (2) silver chelate in aqueous 40% ethanol solution; (3) silver chelate in 0.1% SDS solution, pH 5.5.

Fig. 3. Calibration output for 0—0.8 mg l^{-1} silver and the determination of silver in diluted waste fixing solutions (S_1 and S_2). Each standard and sample was injected three times.

pyridine ring, and thiazolylazo compounds formed chelates which were only slightly affected by the addition of surfactant in terms of absorption characteristics.

The composition of the silver/3,5-diBr-PAEA chelate was examined in 0.1% (w/v) SDS solution by the mole ratio method. The results showed the formation of a 1:2 chelate (AgL_2).

When 4-(4-pyridylazo)dimethylaniline, which may behave as monodentate ligand, was used, the difference in the absorption spectra between the reagent and the silver complex was very small even in the presence of surfactant. From all these results, silver ion may coordinate with the pyridine nitrogen atom and a nitrogen atom in the azo group of 3,5-diBr-PAEA or 3,5-diBr-PAESA. If only the pyridine nitrogen were involved, such a large bathochromic shift would not be observed. The formation of tetrahedral silver(I)/pyridine [3] and diamine complexes [4] have been reported when the concentrations of ligands were large. In the present case, it is considered that the silver chelate (AgL_2) may have a tetrahedral structure, because the chromogenic reagent is probably concentrated in each micelle of the surfactant. Bromine in the pyridine ring may play a role in weakening the basicity of the pyridine nitrogen, so that silver ion could easily replace the proton at a relatively low pH range.

The behaviors of 3,5-diBr-PAEA and 3,5-diBr-PAESA for silver ion were similar, but 3,5-diBr-PAEA was preferred here because of the wider linear range of calibration and smaller reagent blank.

Optimum conditions for the determination of silver(I)

The anionic or nonionic surfactants examined were SDS, sodium decylsulfate (SDeS), sodium tetradecylsulfate (STDS), sodium dodecylbenzenesulfonate (SDBS), Triton X-100 and Brij-35. The absorbance of the silver(I)/3,5-diBr-PAEA chelate at 600 nm was measured for varying surfactant concentrations at pH 5.5 (0.08 M acetic acid/sodium acetate buffer). Maximum and constant absorbance of the silver chelate was observed when more than the c.m.c. (2×10^{-3} M) of SDS was present. The absorbances of the silver chelate in STDS solution could not be measured exactly over a wide concentration range because of the low solubility of STDS in water. The effect of SDBS concentration was constant above 2.0×10^{-3} M. With Triton X-100, the absorbance was increased up to 0.05 M, and then decreased. The behavior of Brij-35 was similar to that of Triton X-100. Cationic surfactants such as tetraalkylammonium ion decomposed the silver chelate. Thus SDS is recommended for the spectrophotometric determination of silver, because of the high sensitivity and the small effect of varying SDS concentrations (in the range 2×10^{-3}—10^{-2} M) on the absorbance.

Because the absorbance of the silver chelate was constant in the presence of more than a four-fold excess of 3,5-diBr-PAEA, 1 ml of 10^{-3} M solution was used for the batch method.

The absorbance of the silver(I)/3,5-diBr-PAEA chelate at different pH values in the presence of SDS was measured at 600 nm. The absorbance

increased with increasing pH in the range pH 3.0—4.5, and was constant from pH 4.5 to 7.

Calibration and interferences

Beer's law was obeyed up to 1.0 mg l^{-1} silver and the molar absorptivity was 8.0×10^4 l mol^{-1} cm^{-1} at 600 nm under the recommended conditions. The limit of detection was 0.03 mg l^{-1}.

Palladium(II), copper(II), nickel(II), cobalt(II) and cobalt(III) react with 3,5-diBr-PAEA in the presence of SDS. The interferences from these metal ions could be eliminated by masking with EDTA.

Among the anions tested, chloride, iodide, bromide, cyanide, thiocyanate and thiosulfate interfered seriously when the pretreatment of samples was omitted. Less than a four-fold amount of fluoride did not interfere.

Application in flow-injection analysis

The manifold shown in Fig. 1 proved satisfactory for the application of 3,5-diBr-PAEA. When the concentration of SDS in the chromogenic reagent solution was increased from 0.2 to 0.6%, the peak heights decreased, but 0.4% SDS gave good reproducibility. When the concentration of 3,5-diBr-PAEA was increased from 10^{-5} M to 8×10^{-5} M, the peak heights became constant over 4×10^{-5} M; therefore, the 5×10^{-5} M solution was employed.

The effect of the length of the mixing coil on the peak height for silver was examined for the range 1—5 m. The peak height decreased with increasing coil length, but the reproducibility was poor with coils of less than 2 m, thus a 3-m coil is recommended. When the flow rate for each solution was varied over the range 0.5—1.0 ml min^{-1}, the peak heights were similar. For good reproducibility and a reasonable sampling rate (about 30 h^{-1}), flow rates of 0.8 ml min^{-1} are recommended. The peak heights increased with increasing sample volumes up to 80 μl; 40 μl was most suitable for the apparatus used.

Under the optimum conditions, calibration graphs were linear for 0.1—1.0 mg l^{-1} silver at 600 nm (Fig. 3). The interferences from other metal ions could be eliminated by adding 10^{-3} M EDTA to the buffer solution.

This method was applied to the determination of silver in diluted waste fixing solutions, which were pretreated by the recommended procedure. Sample solutions diluted finally 800 (S_1) and 1600 (S_2) times were injected (Fig. 3). The results were in good agreement with those obtained by the proposed batch method. The relative standard deviations were less than 0.1% by the flow-injection method and 0.5% by the batch method.

It is interesting that the bidentate 4-(3,5-dibromo-2-pyridylazo)aniline derivatives react with silver ion sensitively in the presence of anionic surfactant. The bidentate reagent, 3,5-diBr-PAEA is better than the terdentate reagent, 3,5-diBr-PADAP, because it is much more selective.

REFERENCES

1 Shui-Chieh Hung, Chan-Ling Qu and Shui-Sheng Wu, Talanta, 29 (1982) 85.
2 K. Ohshita, H. Wada and G. Nakagawa, Anal. Chim. Acta, 176 (1985) 41.
3 K. Nilsson and A. Oskarsson, Acta Chem. Scand., Ser. A: 36 (1982) 605.
4 H. Ohtaki and K. Cho, Bull. Chem. Soc. Jpn., 50 (1977) 2674.

Analytica Chimica Acta, 182 (1986) 163—175
Elsevier Science Publishers B.V., Amsterdam — Printed in The Netherlands

SIMULTANEOUS SEMI-AUTOMATIC CATALYTIC TITRATION OF BINARY MIXTURES OF MERCURY(II) WITH COPPER(II) OR CADMIUM AT THE MICROMOLAR LEVEL

T. RAYA SARO and D. PÉREZ BENDITO*

Department of Analytical Chemistry, Faculty of Sciences, University of Córdoba, Córdoba (Spain)

(Received 19th June 1985)

SUMMARY

Copper(II) and mercury(II) act as catalyst and inhibitor, respectively, for the oxidation of 4,4′-dihydroxybenzophenone thiosemicarbazone by hydrogen peroxide in an ammonium chloride/ammonia medium. The combination of these two effects and blocking of the catalytic cycle by EDTA are used as the basis for titrimetric methods for individual and simultaneous titrations of mercury and copper or cadmium, with catalytic end-point detection. Mixtures can be resolved in the mole ratio range 20.1—4.1 for Cu/Hg and 27.1—1.1 for Cd/Hg. Titrations are viable for 10^{-7}—10^{-6} M mercury(II) and 10^{-6}—10^{-5} M copper(II) or cadmium(II).

The catalytic titration methods described in the literature are usually based on the inhibition of an indicator reaction by blocking the activity of its catalyst, which is normally used as the titrant for the inhibitor [1—3]. This paper introduces a catalytic titration based on the inactivation of one of the substrates taking part in the indicator reaction by interaction between the analyte (inhibitor) and the substrate (which is used as the titrant). The titration is done in the presence of the catalyst, which only acts on the titrant once the analyte has been fully titrated. The onset of the catalyzed reaction indicates the end-point of the titration. These inhibitory effects on the substrate seldom appear at low concentrations and, therefore, their applications to kinetic/catalytic analysis are few [4—6]; no catalytic titration exploiting them seems to have been reported. However, this paper demonstrates that the method allows more selective determinations, with lower detection and determination limits, than those generally attained in catalytic titrations or conventional titrations.

The method is exemplified by the titration of mercury(II), which inhibits the oxidation of 4,4′-dihydroxybenzophenone thiosemicarbazone (DBPT) by hydrogen peroxide, catalyzed by trace copper. The organic reagent is used as the titrant. The catalytic titration of copper(II) by use of the same indicator reaction is also feasible; a solution of EDTA (catalyst inhibitor) and DBPT is used as titrant. The end-point is indicated when the catalyzed

0003-2670/86/$03.50

reaction is stopped by addition of sufficient EDTA to bind with all the copper. This mode of titration [7, 8] allows not only the direct titration of the catalyst but also determination of other metal ions that can react fully with the inhibitor before the catalyst. This novel aspect is exemplified here by the determination of cadmium(II).

A method is proposed for the simultaneous determination of mercury(II) and copper or cadmium, relying on the principles and reactions described above. For this purpose, a solution of DBPT and EDTA is used, the DBPT acting as titrant for mercury and EDTA for copper and cadmium. Only a few other methods have been described for the determination of more than one metal in mixtures by catalytic titrations [9—11], and these entail two separate titrations from two sample aliquots, with the use of a masking agent for one of the components in one titration.

EXPERIMENTAL

Apparatus and reagents

The equipment used consisted of a Memotitrator (Mettler DL40) with autoburette (10 ml), stirrer and titration vessel (100 ml), a scanning photo-titrator (Mettler DK18) with an immersion probe (Mettler DK181), a recorder (Mettler GA14) and a printer (Mettler GA40). A detailed description of the whole system was given earlier [11, 12].

4,4′-Dihydroxybenzophenone thiosemicarbazone was synthesized by condensation of 4,4′-dihydroxybenzophenone with thiosemicarbazide [13]. A 0.1% (w/v) solution of the reagent in ethanol was prepared. This is stable for at least one month.

Distilled water was used throughout. A copper(II) solution (0.994 g l^{-1}) was prepared from $CuSO_4 \cdot 5H_2O$ dissolved in water and standardized iodimetrically. A standard cadmium(II) solution was prepared by dissolving 1 g of metal in the minimum volume of (1 + 1) hydrochloric acid and diluting to exactly 1 l with 1% (v/v) hydrochloric acid. A standard mercury(II) solution was prepared by dissolving 1.08 g of HgO in 20 ml of concentrated nitric acid and diluting to exactly 1 l with water. All diluted solutions were prepared immediately before use. An EDTA solution (0.1 M) was prepared from the disodium EDTA dihydrate dissolved in water and standardized potentiometrically against copper solution [14].

For titrant A, 50 ml of the 0.1% DBPT solution and 1 ml of 0.1 M EDTA were added to a 500-ml volumetric flask and the mixture was diluted to volume with water. For titrant B, 50 ml of 0.1% DBPT was diluted to the mark with water in a 500-ml volumetric flask.

Procedures

Semiautomatic direct titration of copper(II). To a 100-ml titration vessel add an aliquot of the sample containing 0.3—1.25 μmol Cu(II) (for calibration add 1—4 ml of 3.12×10^{-4} M Cu(II)), 5 ml of 0.072% (v/v) hydrogen

peroxide solution and 4 ml of 1.5 M ammonia/0.45 M ammonium chloride buffer pH 10.2, and dilute to ca. 75 ml with water. Stir for 5—10 s and add titrant A at 6 ml min^{-1}, with the stirring speed set at 120 rpm, the slow factor at 1, the absorbance scale at 0.025 cm^{-1}, the chart speed at 10 or 20 mm ml^{-1} (10 for end volume $\geqslant$2 ml and 20 for end volume <2 ml) and the initial absorbance at 0.2 (200 mV). From the titration curve recorded (absorbance at 415 nm as a function of titrant volume) determine the end-point graphically from the interceptor of the straight segments.

Determination of cadmium. To an aliquot of sample containing 0.15—1.2 μmol Cd(II) add 0.5 or 1.0 ml of 3.12×10^{-4} M copper(II) solution and continue as in the titration of copper from the stage of hydrogen peroxide addition.

Semiautomatic direct titration of mercury(II). To an aliquot of sample containing 4×10^{-2}—0.5 μmol of Hg(II) (for calibration add 0.5—6 ml of 8.7×10^{-5} M Hg(II)), add 0.5 ml of 3.12×10^{-4} M copper(II) solution and continue as in the titration of copper from the stage of hydrogen peroxide addition, but with titrant B.

Simultaneous titration of mercury and copper or cadmium. Follow the procedure as for the titration of copper or cadmium.

RESULTS AND DISCUSSION

Study of the copper-catalyzed DBPT hydrogen peroxide reaction as an indicator system

The catalyst of an indicator reaction can be titrated directly by using an inhibitor of the catalytic reaction as titrant [7, 8]. One of the components of the indicator reaction (DBPT) is added with the titrant (EDTA), whereas the other(s) is (are) mixed with the sample before the titration. The titration has two stages; in the first stage, the titration reaction [EDTA/Cu(II)] and indicator reaction [DBPT/H_2O_2//Cu(II)] take place simultaneously. When stoichiometric equivalence between EDTA and copper(II) is attained, catalytic activity is lost and the rate of the indicator reaction decreases sharply to that of the uncatalyzed reaction (second stage).

Continuous recording of the absorbance of the solution at 415 nm against the volume of titrant added yields a titration curve like those shown in Fig. 1. From this curve, the end-point is determined graphically as illustrated in the figure. The initial linearity of the titration curves indicates that, in the presence of an excess of hydrogen peroxide and copper, the reagent added with the titrant is oxidized instantly, and that changes in the rate of this reaction resulting from a decrease in the uncomplexed copper concentration are not significant. Therefore, the rate of the indicator reaction over the linear range can be considered to depend exclusively on the DBPT concentration in the titrant and on the speed of titrant addition. In the vicinity of the end-point, the free copper concentration becomes very low, at which stage the rate of the indicator reaction becomes noticeably dependent

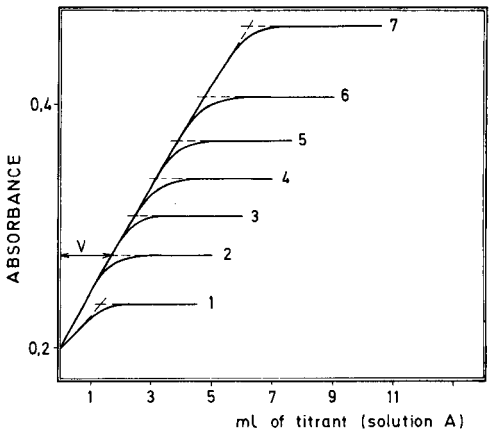

Fig. 1. Titration curves for Cu(II): (1—7) 0.5, 1.0, 1.5, 2.0, 2.5, 3.0 and 4.0 ml of 3.12 × 10^{-4} M Cu(II), respectively, under the recommended conditions.

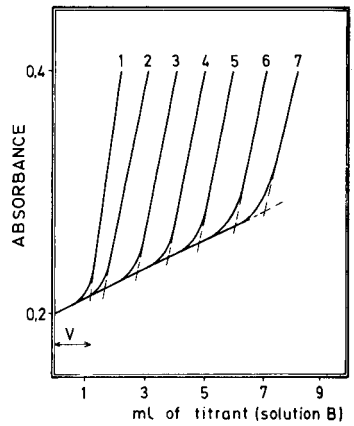

Fig. 2. Titration curves for Hg(II): (1—7) 0.5, 1.0, 2.0, 3.0, 4.0, 5.0 and 6.0 ml of 8.7 × 10^{-5} M Hg(II), respectively, under the recommended conditions.

on the copper concentration. This accounts for the progressive decrease in the slope of the titration curve in the vicinity of the end-point. The linear segment corresponding to the second stage shows the uncatalyzed reaction proceeding so slowly that the increasing reagent concentration has no appreciable effect on the reaction rate.

In order to determine the conditions which allow titration curves suitable for graphical location of the end-point to be achieved, as well as providing accurate and reproducible results, the factors influencing the titration were studied by the univariant method. The addition of DBPT in the titrant produces titration curves with initial segments closer to linearity than if the reagent is present with the sample and the oxidant is added in the titrant. This mode was therefore adopted. The DBPT concentrations investigated ranged from 0.004 to 0.012% (w/v), while that of EDTA was kept at 2×10^{-4} M. The initial slope increases with increasing DBPT concentration; for the final linear segment, the differences between the slopes at different concentrations are insignificant. A 0.010% DBPT solution is recommended because the end-point appears later than the equivalence point with a 0.012% solution, and lower concentrations give smaller slopes.

Hydrogen peroxide concentrations corresponding to 1—8 ml of a 0.072% (v/v) solution did not appreciably affect the initial slope but they did modify the end-point location. The smallest errors were obtained with 3—6 ml of the hydrogen peroxide (ca. 10^{-3} M); higher concentrations led to positive errors in the determination of copper, whereas lower concentrations caused negative errors.

The errors encountered when buffer volumes were between 4 and 10 ml

(NH_4ClNH_3, pH 10.2) and at pH 9.7—10.4 (obtained by addition of HCl or NaOH), were <2% in every case, but the curve corresponding to the development of the indicator reaction had greater linearity when 5—7 ml of buffer (without NaOH or HCl) was added (pH 10.1—10.2); this is the most suitable for the development of the indicator reaction [15]. The effect of ionic strength was studied by adding 0—10 ml of 2.5 M potassium chloride. As the concentration of the electrolyte increased, the end-point became more sluggish, but the indicator reaction was not affected, in that the initial linear slope was unchanged. Addition of electrolytes, therefore, is not required, but the ionic strength should be adjusted to ca. 0.3 M when solutions of high ionic strength are titrated.

The titrant concentration providing the most accurate results for the titration of different copper concentrations was 2×10^{-4} M; this concentration yielded favourable curves when the end-points appeared after adding 1.5—6.30 ml of titrant (Fig. 1). More dilute EDTA solutions favoured the development of the indicator reaction, thus leading to positive errors. Higher concentrations increased the determination limit and detracted from the sensitivity, without expanding the determination range because a distortion in the initial portion of the titration curves appeared for amounts of copper higher than those proposed herein (0.3—1.3 μmol). This can be attributed to the stabilization of the copper/DBPT complex [16] with increasing concentrations of copper (catalyst poisoning). Other variables, both chemical and instrumental, were also studied. The values adopted as optimum are indicated in the Experimental section.

Direct titration of copper(II). The end-points obtained by titration of copper of various concentrations, under the optimum conditions, were evaluated in two ways. The proportional method and the calibration graph method. The former allows the results to be obtained by a simple equivalence relation. For 8×10^{-6}—1.7×10^{-5} M copper (0.3—1.3 μmol in 75 ml), the method was accurate (average error 0.6%) and precise (for 1.0×10^{-5} M copper, 1.6% RSD, $n = 11$). The latter method requires the prior calibration of the titrant volume against known copper concentrations. This afforded a wider determination range (4×10^{-6}—1.7×10^{-5} M) and lower determination limit, and a similar precision.

The selectivity of the method was studied by use of the calibration procedure; 5 ml of 2.5 M potassium chloride was added to the calibration standards and to the samples containing foreign ions in order to swamp any effects of ionic strength. The tolerance limits found are summarized in Table 1. Serious interferences arise from Mn(II), Pb, Bi and Hg(II), which react with DBPT; by Ca, Cd and Zn, which introduce positive interferences; and by copper-complexing species such as cyanide and the aminopolycarboxylic acids. The tolerance to other metal ions at moderate concentrations shows that the titration of copper in this mode is more selective than by indirect methods based on the titration of an excess of ligand with standard catalyst solution [11, 16]. Such methods are generally subject

TABLE 1

Effect of various ions on the individual titration of copper and mercury

Maximum tolerated mole ratio	Foreign ions
Titration of copper (0.78 μmol)	
100	NO_3^-, SO_4^{2-}, CO_3^{2-}, BrO_3^-, ClO_3^-, ClO_4^-, Cl^-, Br^-, I^-, F^-
50	PO_4^{3-}, SO_3^{2-}, SCN^-, $S_2O_3^{2-}$, acetate, oxalate, tartrate, Al^{3+}
25	$P_3O_{10}^{5-}$, citrate, Cr^{3+}
10	$P_2O_7^{4-}$, $S_2O_8^{2-}$, perborate, Co^{2+}, Sn^{2+}
5	Ba^{2+}, Sr^{2+}, Mg^{2+}, Fe^{3+}
2	Ni^{2+}
1	CN^-, IO_4^-, Bi^{3+}
<1	Mn^{2+}, Pb^{2+}, Ca^{2+}, Cd^{2+}, Zn^{2+}, Hg^{2+}, EGTA, NTA, DCTA
Titration of mercury (0.305 μmol)	
100	PO_4^{3-}, NO_2^-, NO_3^-, SO_3^{2-}, SO_4^{2-}, $S_2O_8^{2-}$, SCN^-, ClO_3^-, ClO_4^-, CO_3^{2-}, BrO_3^-, IO_3^-, IO_4^-, I^-, Ag(I), Br^-, F^-, Mg^{2+}, Ca^{2+}, Sr^{2+}, Ba^{2+}, Ni^{2+}, Al^{3+}, acetate, perborate, oxalate, tartrate
50	$P_3O_{10}^{5-}$, citrate, Zn^{2+}, Cd^{2+}, Cr^{3+}, Pd^{2+}, Pb^{2+}[a]
25	Sn(IV), $P_2O_7^{4-}$
20	Mn^{2+}[b], Bi^{3+}[c]
10	Pt^{4+}, Fe^{3+}, Sn^{2+}
5	$S_2O_3^{2-}$, Co^{2+}
1	Bi^{3+}
<1	Mn^{2+}, Pb^{2+}, CN^-, EDTA, NTA, EGTA, DCTA

[a]With $P_3O_{10}^{5-}$ as masking agent. [b]With $P_2O_7^{4-}$ as masking agent. [c]With tartrate as masking agent.

to interferences (catalytic or otherwise) at concentrations lower than that of the analyte of every species liable to interact with the inhibiting ligand, even if they form weaker complexes than that of the catalyst with that ligand. Only those species reacting with the inhibitor prior to or at the same time as the catalyst interfere with the present procedure.

Determination of cadmium. The effect exerted by the presence of Cd, Zn or Ca on the titration of Cu(II) allows the determination of these metal ions by adding a known amount of copper(II) to the sample and following the same titration procedure as above. The end-point is directly related to the concentration of cadmium (or zinc or calcium) plus copper, that of the ion of interest being determined by subtracting the copper concentration. In general, the method requires the analyte to react fully with the inhibitor before the catalyst has been completely complexed. This effect can be considered as a type of activation, and its additive character allows the determination limit for the catalyst to be lowered. For 0.16 μmol of Cu(II) added, the determination range for cadmium was 0.2—1.2 μmol, by both proportional and calibration methods. Under these conditions, the average

relative error was <1% and the mid-range RSD was 2.6% (n = 11) for both methods.

From the precision data obtained for the titration of copper alone, it is possible to calculate the minimum cadmium concentration which can be distinguished from the blank [17]. The titrant volume consumed by 0.31 μmol of Cu(II) in the absence of cadmium was used as the blank. The detection and determination limits found were 0.04 and 0.132 μmol, respectively. The measurement of cadmium concentrations of this order requires the addition of >0.16 μmol of Cu(II), otherwise the titration curves will have too short an initial linear segment. Therefore, the method is proposed for 0.13—1.2 μmol of cadmium, by adding enough copper ion to give an end-point after adding 1.5—7.0 ml of 2×10^{-4} M EDTA. The selectivity of this determination is the same as that for copper alone, and the determination limit for copper can be lowered to 0.132 μmol by adding a suitable, known amount of cadmium.

Catalytic titrations by substrate inactivation

The method of catalytic titration by substrate inactivation uses one of the components of the indicator reaction as titrant. The other component and the catalyst are added to the titration vessel together with the analyte/inhibitor. If R and B are the components of the indicator reaction, catalyzed by C, then the titration will involve the following reactions:

$$\text{R} + \text{inhibitor} \longrightarrow \text{P}' \text{ (titration reaction)}$$

$$\text{R} + \text{B} \xrightarrow{\text{C}} \text{P} \text{ (indicator reaction)}$$

where P and P′ are the various reaction products.

The titration curves obtained are typical of the direct titration of inhibitors, with a pseudo-induction period corresponding to the titration reaction. However, there is a significant difference between this mode and that described above in that the analyte inhibits the catalyzed reaction through interaction with substrate R instead of with the catalyst.

Mercury(II) inhibits the oxidation of DBPT by hydrogen peroxide in the presence of copper(II) ion, which is the basis for the method proposed here for the determination of mercury. The DBPT is used to titrate a solution containing the analyte, oxidant and catalyst. At the beginning of the titration, the reagent added is consumed by complexation of mercury(II); once this is complete, the excess of titrant starts the indicator reaction. The pseudo-induction period of the corresponding titration curves (absorbance at 415 nm vs. volume of titrant added) is directly related to the mercury(II) concentration in the sample (Fig. 2).

Because mercury(II) forms strong complexes with sulphur compounds, its complexation with DBPT takes priority over the indicator reaction. This inhibitory effect is only apparent when there is sufficient mercury to inactivate all the DBPT, so this effect passed undetected in earlier studies of the same reaction [10, 11, 15, 16, 18], in which DBPT was used in large excess with respect to the species of analytical interest.

The complex formed between DBPT and mercury(II) in ammonia/ammonium chloride buffer was studied. The complex was found to have an absorption band with maximum absorbance at 395 nm, which overlapped those of DBPT in its reduced (λ_{max} = 360 nm) and oxidized (λ_{max} = 415 nm) forms. The complex was stable for at least 30 min when the mole ratio of DBPT:Hg was $\geqslant$2:1, whereas at $\leqslant$1:1 the absorbance at 395 nm decreased with time as a new maximum appeared at 415—420 nm, attributable to the oxidation of the ligand to a phenoxy radical by excess of mercury(II) [19]. Hydrogen peroxide did not affect the spectrum of the complex for ligand/metal ratios between 3:1 and 2:1, whereas at higher ratios the excess of ligand was slowly oxidized and at lower ratios a slight increase of the oxidizing effect of the excess of mercury(II) on the complex became apparent. No complexation was detected when mercury(I) (obtained by prior reduction of mercury(II) with ascorbic acid) was used, which suggests that mercury(II) is involved in complex formation.

From the above statements the impossibility of clearly establishing the stoichiometry of the complex can readily be understood. The stoichiometry of thiosemicarbazonate/mercury(II) is usually 2:1 [20, 21], however.

Influence of variables on the titration of mercury(II). Because the stoichiometry of the titration reaction is unknown, the application of the proportional method is not feasible; however, under the reaction conditions indicated in the Experimental section, there is a linear relationship between the volume of titrant added up to the end-point and the mercury(II) concentration. Therefore, the titration is made possible by previously calibrating the titrant against standard mercury(II) solutions. This has the advantage of requiring no knowledge of the exact titrant concentration.

The study of experimental variables was aimed at establishing a set of conditions to give a linear relationship between the volume of the titrant and mercury(II) concentration over a wide range, maximum sensitivity (maximum calibration slope), and minimum deviations of the end-points arising from slight changes in the variables studied. The influence of each variable on the titration reaction (without adding copper(II) to the samples) and on the indicator reaction (without adding mercury(II)) was studied. The optimal conditions are summarized in Table 2.

Of all the variables investigated, the pH exerted the greatest influence on the titration reaction. Above pH 10.2, the inhibitory effect of mercury(II) lessened considerably, which can be attributed to the formation of hydroxo complexes of mercury. The remaining variables mainly affected the indicator reaction. The variations in end-points are due to changes in the blank, and therefore can be compensated by keeping constant all reaction conditions during calibration and titration of samples.

Direct titration of mercury(II). Under the optimal conditions, 5.8×10^{-7}—7.0×10^{-6} M mercury(II) (4.4×10^{-2}—0.5 μmol in 75 ml) can be determined. The experimental curve is defined by $V = 12.16\ [Hg^{2+}] + 0.62$ (r^2 = 0.9991; 10 points), V being the volume of titrant (in ml) added up

TABLE 2

Optimal conditions for the direct titration of mercury(II)

Chemical factors		Instrumental factors	
Variable	Optimal range	Variable	Optimal range
Cu(II)	5—10 μg	Titrant addition rate	6 ml min^{-1}
H_2O_2	3—10 ml of 0.072% (v/v)	Slow factor	1
pH	10.0—10.2	Stir	100—200 rpm
Buffer	4—5 ml of NH_4Cl/NH_3, (pH 10.2)	Initial absorbance	0.2 (200 mV)
		Absorbance scale	0.025 cm^{-1}
Dilution of sample	50—80ml	Chart speed	1 or 2 cm ml^{-1}
Volume of titrant at end-point	1—7 ml		
Titrant solution	0.01% (w/v) of DBPT in 10% ethanol		
Ionic strength	<0.4 M KCl		

to the end-point, and $[Hg^{2+}]$ the amount in μmol. The titration of eleven identical samples containing 0.26 μmol Hg(II) gave an RSD of 1.8%. The detection and determination limits calculated from the precision data of the blank [17] were 1.4×10^{-7} and 5.2×10^{-7} M, respectively.

Table 1 lists the maximum ratios of foreign ion to mercury tolerated for an error limit of ±2%. As expected, this mode is more selective than the usual catalytic titrations because of the high selectivity of the titration reaction. Thus, the direct titration of mercury(II) with iodide, using the Ce(IV)/As(III) indicator system [22—27] (the only system reported to date), is subject to interferences from Ag(I), Pd(II) and all metal ions forming precipitates with iodide. In addition, the determination limits are higher. This is also the case for the determination of mercury(II) by back-titration methods using an aminopolycarboxylic acid as inhibitor [9, 28—31]; these titrations afford lower determination limits than a direct titration, but generally higher than that of the present method. In addition, many metal ions interfere at all levels.

Simultaneous titration of metal ions by a combined method

The combination of two inhibitory effects on the same indicator reaction acting independently on different reactants (substrate and catalyst) involved in this reaction makes it possible to determine metal mixtures by catalytic titration. This is described here for the resolution of binary mixtures of mercury(II) with copper or cadmium. Such a method employs conditions identical with those for the titration of copper (or cadmium), which requires the copper plus cadmium concentration to be higher than that of mercury(II).

Copper/mercury mixture. The process for the simultaneous titration of copper and mercury(II) requires three stages as shown in the following scheme.

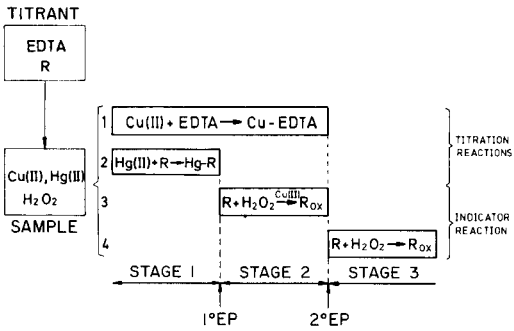

Scheme I

In the first stage both titration reactions occur, copper with EDTA and mercury with DBPT. When mercury has been fully titrated, the second stage starts, the DBPT beginning its oxidation by hydrogen peroxide, catalyzed by the copper not complexed by EDTA. This stage is complete when the copper has been fully complexed by EDTA, after which only the uncatalyzed reaction proceeds (third stage). Figure 3 shows the titration curves obtained for different mercury concentrations and a fixed copper concentration. For <0.42 μmol of mercury, the curves show two end-points; the first, V_1, corresponds to the titration of mercury(II) by DBPT, whereas the second, V_2, corresponds to the titration of copper by EDTA.

The correct application of the method requires mercury(II) not to react with EDTA at any stage of the titration, and the indicator reaction not to start before mercury(II) has been completely titrated. It is also necessary that there should be sufficient free copper ions at V_1 to enable the indicator

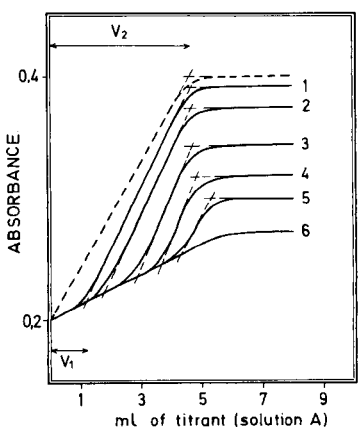

Fig. 3. Titration curves for 0.94 μmol of Cu(II) and different amounts of Hg(II) (μmol): (1) 0.045; (2) 0.09; (3) 0.18; (4) 0.24; (5) 0.30; (6) 0.42. (- - - -) No Hg(II) present. Conditions as recommended.

reaction to develop so that the linear segments can be extrapolated. These requirements are met when the mole ratio of Cu:Hg is between 20:1 and 4:1 and when at the end-point of the mercury titration the amount of copper ions is 0.2—0.7 μmol, i.e., the difference between V_2 and V_1 is 1—3.5 ml of titrant (2×10^{-4} M EDTA). The determination limits were 4.5×10^{-2}—0.24 μmol of Hg(II) and 0.46—0.94 μmol of Cu(II). Table 3 gives the results of analyses of synthetic mixtures. All mixtures were resolved satisfactorily.

Cadmium/mercury mixture. Cadmium/mercury mixtures are analyzed as for copper/mercury mixtures, but known amounts of copper(II) are added to the samples. The investigation of numerous samples containing various concentrations of both metals showed the simultaneous determination of mercury and cadmium to be feasible in the concentration ranges 4.3×10^{-2}—0.44 μmol of Hg(II) and 0.3—1.2 μmol of Cd(II) when 0.16 μmol of Cu(II) was added to the samples. An increase in the copper concentration decreased the determination limit of cadmium, whereas that of mercury remained unchanged. Table 3 shows some of the results obtained.

Selectivity. The selectivity of the combined method for simultaneous analysis of metal mixtures can be assessed from the results obtained in the individual determination of each metal. Because the determination of copper (or cadmium) is subject to more interferences than that of mercury, the proposed mixtures can only be resolved favourably in the presence of species not interfering with the determination of copper (cadmium), as specified in Table 1. However, the use of EDTA plus DBPT as titrant allows the determination of mercury alone with a higher tolerance for several cations than

TABLE 3

Resolution of mixtures of Hg(II) with Cu(II) or Cd(II)

Mercury/copper (10^{-2} μmol)				Mercury/cadmium (10^{-2} μmol)			
Hg(II)		Cu(II)		Hg(II)		Cd(II)	
Added	Found[a]	Added	Found[a]	Added	Found[a]	Added	Found[a]
4.5	4.6	93.6	93.7	4.35	4.27	120	118
6.0	6.0	93.6	94.0	8.70	8.40	120	117
7.5	7.6(6.0)	93.6	93.9(1.0)	17.4	17.2	120	119
9.0	9.2	93.6	93.3	26.1	26.0	120	118
12.0	12.2	93.6	94.0	34.8	34.9	120	120
18.0	18.3	93.6	94.0	43.5	43.4	120	118
24.0	24.6	93.6	94.7	34.8	34.6	100	100
15.0	15.0	78.0	78.0	26.1	25.8	80	80
12.0	11.9	62.4	62.7	21.7	21.8(2.3)	80	80(1.7)
9.0	9.0	54.6	54.3	17.4	17.5	60	60
6.0	6.1	54.6	55.0	8.70	8.69	30	30
4.5	4.4	46.8	46.7	4.35	4.41	30	30

[a]Average of 3 determinations. RSD (%) in brackets (n = 11).

TABLE 4

Analysis of synthetic samples

Composition (mg) of sample with 30.0 μg of Hg(II) added			Hg found (μg)	Cu found (μg)	Cd found (μg)
1.00 Pb^{2+}	0.50 Cd^{2+}		30.3	—	—
0.30 Fe^{3+} [a]	0.20 Mn^{2+} [b]		29.7	—	—
0.50 Al^{3+} [a]	0.50 Ca^{2+}		30.3	—	—
2.00 Ag^{+}	0.50 Pb^{2+}		29.1	—	—
0.50 Cd^{2+}	0.50 Zn^{2+}		30.3	—	—
0.10 Ni^{2+}	0.25 Co^{2+}	0.0600 Cu^{2+}	29.3	60.4	—
0.25 Fe^{3+} [a]	0.50 Al^{3+} [a]	0.0600 Cu^{2+}	30.1	59.7	—
0.50 Cr^{3+}	0.50 Al^{3+} [a]	0.0600 Cu^{2+}	29.3	60.4	—
0.10 Mg^{2+}	0.50 Al^{3+} [a]	0.0900 Cd^{2+}	29.7	—	90.4
0.50 Cr^{3+}	0.25 Fe^{3+}	0.0900 Cd^{2+}	30.3	—	89.2

[a] Triethanolamine as masking agent. [b] Pyrophosphate as masking agent.

that afforded by the simple method. This is true for lead and copper, which are tolerated in ratios 100:1 and 20:1, respectively, to mercury in the combined method. In order to illustrate the selectivity of these determinations, Table 4 shows the results obtained for the analysis of synthetic samples.

This work is part of Project No. 0248, sponsored by Spanish CAICYT.

REFERENCES

1 H. A. Mottola, Talanta, 16 (1969) 1265.
2 T. P. Hadjiioannou, Rev. Anal. Chem., 3 (1976) 82.
3 T. F. A. Kiss, Talanta, 30 (1983) 771.
4 M. Ternero, F. Pino, D. Pérez-Bendito and M. Valcárcel, Microchem. J., 25 (1980) 102.
5 H. Weisz, S. Pantel and W. Meiner, Anal. Chim. Acta, 82 (1976) 145.
6 A. Moreno, M. Silva and D. Pérez-Bendito, Anal. Lett., 16 (1983) 747.
7 H. Weisz and S. Pantel, Z. Anal. Chem., 268 (1973) 389.
8 H. Weisz, S. Pantel and H. Ludwig, Z. Anal. Chem., 262 (1972) 269.
9 E. A. Piperaki and T. P. Hadjiioannou, Chim. Chron., 6 (1977) 375.
10 T. Raya Saro and D. Pérez-Bendito, Quim. Anal., 4 (1985) 259.
11 T. Raya Saro and D. Pérez-Bendito, Anal. Chim. Acta, 172 (1985) 273.
12 A. Moreno, M. Silva, D. Pérez-Bendito and M. Valcárcel, Analyst (London), 109 (1984) 249.
13 F. Toribio, J. M. López-Fernández, D. Pérez-Bendito and M. Valcárcel, Quim. Anal., I (1982) 21.
14 J. Veselý, D. Weiss and K. Stulik, Analysis with Ion-selective Electrodes, Ellis Horwood, Chichester, 1978, p. 194.
15 J. L. Ferrer and D. Pérez-Bendito, Anal. Chim. Acta, 132 (1981) 157.
16 T. Raya Saro and D. Pérez-Bendito, Analyst (London), 108 (1983) 857.
17 G. L. Long and J. D. Winefordner, Anal. Chem., 55 (1983) 712A.
18 T. Raya Saro and D. Pérez-Bendito, Mikrochim. Acta, I (1984) 467.

19 S. Patai, The Chemistry of the Hydroxyl Group, Part I, Interscience, New York, 1971, p. 577.
20 A. Gallardo Cespedes, D. Pérez-Bendito and M. Valcárcel, Microchem. J., 30 (1984) 105.
21 F. Lázaro, M. D. Luque de Castro and M. Valcárcel, Microchem. J., 30 (1984) 235.
22 T. P. Hadjiioannou and E. A. Piperaki, Anal. Chim. Acta, 90 (1977) 329.
23 H. Weisz, D. Klockow and F. A. Kiss, Z. Anal. Chem., 247 (1969) 248.
24 F. F. Gaal and B. F. Abramovic, Mikrochim. Acta, I (1982) 465.
25 H. Weisz and D. Klockow, Z. Anal. Chem., 232 (1967) 321.
26 K. C. Burton and H. M. Irving, Anal. Chim. Acta, 52 (1970) 441.
27 F. F. Gaal and B. F. Abramovic, Talanta, 27 (1980) 733.
28 H. Weisz and V. Z. Muschelknautz, Anal. Chem., 215 (1966) 17.
29 H. Weisz and T. F. Kiss, Z. Anal. Chem., 249 (1970) 302.
30 A. Gómez-Hems, M. Ternero, D. Pérez-Bendito and M. Valcárcel, Mikrochim. Acta, I (1979) 375.
31 H. Weisz and T. J. Janjíc, Anal. Chem., 227 (1967) 1.

Analytica Chimica Acta, 182 (1986) 177—183
Elsevier Science Publishers B.V., Amsterdam — Printed in The Netherlands

SELECTIVE DETERMINATION OF *N*-TERMINAL TYROSINE-CONTAINING PEPTIDES BY A NOVEL FLUORESCENCE REACTION WITH BORATE, HYDROXYLAMINE AND COBALT(II)

MASAAKI KAI and YOSUKE OHKURA*

Faculty of Pharmaceutical Sciences, Kyushu University 62, Maidashi, Higashi-ku, Fukuoka 812 (Japan)

(Received 25th June 1985)

SUMMARY

A fluorimetric method is proposed for determining *N*-terminal tyrosine-containing peptides, of which some peptides such as enkephalins and kyotorphin are of physiological importance. An intense fluorescence is produced when the peptide is heated at 100°C for 3 min in a weakly alkaline medium containing borate, hydroxylamine and cobalt(II). The fluorescent species is stabilized with β-mercaptoethanol, with excitation and emission maxima at 335 and 430 nm, respectively. The method is highly selective for *N*-terminal tyrosine-containing peptides, with a detection limit of 43—69 pmol ml^{-1}.

Opiate peptides such as leucine- and methionine-enkephalins [1], endorphin [2], dynorphin [3] and kyotorphin [4], which have recently been isolated and identified from mammalian tissues, all have a tyrosyl residue at the terminal amino group of the amino acid sequence. The determination of these peptides is usually by radioimmunoassay (RIA) or liquid chromatography. Although the RIA methods [5, 6] offer sufficient sensitivity and selectivity for determining the individual peptides, there is still difficulty in preparing a specific antibody especially for the oligopeptides. Peptide detection in chromatography is generally by u.v. absorption between 200 and 230 nm [7], on-line post-column fluorescence derivatization in which the primary amino groups of peptides react with a fluorogenic reagent (fluorescamine [8] or *o*-phthalaldehyde [9]), or electrochemical activity [10] of tyrosine in the peptide molecule. However, these detection methods are not specific for *N*-terminal tyrosine-containing peptides.

In this paper, a new spectrofluorimetric method is described which permits the highly selective determination of *N*-terminal tyrosine-containing peptides. The method is based on the formation of fluorescent compounds from the peptides under weakly alkaline conditions on heating in the presence of borate, hydroxylamine and cobalt(II) ions. Two oligopeptides, Tyr-Arg (kyotorphin) and Tyr-Gly-Gly (Tyr = tyrosine, Gly = glycine), were used as model compounds to establish reaction conditions for a more general analytical method.

0003-2670/86/$03.50

EXPERIMENTAL

Reagents, solutions and apparatus

Deionized and distilled water was used throughout. Peptides were purchased from the Protein Research Foundation (Osaka, Japan) or Sigma Chemical Co. Peptide solutions were prepared in water and stored at −80°C until used. The solutions were stable for at least two weeks. All other chemicals were of reagent grade, unless otherwise noted.

Hydroxylamine (10 mM)/cobalt (50 μM) solution was prepared by dissolving 64.5 mg of hydroxylammonium chloride and 1.2 mg of cobalt(II) chloride hexahydrate in ca. 50 ml of water and diluting with water to exactly 100 ml. Borate buffer (0.3 M, pH 8.8) was prepared by dissolving 1.854 g of boric acid in ca. 70 ml of water, adjusting the pH to 8.8 with 1.0 M sodium hydroxide and diluting with water to 100 ml. β-Mercaptoethanol solution (50 mM) was obtained by dissolving 0.39 g of freshly distilled β-mercaptoethanol in 100 ml of water. The three reagent solutions were usable for at least a month when stored in a refrigerator.

Uncorrected fluorescence excitation and emission spectra and intensities were measured with a Hitachi MPF-4 spectrofluorimeter in 10 × 10-mm quartz cells; spectral bandwidths of 10 nm were used in the excitation and emission monochromators.

Procedure

A 1.0-ml portion of peptide solution was placed in a test tube, to which were added 1.0 ml each of the hydroxylamine/cobalt solution and the borate buffer. The mixture was heated in a boiling water bath for 3 min, and a 200-μl portion of the β-mercaptoethanol solution was quickly added, with cooling in ice-water. The reagent blank solution was prepared in the same way except that 1.0 ml of the peptide solution was replaced with 1.0 ml of water. The fluorescence intensity was measured at the wavelength of the emission maximum with irradiation at the excitation maximum (see Table 2).

RESULTS AND DISCUSSION

The excitation and emission maxima for the fluorescent product from Tyr-Arg are at 335 and 430 nm, respectively (Fig. 1). The product from Tyr-Gly-Gly shows almost identical spectra, with maxima at 335 and 435 nm, respectively. On irradiation at 335 nm, a weak fluorescence is observed from the reagent blank (Fig. 1); the intensity is 0.8% of that given by 5 nmol ml^{-1} Tyr-Arg.

Effects of reaction conditions

Borate buffer (pH 8.8, $\geqslant$0.2 M) gives maximum and constant fluorescence for both peptides, although no fluorescence is produced in the absence of borate (Fig. 2A). The pH of the buffer also affects significantly the

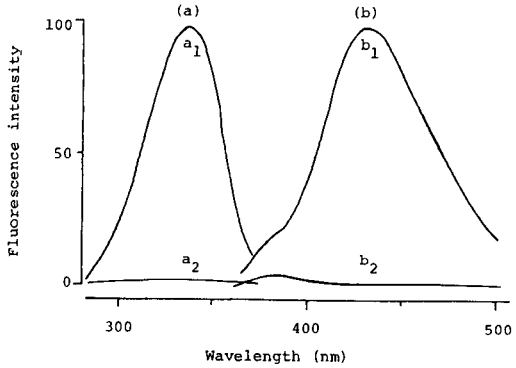

Fig. 1. (a) Excitation (emission measured at 430 nm) and (b) emission (excitation at 335 nm) spectra of the reaction mixture of Tyr-Arg (a_1, b_1) and the reagent blank (a_2, b_2). Portions (1.0 ml) of 5 nmol ml^{-1} Tyr-Arg solution or water were treated by the recommended procedure.

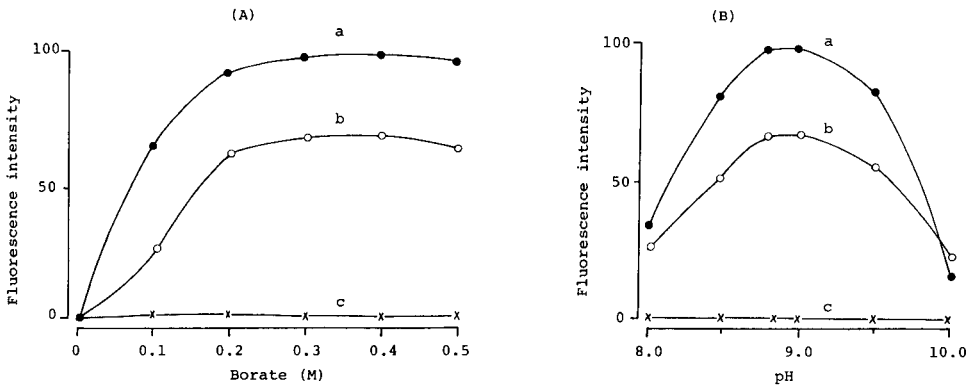

Fig. 2. Effects of (A) concentration and (B) pH of the borate buffer on the fluorescence intensity. Portions (1.0 ml) of 5 nmol ml^{-1} solutions of (a) Tyr-Arg, (b) Tyr-Gly-Gly and (c) water were treated as recommended with buffer of various concentrations at pH 8.8, or of various pH values at a concentration of 0.3 M.

development of the fluorescence (Fig. 2B). The pH that gives greatest intensity is 8.8 or 9.0, but at pH values <6.0, there is no fluorescence. Thus, 0.3 M borate buffer of pH 8.8 was selected for the procedure. When 0.2 M phosphate (pH 5—9) or carbonate (pH 9—11) buffer is used in place of the borate, only slight fluorescence is produced, at pH 9; the intensities from both peptides are $<2\%$ of those obtained with the borate buffer. With 0.2 M Tris hydrochloride buffer, no fluorescence from the peptides is observed at any pH.

Hydroxylamine is also an essential reactant for fluorescence production; the concentration that produces the greatest intensity is estimated to be 10 mM (Fig. 3A). The hydroxylamine derivatives *N*-methylhydroxylamine, *O*-methylhydroxylamine and *N*-phenylhydroxylamine (all 10 mM) were also

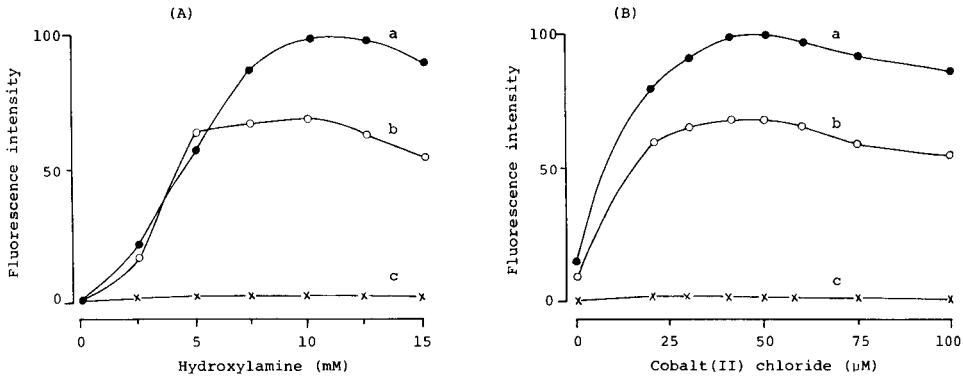

Fig. 3. Effects of the concentrations of (A) hydroxylamine (B) cobalt(II) chloride on fluorescence intensity. Portions (1.0 ml) of (a) a 5 nmol ml^{-1} solution of Tyr-Arg, (b) a 5 nmol ml^{-1} solution of Tyr-Gly-Gly and (c) water were treated as recommended with various concentrations of hydroxylamine or cobalt(II) chloride.

tested for fluorescence production from the peptides. Of these, only *N*-methylhydroxylamine gives any fluorescence, but the intensity is ca. 20% of that obtained with 10 mM hydroxylamine.

Cobalt(II) ions are required to develop intense fluorescence from the peptides. The maximum intensities from both peptides obtained at 50 μM cobalt (Fig. 3B) are an order of magnitude higher than those obtained in the absence of cobalt ion. However, there is no enhancement of the fluorescence when cobalt ion is added to the reaction mixture after heating. The effect of other metal ions is shown in Table 1. Only manganese(II) and nickel have any enhancing effect, but both are much less effective than cobalt.

The fluorescence reaction proceeds rapidly at temperatures higher than ca. 50°C (Fig. 4); fluorescence is not observed within at least 20 min at <30°C. At 100°C, which was selected for convenience, the maximum intensities from both the peptides are attained by heating for 3 min.

β-Mercaptoethanol stabilizes the fluorescence produced but does not affect its intensity. In its absence, the fluorescence intensities from Tyr-Arg and Tyr-Gly-Gly decrease at ca. 90% h^{-1} in daylight at room temperature. The addition of β-mercaptoethanol (>10 mM) prevents this decrease; a 50 mM solution is used in the recommended procedure. The stabilizing effect was also observed with other reductants such as sodium sulfite and thioglycollic acid at >10 mM concentrations.

Calibration and precision

The calibration graphs for Tyr-Arg and Tyr-Gly-Gly were linear over the concentration range 0.02—10 nmol ml^{-1}. The precision of the method was evaluated from the results of 20 determinations of 5 nmol ml^{-1} solutions of Tyr-Arg and Tyr-Gly-Gly. The relative standard deviations were 1.7 and 2.0%, respectively.

TABLE 1

Effects of various metal ions on the fluorescence intensity

Peptide	Conc. of salt (μM)	Relative fluorescence intensity							
		$CoCl_2$	$CuSO_4$	$MnCl_2$	$NiCl_2$	$FeSO_4$	$FeCl_3$	$Al(NO_3)_3$	None
Tyr-Arg	25	85	2	23	21	9	9	11	11
	50	100[a]	2	15	24	9	8	12	
	100	88	3	11	22	8	7	12	
Tyr-Gly-Gly	25	96	1	26	21	12	11	14	12
	50	100[a]	2	16	20	11	11	14	
	100	83	3	9	22	9	11	14	

[a]Fluorescence intensities are relative to this value, taken as 100.

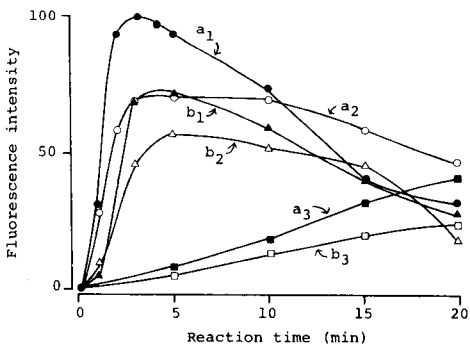

Fig. 4. Effect of reaction time and temperature on the fluorescence intensity: (a_1, b_1) 100° C; (a_2, b_2) 80° C; (a_3, b_3) 60° C. Portions (1.0 ml) of 5 nmol ml^{-1} solutions of (a) Tyr-Arg and (b) Tyr-Gly-Gly were otherwise treated as recommended.

Reaction of other substances

All the *N*-terminal tyrosine-containing peptides tested fluoresce intensely under the reaction conditions estbalished and they can be determined at concentrations as low as ca. 50 pmol ml^{-1} (Table 2). The excitation and emission spectra of the fluorescences from these peptides have similar structures and maxima to those of that from Tyr-Arg, and are not characteristic of individual compounds (Table 2).

In contrast, the present method does not permit any fluorescence development from the following peptides: Gly-Gly, Gly-Tyr, Phe-Arg-Gly, acetyl-Leu-Leu-Arg, Thr-Lys-Pro-Arg (tuftsin), Arg-Val-Tyr-Ile-His-Pro-Phe (angiotensin III), Lys-Arg-Pro-Pro-Gly-Phe-Ser-Pro-Phe-Arg (kallidin) or pyro-Glu-His-Trp-Ser-Tyr-Gly-Leu-Arg-Pro-Gly-NH_2 (luteinizing hormone-releasing hormone); because they have no tyrosyl residue at the terminal nitrogen of the amino acid sequence.

Tyrosine, tyramine and tyrosinamide fluoresce slightly in the recommended procedure; their intensities are 4, 1 and 36%, respectively, of that given by

TABLE 2

Spectral characteristics of the fluorescences from *N*-terminal tyrosine-containing peptides, and the lower limits of determination[a]

Peptide	Excitation maximum (nm)	Emission maximum (nm)	Relative fluorescence intensity	Lower limit of determination[b] (pmol ml^{-1})
Tyr-Arg	335	430	100	43
Tyr-Gly	335	430	88	49
Tyr-Phe	335	430	62	69
Tyr-Tyr	335	430	67	64
Tyr-Gly-Gly	335	435	68	63
Tyr-Gly-Gly-Phe	340	435	65	66
Tyr-Gly-Gly-Phe-Met (methionine enkephalin)	340	435	73	59
Tyr-Gly-Gly-Phe-Leu (leucine enkephalin)	340	435	81	53

[a]Portions (1.0 ml) of 5 nmol ml^{-1} solutions of the compounds were treated by the recommended procedure. The fluorescence intensity from Tyr-Arg was taken as 100. [b]The concentration which gives a fluorescence intensity twice that of the blank.

an equimolar concentration of Tyr-Arg. The following substances do not fluoresce at concentrations as high as 500 nmol ml^{-1}: sugars (glucose, fructose, galactose, xylose, maltose, sucrose, galactosamine, ribose and 2-deoxyglucose), steroids (estriol, β-estradiol, estrone and estrone-3-sulphate), keto acids (pyruvic acid, phenylpyruvic acid and 4-hydroxyphenylpyruvic acid), carboxylic acids (acetic acid and propionic acid), aldehydes (acetaldehyde, glyceraldehyde and glutaraldehyde), 16 L-α-amino acids other than tyrosine, amines (putrescine, spermidine, serotonin, tryptamine, adrenaline and guanidine), urea and purine and pyrimidine bases (adenine, guanine, uracil and cytosine).

The above results demonstrate that the proposed method is highly selective for *N*-terminal tyrosine-containing peptides. The chemical structure of the fluorescent compounds produced from the peptides remains unknown, and studies of the mechanism of the fluorescence reaction are necessary. The method is simple, rapid and sensitive, and should be applicable to an automatic detection system after chromatographic separation of enkephalins and related peptides in biological samples. Such work is in progress.

This work was supported in part by a Grant-in-aid for Scientific Research from the Ministry of Education, Science and Culture of Japan. The skilful assistance of Miss S. Takita is also acknowledged.

REFERENCES

1 J. Hughes, T. W. Smith, H. W. Kosterlitz, L. A. Fothergill, B. A. Morgan and H. R. Morris, Nature (London), 258 (1975) 577.
2 N. Ling, R. Burgs and R. Guillemin, Proc. Natl. Acad. Sci., 73 (1976) 3942.
3 A. Goldstein, S. Tachibana, L. I. Lowney, M. Hunkapiller and L. Hood, Proc. Natl. Acad. Sci., 76 (1979) 6666.
4 H. Shiomi, H. Ueda and H. Takagi, Neuropharmacology, 20 (1981) 633.
5 H. Y. Yang, J. S. Hong and E. Costa, Neuropharmacology, 16 (1977) 303.
6 R. J. Miller, K. J. Chang, B. Cooper and P. Cuatrecasas, J. Biol. Chem., 253 (1978) 531.
7 S. Mousa, D. Mullet and D. Couri, Life Sci., 29 (1981) 61.
8 S. Stein and J. Moschera, Methods Enzymol., 79 (1981) 7.
9 H. Nakamura, C. L. Zimmerman and J. J. Pisano, Anal. Biochem., 93 (1979) 423.
10 M. W. White, J. Chromatogr., 262 (1983) 420.

Analytica Chimica Acta, 182 (1986) 185—191
Elsevier Science Publishers B.V., Amsterdam — Printed in The Netherlands

PHASE-RESOLVED FLUOROIMMUNOASSAY OF HUMAN SERUM ALBUMIN

YAHYA R. TAHBOUB and LINDA B. McGOWN*
Department of Chemistry, Oklahoma State University, Stillwater, OK 74078 (U.S.A.)
(Received 23rd December 1985)

SUMMARY

In the homogeneous immunoassay of human serum albumin described, a difference in fluorescence lifetime is used along with a small difference in fluorescence intensity to discriminate between the free and the antibody-bound labelled antigen. The immunoassay is based on the use of phase-resolved fluorescence measurements, in which sinusoidally-modulated excitation is combined with phase-sensitive detection to generate time-dependent signals which are integrated over a pi-interval to produce phase-resolved intensities. Texas Red was used as the fluorescent label. Negligible matrix effects were observed from serum, and a comparison of values determined by using the phase-resolved fluoroimmunoassay with values provided by the hospital from which the samples were obtained yielded a correlation coefficient of 0.996.

The use of phase-resolved fluorescence spectrometry for the homogeneous (non-separation) immunoassay of phenobarbital has been described [1], and demonstrates the application of fluorescence lifetime selectivity to the determination of a hapten (small molecule non-antigenic) species. The work described here demonstrates the use of the same phase-resolved fluoroimmunoassay (PRFIA) approach for the determination of a macromolecular (antigenic) species, human serum albumin (HSA). In addition to serving as a model system, the determination of HSA in serum is of clinical significance and is a routinely performed test in clinical laboratories. Results for PRFIA determinations of HSA in serum samples obtained from a local hospital are compared with values provided by the hospital, and experiments to evaluate matrix effects from serum are discussed.

The labelled antigen used for this work was HSA covalently labelled with the fluorescent species, Texas Red, which is the sulfonyl chloride derivative of Sulforhodamine-101 [2]. Texas Red offers the advantages of high absorptivity and quantum yield, a lower rate of photobleaching than fluorescein (which was used in the previous PRFIA study [1]), and has excitation and emission maxima at significantly longer wavelengths than most species likely to contribute to the fluorescence background in serum, including bilirubin which has high spectral overlap with fluorescein.

0003-2670/86/$03.50

THEORY

The theory and instrumentation of phase-resolved fluorescence spectrometry have been described [3—5]. The technique is based on the use of an excitation beam sinusoidally modulated with an angular frequency ω to produce fluorescence emission that is phase-delayed and demodulated to an extent that depends upon the fluorescence lifetime of the emitter(s). The observed fluorescence lifetime, τ, can be calculated from the phase-delay, ϕ

$$\tau_\phi = (1/\omega) \tan \phi \tag{1}$$

or from the demodulation D

$$\tau_m = (1/\omega) [(1/D^2) - 1]^{1/2} \tag{2}$$

where both ϕ and D are measured relative to a reference scattering solution ($\tau = 0$).

In phase-resolved spectrofluorimetry, the alternating current (a.c.) component of the modulated emission signal is integrated over a pi-interval (one half cycle), resulting in a wavelength-dependent, time-independent phase-resolved fluorescence intensity (PRFI) which is a function of the relative position of the integration interval (the detector phase angle setting, ϕ_D), the modulation of the excitation beam (m_{ex}), the demodulation of the emitted signal (m) and the relative phase of the emission (ϕ) (both m and ϕ are fluorescence-lifetime-dependent), and steady-state fluorescence intensity parameters (A) including molar absorptivity, quantum yield and instrumental factors. The PRFI can therefore be expressed as

$$F(\phi_D) = A[1 + m_{ex} m \cos(\phi_D - \phi)] \tag{3}$$

Phase-resolved fluorescence immunoassay involves the use of PRFI measurements at one or more ϕ_D settings, as previously described [1]. The competitive immunoassay equilibrium can be represented as

$$Ag^* + Ag + Ab \rightleftharpoons Ag^*—Ab + Ag—Ab \tag{4}$$

where Ag* represents the fluorescent-labelled antigen (Texas Red/HSA), Ag represents the analyte antigen (standard or sample HSA), and Ab is the antibody (anti-HSA). In PRFIA, the difference in fluorescence lifetime between Ag* and Ag*—Ab provides the basis for the simultaneous determination of the two species without physical separation.

Because PRFI contributions are additive in mixtures of non-interacting emitters, the PRFI of the immunoassay solutions can be given as

$$F(\phi_D) = I_f C_{Ag^*} + I_b C_{Ag^*—Ab} \tag{5}$$

where $F(\phi_D)$ is the PRFI of a sample or standard solution, I_f is the unit PRFI of free Ag*, I_b is the unit PRFI of Ag*—Ab, and C_{Ag^*} and $C_{Ag^*—Ab}$ are the concentrations of free and bound Ag*, respectively. When Ag is added to a solution containing Ag* and Ab, C_{Ag^*} will increase by an amount

ΔC and C_{Ag^*-Ab} will decrease by the same amount:

$$F'(\phi_D) = I_f(C_{Ag^*} + \Delta C) + I_b(C_{Ag^*-Ab} - \Delta C) \quad (6)$$

Subtraction of Eqn. 5 from Eqn. 6 gives

$$\Delta C = [F'(\phi_D) - F(\phi_D)]/(I_f - I_b) \quad (7)$$

A plot of ΔC as a function of C_{Ag} for a series of standard solutions yields a calibration curve.

EXPERIMENTAL

Reagents, samples and equipment

Demineralized distilled water was used for all preparations.

Non-specific immunoglobulin G (IgG), the anti-HSA stock solution (containing 48 mg protein per ml, prepared from the IgG fraction of anti-HSA antiserum) and HSA standard solutions (in 0.85% NaCl) were purchased from Sigma Chemical Co. The Texas Red/HSA stock solution (4.1 mg ml^{-1}) was purchased from Accurate Chemical and Scientific Corp.

Phosphate buffer (0.010 M, pH 7.5) was prepared from NaH_2PO_4 and Na_2HPO_4. Freshly prepared solutions were used for each set of experiments.

Texas Red/HSA reagent was prepared by diluting 125 μl of the stock solution to 25 ml. Anti-HSA reagent was prepared by diluting 500 μl of the stock solution to 50 ml. Albumin standards were prepared by diluting 43 μl of the 4.0 g dl^{-1} HSA standard solution to 50 ml, followed by dilution of volumes ranging from 40 to 800 μl of the latter solution to 5.0 ml.

All fluorescence measurements were made with an SLM 4800S spectrofluorimeter (SLM Instruments) with a 450-W xenon arc lamp source, Hamamatsu R928 photomultiplier tube detectors, and a Glan-Thompson calcite prism polarizer in the excitation beam at 35° from the vertical axis. Sample-turret temperature was maintained at 25.0 ± 0.1°C for all measurements by a Haake A81 temperature controller.

Serum samples were obtained from a local hospital. A 40-μl aliquot of each sample was diluted to 50 ml, and 120 μl of this solution was diluted to 5.0 ml.

Procedures

For each run, 600 μl of Texas Red/HSA, 800 μl of anti-HSA and 800 μl of the HSA sample or standard were mixed in a disposable polyethylene fluorescence cuvette (Precision Cells) to give concentrations of HSA ranging from 0.10 to 2.0 μg ml^{-1}.

The excitation and emission monochromators were set at 590 and 610 nm, respectively. The slit settings were 16 and 0.5 nm for the excitation monochromator entrance and exit, respectively, 0.5 nm for the modulation tank exit, and 16 and 8 nm for the emission monochromator entrance and exit, respectively.

Phase-resolved intensities and phase-modulation lifetimes were all measured at a modulation frequency of 30 MHz, in the delta-phase mode (a ratiometric mode) to minimize the effects of fluctuations in the source output and excitation modulation.

All measurements were made in triplicate, each measurement being the average of 100 samplings made during a 30-s period, performed internally by the spectrofluorimeter electronics.

An APPLE II+ microcomputer on-line with the spectrofluorimeter was used for data acquisition and processing.

RESULTS AND DISCUSSION

Uncertainties for all quantitative results are given as one standard deviation unit. Fluorescence lifetimes were all calculated from phase-shift measurements.

Fluorescence spectra for the Texas Red/HSA (Ag*) indicated excitation and emission maxima at 590 and 610 nm, respectively with the antibody-bound Ag* (Ag*—Ab) having an excitation maximum at 592 nm.

To avoid the precipitation of bound Ag* via the precipitin reaction in the presence of excess Ab, it was necessary that all solutions contain excess Ag*. Therefore, the standard solution containing no Ag was used to find the "I_b" value for Eqns. 5—7, even though this solution contains both Ag* and Ag*—Ab. Because all results are skewed to this assignment of I_b, the axes on the calibration curves are given as relative ΔC in arbitrary units. To simplify the discussion below, the zero Ag standard solution will be referred to as the Ag*—Ab standard solution.

Fluorescence lifetimes were determined by using a reference scattering solution and values of 3.98 ± 0.03 ns and 4.07 ± 0.03 ns were obtained for the Ag*—Ab standard solution and the 2.0 μg ml^{-1} Ag standard solution (corresponding to "free Ag*"), respectively, using phase-shift measurements. Additional Ag did not cause a further increase in the observed lifetime of the latter solution, so it was assumed that this represented essentially complete displacement of the Ag* from the Ab. This solution will hereinafter be referred to as the Ag* standard solution. A solution containing only Ag* (no Ab) gave a lifetime of 4.11 ± 0.05 ns, indicating an effect from the presence of the antibody in the standard solution despite the apparently complete displacement of the Ag*.

Similar lifetimes were obtained with and without the polarizer in the excitation beam, and the polarizer was used in subsequent experiments as a safeguard against rotational artifacts. In initial experiments comparing lifetimes of Ag* and Ag*—Ab fluorescence, non-specific IgG was added to the solutions of Ag* to give the same IgG concentration as in the Ag*—Ab solutions, thereby preventing differences in lifetime caused by the presence of the protein rather than by specific binding of the Ag*. The same lifetime was observed for Ag* whether or not IgG was present in the solution, and the addition of IgG was not continued.

The plots of relative PRFI vs. ϕ_D for the Ag* and the Ag*—Ab standard solutions indicated a phase-angle difference between the two species corresponding to a fluorescence lifetime difference of 0.09 ns. This is consistent with the direct lifetime determinations.

Figure 1 shows a typical calibration curve generated by using measurements at three detector phase angles (10.7°, 55.7° and 100.7°, where 74° is the angle corresponding to maximum PRFI for Ag*—Ab). The relative standard deviation for four calibration curves generated on four consecutive days was 5.8%.

A steady-state version of the immunoassay was also attempted, in which conventional steady-state measurements were made at the same wavelengths used for the PRFIA, and results were calculated using a version of Eqn. 7 in which all of the intensities are steady-state instead of phase-resolved. This approach exploits only the small difference in unit intensity between Ag* and Ag*—Ab, without the additional lifetime selectivity used in PRFIA. Calibration curves generated in the steady-state mode for the same solutions on the same four days as the PRFIA curves, and using the same total number of measurements per solution, gave a relative standard deviation of 14%. The improvement in precision gained by the incorporation of lifetime selectivity into the determination technique, previously observed for the phenobarbital immunoassay [1], was therefore also observed for the immunoassay of the macromolecular antigen HSA.

Serum samples

Serum samples were obtained from a local hospital. Values for HSA were supplied for each sample as determined by the hospital laboratory using the bromocresol green method [6] on a Technicon RA-1000 Autoanalyzer system.

The fluorescence lifetime for a solution containing Ag*, Ab and Ag in

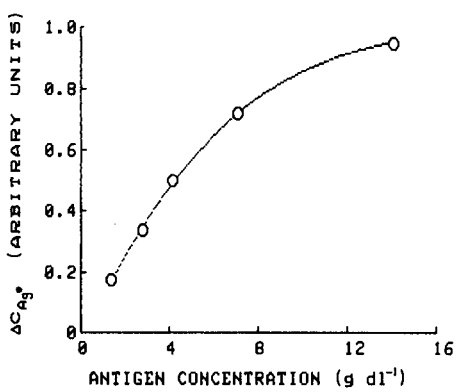

Fig. 1. Phase-resolved fluoroimmunoassay calibration curve generated by using three detector phase angles. The relative change in the concentration of Ag* is plotted as a function of antigen concentration in undiluted serum.

TABLE 1

Comparison of the results for determination of HSA in serum samples by PRFIA with those by the bromocresol green method[a]

Detector phase angle(s) ϕ_D (°)	Slope	Intercept (g dl^{-1})	Std. error of estimate (g dl^{-1})	Correlation coefficient
10.7	$1.2_8 \pm 0.2_1$	$-0.9_7 \pm 0.8_5$	0.33	0.96
55.7	$1.2_2 \pm 0.2_0$	$-0.6_4 \pm 0.8_1$	0.32	0.96
100.7	$0.9_0 \pm 0.1_7$	$0.5_8 \pm 0.6_9$	0.27	0.96
55.7, 100.7	$0.9_9 \pm 0.0_4$	$0.2_6 \pm 0.1_7$	0.06	0.996
10.7, 55.7, 100.7	$1.1_1 \pm 0.1_3$	$-0.4_4 \pm 0.4_6$	0.19	0.99

[a]24 serum samples with HSA concentrations in the range 2.5—5.0 g dl^{-1}.

which an undiluted serum sample was used, was found from phase-shift measurements to be 4.06 ± 0.03 ns. This is in good agreement with the value of 4.07 ± 0.03 ns obtained when the HSA standard was used (see above). In a second experiment, two sets of six solutions were prepared. In the first set, a serum sample containing 4.7 g dl^{-1} HSA (as determined by the hospital lab) was used to provide concentrations in the range 0.10—1.0 μg ml^{-1}. The second set of solutions was prepared to have the same six concentrations as the first set, using the 4.0 g dl^{-1} standard HSA solution. Data for HSA concentrations obtained using the PRFIA for the serum solutions (y) vs. those similarly obtained for the standard solutions (x) were fitted by the method of least squares and yielded the equation $y = (1.02 \pm 0.03)x - 0.04 \pm 0.05$. The standard error of estimate was 0.05 and the correlation coefficient was 0.999. These two experiments indicate the absence of a significant matrix effect, probably because of the large sample dilution factor (7×10^{-6}).

In another experiment, HSA was quantified in individual serum samples by using PRFIA, and the values obtained were compared with those provided by the hospital. The results for the comparison of the two techniques are summarized in Table 1. Five sets of PRFIA results were used for the comparison, including one set obtained at each of the three detector phase angles used, one set obtained by averaging the results for two of the angles (best-case results shown), and one set obtained by averaging the results of all three detector phase angles. The comparative results for the two-angle average are better than those for any of the single-angle results. They are also better than the comparative results for the three-angle average. This is not surprising because the errors for the two angles tended to cancel each other. Optimization of the PRFIA with respect to the choice of detector phase angles has not yet been studied systematically.

The authors are grateful to the Stillwater Medical Center Laboratory and to Charles R. Mullins at the Laboratory for providing the serum samples and

results. This work was supported by the National Science Foundation (Grant No. CHE-8403759).

REFERENCES

1 F. V. Bright and L. B. McGown, Talanta, 32 (1985) 15.
2 J. A. Titus, R. Haugland, S. O. Sharrow and D. M. Segal, J. Immunol. Methods, 50 (1982) 193.
3 T. V. Vesalova, A. S. Cherkasov and V. I. Shirokov, Opt. Spectrosc., 29 (1970) 617.
4 J. R. Lakowicz and H. Cherek, J. Biochem. Biophys., 5 (1981) 19.
5 J. R. Mattheis, G. W. Mitchell and R. D. Spencer, in D. Eastwood (Ed.), New Directions in Molecular Luminescence, ASTM Special Technical Publication 822, Baltimore, 1983, pp. 50—64.
6 B. T. Doumas, W. A. Watson and H. G. Biggs, Clin. Chim. Acta, 31 (1971) 87.

Analytica Chimica Acta, 182 (1986) 193—202
Elsevier Science Publishers B.V., Amsterdam — Printed in The Netherlands

DESIGN OF A PROLOG-BASED EXPERT SYSTEM FOR PLANNING SEPARATIONS OF STEROIDS BY HIGH-PERFORMANCE LIQUID CHROMATOGRAPHY

HARI GUNASINGHAM*

Department of Chemistry, National University of Singapore, Kent Ridge, 0511 (Singapore)

B. SRINIVASAN

Department of Computer Science, Monash University, Clayton, Victoria (Australia)

A. L. ANANDA

Department of Information Systems and Computer Science, National University of Singapore, Kent Ridge, 0511 (Singapore)

(Received 18th January 1985)

SUMMARY

A Micro-PROLOG-based expert system is described for planning separations by high-performance liquid chromatography. The criteria for the system design are presented together with details of the PROLOG implementation and its application to the separation of steroids.

Expert or knowledge-based systems can be powerful for problem-solving when the solution is based on incomplete or uncertain information. In such "fuzzy" situations, they can achieve performance levels that are rarely matched by conventional programming based on rigidly defined algorithms. In recent years, expert systems have been used in a wide variety of applications ranging from medical consultation and analysis of chemical structures to the configuration of computer systems [1—3].

Expert systems differ from conventional software systems in the differentiation between the knowledge base and the inference procedure. In conventional systems, there is usually no such distinction. One obvious benefit of keeping the two apart is that the knowledge base can easily be altered by addition or deletion. The knowledge base contains expert information in the form of rules and facts regarding the application, which are obtained from experts in the field concerned. For example, rules encoded in the knowledge base are often heuristic and so are somewhat uncertain because of the uncertainty in the data and the subjective nature of human judgements based on such data. The usefulness of an expert system therefore depends on the accuracy and completeness of the knowledge base. However, if the knowledge base is good, then an expert system is capable of a high level of performance.

0003-2670/86/$03.50

Some of the best known applications of expert systems have been to chemistry. Indeed, the earliest and, perhaps, most successful system is DENDRAL, which analyzes the molecular structures of organic compounds based on mass spectrometric (m.s.) data [4—6]. The m.s. specialist relies on past experience for the interpretation of data; usually, this now involves computerized pattern recognition but ambiguity in the data and interpretation means that the results have only some probability of being correct.

Dessy [7, 8] has set out a tutorial description of expert systems and the scope of their applications to chemistry. Broadly, applications area include planning of chemical synthesis [9, 10], and structure elucidation through the interpretation of molecular spectra [8]. A commercial expert system for planning liquid chromatographic (l.c.) separations has been described briefly [8]; little detail regarding the implementation of the system was given.

The knowledge base of an expert system is usually a set of facts and rules relevant to the particular problem, e.g., in DENDRAL, the knowledge base includes prior experience on the fragmentation of organic molecules. The inference procedure controls and updates the current status of the knowledge about the case to hand. In the case of DENDRAL, the inference procedures are the INTERLISP functions. And in the present application, the inference procedures are implemented by the PROLOG functions.

In this paper, an expert system is described for planning l.c. separations of steroids. The design criteria and structure of the system and the approach to problem-solving and knowledge representation in PROLOG are emphasized. The system is implemented in micro-PROLOG running under the CPM operating system on an Apple IIe computer (with Z80 processor).

High-performance liquid chromatography of steroids

Several hundred naturally-occurring steroids and a constantly-expanding number of synthetic steroids are known; they are divided into four main categories, the corticosteroids, androgens, estrogens and progestins. Steroids vary considerably in their physical characteristics and chromatographic properties. The difficulty of analyzing for steroids in biological samples is that there are many interfering compounds, some of which may be closely related analogues.

Major developments in the l.c. of steroids up to 1979 have been reviewed [11, 12]. Most of the facts and rules for the knowledge base in this work were obtained from these sources, and especially from Hara and Hayashi [13] who made a detailed study of the retention behaviour of 43 steroids in reverse-phase and normal-phase l.c. In the present work, attention was limited to pregnane, androstane and estrogen derivatives.

There are several quantitative expressions for relating chromatographic optimization parameters to solute, eluent and stationary phase properties, but in practice most chromatographers rely on experience and information in the literature. However, attempts have been made to rationalize such information by the use of selection tables or selection diagrams. In the present

approach to designing an expert system, an attempt is made to emulate the way by which an experienced chromatographer might tackle a separation problem.

The choice of a particular separation method is usually governed by the nature of the sample, the type of separation selectivity required, experimental convenience and experience with the method [14]. The sample is obviously the principal guide; knowledge of what compounds are present in the sample mixture greatly simplifies the approach. There are then two options. First, a literature search could produce an earlier successful separation for the compounds of interest, or at least separations of a similar class of compounds which could act as a guide. Alternatively, a separation method could be devised from basic principles; this process involves choice of the l.c. system and optimization of the separation. A successful separation is achieved when a proper balance is established between the sample intermolecular forces, mobile phase and stationary phase; a common approach is to match the polarity of the sample and stationary phase and then use a mobile phase of different polarity. The first step is therefore to obtain information about the molecular weight, solubility and polarity of the constituents of the sample; these provide a rough guide to an appropriate method. Constraints may then be imposed; e.g., the choice of eluent may be governed by cost, purity, viscosity, ability to dissolve sample, compatibility with the detector and solvent selectivity. Obviously, the criteria for a particular separation can vary from case to case. In one application, the best resolution for a pair of compounds or several pairs may be needed, and in another, good separation of all compounds in the sample mixture may be demanded. Attempts have been made to quantify separation criteria on the basis of a chromatographic response function (CRF) [15], but its practical application has far to go.

DESIGN CONSIDERATIONS IN THE PROLOG IMPLEMENTATION

Procedural knowledge may be represented by conventional programs but problems arise when the precise number of steps leading to the solution are not known. An alternative to this combinatorial problem is to encode the knowledge base in the form of pattern-invoked programs, which are activated by the control structure whenever the data fulfil certain conditions. In PROLOG, procedural knowledge is represented in first-order predicate logic and is structured to allow pattern-driven call-up. Thus, one of the characteristics of PROLOG is its ability to extract inferences automatically, and this makes it well suited to the development of expert systems [16—23].

Logic programming languages such as PROLOG afford a powerful alternative to LISP. The most significant difference is that the PROLOG interpreter already incorporates the pattern-matching facilities which have to be explicitly programmed in the case of LISP. The other advantage of PROLOG lies in its ability to represent real-world knowledge efficiently [17]: it is precise (unambiguous), flexible in that facts and rules can be placed in the knowledge

base without having to be committed to any deduction processes, and it is modular, i.e., items can be added to the knowledge base independently of each other. With regard to its performance, a PROLOG compiler/interpreter has been developed which is comparable to LISP [16].

Representing knowledge in PROLOG

PROLOG can be used to represent both declarative and procedural knowledge. A fact is represented by a predicate name which links together a list of arguments. Micro-PROLOG has two forms: the surface syntax and the internal syntax. Programs described in this paper are written in the surface syntax so as to make them more readable. Although there is only a superficial difference, it should be noted that micro-PROLOG understands only the internal syntax [17]. An example of the surface syntax is as follows:

```
estriol has-property aromatic
aromatic suited-for ultraviolet-detection
```

This predication can be used to represent the fact that estriol has an aromatic character and that aromatic compounds may be detected with an ultraviolet detector.

Rules have the form P1 if P2 and P3 and ... and P*n*. For example, the rule

```
X detects Y if
Y has-property Z
and X suited-for Z
```

may be used to describe the general rule for choosing a mode of detection. The above rule is assumed to apply for all possible values of the variable X Y Z. The internal syntax of this rule is given by

```
((detects (X Y))
(has-property (Y Z))
(suited-for (X Z)))
```

Generating inferences

PROLOG can be used to ascertain whether any assumptions about the applications (in this case the h.p.l.c. of steroids) are consistent with the description (rules and facts) present in the knowledge base. It does so through a deductive process. The request "Which(X X detects estriol)" causes PROLOG to find cases of the above predication that make it true, and the answer found is "X = ultraviolet-detection".

PROLOG answers a query P1 and P2 and ... and P*n* by taking each P*i* in turn and trying to find it among the expanded facts and rules, either as a fact or as the left-most predication of a rule. If found among the facts, P*i* is considered proven. If it appears in a rule of the form P*i* if Q1 and Q2 ... and Q*m*, then PROLOG simply tries to prove each and all of Q1 ... Q*n* in the same way.

Obtaining rules by induction

The first step in developing an expert system is to build the knowledge base. One route to acquisition of knowledge is by induction. Examples of how the expert system should behave are taken and then generalized to a higher-level rule that can guide the inference procedure. A spin-off of using an inductive process to build the knowledge base is that regularities can be discovered [23]. The DENDRAL program is an example of automation of the inductive process for establishing rules. Meta-DENDRAL was designed as the learning element for Heuristic DENDRAL in obtaining rules for the fragmentation of analogous structures [5].

The inductive process can also be applied to establish rules for the separation of steroids. The specific examples are the validated results of successful separations reported in the literature. Hara and Hayashi [13] found that 17B-acetoxyandrostrane-4-en-3-one and 17B-hydroxyandrostrane-4-en-3-one are better separated by reverse-phase l.c. From this and other similar examples, the following general rule was derived: reversed-phase systems are preferred for the separation of hydroxy steroids and the corresponding acyloxy steroids [13]. This rule can be represented by the following PROLOG statement:

```
reversed-phase can-separate (X¦Y) if
   Z belongs-to (X¦Y)
and X1 belongs-to (X¦Y)
and Z is-a hydroxy-steroid
and X1 is-a acyloxy-steroid
and Z same-parent X1
```

(X¦Y) is the list of compounds which are to be separated. The PROLOG rule states that if Z and X1 are members of this list and are hydroxy and acyloxy steroids having the same parent, then they can be separated by reverse-phase l.c.

Planning and problem-solving by problem reduction

Problem reduction was used in some of the early problem-solving systems such as GPS [23]. The problem to be solved is divided into subproblems that can be solved separately, in such a way that combination of these solutions will yield a solution to the original problem. Each subproblem can be divided further until elementary problems which can be solved directly are generated. All possible divisions of a problem can be represented in a problem-reduction graph or AND/OR graph in which each OR branch represents a choice of several divisions, and each AND branch represents a particular way of dividing up a problem.

SYSTEM DESIGN

In the present application, the problem is to select an appropriate separation system for a given number of compounds. The separation problem can

be reduced to an AND/OR graph (Fig. 1) and the solution to this problem can be expressed in terms of a search of this graph from the bottom. Although the AND/OR graph dictates a goal-driven (backward chaining) structure, the move from one node to another, along a particular branch may require data inputs from the user which poses constraints on the search. This data-driven strategy aims to narrow the search and so reduce the time required to reach a solution.

The search proceeds from left to right. The first step is to seek a case in the knowledge base in which some or all of the compounds of interest in the sample have been separated. If this fails, the search backtracks to the first node of the second branch and an approximate match is sought, i.e., similar compounds or class of compounds which have been separated successfully. Finally, if all these fail, the system backtracks to the first node of the last branch from which the system plans the separation from first principles.

The structure of the procedural knowledge is thus an AND/OR tree, each node of which is a rule which can be invoked if the conditional part of the rule is satisfied. Associated with these rules are various facts regarding properties of the steroids, eluent, stationary phase and detector and additional rules which pose the constraints to the search. These rules and facts are particular to the problem at hand, but there are also more general rules which define list processing. When the user wants to query the expert system about a particular separation problem, he has to input a list of compounds suspected to be present in the sample, and a list of the compounds which must be especially well separated.

The PROLOG representation of a list is of the form (x¦y) where x is the head of the list and y is the tail. The processing of such lists is defined by a

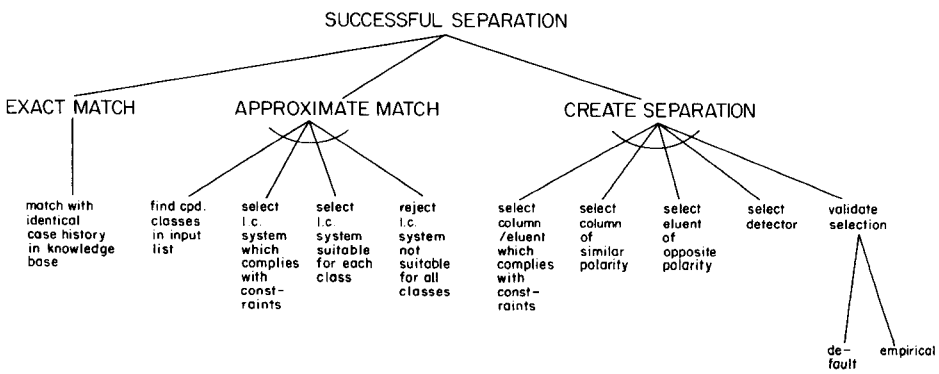

Fig. 1. AND/OR graph outlining the solution to the problem of planning l.c. separations. The graph can be represented by the statements:

(X Y Z) will-separate (x¦y) if
(X Y Z) exact-match (x¦y)
(X Y Z) will-separate (x¦y) if
(X Y Z) approximate-match (x¦y) if
(X Y Z) will-separate (x¦y) if
(X Y Z) create-match (x¦y)

set of PROLOG relationships which enables access to members of the list. PROLOG statements for list processing used include those listed in Table 1. The permutation-of relationship enables the matching of two lists even though members of each are in different order. The has-length relationship enables the length of a list to be established. The intersection-of relationship enables construction of a list of elements which are common to two other lists. All these relationships use a recursive definition. A detailed discussion of PROLOG list processing is given by Clocksin and Mellish [19].

The creation of a separation may be reduced to four subproblems: (1) establishing the characteristics of the sample, i.e., the compounds of interest and their polarity indexes; (2) finding a stationary phase of similar polarity; (3) finding an eluent mixture of opposite polarity; and (4) finding a compatible detector. Solution to these subproblems may be sought at a lower level. (The polarity index is taken to be the mean polarity of the compounds of interest in the scale 1—10; polarity is defined in relative terms from the retention data of Hara and Hayashi [13].) The preceding steps can produce a very large number of candidate solutions. In order to narrow the search, constraints can be imposed and this should be done as early as possible. In the continued search, candidate solutions which do not satisfy the constraints are ignored. Finally, the validity of the candidate solution can be checked empirically by running an actual chromatogram.

RESULTS AND DISCUSSION

For simplicity, the 43 steroids considered by Hara and Hayashi [13] were classified according to polarity. In the following example, the problem is limited to finding a suitable separation for the estrogen steroids listed in Table 2. Table 3 lists the micro-PROLOG statements that implement the search along the approximate-match branch of Fig. 1. In order to invoke the search of this branch to generate an inference, the user must query the system. For example, the user types in "which (x x will-separate (a b c e d f g j k m l o n))". The expert system then asks the user to input constraints to

TABLE 1

PROLOG statements for list processing

```
(( ) X) appends-to X
((X¦Y) Z) appends-to (X¦x) if
   (Y Z) appends-to x
DELETE (X Y Z) if
   (x (X¦y)) appends-to Y and
   (x y) appends-to Z
( ) permutation-of ( )
(X¦Y) permutation-of Z if
   DELETE (X Z x)
   and Y permutation-of x
( ) has-length 0
(X¦Y) has-length Z if Y has-length x
   and SUM (x 1 Z)
X intersection-of (Y Z) if
   X Is-All (x x belongs-to Y and x belongs-to Z)
X belongs-to (X¦Y)
X belongs-to (Y¦Z) if
   X belongs-to Z
```

TABLE 2

Polarity index for the estrogen steroids

	Steroid	Polarity index
a	3,17B-Dipropionyloxy-E-1,3,5(10)triene	1
b	3-Methoxy-17-Etin-E-1,3,5(10)trien-17B-ol	1.3
c	17B-Valeryloxy-E-1,3,5(10)-trien-3-ol	1.3
d	3-Benzoyloxy-16,17B-diacetoxy-E-1,3,5(10)-triene	2.0
e	17-Etin-E1,3,5(10)-triene-3,17B-diol	2.3
f	3-Hydroxy-E-1,3,5(10)-trien-17-one (estrone)	2.4
g	17B-[B-(Phenypropionyloxy)]-E-4-en-3-one	2.6
h	17B-[B-(Furylpropionyloxy)]-E-4-en-3-one	2.6
i	3-Benzoyloxy-E-1,3,5(10)-trien-17B-ol	2.7
j	E-1,3,5(10)-triene-3,17B-diol (estradiol)	2.9
k	17B-Hydroxy-17a-Etin-E-4-en-3-one	3.7
l	17B-Hydroxy-17a-Et-E-4-en-3-one	4.6
m	17B-Hydroxy-17a-Me-E-4-en-3-one	5.7
n	17B-Hydroxy-17a-Me-E-4-en-3-one	6.5
o	E-1,3,5(10)-triene-3,16a,17B-triol (estriol)	10

the search: e.g., "sample origin ? urine; patient condition ? pregnancy; constraints ? (f j)". The user responses assist in narrowing down the search. Thus, in this example, only column/eluent systems which can handle pregnancy urine samples (which contain potentially interfering compounds) are selected. The further constraint regarding selectivity is that estrogens f and j (estrone and estradiol) should be well resolved.

Finally, micro-PROLOG searches through its list of rules and facts to find a suitable match to the user query. It returns with the answer: (Lichrosorb-ODS diethyl-ether-acetonitrile-water UV). This gives the column, eluent and detector needed to solve the estrogen steroid separation problem.

Generality vs. expertness

In the above example, constraints were applied to narrow the search; for maximum efficiency, this is done as early as possible to prevent searching of the knowledge base for all possible solutions. This means that the user-generated constraints must be satisfied before the program outputs the column, eluent and detector. The other approach would have been to select the column, eluent and detector and then apply the constraint to see if the selection was valid. The latter is an exhaustive search whereas the former is selective and produces a solution more economically. Differences in performance become more significant as the number of possible solutions increases. The trade-off between generality and expertness is a major issue in the design of expert systems. By increasing expertness (by, for example, heuristic search), the cost is lowered but the scope is narrowed.

The present implementation is limited to quite simple separations. How-

TABLE 3

Micro-PROLOG rules (in surface syntax) for searching the "approximate-match" branch of the AND/OR graph

```
(X Y Z) will-separate (x¦y) if
        sample-input (z) and
        / ( ) and
        constraints PP ? and
        R (X1) and
        Y1 intersection-of ((x¦y) X1) and
        Y1 has-length Z1 and
        / ( ) and
        (X Y) suitable X1 and
        (X Y Z) separates (x¦y)

(X Y Z) separates (x¦y) if
        sample (z) and
        patient (X1) and
        / ( ) and
        Y1 parent-to (x¦y) and
        (X Y) is-compatible (z X1 Y1) and
        (X Y Z) can-separate Y1

X parent-to (Y¦Z) if
        X parent-of x and
        (Y¦Z) permutation-of x and
        x has-length y and
        (Y¦Z) has-length z and
        z EQ y

X parent-to (Y¦Z) if
        X parent-of x and
        Y intersection-of ((Y¦Z) x) and
        (Y¦Z) has-length z and
        y has-length X1 and
        Not (z EQ X1) and
        2 LESS X1 and
        PROD (X1 Y1 z Z1) and
        Y1 LESS 2

(X Y Z) can-separate x if
        X column-for x and
        Y eluent-for x and
        Z detector-for x
```

ever, this limitation is due to insufficient information in the knowledge base rather than to deficiencies in the system structure or the approach to problem solving. This is inevitable in the development of expert systems because building of the knowledge base is usually an incremental process.

The provision of a University research grant, RP37/82, for this work is gratefully acknowledged.

REFERENCES

1 D. Nau, Computer, 15 (1983) 63.
2 A. Barr and E. Feigenbaum (Eds.), Handbook of Artificial Intelligence, Vol. 1, W. Kaufman, California, 1982.
3 M. Stelfik, Artificial Intelligence, 18 (1982) 135.
4 R. K. Lindsay, B. Buchanan, E. A. Feigenbaum and J. Lederberg, Applications of Artificial Intelligence for Organic Chemistry, the Dendral Project, McGraw-Hill, New York, 1980.
5 B. G. Buchanan and T. M. Mitchell, in D. A. Waterman and F. Hayes-Roth (Eds.), Pattern-Directed Inference Systems, Academic Press, New York, 1978.
6 E. Feigenbaum, G. Buchanan and J. Lederberg, in D. Meltzer and D. Mitchie (Eds.), Machine Intelligence, Vol. 6, Edinburgh Univ. Press, 1971, p. 165.
7 R. E. Dessy, Anal. Chem., 56 (1984) 1200A.
8 R. E. Dessy, Anal. Chem., 56 (1984) 1312A.
9 E. J. Corey, Quart. Rev., 25 (1971) 455.
10 R. D. Stolow and L. J. Joncas, J. Chem. Educ., 57 (1980) 868.
11 E. Heftman, Chromatography of Steroids, Elsevier, Amsterdam, 1976.
12 E. Heftman and I. R. Hunter, J. Chromatogr., 165 (1979) 283.
13 S. Hara and S. Hayashi, J. Chromatogr., 142 (1977) 689.
14 L. R. Snyder and J. J. Kirkland, Introduction to Modern Liquid Chromatography, 2nd edn., Wiley, New York, 1979.
15 J. L. Glajch, J. J. Kirkland, K. M. Squire and J. M. Minor, J. Chromatogr., 199 (1980) 57.
16 D. Warren, in D. Mitchie (Ed.), Expert Systems in the Micro-electronic Age, Edinburgh Univ. Press, Edinburgh, 1979, p. 112.
17 V. Dahl, Computer, 16 (1983) 106.
18 E. W. Elcock, Computer, 16 (1983) 114.
19 W. F. Clocksin and C. S. Mellish, Programming in Prolog, Springer Verlag, Berlin, 1981.
20 D. H. D. Warren, L. M. Pereira and F. Pereira, Sigart Newsletter, 64 (1978) 109.
21 K. L. Clark and F. C. McCabe, in D. Mitchie (Ed.), Expert Systems in the Micro-electronic Age, Edinburgh Univ. Press, Edinburgh, 1979, p. 122.
22 R. A. Kowalski, Logic for Problem Solving, North Holland, Elsevier, New York, 1979.
23 A. Barr and E. Feigenbaum (Eds.), Handbook of Artificial Intelligence, Vol. 3, W. Kaufman, California, 1982.

Analytica Chimica Acta, 182 (1986) 203—206
Elsevier Science Publishers B.V., Amsterdam — Printed in The Netherlands

Short Communication

TWO NEW FLUOROGENIC SUBSTRATES FOR THE DETECTION OF PENICILLIN-G-ACYLASE ACTIVITY

TH. SCHEPER, M. WEISS and K. SCHÜGERL*

Institut für Technische Chemie, Universität Hannover, Callinstrasse 3, 3000 Hannover 1 (Federal Republic of Germany)

(Received 25th October 1985)

Summary. Two fluorogenic substrates are described for the detection of Penicillin-G-acylase (EC 3.5.1.11) activity in coloured cell-containing media and inside single cells. A sensitive enzyme assay is based on the use of 7-phenylacetyl-4-alkylcoumarinylamides. Linear response is obtained in the range 20—300 μU ml^{-1}. After the cells have been made permeable, intracellular enzyme activity can be monitored. It is thus possible to label enzyme-containing cells and to distinguish them from enzyme-free cells by fluorescence microscopy or laser-flow cytometry.

Penicillin-G-acylase is needed for the industrial production of 6-amino-penicillanic acid from penicillin-G and for the production of semisynthetic penicillins. Several conventional tests are available for the detection of the enzyme [1, 2] but there are no fluorogenic assays for this enzyme. It is well known that penicillin-G-acylase hydrolyzes several amido and ester derivatives of phenylacetic acid. The selectivity of the enzyme for the 6-APA nucleus of penicillin-G is very low [3]. Several authors have reported amino-coumarin derivatives as substrates for peptidases [4—6]. Aminocoumarins react easily with phenylacetyl chloride to yield an amido ester of phenylacetic acid. Two fluorogenic substrates were synthesized and tested for a fluorogenic enzyme assay and as a specific marker for intracellular enzyme activity.

Experimental

The two substrates, 7-phenylacetyl-4-methylcoumarinylamide (PMC) and 7-phenylacetyl-4-trifluoromethylcoumarinylamide (PFC), were synthesized by the following procedure. The coumarin (1 mmol; 7-amino-4-methylcoumarin or 7-amino-4-(trifluoromethyl)coumarin; Aldrich Chemical Co.) was dissolved in 60 ml of dioxan (Merck), and 1.1 mmol of pyridine (Merck) was added while stirring. Then, 1.1 mmol of phenylacetyl chloride was added dropwise over 2 min. The reaction mixture was stirred for 3 h, poured on ice-water and acidified with concentrated (32%) hydrochloric acid. The precipitate was collected, washed with cold water and recrystallized from

0003-2670/86/$03.50

ethanol (yield, 77% PMC or 60% PFC) to give products pure by i.r. and n.m.r. spectroscopy. The coumarinylamides were stored (protected from light and moisture) below −5°C.

Both substrates are poorly soluble in water. Concentrations up to 10 mg l^{-1} (in 5% ethanol) can be obtained, if the amides are first dissolved in ethanol. This stock solution can be diluted with phosphate buffer (50 mM, pH 8) to the required amide and ethanol concentration.

The enzyme was assayed in a spectrofluorimeter (at 25°C). The excitation wavelength for all tests was 365 nm and the reaction was started by adding different amounts of enzyme solution to the substrate mixture (50 mM potassium phosphate buffer, pH 8, containing different amounts of ethanol).

Results and discussion

The mechanism of the enzymatic reaction is as follows:

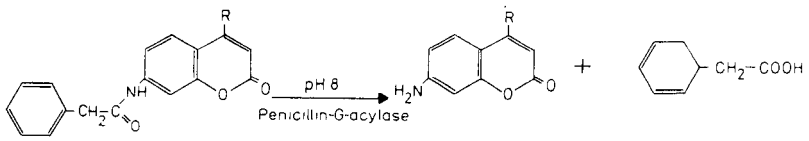

I R = $-CH_3$
II R = $-CF_3$

During the reaction, the highly fluorescent aminocoumarins are formed. The substrates and products differ greatly in their fluorescence emission behaviour, as shown in Fig. 1. The emission spectra for both substrates are shown before and after the addition of the enzyme.

The calibration gaphs for both substrates are shown in Fig. 2. The linear increase of the fluorescence was measured over 3 min and is plotted as a function of the enzyme concentration in the assay mixture. The calibration graphs are linear in the range 20—300 μU ml^{-1} for both substrates. This is a very sensitive enzyme assay for the detection of penicillin-G-acylase activity.

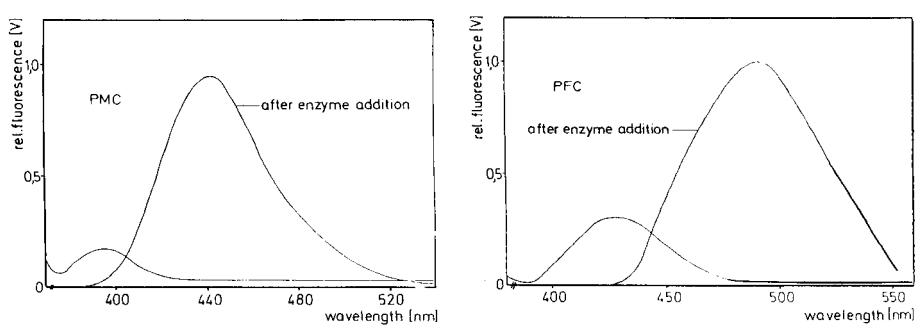

Fig. 1. Emission spectra of PMC and PFC in 50 mM phosphate buffer, pH 8, before and after addition of 10 μl of enzyme to 3 ml of substrate solution.

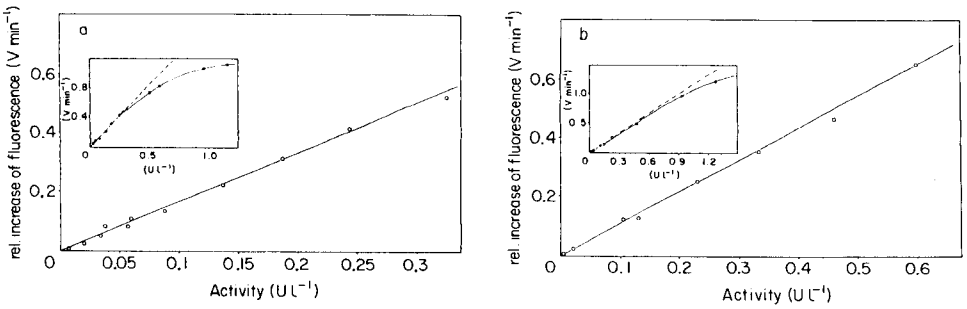

Fig. 2. Calibration graphs: (a) PMC, 1 μg ml^{-1}, 50 mM buffer, no ethanol, pH 8; (b) PFC, 3 μg ml^{-1}, 50 mM buffer, 5% ethanol, pH 8. Excitation at 365 nm; emission measured at 440 nm for PMC and 495 nm for PFC.

The enzyme is inhibited by the substrates, as shown by the Lineweaver-Burk plot [7]. The best substrate concentration was found to be 3 μg ml^{-1}. The kinetic parameters for the substrates were estimated from the Lineweaver-Burk plots to be v_{max} = 11.07 μmol l^{-1} min^{-1} and K_M = 83.1 μmol l^{-1} for PMC, and v_{max} = 3.33 μmol l^{-1} min^{-1} and K_M = 44.7 μmol l^{-1} for PFC.

Both substrates can be used for the detection of intracellular penicillin-G-acylase activity in micro-organisms. Enzyme-containing cells (*E. coli* ATCC 11105 after induction with phenylacetic acid [1] or the recombinant *E. coli* 5 K (pHM 12) [8]) were treated with 10% ethanol in water to make the cell walls permeable. The cells were next suspended in the substrate solution for 5—10 min. The substrate is hydrolyzed by the enzyme directly in the cells and the fluorescent coumarins are liberated intracellularly. Within 60 min, the cells can be observed under a fluorescence microscope or can be analyzed in a flow cytometry system [7]. Enzyme-containing cells fluoresce and can be separated from enzyme-free cells. This procedure is very important for studies on recombinant *E. coli* cells.

Cell-containing samples from cultivation processes can be used for the enzyme assay directly. Figure 3 shows the increase of the relative fluorescence, when 20 μl of a cell suspension of *E. coli* 5 K (pHM 12) was added to the substrate solution (the cells were made permeable by suspending them for 5 min in 50% ethanol). Very low concentrations of the enzyme can be detected by this method in cell-containing media.

Conclusions

The application of these fluorogenic substrates for the detection of penicillin-G-acylase is very interesting for various research purposes. Work is in progress on the continuous detection of the intracellular enzyme by an automated segmented-flow analyzer using this fluorogenic enzyme assay. Flow-cytometric studies will be continued for monitoring enzyme production and plasmid stability in single cells, and microscopic techniques will also

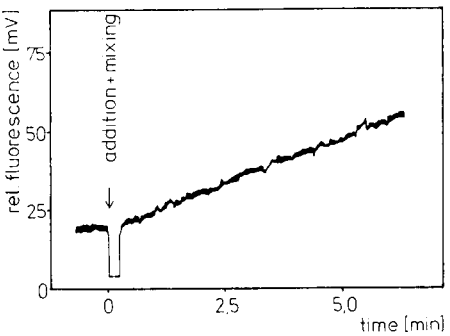

Fig. 3. Spectrofluorimetric detection of penicillin-G-acylase in a sample of a cultivation of *E. coli* 5K (pHM 12), showing increase in fluorescence intensity with time.

be used for strain improvement. These applications are important for studies of different cultivation processes of the genetically modified *E. coli* 5K (pHM 12), regarding gene expression, plasmid stability and process optimization.

REFERENCES

1 C. Kutzenbach and E. Rauenbusch, Z. Physiol. Chem., 354 (1974) 45.
2 A. Firley, Diploma thesis, University of Hannover, 1983.
3 M. Cole, Biochem. J., 115 (1969) 741.
4 R. E. Smith and E. R. Bissell, Eur. Pat. Appl., 18, 112, Oct. 1980; U.S. Appl., 32, 444, Apr. 1979. Chem. Abs., 94 (1981) 60672w.
5 T. Sekine, H. Itakura, T. Namihisa, T. Takahashi, H. Nakayame and Y. Kanaoka, Chem. Pharm. Bull., 29 (1981) 3286.
6 Y. Kanaoka, T. Takahashi, H. Nakayama, T. Ueno and T. Sekine, Chem. Pharm. Bull., 30 (1982) 1485.
7 Th. Scheper, Dissertation, University of Hannover, 1985.
8 H. Mayer, J. Collins and F. Wagner, Enzyme Eng., 5 (1980) 61.

Analytica Chimica Acta, 182 (1986) 207—211
Elsevier Science Publishers B.V., Amsterdam — Printed in The Netherlands

Short Communication

NEPHELOMETRIC DETERMINATION OF TRACE AMOUNTS OF THIOSULFATE IN AQUEOUS SAMPLES BY PRECIPITATION WITH BIS(1,10-PHENANTHROLINE)SILVER(I)

ROBERTO ARUGA* and ENNIO CAMPI

Department of Analytical Chemistry, University of Turin, Via Giuria 5, 10125 Turin (Italy)

(Received 7th October 1985)

Summary. The proposed nephelometric determination of thiosulfate in aqueous solution is based on precipitation of the slightly-soluble salt of thiosulfate with bis(1,10-phenanthroline)silver(I) cation from an aqueous ethanolic medium. Thiosulfate is determined in the range 3—70 mg l^{-1}, with a relative standard deviation of 2.6% and a relative accuracy of 2.5%. The method is simple and convenient. Iodide and thiocyanate interfere, but sulfite does not, even at 200 mg l^{-1}, which is an advantage over the usual iodimetric method.

Various methods for the determination of thiosulfate in aqueous samples have been proposed. The most widely applicable are generally thought to be the iodimetric techniques [1], with either visual or instrumental end-point indication [2, 3]. Another oxidimetric method makes use of cerium(IV) sulfate as titrant, with an amperometric end-point [4]. Polarographic [5], spectrophotometric [6—9] and kinetic [10—12] methods have also been proposed. Some methods have been based on the oxidation of thiosulfate by oxidizing agents (H_2O_2, mercury(II), etc.) followed by titration of the acid formed [1], but they are not considered sufficiently selective or reliable. No nephelometric or turbidimetric methods seem to have been proposed for the determination of thiosulfate.

Thiosulfate gives a slightly soluble salt with the silver(I) ion in the presence of 1,10-phenanthroline [13, 14], and the nephelometric technique is simple and rapid [15]. Thus it was thought worthwhile to develop a method of this type for the determination of thiosulfate in aqueous samples. The proposed method, after careful optimization of experimental conditions, provides good reproducibility and accuracy in the concentration range 3—70 mg l^{-1} thiosulfate (2.7×10^{-5}—6.2×10^{-4} mol l^{-1}) in the sample.

Experimental

Reagents and solutions. The following analytical-grade reagents (C. Erba) were used: 1,10-phenanthroline monohydrate, silver acetate, 95% ethanol, sodium acetate/acetic acid buffer pH 4.62, aqueous 0.1 N sodium thiosulfate.

0003-2670/86/$03.50

Merck "suprapur" sodium thiosulfate was also used; its purity was checked by iodimetric titration. Polyvinylpyrrolidone was from Fluka (purum K25). Doubly-distilled and filtered water (Millipore HA 0.45-μm membrane) was always used. In order to eliminate the interferences of cations, Bio-Rad Ag-50W-X8 cation-exchanger was used. The salts used in interference studies were analytical-grade reagents (C. Erba).

Precipitant solution (A). Silver acetate (6.726 g), 15.974 g of 1,10-phenanthroline monohydrate and 25.0 g of polyvinylpyrrolidone were placed in 400 ml of water, 420 ml of 95% ethanol was added, and the suspension was stirred until the solid dissolved completely. The solution was filtered (0.45-μm membrane) and diluted to 1 l with water. The yellow solution of the $[Ag(I)phen_2]^+$ complex was stable for at least 20 days at room temperature, as shown by the u.v.-visible spectra [15].

Standard solution of thiosulfate (B). Exactly 17.84 ml of 0.1 N sodium thiosulfate was diluted to 200 ml with water (final concentration 1000 mg l^{-1} $S_2O_3^{2-}$).

Equipment. A commercial HF-DRT-1000 nephelometer (HF Instruments, Bolton, Canada) was used. The main characteristics are: unfiltered light from a tungsten lamp, 90° observation, cylindrical 25.4-mm diameter cell with observation between 15 and 35 mm from the bottom, and an optional flow-through facility. Ultrasonic treatment was done by means of a Branson Sonifier B-15 generator.

Instrument calibration. The instrument was calibrated in formazine turbidity units FTU (or nephelometric turbidity units NTU) with the following standard [16]: 5.00 g of hydrazinium sulfate was dissolved in 400 ml of water, 50.00 g of hexamethylenetetramine was dissolved in 400 ml of water, and the solutions were mixed in a 1-l volumetric flask and diluted to volume. The mixture was allowed to stand at 20 ± 2°C for 48 h during which time a white suspension of formazine polymer developed. The turbidity of this mixture is conventionally considered to be 4000 FTU. Dilution of this suspension with water gives reference suspensions of the desired turbidity. The instrument output was linear between 0.1 and 300 FTU.

Procedure

Calibration. Known amounts of the thiosulfate standard solution (B) were placed in 50-ml volumetric flasks (the concentration of thiosulfate after dilution to the final volume should be between 2.5 and 60 mg l^{-1}). The solution was diluted to about 40 ml with water, and 5.00 ml of precipitant solution A and 1.00 ml of the 0.1 mol l^{-1} acetate buffer (pH 4.62) were added. After dilution to 50 ml with water, the suspension was shaken for a few seconds and kept for 5 h at 20—22°C. Then it was subjected for 3 min to alternating ultrasonic treatment at 20 kHz (i.e., treatment in 1-s spurts at 1-s intervals). The turbidity was immediately measured. The turbidity values as a function of the thiosulfate concentration gave a linear calibration (see below).

Determination. A known volume (42.5 ml) of the thiosulfate sample containing 3—70 mg l^{-1} thiosulfate at pH 3—10) was treated as above. The thiosulfate content was evaluated from the linear regression parameters of the calibration plot.

Results and discussion

Ten determinations were done for each of five concentrations of thiosulfate studied (Table 1). The linear regression equation for the mean turbidity values (in FTU) vs. the thiosulfate concentration (in mg l^{-1}) was $Y = (4.89 \pm 0.03)X - (11 \pm 1)$. The reproducibility and accuracy of the method were evaluated as generally suggested for quantitative methods [16]. Reproducibility is expressed by percent standard deviation (RSD = $100 \times D[C']/\bar{C}'$, where $\bar{C}'$ is the mean value of the concentrations found, and $D[C']$ is the estimated standard deviation). Accuracy is expressed by the relative error calculated in the usual manner. All the values are reported in Table 1.

Optimization of the procedure. The procedure reported above was developed after careful examination of the influence of experimental conditions on the determination. Reliable results are given by nephelometric methods only if the suspended particles are of uniform and reproducible dimensions. It was shown that the pH of the suspension during the turbidity measurement did not affect the final results between pH 4.5 and 6.5; this range, given that acetate buffer is added to the sample, corresponds to pH 3—10 for the initial sample. The amount of polyvinylpyrrolidone (used as suspension stabilizer) affected the final values; when its concentration was lower than that recommended, lower turbidity values were obtained for the same concentration of thiosulfate. Without ultrasonic treatment, lower values are again

TABLE 1

The nephelometric determination of thiosulfate in aqueous samples[a]

Thiosulfate taken (mg l^{-1})	Turbidity (FTU)	Thiosulfate found (mg l^{-1})	RSD (%)	Relative error (%)
2.94	6.8 ± 0.6	3.2 ± 0.1	3.1	8.8
11.8	47.8 ± 1.0	11.7 ± 0.3	2.6	—0.8
29.4	130 ± 4	28.7 ± 0.8	2.8	—2.4
58.8	277 ± 5	59.0 ± 1.1	1.9	0.3
70.6	334 ± 8	70.7 ± 1.7	2.4	0.1
			Mean 2.6	2.5

[a]The uncertainty of the measured values is expressed as the estimated standard deviation for 10 separate determinations.

obtained, and the concentration range of thiosulfate determinable was reduced. The temperature of precipitation greatly affected the results; room temperature was best. At 50° C turbidities were less and at 0° C precipitation was too slow.

Interferences. Interferences with the thiosulfate determination by various ions were studied. The results are reported in Table 2. Among the anions considered, iodide, thiocyanate and sulfide are the main interfering species. The interference of sulfide was eliminated simply by treating the sample with a zinc carbonate suspension, stirring for about 15 min, filtering and washing the precipitate with water, as suggested by Karchmer and Dunahoe [17] (suspensions were obtained by mixing equimolar amounts of zinc acetate and sodium carbonate solutions). Elimination of the iodide and thiocyanate interferences, however, was not possible. Precipitation of these species by silver or thallium(I) acetate was unsatisfactory because of interactions of thiosulfate with both silver and thallium(I). Lead was also tested, but lead itself interfered with the thiosulfate determination. Although iodides and thiocyanates are not often present in large amounts in aqueous samples, their presence may prove a limitation of the proposed method. Semiquantitative tests with bromide showed that its interference was intermediate between those of chloride and iodide, in accordance with earlier conductometric data [14].

As regards interferences by metal ions, it was observed that the simultaneous presence of various cations in the sample could interfere with the thiosulfate determination even when each cation was present at a concen-

TABLE 2

Interference of various ions with the nephelometric determination of thiosulfate in aqueous samples[a]

Ion	C (mg l^{-1})	C' (mg l^{-1})	Ion	C (mg l^{-1})	C' (mg l^{-1})
Sodium	230	340	Sulfide	—	6
Ammonium	—	12	Nitrate	29	35
Magnesium	120	235	Nitrite	12	18
Magnesium[b]	470	590	Sulfate	590	—
Calcium	350	470	Sulfite	200	—
Calcium[b]	470	590	Sulfite[c]	200	—
Zinc	6	12	Acetate	580	880
Cadmium	—	6	Salicylate	18	23
Chloride	295	—	Tartrate	59	76
Iodide	—	0.6	Citrate	—	6
Thiocyanate	—	6			

[a] C: highest ion concentration at which no interference was observed. C': ion concentration at which the beginning of interference was observed. Thiosulfate concentration in the sample was 60 mg l^{-1}, unless specified otherwise. Cations were added as their acetate salts and anions as their sodium salts. [b] Thiosulfate concentration, 3 mg l^{-1}. [c] Thiosulfate concentration, 30 mg l^{-1}.

tration lower than C' (Table 2). All the interfering cations could be eliminated simultaneously by batch treatment of a portion of the sample with an excess of a cation-exchange resin, followed by filtration. For example, when an aqueous sample of sodium thiosulfate (60 mg l^{-1} thiosulfate) containing 70 mg l^{-1} Ca^{2+}, 70 mg l^{-1} Mg^{2+}, 6 mg l^{-1} NH_4^+, 6 mg l^{-1} Zn^{2+} and 6 mg l^{-1} Cd^{2+}, was stirred for 30 min with three times the stoichiometric amount of Bio-Rad AG-50W-X8 cation-exchange resin, any interference on the thiosulfate determination was eliminated.

Conclusions

The proposed method has a linear range of 3—70 mg l^{-1} thiosulfate (Table 1) which is not very different from a useful range of the iodimetric titrations which are generally considered as the most widely applicable method for thiosulfate. The lower limit of determination is about 10 mg l^{-1} thiosulfate for iodimetry with usual end-point indication [5]; the range is 50—100 mg l^{-1} thiosulfate for coulometric iodimetry [2]. Although no data directly referring to thiosulfate determinations were given, an iodimetric/amperometric method [3] seems more sensitive than the present one.

The proposed nephelometric method is simple and fairly rapid, and interfering species are easily eliminated, except for iodide and thiocyanate. Sulfite does not interfere whereas it interferes quantitatively in the iodimetric determination [5].

REFERENCES

1 I. M. Kolthoff and P. J. Elving (Eds.), Treatise on Analytical Chemistry, Part II, Vol. 7, Interscience, New York, 1961, p. 84.
2 M. A. V. Devanathan, Q. Fernando and P. Peries, Anal. Chim. Acta, 16 (1957) 292.
3 G. Knowles and G. F. Lowden, Analyst (London), 78 (1953) 159.
4 A. K. Zhdanov, G. Akhmedov and T. V. Luk'yanova, Uzb. Khim. Zh., 13 (1969) 12.
5 N. W. Hanson (Ed.), Official, Standardised and Recommended Methods of Analysis, The Society for Analytical Chemistry, London, 1973.
6 B. Sorbo, Biochim. Biophys. Acta, 23 (1956) 412.
7 O. A. Efremenko, O. B. Esenina and N. A. Ovesnova, Izv. Vyssh. Uchebn. Zaved., Khim. Khim. Teknol., 22 (1979) 927.
8 Yu. G. Eremin and K. S. Kiseleva, Zh. Anal. Khim., 24 (1969) 1201.
9 T. Koh, Y. Miura and M. Katoh, Talanta, 24 (1977) 759.
10 J. B. Risk and J. D. H. Strickland, Anal. Chem., 29 (1957) 434.
11 E. Michalski and A. Wtorkowska, Chem. Anal. (Warsaw), 7 (1962) 783.
12 D. P. Nicolelis and T. P. Hadijoannou, Mikrochim. Acta, 1 (1957) 125.
13 I. Hayashida, H. Yoshida, M. Taga and S. Hikime, Bunseki Kagaku, 29 (1980) 304.
14 I. Hayashida, M. Taga and H. Yoshida, Talanta, 28 (1981) 340.
15 R. Aruga, C. Baiocchi, E. Campi, M. C. Gennaro and E. Mentasti, Ann. Chim. (Rome), 74 (1984) 87.
16 Standard Methods for the Examination of Water and Wastewater, American Public Health Association, Washington, 1975.
17 J. H. Karchmer and J. W. Dunahoe, Anal. Chem., 20 (1948) 915.

Analytica Chimica Acta, 182 (1986) 213—218
Elsevier Science Publishers B.V., Amsterdam — Printed in The Netherlands

Short Communication

ANALYSIS OF BINARY AND TERNARY MIXTURES OF COBALT, NICKEL AND COPPER BY DIFFERENTIAL KINETIC METHODS BASED ON LIGAND SUBSTITUTION REACTIONS

L. BALLESTEROS and D. PÉREZ-BENDITO*

Department of Analytical Chemistry, Faculty of Sciences, University of Córdoba, Córdoba (Spain)

(Received 14th June 1985)

Summary. The methods are based on displacement of pyridoxal thiosemicarbazone from its complexes with cobalt(II), nickel and copper(II) with DCTA. The reactions are monitored spectrophotometrically at 425 nm. The Ni/Cu and Co/Ni/Cu mixtures are analyzed by the single-point method and the Co/Ni and Co/Cu mixtures by the logarithmic extrapolation method. In all determinations the relative standard deviation is <3%, at the μg ml^{-1} level.

The number of applications of differential rate methods in inorganic analysis is small, probably because of the difficulty of finding reactions of closely related species occurring at sufficiently different rates [1]. The present authors [2—4] have recently described methods for the simultaneous determination of various binary mixtures of iron, cobalt, nickel and copper by differential kinetic methods based on direct complex formation reactions with pyridoxal thiosemicarbazone (PTC). Here, the study is extended to ligand substitution reactions between PTC and 1,2-diaminocyclohexane-*N,N,N',N'*-tetraacetate (DCTA), i.e., M—PTC + DCTA → M—DCTA + PTC. This reaction is particularly useful, as it allows copper/nickel/cobalt mixtures to be analyzed by a differential kinetic procedure. Only one method of kinetic analysis of such a mixture has been published previously [5].

Experimental

Reagents. All reagents and *N,N*-dimethylformamide were of analytical reagent grade. Pyridoxal thiosemicarbazone was synthesized by condensation of pyridoxal hydrochloride with thiosemicarbazide [6]. A 0.1% (w/v) solution of the reagent in dimethylformamide was used. Solutions of cobalt(II) (0.952 mg ml^{-1}) and nickel (1.848 mg ml^{-1}) were standardized gravimetrically, and that of copper(II) (0.925 mg ml^{-1}), iodimetrically. The sodium acetate/acetic acid buffer (1.70 M) was pH 3.85.

Apparatus. A Perkin-Elmer 575 u.v.-visible spectrophotometer was used with 1.0-cm glass cells; an electronic thermostat was added for the kinetic

0003-2670/86/$03.50

measurements. A Radiometer PHM-62 pH meter with a combined glass/calomel electrode was also used.

Procedure. To a 10-ml volumetric flask containing $\leqslant 30$ μg of the metal ions in a mixture, add 3 ml of 1 M potassium nitrate, 2 ml of the acetate buffer, 0.7 ml of the PTC solution and an appropriate volume of distilled water, so that when the DCTA solution is finally added, the total volume is 10.0 ml. Shake the mixture and warm in a water-bath at 25.0 ± 0.1°C for 5 min. Add 0.25 ml of 0.02 M DCTA solution (0.1 M DCTA for the Co/Cu mixture) with great care (to prevent any prior mixing of the solutions). Shake again (t = 0) and transfer one portion to a 1.0-cm cell thermostatted at 25.0 ± 0.1°C. Record the change of absorbance at 425 nm every 15 s between 1 and 2 min. Also, measure the absorbance after 5 min for the Ni/Cu and Co/Ni/Cu mixtures. Allow samples containing cobalt to stand until complete reaction. Treat the data as described below.

Results of kinetic study

At pH 3.95 DCTA does not react with the Co/PTC complex whereas PTC is displaced from its complexes with nickel and copper(II). The rate of the ligand substitution reaction is monitored spectrophotometrically by recording the decrease in absorbance at 425 nm. Figure 1 shows that the nickel complex is completely substituted within 15 min and the copper complex within 60 min.

When the reagent concentrations are significantly greater than that of the PTC complexes, the ligand substitution reactions involved are pseudo-first order in the PTC complexes. When the substitution by DCTA is complete, the absorbance is zero (A_∞ = 0). Thus the integrated rate equation, in terms

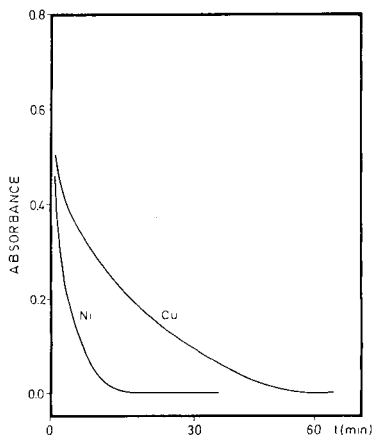

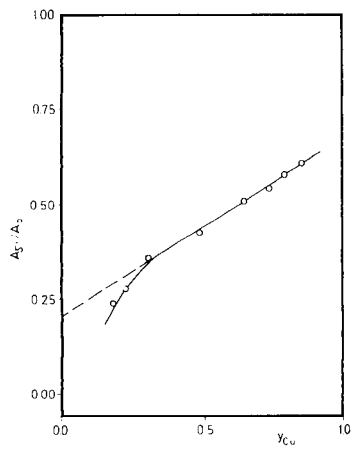

Fig. 1. Absorbance/time curves for PTC displacement from its nickel and copper complexes by DCTA.

Fig. 2. Calibration graph obtained by the single-point method for the simultaneous determination of nickel and copper.

of absorbance, can be written as $\log A_t = \log A_0 - k'_M t/2.303$, where k'_M is the conditional rate constant when metal M is studied, A_0 is the initial absorbance, and A_t is the absorbance at time t. By plotting $\log A_t$ vs. time a straight line is obtained; its slope allows the determination of the conditional rate constant of the ligand substitution reaction. For 11 determinations, the average values found were $k'_{Ni} = 0.404 \pm 0.007$ min^{-1} and $k'_{Cu} = 0.094 \pm 0.002$ min^{-1}.

Effect of reaction variables on the rates of ligand displacement. The conditional rate constant is not appreciably affected by the ionic strength, which was fixed at 0.3 M with potassium nitrate. It increases with increasing dimethylformamide concentration; a 7% concentration was chosen for further studies.

The variation of the conditional rate constant with temperature was studied between 20 and 40°C. The rate constant increased with temperature; 25°C was used in further work. From the data obtained, the activation energies found were 13.2 kcal mol^{-1} for the nickel complex and 10.1 kcal mol^{-1} for the copper complex.

The effect of the PTC concentration on the conditional rate constant was studied in the range 2.92×10^{-4}—5.00×10^{-4} M. The rate constant was independent of the PTC concentration in this range for the copper complex, but it decreased for the nickel complex at $> 3.8 \times 10^{-4}$ M PTC. Therefore, 2.92×10^{-4} M PTC (0.7 ml of 0.1% solution) was used in further studies.

The influence of the acetate concentration was studied in the range 1.2×10^{-2}—7.2×10^{-2} M, and 4.8×10^{-2} M (2 ml of pH 3.85 buffer) was chosen for further work. The partial reaction order with respect to acetate concentration over this range was 1/3 for both complexes. The pH of the acetate buffer was adjusted in the range 3.6—4.5, by addition of sodium hydroxide. The rate decreased as the pH increased.

Increase of the DCTA concentration over the range 3.0×10^{-4}—8.0×10^{-4} M did not affect the conditional rate constant for the nickel complex, whereas that for the copper complex increased. A DCTA concentration of 5×10^{-4} M (0.25 ml of 0.02 M DCTA) is recommended. The partial reaction order for the copper complex was 0.5.

From the kinetic data obtained, the following rate equations can be suggested for the ligand substitution reactions between the nickel/PTC and copper/PTC complexes and DCTA in an acetate medium, under the recommended analytical conditions:

$$v_{Ni} = k_{Ni}\,[\text{Ni—PTC}]\,[\text{acetate}]^{1/3}\,[\text{H}^+]^{1/3}$$

$$v_{Cu} = k_{Cu}\,[\text{Cu—PTC}]\,[\text{acetate}]^{1/3}\,[\text{H}^+]^{-1/3}\,[\text{DCTA}]^{1/2}$$

Analysis of binary and ternary mixtures

The nickel and copper substitution reactions are pseudo-first order in metal complex. Under the recommended experimental conditions, $k'_{Ni}/k'_{Cu} = 4.4$. This ratio is large enough to allow the analysis of nickel/copper mixtures

by the single-point method but not by the logarithmic extrapolation method. The cobalt/PTC complex is not affected by DCTA, so that binary mixtures of cobalt with copper or nickel, as well as mixtures of all three metals can be analyzed.

Single-point method for nickel/copper mixtures. The absorbance at time t is given by

$$A_t = \epsilon_{Ni}\,[Ni^{2+}]_0 \exp(-k'_{Ni}t) + \epsilon_{Cu}\,[Cu^{2+}]_0 \exp(-k'_{Cu}t)$$

If this equation is divided by the initial absorbance $A_0 = \epsilon_{Ni}[Ni^{2+}]_0 + \epsilon_{Cu}[Cu^{2+}]_0$, the following expression is obtained:

$$A_t/A_0 = [\exp(-k'_{Cu}t) - \exp(-k'_{Ni}t)]\ Y_{Cu} + \exp(-k'_{Ni}t)$$

where Y_{Cu} is the absorbance fraction of copper(II) which is defined by $Y_{Cu} = \epsilon_{Cu}[Cu^{2+}]_0/(\epsilon_{Cu}[Cu^{2+}]_0 + \epsilon_{Ni}[Ni^{2+}]_0)$ so that $Y_{Cu} + Y_{Ni} = 1$. The $\epsilon_{Cu} = 1.58 \times 10^4$ l mol^{-1} cm^{-1} and $\epsilon_{Ni} = 1.19 \times 10^4$ l mol^{-1} cm^{-1} are calculated by kinetic measurements. By using the Lee and Kolthoff equation [7], the optimum time is 5 min. Figure 2 shows the calibration curve corresponding to this optimum time. When $Y_{Cu} \leqslant 1/3$ (or $Y_{Ni} \geqslant 2/3$) the calibration graph is linear; a typical equation is $A_5/A_0 = 0.427\ Y_{Cu} + 0.207$ ($r^2 = 0.9973$, 9 points). The deviation from linearity was also found previously [3] when this mixture was analyzed by direct complex-formation reactions. However, the non-linear range for the present substitution reactions is shorter than that for the direct complex-formation reactions.

Logarithmic extrapolation method for cobalt binary mixtures. The cobalt/PTC complex does not react with DCTA, so it is a simple matter to resolve mixtures of cobalt with nickel or copper. This can be considered as a differential kinetic method for which the conditional rate constant for the cobalt complex is zero. Accordingly, the absorbance of each sample at time t is

$$A_t = \epsilon_M\,[M^{2+}]_0 \exp(-k'_M t) + \epsilon_{Co}\,[Co^{2+}]_0$$

where M denotes Cu^{2+} or Ni^{2+}. As $\epsilon_{Co}[Co^{2+}]_0 = A_\infty$, $\log(A_t - A_\infty) = \log \epsilon_M[M^{2+}]_0 - k'_M t/2.303$. Thus, logarithmic extrapolation to $t = 0$ allows the calculation of the initial concentration of nickel or copper. The initial concentration of cobalt is obtained from the final absorbance.

Analysis of cobalt/nickel/copper mixtures by the single-point method. For the ternary mixture, the absorbance at time t is given by

$$A_t = \epsilon_{Ni}\,[Ni^{2+}]_0 \exp(-k'_{Ni}t) + \epsilon_{Cu}\,[Cu^{2+}]_0 \exp(-k'_{Cu}t) + \epsilon_{Co}\,[Co^{2+}]_0$$

or

$$A_t - A_\infty = \epsilon_{Ni}\,[Ni^{2+}]_0 \exp(-k'_{Ni}t) + \epsilon_{Cu}\,[Cu^{2+}]_0 \exp(-k'_{Cu}t)$$

Dividing this expression by $A_0 - A_\infty = \epsilon_{Ni}\,[Ni^{2+}]_0 + \epsilon_{Cu}\,[Cu^{2+}]_0$ gives

$$(A_t - A_\infty)/(A_0 - A_\infty) = [\exp(-k'_{Cu}t) - \exp(-k'_{Ni}t)]\,Y_{Cu} + \exp(-k'_{Ni}t)$$

From the calibration curve for the nickel/copper mixture (Fig. 2) and the value of $(A_t - A_\infty)/(A_0 - A_\infty)$, the absorbance fraction of copper, Y_{Cu}, and

hence the initial concentrations of nickel and copper can easily be calculated. The initial concentration of cobalt is obtained from the final absorbance.

Analysis of some synthetic mixtures. The results for the kinetic resolution of copper/nickel mixtures, with and without cobalt, are given in Tables 1

TABLE 1

Simultaneous determination of cobalt, nickel and copper in synthetic mixtures

Added (μg ml^{-1})			Found (μg ml^{-1})		
Co^{2+}	Ni^{2+}	Cu^{2+}	Co^{2+}	Ni^{2+}	Cu^{2+}
0.48	0.55	1.48	0.51	0.53	1.42
0.48	1.11	1.48	0.50	1.08	1.42
0.48	1.11	0.74	0.47	1.09	0.79
0.48	2.22	0.74	0.48	2.28	0.73
0.95	0.55	2.22	1.04	0.51	2.20
0.95	0.55	1.48	1.03	0.53	1.49
0.95	0.55	0.74	0.94	0.61	0.71
0.95	1.11	0.74	0.93	1.17	0.70
1.90	0.55	1.48	1.99	0.58	1.34
1.90	0.55	0.74	1.90	0.56	0.81

TABLE 2

Simultaneous determination of nickel and copper in synthetic mixtures

Added (μg ml^{-1})		Found (μg ml^{-1})		Relative error (%)	
Ni^{2+}	Cu^{2+}	Ni^{2+}	Cu^{2+}	Ni^{2+}	Cu^{2+}
0.55	2.96	0.58	2.94	4.9	−0.5
0.55	2.22	0.53	2.24	−3.9	0.9
0.55	1.48	0.54	1.49	−3.1	0.9
1.11	2.22	1.16	2.18	4.6	−1.6
1.11	1.48	1.11	1.48	0.2	−0.1
1.11	0.74	1.12	0.73	0.8	−0.8
2.22	0.74	2.18	0.77	−1.6	2.6

TABLE 3

Relative standard deviations (n = 11) and concentration ratio ranges for the mixtures

Mixture M_1/M_2	RSD (%)			Applicable conc. ratio range (M_1:M_2)
	Co^{2+}	Ni^{2+}	Cu^{2+}	
Ni^{2+}/Cu^{2+}	—	0.7	0.7	3:1—1:6
Co^{2+}/Ni^{2+}	0.7	0.7	—	7:1—1:7
Co^{2+}/Cu^{2+}	0.5	—	0.7	4:1—1:6
$Co^{2+}/Ni^{2+}/Cu^{2+}$	0.6	1.0	1.3	—

and 2, respectively. Mixtures of cobalt (0.5—3.8 μg ml^{-1}) with copper (0.7—3.0 μg ml^{-1}) or nickel (0.5—3.3 μg ml^{-1}) so that the total metal concentration was $\geq$4.4 μg ml^{-1} all gave relative errors of $\leq$5%. The relative standard deviations and the concentration ratio ranges which are suitable for each mixture are summarized in Table 3.

REFERENCES

1 D. Pérez-Bendito, Analyst (London), 109 (1984) 891.
2 L. Ballesteros and D. Pérez-Bendito, Analyst (London), 108 (1983) 443.
3 L. Ballesteros and D. Pérez-Bendito, Mikrochim. Acta, in press.
4 L. Ballesteros and D. Pérez-Bendito, Quím. Anal., 4 (1985) 272.
5 S. Ito, K. Haraguchi, K. Nakagawa and K. Yamada, Bunseki Kagaku, 26 (1977) 554.
6 D. Pérez-Bendito and M. Valcárcel, Afinidad, 37 (1980) 123.
7 T. S. Lee and I. M. Kolthoff, Ann. N.Y. Acad. Sci., 53 (1951) 1093.

Analytica Chimica Acta, 182 (1986) 219—223
Elsevier Science Publishers B.V., Amsterdam — Printed in The Netherlands

Short Communication

THE SPECTROPHOTOMETRIC DETERMINATION OF COBALT AFTER EXTRACTION OF TETRAMETHYLENE-BIS(TRIPHENYLPHOSPHONIUM) TETRATHIOCYANATOCOBALTATE(II) WITH MICROCRYSTALLINE BENZOPHENONE

D. THORBURN BURNS* and N. TUNGKANANURUK

Department of Analytical Chemistry, The Queen's University, Belfast BT9 5AG (Northern Ireland)

(Received 18th October 1985)

Summary. Cobalt (0—130 μg) is determined spectrophotometrically at 625 nm after its adsorptive extraction as tetramethylene-bis(triphenylphosphonium) tetrathiocyanatocobaltate(II) on microcrystalline benzophenone at pH 6.5 after dissolution of the solid phase in acetylacetone. The system is applied to the determination of cobalt (0.2—10%) in high-speed tool steels without prior separation of iron.

A variety of onium cations has been proposed for the extraction of complex anions of transition metals [1]. So far no applications have been reported for the tetramethylene-bis(triphenylphosphonium) cation which, being bifunctional, can be regarded as the ion-pairing equivalent for anions to a chelating ligand for cations [2]. Among the anions formed from transition metals, tetrathiocyanatocobaltate(II) has been widely studied in conventional liquid/liquid extraction [3] but not in solid/liquid systems [4], which have been applied mainly to extract cobalt(II) chelates [5—10]. Only two ion-pair systems, the tetraphenylborate ion-pairs with [4′-(4-methoxyphenyl)-2,2′:6′,6″-terpyridine]cobaltate(II) [11] and [3-(4-phenyl-2-pyridyl)-5,6-diphenyl-1,2,4-triazine]cobaltate(II) [12]. All systems were extracted into molten or microcrystalline naphthalene.

The present communication reports on the novel absorptive extraction of tetramethylene-bis(triphenylphosphonium) tetrathiocyanatocobaltate(II) with microcrystalline benzophenone. The solid benzophenone may be dissolved in acetylacetone and the determinations completed spectrophotometrically at 625 nm. The system is applied to the determination of cobalt in tool steels.

Experimental

Apparatus. Pye-Unicam SP8-400 and SP6-550 u.v.-visible spectrophotometers were used for recording absorption spectra and for routine measurements, respectively, with matched quartz 1-cm cells.

0003-2670/86/$03.50

Reagents and solutions. Tetramethylene-bis(triphenylphosphonium) bromide [1,4-bis(triphenylphosphonium)butane dibromide; Lancaster Synthesis; 98+%] was used as supplied. Elemental analysis gave 64.6% C, 5.2% H (theor. for $C_{40}H_{38}P_2Br_2$, 64.9% C, 5.2% H). A 0.003 M stock solution was made by dissolving 1.1107 g of the reagent in 500 ml of distilled water. This solution was stored in a dark brown glass bottle. A stock 1000 μg ml^{-1} cobalt(II) solution was prepared by dissolving 2.630 g of anhydrous cobalt(II) sulphate (analytical grade dried to constant weight at 400°C) in 1 l of distilled water. More dilute standard solutions were prepared as required. For the pH 6.5 buffer, 10.89 g of potassium dihydrogenphosphate and 5.65 g of disodium hydrogenphosphate were dissolved in 1 l of distilled water. The benzophenone solution was 20% (w/v) in acetone. All other reagents were of analytical grade. Twice-distilled water was used throughout.

General procedure. Place an aliquot containing up to 130 μg of cobalt(II) in an Erlenmeyer flask with ground-glass stopper. Add 3.0 ml of 5 M ammonium thiocyanate, 2 ml of pH 6.5 buffer and 2.0 ml of the 0.003 M reagent solution, and dilute to 10—15 ml with water. Swirl to mix. Add 2.0 ml of 20% benzophenone solution, stopper the flask and shake vigorously for 30 s. Filter the blue-coloured separated solid through a filter paper (Whatman No. 1) or a sintered glass filter (No. 2). Wash with water, drain or suck dry, dissolve the solid in acetylacetone and make up to volume with that solvent in a 10-ml volumetric flask. Dry the solution by addition of 1—2 g of anhydrous sodium sulphate. Measure the absorbance at 625 nm against a reagent blank prepared in the same way.

Procedure for steel samples. For steel samples containing 2—10% or 0.2—1% cobalt, dissolve accurately weighed 0.05- or 0.5-g samples, respectively, in a mixture of 3 or 30 ml of concentrated hydrochloric acid and 1 or 10 ml of concentrated nitric acid, respectively, in 250-ml conical flasks. Warm to aid dissolution. When dissolved, boil to near dryness, cool, add 1 or 10 ml of concentrated hydrochloric acid, and evaporate to near dryness. Cool, add 50 ml of distilled water and warm to dissolve the solid. Cool, and filter through a Whatman No. 1 paper into a 100-ml volumetric flask. Wash the residue (silica, tungstic acid) with a small volume of hot 2% (v/v) hydrochloric acid followed by distilled water and make up to volume with distilled water. Dilute (1 + 4) with distilled water. Transfer 5- or 10-ml aliquots containing 10—60 μg of cobalt to a ground-glass-stoppered Erlenmeyer flask. Add 5 ml of saturated ammonium-D(+)-tartrate solution (for a steel containing copper, add 2 ml of 10% (w/v) sodium thiosulphate solution after the tartrate) and proceed as in the general procedure.

Prepare a calibration graph for the range 0—130 μg of cobalt after adding 10 ml of iron(III) nitrate solution, containing about the same amount of iron as in the steel sample solutions to the standard cobalt solution.

Examination of main experimental variables

Naphthalene, diphenyl, benzophenone and 1,4-dichlorobenzene were each examined for their adsorptive/extraction properties using the microcrystalline

solid formation procedure from acetone solution. Benzophenone showed the highest recovery (i.e., absorbance) of the solids examined when dissolved, and was adopted for use.

A variety of solvents with a range of functional group types, including alcohols, ketones, esters, ethers and chlorinated and aromatic hydrocarbons, was examined to dissolve the complex along with the benzophenone. The ion-pair was soluble in acetylacetone, acetonitrile, propylene carbonate, diethyl ketone, methyl ethyl ketone, dichloromethane, dimethylformamide and dimethylsulphoxide but was not soluble in the other solvents examined. The solutions in dimethylformamide and dimethylsulphoxide were unstable. Acetylacetone was chosen for further study because the ion-pair gave the greatest molar absorptivity (at 625 nm) in this solvent.

The effect of pH was examined for 80 μg of cobalt(II) by addition of 1 M hydrochloric acid or 1 M ammonia solution prior to extraction. The absorbances were measured as before and were almost independent of pH in the range 2.0—8.0, decreasing rapidly outside these limits. In subsequent work the aqueous phase was buffered at pH 6.5.

The effects of varying the amounts of ammonium thiocyanate and tetramethylene-bis(triphenylphosphonium)bromide were examined for 80 μg of cobalt(II). For both reagents, the absorbance of the dissolved extracts increased up to a constant value with increase in volume of reagent. Convenient amounts in the plateau regions are specified in the general procedure. The extent of extraction was found to be unaffected by ionic strength (provided that the pH remained at 6.5), by phase volume ratios up to 10:1 water/benzophenone in acetone, or by time of shaking. Dissolved extracts were stable for up to 3 days in direct daylight but for at least 10 days in diffuse daylight.

The composition of the complex was established spectrophotometrically by Job's method [13] and by the mole ratio method [14, 15] to be $[(C_6H_5)_3P(CH_2)_4P(C_6H_5)_3][Co(NCS)_4]$. Elemental analysis of the precipitate formed from aqueous solution was consistent with that composition (required 60.6% C, 4.4% H, 6.4% N; found 60.5% C, 4.5% H, 6.3% N).

Results and discussion

A linear calibration graph was obtained over the range 0—130 μg of cobalt in 10 ml of final solution in acetylacetone (molar absorptivity 1.5×10^3 l mol^{-1} cm^{-1}). For the determination of 40 μg of cobalt the relative standard deviation was 0.46% (10 results).

The possible interferences of various anions and cations, chosen on the basis of previous studies of onium extraction of tetrathiocyanatocobaltate(II) for the analysis of steels [16] were checked spectrophotometrically for 40 μg of cobalt. Slightly decreased extraction occurred at high adverse ratios of iron(III) to cobalt (−2.8% for 40 mg of iron, −1.9% for 4 mg of iron) when 3.0 ml of saturated ammonium-D(+)-tartrate solution was used to mask iron(III). This effect may be compensated by addition of an equivalent amount

of iron to the standards and blank, for construction of a low concentration range calibration graph. The results of the interference and masking study are summarised in Table 1. The only ions which interfered significantly and are of interest in the analysis of steels were iron(III) (≥500:1), niobium and tin (≥300:1) and copper (≥200:1). The interferences of iron(III), niobium and tin can be masked by addition of ammonium tartrate and that of copper by sodium thiosulphate. Under the conditions of the procedure, the following cations in the weight ratio 500:1 were without significant effect: Na^+, K^+, NH_4^+, Mg^{2+}, Ca^{2+}, Cd^{2+}, Ni^{2+}, Mn^{2+}, Al^{3+} and Zr(IV). Other cations which

TABLE 1

Effect of various ions on the determination of 40 μg of cobalt

Ion[a]	Ratio to Co(II) (w/w)	Error in absorbance (%)[f]	Ion[a]	Ratio to Co(II) (w/w)	Error in absorbance (%)[f]
Pd^{2+}	100	0	Fe^{3+}	300	−79
Hg^{2+}	500[b]	−21		500[c,d]	−84
	100	0	Cu^{2+}	200[e]	−17
Bi^{3+}	250[c]	+13		100	0
Cr^{3+}	500[c]	+10	VO_3^-	2500	−16
Zn^{2+}	500	−82		500	−7
U(IV)	500[c]	−24		250	0
Sn(IV)	300[c]	+16	WO_4^{2-}	2500	−18
Nb(V)	300[c]	−7		500	0
Fe^{2+}	300[b]	−41	CN^-	25	−100
			EDTA	25	−100

[a]Cations added as chloride, sulphate or nitrate, anions added as sodium salts. [b]When 1 drop of hydrazine hydrate was added, there was no error in absorbance. [c]No error with 1.5 ml of 30% (w/v) NH_4F added. [d]No error with 3 ml of saturated ammonium tartrated added. [e]No error with 2 ml of 10% (w/v) $Na_2S_2O_3$ added. [f]Ions causing less than a 5% change in absorbance.

TABLE 2

Analysis of high-speed tool steels

BCS Steel	Cobalt content (%, w/w)		
	Certified value	Certified range	Found[a]
220/2	0.32	0.31—0.33	0.330 ± 0.015
241/2	5.70	5.66—5.73	5.73 ± 0.04
481	0.21	0.19—0.22	0.220 ± 0.002
482	0.24	0.21—0.27	0.235 ± 0.013
483	1.94	1.90—1.99	1.955 ± 0.013
484	10.20	10.10—10.39	10.25 ± 0.08
485	5.06	5.00—5.11	5.03 ± 0.05

[a]Mean ± 95% confidence limits for 4 replicates.

interfered were Cr^{3+}, U(IV), Hg^{2+} and Zn^{2+} at 500:1 ratios and Bi^{3+} and Fe^{2+} at 300:1. The effects of iron(II) and mercury(II) were overcome by the addition of hydrazine hydrate and those of Bi(III) and Cr(III) by ammonium fluoride. Among ions which did not interfere were fluoride, chloride, bromide, iodide, hydrogenphosphate, acetate, perchlorate, sulphate, thiosulphate, molybdate, tartrate and ascorbate. Cyanide and EDTA should be absent.

The results for the determination of cobalt in seven British Chemical Standard steel samples (Table 2) are in excellent agreement with the certificate values. The method is rapid and more precise than liquid/liquid extractions for the same complex anion.

REFERENCES

1 A. J. Bowd, D. T. Burns and A. G. Fogg, Talanta, 16 (1969) 719.
2 D. T. Burns, Anal. Proc., 19 (1982) 355.
3 D. T. Burns and S. Kheawpintong, Anal. Chim. Acta, 162 (1984) 439 and references therein.
4 D. T. Burns, J. M. Jones and N. Tungkananuruk, Trends Anal. Chem., 4(2) (1985) VI.
5 M. Gautam and B. K. Puri, Mikrochim. Acta, I (1979) 515.
6 M. Gautam, R. K. Bansal and B. K. Puri, Bull. Chem. Soc. Jpn., 54 (1981) 3178.
7 M. Satake, B. K. Puri, J. C. Yuh and L. F. Chang, Mem. Fac. Eng. Fukui Univ., 30 (1982) 63.
8 B. K. Puri, C. L. Sethi and A. Kumar, J. Chin. Chem. Soc. (Taipei), 28 (1982) 173.
9 A. Wasey, R. K. Bansal, M. Satake and B. K. Puri, Bunseki Kagaku, 32 (1983) E211.
10 C. L. Sethi, A. Kumar, B. K. Puri and M. Satake, Analyst (London), 108 (1983) 528.
11 T. Nagahiro, M. Satake, J. L. Lin and B. K. Puri, Analyst (London), 109 (1984) 163.
12 J. L. Lin, L. F. Chang, M. Katyal and M. Satake, Z. Anal. Chem., 319 (1984) 308.
13 P. Job, Ann. Chim. (Paris), 9 (1928) 113.
14 J. H. Yoe and A. L. Jones, Ind. Eng. Chem. Anal. Ed., 16 (1944) 111.
15 K. Momoki, J. Sekino, H. Sato and N. Yamaguchi, Anal. Chem., 41 (1969) 1286.
16 D. T. Burns, P. Hanprasopwattana and B. P. Murphy, Anal. Chim. Acta, 134 (1982) 397 and references therein.

Analytica Chimica Acta, 182 (1986) 225—229
Elsevier Science Publishers B.V., Amsterdam — Printed in The Netherlands

Short Communication

ATOMIC ABSORPTION SPECTROMETRIC STUDIES OF THE ATOMIZATION OF BORON FROM A CARBON ROD ATOMIZER

NEELAM GOYAL, A. R. DHOBALE, B. M. PATEL and M. D. SASTRY*

Radiochemistry Division, Bhabha Atomic Research Centre, Trombay, Bombay-400085 (India)

(Received 30th May 1985)

Summary. Boron ($\leqslant 20$ μg ml^{-1}) in aqueous solutions gives no absorbance but addition of ascorbic acid, especially with titanium greatly enhances the signal, leading to a detection limit of 0.2 μg ml^{-1} boron. The presence of uranium ($\leqslant 10$ mg ml^{-1}) only slightly decreases the boron signal.

Atomic absorption spectrometry (a.a.s.) with electrothermal atomization is quite useful for the determination of traces of metals in nuclear reactor fuels such as uranium(IV) oxide and mixed uranium(IV)/plutonium(IV) oxide [1—6]. However, a few elements such as boron and gadolinium, which are crucial for the quality assurance of nuclear fuels, pose problems in determinations below their specified upper limits. This is presumably due to the inefficient atom formation of these elements on account of factors such as carbide formation, the large dissociation energies of their oxides and possible loss as volatile products [7]. Therefore, there is a need to understand the atomization mechanism for these elements which may help in optimizing conditions of high temperature reactions leading to larger atom densities in the carbon rod atomizer (CRA). Strong interelement effects on the atom density of boron particularly by alkaline earth elements have been reported [8—10].

The results of studies of the determination of boron by a.a.s. with a carbon rod atomizer in the presence of titanium and ascorbic acid are presented here. The effect of uranium on the atomization of boron is also investigated.

Experimental

Apparatus. A Varian-Techtron atomic absorption spectrometer (model AA-6) equipped with a carbon "rod" atomizer (CRA-63) and BC-6 background corrector was used. The atomizer portion was enclosed in a glove box to facilitate handling the radioactive samples. A boron hollow-cathode lamp operated at 15 mA was used. The atomization program was: ashing, 30 s at 00°C; atomization, 4 s at 2850°C (manufacturer's values). Peak-height gnals were measured.

)03-2670/86/$03.50

Preparation of standards and samples. Spectroscopically-pure chemicals and high-purity preanalysed uranium were used in the preparation of stock solutions for the elements of interest. Quartz double-distilled water and electronic-grade nitric acid were used in their preparation. Three sets, each of seven graded multi-element 10-ml standard solutions, were prepared containing boron in the range 0—10 μg ml^{-1} and concomitant elements (Ag, Al, Be, Bi, Ca, Cd, Co, Cr, Cu, Fe, Mg, Mn, Mo, Ni, Si, Sn, V and Zn) in the range 0.01—10 μg ml^{-1}. All solutions in a given set contained 250 mg of ascorbic acid, or 250 mg of ascorbic acid and 100 μg of titanium, or 100 mg of uranium in addition to these amounts of ascorbic acid and titanium. The blank solutions for all the three sets were prepared with the same reagents and starting materials, but without the boron and concomitant elements. Freshly prepared standard solutions were used each time.

Multi-element reference standards, obtained from Jarrell-Ash and Spex Industries, were suitably diluted and mixed with appropriate amounts of titanium and ascorbic acid to serve as reference samples for boron determination. Aliquots (5 μl) of an intermediate-concentration standard were used in optimization of experimental parameters.

Results and discussion

Figure 1 shows the influence of 0.25% ascorbic acid and titanium on the atomic absorption of 5 μg ml^{-1} boron. Atomization of boron is markedly increased in the presence of ascorbic acid. However, further increase of ascorbic acid concentration increases the viscosity of the solution and contributes to inaccuracy in sample injection.

The presence of trace metals also significantly affects the atomization of boron. Strong interelement effects, particularly that of calcium, have been reported by van der Geugten [8] and Szydlowski [9], suggesting that calcium (1—2 mg ml^{-1}) and barium in the presence of calcium enhance boron absorbance. Such effects were investigated. Titanium was found to have the most significant effect in increasing the boron absorbance, in the absence or presence of ascorbic acid (Fig. 1).

A series of standards containing the concomitant elements, titanium and

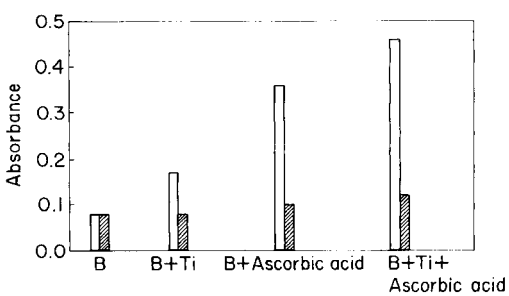

Fig. 1. Effect of 10 μg ml^{-1} titanium and 0.25% ascorbic acid on the absorbance of 5 μg ml^{-1} boron. The shaded portion shows the contribution of the non-specific absorbance at 249.7 nm.

ascorbic acid as well as boron was analysed. A linear calibration graph was obtained in the range of 0.2—10 μg ml^{-1} (Fig. 2). The reference standards were analysed with reference to this graph. The results (Table 1) were in good agreement with the certified values. The absolute 2σ limit of detection, 0.2 μg ml^{-1} in 5 μl of sample (i.e., 1 ng of boron), compares favourably with that reported by Slavin et al. [10] who used calcium as a matrix modifier, viz. 50 ng ml^{-1} in 20 μl of sample (again 1 ng of boron). Other workers [8, 9] reported 20—25 ng ml^{-1} as the limit of detection for a 20-μl sample. This improvement is probably due to more efficient atomization of boron under their experimental conditions.

Atomization mechanism. The ln(absorbance) vs. $1/T$ plot (T is the surface

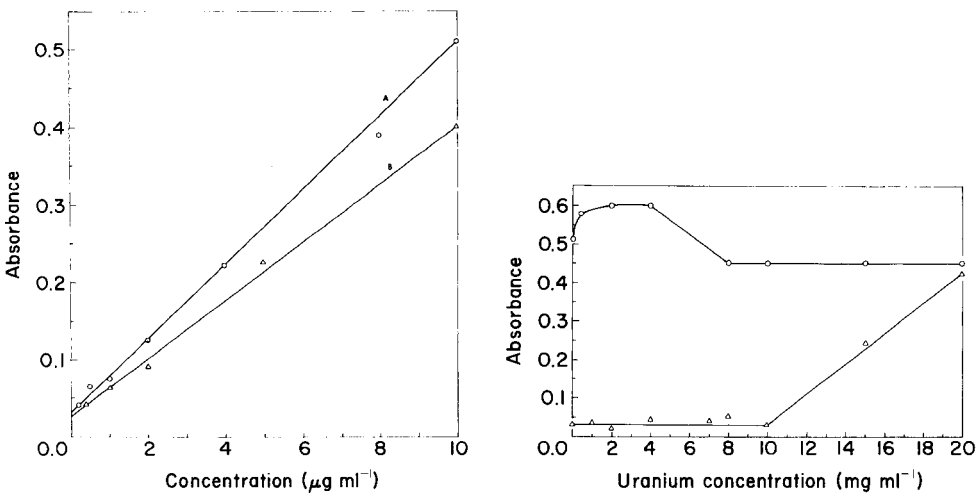

Fig. 2. Calibration graphs for boron: (A) standards contain boron and the concomitant elements given in the text; (B) standards used for (A) with addition of 10 mg ml^{-1} uranium.

Fig. 3. Effect of uranium on the absorbance of boron at 249.7 nm: (○) specific absorbance; (△) non-specific absorbance.

TABLE 1

Comparison of the boron concentration found in certified standard solutions[a]

Sample	Boron concentration (μg ml^{-1})		Sample	Boron concentration (μg ml^{-1})	
	Expected	Found		Expected	Found
M-Spex	0.25	0.26	B-Spex	2.50	2.50
M-Spex	0.50	0.50	B-Spex	4.00	3.40
M-Spex	2.00	2.25	Jarrell-Ash std. 4	2.50	2.50

[a]With addition of 0.25% ascorbic acid and 10 μg ml^{-1} titanium. The Jarrell-Ash standard was diluted 4-fold.

temperature of the graphite furnace as given by the manufacturer) was linear for boron in aqueous samples containing titanium and ascorbic acid. The slope gave an activation energy of 93 ± 2 kcal mol^{-1}. In the presence of ascorbic acid only, boron absorbance was decreased, but the linear ln(absorbance) vs. $1/T$ plot gave an activation energy of 88 ± 3 kcal mol^{-1}. These values compare reasonably well with the reported value of 97 ± 3 kcal mol^{-1} for the sublimation of solid boron [11]. This strongly suggests that the formation of boron atoms under the present conditions is primarily due to the sublimation of solid boron; the presence of ascorbic acid enhances the formation of solid boron and the presence of titanium further improves the conditions for solid boron formation. A detailed understanding of the role of ascorbic acid and titanium in this process is impossible from these studies, as they do not throw light on any reaction intermediates. It is possible, however, that the titanium decreases boron carbide formation.

Determination of boron in uranium. With a view to application of this approach to nuclear fuel analysis, the determination of boron in the presence of uranium was studied. Earlier studies [1—3, 6] showed that uranium has a marked effect on the atomization mechanisms of various analytes. Therefore, experiments were done to investigate the effect of uranium on the absorbance of 5 $\mu g\ ml^{-1}$ boron. The absorbance decreased with increasing uranium concentration up to 8 mg ml^{-1}, above which the absorbance was unaffected (Fig. 3). Non-specific absorbance from uranium increased at higher concentrations of uranium, thereby limiting the permissible uranium concentration to 10 mg ml^{-1} (Fig. 3). The calibration graph for boron in the presence of 10 mg ml^{-1} uranium (Fig. 2) is linear for 0.4—10 $\mu g\ ml^{-1}$ boron. If a uranium solution is diluted to a concentration of 10 mg ml^{-1}, then boron can be determined in the concentration range 40—1000 $\mu g\ g^{-1}$. This is much larger than the fractional $\mu g\ g^{-1}$ boron concentrations found in most nuclear fuels. This necessitates separation of boron from uranium in order to make the present method applicable for quality control of nuclear fuel materials.

The authors are grateful to Dr. M. V. Ramaniah, Director, Radiological Group and Dr. P. R. Natarajan, Head, Radiochemistry Division, for their constant encouragement.

REFERENCES

1 B. M. Patel, P. M. Bhatt, N. Gupta, M. M. Pawar and B. D. Joshi, Anal. Chim. Acta, 104 (1979) 113.
2 B. M. Patel, N. Gupta, P. J. Purohit and B. D. Joshi, Anal. Chim. Acta, 118 (1980) 163.
3 B. M. Patel, N. Goyal, P. Purohit, A. R. Dhobale and B. D. Joshi, Fresenius Z. Anal. Chem., 315 (1983) 42.
4 A. G. Page, S. V. Godbole, S. B. Deshkar and B. D. Joshi, Anal. Lett., 11A (1978) 619.
5 A. G. Page, S. V. Godbole, M. J. Kulkarni, S. S. Shelar and B. D. Joshi, Fresenius Z. Anal. Chem., 296 (1979) 40.
6 M. D. Sastry, M. K. Bhide, K. Savitri, Y. Babu and B. D. Joshi, Fresenius Z. Anal. Chem., 296 (1979) 367.

7 W. C. Campbell and J. M. Ottaway, Talanta, 21 (1974) 837.
8 P. van der Geugten, Fresenius Z. Anal. Chem., 306 (1981) 13.
9 F. J. Szydlowski, Anal. Chim. Acta, 106 (1979) 121.
10 W. Slavin, G. R. Carnrick, D. C. Manning and E. Pruszkowska, At. Spectrosc., 4(3) (1983) 69.
11 Handbook of Chemistry and Physics, Chemical Rubber Company, Cleveland, 1970, p. D-63.

Analytica Chimica Acta, 182 (1986) 231—237
Elsevier Science Publishers B.V., Amsterdam — Printed in The Netherlands

Short Communication

ELECTROTHERMAL ATOMIC ABSORPTION SPECTROMETRY OF SILICON VAPORIZED FROM DIFFERENT SURFACES

M. TADDIA

"G. Ciamician" Chemical Institute, University of Bologna, I-40126 Bologna (Italy)

(Received 27th February 1985)

Summary. The dependence of silicon absorbance on inert gas flow rate, ashing temperature and the amount injected was studied for uncoated, pyrolytically coated and tantalum carbide-coated graphite tubes. The reasons for the anomalous curvature of the calibration graphs and other unusual phenomena are discussed. Most sensitive results for silicon were obtained by isothermal atomization from a tantalum-treated tube and platform.

Despite the increasing number of applications of electrothermal atomic absorption spectrometry (a.a.s.) to elemental trace analysis, few of them deal with the determination of silicon. Recently, only methods for brines [1] and deionized water [2] have been published, perhaps because of the difficulty of obtaining good results without using a suitable graphite coating. The chemical reactions occurring in the furnace during the determination of silicon have been investigated both from the thermodynamic [3] and kinetic [4] point of view. These studies have stressed that the formation of species like SiO(g) and, above 1700° C, SiC(s), affects the atomization process. Treatment with carbide-forming elements, such as tantalum [5—7], tungsten [6] and niobium [4] has proved effective. The effect of tantalum was explained on the basis that atomization of silicon was more favoured from a tantalum carbide surface than a carbon surface [6]. It seems evident, however, that the tantalum carbide layer does not act merely by preventing the reaction between silicon and carbon.

The work described here was undertaken to investigate systematically conditions for the determination of silicon vaporized from different surfaces. It became evident that unusual phenomena observed were worthy of detailed investigation. The effect of the inert gas flow, curvature of calibration graphs and isothermal atomization were then investigated. There is reasonable evidence that traces of oxygen play an important role in determining the behaviour of silicon [8—10].

Experimental

Apparatus. The Perkin-Elmer 372 atomic absorption spectrometer used was equipped with a HGA-500 graphite furnace and a Leeds-Northrup 681A

0003-2670/86/$03.50

chart recorder. A Pye-Unicam silicon hollow-cathode lamp (19 mA, 251.6 nm) was used at the minimum spectral bandwidth of 0.2 nm. Sample aliquots (10, 20 or 50 μl) were injected manually with Brand micropipettes. Argon (3 ppm O_2) and nitrogen (2 ppm O_2) were used to provide the inert atmosphere. Pyrolytically-coated graphite tubes (Perkin-Elmer no. 091504) and pyrolytic graphite L'vov platforms (Perkin-Elmer no. 121091) were used. Tantalum carbide-coated tubes and platforms were prepared from uncoated tubes (Perkin-Elmer no. 121093 and no. 070699) and pyrolytic platforms, by modifying a procedure given by Zatka [11]; in particular, the total concentration of oxalic acid in the soaking solution was halved, to avoid crystallization and to reduce the blank value. A Philips 1710 diffractometer was used for x-ray diffraction analyses.

To minimize contamination from silicon, only polypropylene, polymethylpentene or, when necessary, PTFE vessels were used. They were cleaned with (1 + 1) ammonia and (1 + 9) sulphuric acid and finally rinsed with deionized water.

Reagents. A stock standard solution (1000 mg Si l^{-1}) was prepared by diluting with deionized-distilled water a commercial standard solution of silicon tetrachloride in sodium hydroxide (Titrisol, Merck). Working standards were prepared daily. Tantalum powder (99.7%, Riedel de Haen) was used to prepare the tantalum soaking solution.

Procedure. The temperature programs used for studying silicon behaviour with the different surfaces are reported in Table 1. Standard addition calibration graphs were drawn from the results obtained after adding to 50 ml of 0.2% (w/v) nitric acid, 50-μl aliquots of a 200 μg Si ml^{-1} standard. The amount of acid present was found to be adequate to keep the acidity unaltered (pH 1.60) during the whole experiment. Unless otherwise specified, peak heights were measured.

TABLE 1

Conditions for the HGA-500 furnace with different surfaces[a]

	Uncoated wall (NPG)	TaC-coated wall (NPTG)	TaC-coated and platform
Dry	120/8/20	120/8/20	150/5/20
Ash	1400[b]/10/60	900/10/30	900/30/30
Atomize[c]	2700/1/10	2700/1/10	2700/0/7
Clean	—	2800/1[d]/5	2800/1/5
Cool	—	—	20/1/30

[a]The values in each entry are the temperature (°C)/ramp time (s)/hold time (s). [b]The ashing temperature was 1300°C when atomizing from a pyrolytically coated wall. [c]The internal argon flow during atomization was 50 ml min^{-1}. [d]Some experiments were done with maximum power heating (Ramp = 0 s).

Results and discussion

Ashing temperature. The influence of ashing temperature on the absorbance signal of silicon vaporized from different tubes and platform is shown in Fig. 1. A maximum between 1300 and 1400° C, as previously reported [3], is observed from nonpyrolytic graphite (NPG). Sampling from nonpyrolytic tantalum-treated graphite (NPTG), with or without a pyrolytic tantalum-treated platform (PTG), gives drastic differences in the shapes of the absorbance profiles, so indicating a different surface activity. Without a platform, the absorbance decrease between 900 and 1300° C seems to proceed stepwise as a result of vapour/surface interactions. As the ashing temperature is increased still further, the signal does not drop to zero even at 2000° C, whereas this occurs at 1700° C in the untreated tubes. Although the exact mechanism responsible for the peak-height decrease above 900° C cannot be proven, the corresponding peak-area results show a similar trend (see Fig. 1), suggesting that the losses are due to lower atomization efficiency. The difference between treated and untreated tubes, particularly with respect to the retention of silicon at temperatures higher than 1700° C, may result from a stable ternary phase TaSiC. A study of the Ta/Si/C system by Nowotny et al. [12] using x-ray analysis, showed that a ternary phase exists in the range 0.5—10% carbon, with stability at 5% carbon. Although the experimental conditions used by these authors (1600° C, 12 h) are different from those of the a.a.s. determination, the formation of a Ta/Si/C phase cannot be excluded.

In evaluating the profiles shown in Fig. 1, the results obtained by Hennig [13], who measured the retention of tritiated water on the graphite crystals,

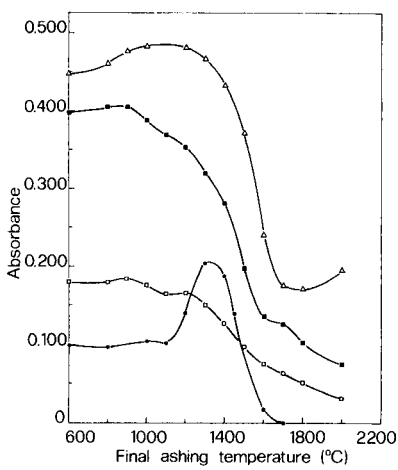

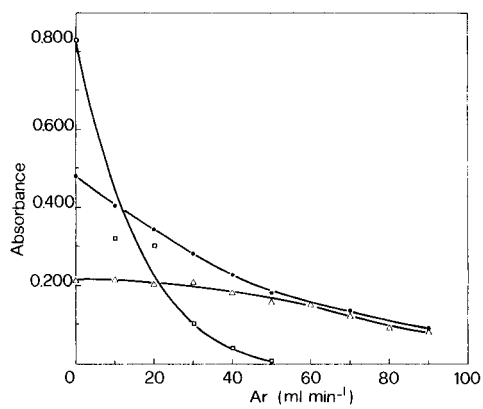

Fig. 1. Absorbance signals for 10 ng Si as a function of the final ashing temperature, from different tubes: (•) NPG; (▪) NPTG with signal integration; (□) NPTG without signal integration; (△) PTG platform in a NPTG tube.

Fig. 2. Effect of argon internal flow rate on the peak absorbance of 10 ng Si: (•) NPG, (□) pyrolytic graphite; (△) NPTG (no platform).

should also be considered. It was found that 6.8% of the initial water was retained even after treatment at 900° C for 10 min. It is reasonable to assume that NPTG has fewer active sites than NPG, so that the total amount of water retained by NPTG should be lower. To investigate this further, 50 μl of water was injected into the NPTG tube after a sample containing 28 ng of silicon had been ashed at 900° C. The water sample was dried, ashed and atomized. An absorbance of 0.675 ± 0.005 (n = 3) was measured; without the supplementary injection of water the value was practically the same. A slight difference was noted when the water was added after the drying step at 120° C; in this case the absorbance was 0.636 ± 0.012 (n = 4). It is interesting to compare these results with those reported by Frech and Cedergren [3] who did the same experiment with NPG; they found an absorbance decrease of about 35% by injecting 10 μl of water after ashing at 1600 K. It follows therefore that the NPTG is adequate for decreasing the influence of water on the silicon signal.

Inert gas flow. The effect of argon internal flow during the atomization stage on the silicon absorbance is shown in Fig. 2. On decreasing the gas flow rate, the absorbance generally increases but the three surfaces do not exhibit uniform behaviour. In particular, there is an abrupt increase in sensitivity from pyrolytic graphite when the gas-stop mode is used. The absorbance from NPTG increases by a factor of 1.4 when the flow is decreased from 50 to 0 ml min^{-1} and by a factor of 90 from pyrolytic graphite. When nitrogen is used instead of argon, the absorbance still depends markedly on the gas flow for pyrolytic graphite but much less so from NPG (Fig. 3). Peak-area measurements follow a similar trend. Obviously if a simple decrease in diffusional losses, without interaction of the gas with the surface or the analyte,

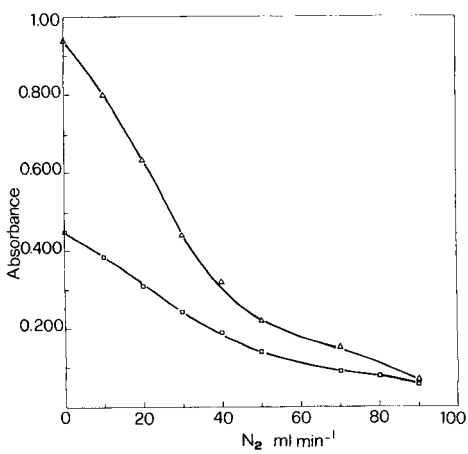

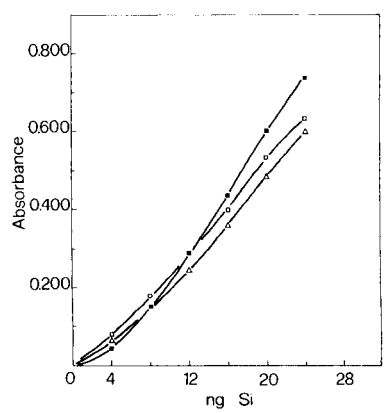

Fig. 3. Effect of nitrogen internal flow rate on the peak absorbance of 10 ng Si: (□) NPG; (△) pyrolytic graphite (no platform).

Fig. 4. Calibration graphs for silicon (NPG, no platform): (□) pH 1.60, 0.2% w/v HNO_3; (△) pH 5.05, acetate buffer; (■) pH 12.65, 0.2% w/v NaOH.

were responsible for such a sensitivity increase, differences between various surfaces should be less marked. Furthermore, it was noted that with an increased number of firings, the absorbance dependence on the gas flow rate for pyrolytic graphite becomes less pronounced. These results will be discussed further below.

These experiments do not confirm that nitrogen is better than argon for silicon determination in NPG, as reported by Manning and Fernandez [14]. However, these authors used a higher gas flow rate (1.1—2.5 l min^{-1}).

Calibration graphs. Figure 4 shows typical calibration curves obtained by plotting peak-height absorbance vs. ng Si for NPG tubes; each curve refers to a particular pH of the solution injected. All these graphs show an anomalous bending near the origin, and the tendency to give sigmoidal curves increases with increasing pH. It has been reported [1] that pH has a drastic effect on silicon sensitivity; for determinations of silicon in brines, pH 5 was recommended, to avoid almost total suppression of the signal. Although the shapes of the calibration curves do not permit an unambiguous comparison of the sensitivity at different pH values, there is no dramatic difference. The characteristic amount of silicon calculated from the linear portions is 0.15 ng at pH 1.60, 0.16 ng at pH 5.05 and 0.12 ng at pH 12.65. The sensitivity for silicon varied with an increased number of firings by as much as 30%. Therefore the above sensitivity data must be considered only as indicative.

Atomization of silicon from pyrolytic graphite surfaces results in a shift of the linear part of the graph as shown in Fig. 5. The displacement appears to be controlled by the gas flow rate, and is less pronounced in the gas-stop mode. No substantial difference resulted from integration of the signal,

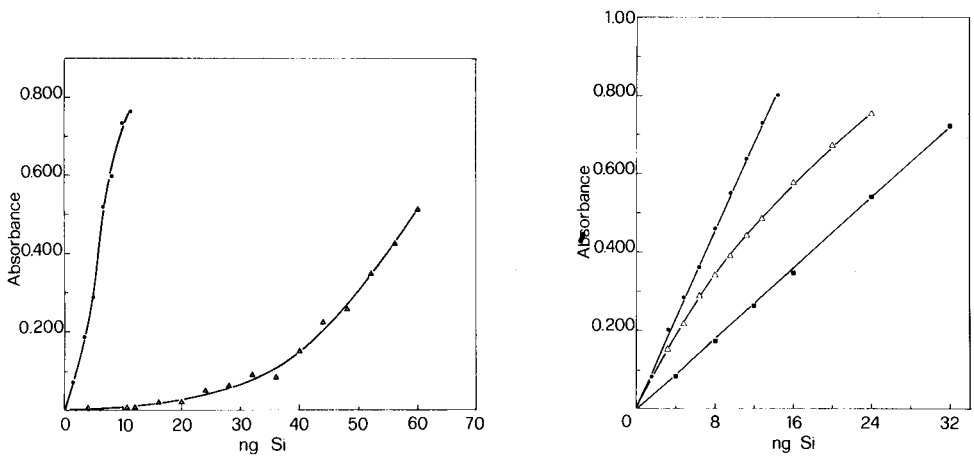

Fig. 5. Calibration graphs for silicon (pyrolytic graphite, no platform): (•) without argon; (△) 50 ml min^{-1} argon.

Fig. 6. Calibration graphs for silicon: (▪) NPTG (no platform); (•) PTG platform in NPTG tube with signal integration; (△) PTG platform in NPTG tube without integration.

compared to peak-height measurements. Conversely, tube aging has a marked effect on the sensitivity difference between the gas-stop and decreased flow modes. The difference progressively decreases as the number of firings increases.

The benefits of using tantalum carbide-coated tubes are significant (Fig. 6). The peak-height absorbance is a linear function of the amount of silicon injected over the whole range examined. The sensitivity (characteristic amount) was about 0.20 ng of silicon; this varied by as much as 30% from tube to tube and became worse with an increased number of firings (by about 16% over a tube lifetime). With the tantalum-treated platform and maximum power heating, the peak-area and peak-height sensitivities were 0.078 and 0.10 ng Si respectively. In this case, peak-area measurements gave better linearity (Fig. 6), good peak-to-peak reproducibility (2% at the 10 ng level), and a nearly constant calibration slope during the tube lifetime.

Integration of the signal also provided better sensitivity when sampling was from NPG and NPTG walls, without a platform, at the standard heating rate (ramp = 1 s). The enhancement factors were 1.7 and 2.2, respectively. Analogously, maximum power heating doubled the peak-height sensitivity for both NPG and NPTG, without a platform. As a consequence, maximum power heating is recommended in order to achieve maximum sensitivity when any of the surfaces examined is used.

To account for the different curve shapes resulting from this work, it is necessary to consider the presence of oxygen in a Massmann-type furnace. Although the real values of the oxygen partial pressure are still controversial [8—10], they seem to be many orders of magnitude higher than the predicted thermodynamic values. It has been assumed [8] that the free oxygen comes mainly from impurity in the inert gas and that the partial pressure of oxygen controls the thermal dissociation of silicon oxide. It has been calculated [8] and then measured [10], that the efficiency of graphite in decreasing the partial pressure of oxygen depends strongly on the internal flow rate. For pyrolytic graphite tubes, flow rates above 3.0 ml s^{-1} produced an insignificant reduction in the oxygen partial pressure while the reaction between carbon and oxygen was also insignificant below 1300 K [10]. Tubes made with NPG seem to be more reactive at lower temperatures but the extent of the reaction still depends on the flow rate. Free atoms of the analyte can participate in oxygen removal, the result being a displacement of the linear part of the calibration graph. In the present system, the existence of gaseous SiO above 1600 K [3] has to be taken into account in determining the vapour composition, but the atomization mechanism proposed by L'vov and Ryabchuk [8] helps to explain the phenomena observed. When pyrolytic graphite is used, these effects are more evident because of its lower efficiency in removing oxygen. This lower efficiency may also account for the drastic difference in sensitivity between operation in the gas-stop and decreased flow modes.

To explain the behaviour on tantalum carbide-coated surfaces, an implication of the Nowotny Ta/O/C system should be considered [15]. This reaction

should play an active role in removing oxygen from the furnace environment, so that losses of silicon as gaseous SiO should be decreased and better linearity achieved. Other mechanisms, based on the oxygen removal as Ta_2O_5, which may be valid for tantalum furnaces [10], should be excluded. On the surfaces of new and old NPTG tubes, only carbon and tantalum carbide were detected by x-ray diffraction analysis. The efficiency of tantalum-treated tubes may also be due to faster release of silicon from the tantalum carbide surface and slower capture of the free atoms to form silicon carbide [7]. This view is supported by the results obtained on niobium-coated tubes [4]; the rate of silicon carbide formation at 1960°C was 0.4 mol mol^{-1} min^{-1} on niobium-coated tubes and 0.94 on the uncoated tubes [4]. Although these data provide useful information, further studies are needed to estimate the oxygen partial pressure in tantalum carbide-coated tubes, and to propose a more definite mechanism for free atom formation from this substrate.

REFERENCES

1 L. A. Powell and R. L. Tease, Anal. Chem., 54 (1982) 2154.
2 F. Fehse, Spectrochim. Acta, Part B: 39 (1984) 597.
3 W. Frech and A. Cedergren, Anal. Chim. Acta, 113 (1980) 227.
4 G. Müller-Vogt and W. Wendl, Anal. Chem., 53 (1981) 651.
5 P. Hocquellet and N. Labeyrie, Analusis, 3 (1975) 505.
6 H. M. Ortner and E. Kantuscher, Talanta, 22 (1975) 581.
7 D. J. Lythgoe, Analyst (London), 106 (1981) 743.
8 B. V. L'vov and G. N. Ryabchuk, Spectrochim. Acta, Part B: 37 (1982) 673.
9 A. Cedergren, W. Frech and E. Lundberg, Anal. Chem., 56 (1984) 1382.
10 R. E. Sturgeon, K. W. M. Siu and S. S. Berman, Spectrochim. Acta, Part B: 39 (1984) 213.
11 V. J. Zatka, Anal. Chem., 50 (1978) 538.
12 H. Nowotny, B. Lux and H. Kudielka, Monatsh. Chem., 87 (1956) 447.
13 R. Hennig, J. Chem. Phys., 58 (1961) 12.
14 D. C. Manning and F. Fernandez, At. Abs. Newsl., 3 (1970) 65.
15 H. M. Ortner, H. Krabichler and W. Wegscheider, in Fortschritte in der Atomspektrometrischen Spurenanalytik, Vol. 1, Verlag Chemie, Weinheim FRG, 1984, p. 94.

Analytica Chimica Acta, 182 (1986) 239—244
Elsevier Science Publishers B.V., Amsterdam — Printed in The Netherlands

Short Communication

OCCURRENCE OF MONOALKYLLEAD SPECIES DURING THE SPECIATION OF ORGANOLEAD

RUDY J. A. VAN CLEUVENBERGEN, DIPANKAR CHAKRABORTI and FRED C. ADAMS*

Department of Chemistry, University of Antwerp (U.I.A.), Universiteitsplein 1, B-2610 Wilrijk (Belgium)

(Received 6th September 1985)

Summary. When tri- and dialkyllead levels are determined in environmental samples by a method based on Grignard derivatization and subsequent gas chromatography/atomic absorption spectrometry, monoalkyllead species are sometimes detected. A rearrangement process during or following Grignard derivatization explains this occurrence at least partly. The accuracy of the determination does not suffer significantly from this limited-scale reaction but the detection of a monoalkyltributyllead species does not necessarily mean that the sample contains monoalkyllead compounds.

The environmental occurrence and fate of the highly toxic tetraalkyllead compounds used commercially as antiknock agents in gasoline, have been studied extensively. At first, efforts were mainly focused on monitoring the concentrations of these compounds in the atmosphere [1], but attention gradually shifted to the role of the degradation products, the trialkyllead and dialkyllead compounds. Consequently, during recent years, sensitive analytical methods have been developed to speciate the ionic breakdown products in an aqueous matrix. The use of Grignard derivatization and measurement by gas chromatography/atomic absorption spectrometry (g.c./a.a.s.) has proved to be very suitable for this purpose [2—5]. In addition to the ionic organolead compounds derived from tetramethyllead and tetraethyllead (trimethyllead, dimethyllead, triethyllead and diethyllead), all the research groups following this approach have reported the detection of mixed methylethyllead species. It was shown here that these products are formed when a mixture of tetraalkyllead compounds is added to natural water. The mixed tetraalkyllead precursors were also indicated as minor atmospheric pollutants [6]; therefore the occurrence of the mixed ionic species in rain water is probable. More unexpectedly, two additional peaks have been ascribed to monomethyllead and monoethyllead on the basis of their retention characteristics [3—5].

Ever since the first studies on the decomposition of alkyllead compounds by Calingaert et al. [7], monoalkyllead salts have generally been stated to be too unstable to permit their isolation in the environment, although they can

0003-2670/86/$03.50

be considered as intermediates in the final conversion of organolead to inorganic lead [8—11]. The inability to detect a stable monoalkyllead complex in water has provided a major argument against the possibility of biomethylation of lead in the environment [12, 13]. The assumed chemical instability of monoalkyllead compounds, however, is not evident; Chobert and Devaud [14] described the synthesis of $RPbI_3$ products (R = C_2H_5, C_3H_7, C_4H_9) with a carbon—lead bond which is stable towards water, and stable monoaryllead compounds have been known for many years, being applied industrially as catalysts in the preparation of polyurethane foams [8]. Regardless of the stability of the monoalkyllead compounds, however, the excellent detection limits of the recently reported methods, which are around 1 ng l^{-1} [3], makes their detection more plausible than before.

A possibility that must be eliminated before it can be concluded that monoalkyllead species occur in natural water, is rearrangement after sampling. The exchange of alkyl groups between different organolead compounds, commonly referred to as a redistribution reaction, is fairly well documented [9, 15]. It has been suggested that such a process in the g.c. injection port [4] or somewhere in the analytical pathway [3] could be responsible for the regular chromatographic appearance of butylated monoalkyllead species. In this study, a series of experiments was designed to elucidate the detection of the monoethyllead species in water samples.

Experimental

The method applied is based on the chelate extraction of the diethyldithiocarbamate complexes of the ionic alkyllead species into pentane, further enrichment into n-nonane, derivatization with n-butyl Grignard reagent and measurement by g.c./a.a.s. It has been described in detail elsewhere [3, 5]. The alkyllead compounds were kindly supplied by the Associated Octel Company (South Wirral, England); they included a mixture of the five tetraalkylleads in diisopropyl ether, a solution of tetraethyllead in diisopropyl ether, and trimethyllead chloride, triethyllead chloride, dimethyllead dichloride and diethyllead dichloride in powder form. The latter were used to prepare individual stock solutions in water, each containing about 10 μg ml^{-1} lead. Working standards, obtained by dilution, were prepared daily. The Grignard reagent used, 2.0 M n-butylmagnesium chloride in tetrahydrofuran (THF; Alfa Ventron), was stored and handled under argon. The butylation was done in 250 μl of nonane.

Results and discussion

In the procedures for determining ionic alkyllead species, the butylation is clearly the most critical step. Not only must the reagent itself be appropriately handled to prevent loss of activity; even the smallest traces of water resulting from an imperfect separation during the liquid-liquid extraction can be expected to have a drastic effect on the efficiency of derivatization. Furthermore, other species may be present, possibly reacting with the butylating

agent and hence affecting the butylation of the ionic alkyllead species. Unfortunately, these parameters are not always fully controllable.

The concentration of the Grignard reagent used can be considered to correlate with the factors mentioned above. Table 1 demonstrates the effect of the amount and the concentration of the butylating reagent on the recovery of 350 ng of trimethyllead from deionized water; a similar trend was obtained for triethyllead and for spiked natural waters. The standard 2.0 M Grignard reagent in THF was either previously diluted with THF or used directly after addition to the sample of a known amount of dry THF; in each case, 1 ml of butylating reagent was added. In this way, the effect of varying both the absolute amount of reagent and its concentration could be monitored. It appears that derivatization with excessive amounts of Grignard reagent produces some rearrangement; part of the organolead species is eventually converted to tetrabutyllead. Yet, the amount used must be large enough to provide complete derivatization of the species present. Predilution to a 0.5 M concentration looks like the best compromise. It was applied in all further determinations, and in the environmental survey reported elsewhere [5].

In view of these results, it is tempting to assume a similar rearrangement process to explain the occurrence of the small monoalkyllead peaks in rain and snow samples. Indeed, regularly, but not consistently, a monoethyltributyllead peak was observed, with an absorbance corresponding to <5% of that from the tri- and diethyllead derivatives; the monomethyltributyllead signal was rarely present. Accordingly, the ethyllead compounds were preferred in the following experiments aimed at corroborating the existence of rearrangement reactions leading to monoethyltributyllead. The concentration of Grignard reagent applied to the determination of triethyllead in spiked deionized water seemed not to affect the abundance of monoethyllead, whether at environmentally significant (440 ng l^{-1}) or at higher (1300 ng l^{-1}) concentrations. In all these synthetic samples, monoethyllead occurred consistently, at an absorbance level of about 5% relative to triethyllead; the

TABLE 1

Effect of the concentration and amount of Grignard reagent on the recovery of trimethyllead (350 ng) and the formation of tetrabutyllead (Me = $-CH_3$, Bu = $-C_4H_9$)

Grignard reagent		Recovery of $PbMe_3^+$ (%)	
Concentration (M)	Amount (mmol)	$PbMe_3Bu$	$PbBu_4$
2.0	2.0	43	63
1.0	1.0	90	10
0.5	0.5	96	<4
0.2	0.2	96	<4
0.1	0.1	7	<4
1.0	2.0	70	31
0.5	2.0	93	9

recovery of the analyte was satisfactory (above 90%) except when rearrangement to tetrabutyllead was observed. Preparing fresh stock solutions, or purifying them by a salting-out procedure for trialkylleads [16], neither eliminated the monoethyllead derivative nor altered significantly its relative abundance. Consequently, it was considered unlikely that this species was present as a decomposition product in the alkyllead standards; because the kinetics of its possible formation and degradation are unknown, the existence of monoethyllead in the aqueous solutions cannot be ruled out completely.

As the consistent occurrence of the monoethyllead species in synthetic samples seemed likely to be due to a rearrangement reaction, attention was focused on another parameter of the derivatization reaction, the amount of organolead present. In Fig. 1, the peak intensity ratio of monoethyllead to triethyllead is plotted versus the input of triethyllead. The butylation was done with 0.5 M reagent; care was taken that neither traces of water nor any species capable of being butylated other than the analyte were present. Clearly, the relative intensity of monoethyllead increases as the input triethyllead is lowered. This points to a rearrangement process: the larger the excess of butylating agent present, the higher the risk of redistribution, in which one (or more) of the alkyl groups originally bound to the lead atom is replaced by a butyl group. The occasional detection of traces of tetraethyllead provided additional evidence to support this suggestion; there is indeed a chance that the ethyl group replaced can ethylate another analyte molecule. The tetrabutyllead signal did not differ markedly throughout this experiment, and diethyllead derivatives could hardly be detected. When this experiment was repeated, highly variable relative intensities of the monoethyllead species were obtained, with an absorbance rarely exceeding a tenth of the triethyllead peak. Apparently, the parameters involved are largely uncontrollable. It should be noted that an absorbance ratio of 10% would induce a similar relative error on the analyte determination; in environmental samples, how-

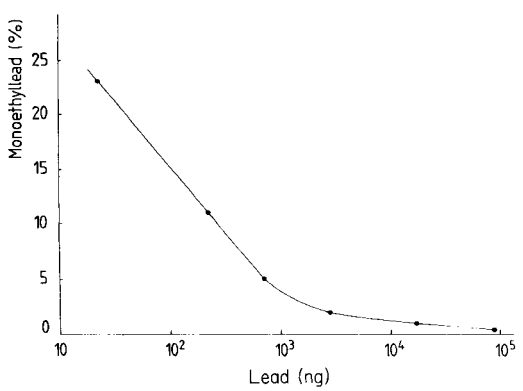

Fig. 1. Relative intensity ratio of monoethyllead to triethyllead (%) as a function of the original triethyllead concentration used for derivatization (ng Pb per 500 ml of water).

ever, the monoalkylleads tend to occur at much lower levels, probably because the derivatization is done in a complex medium. The resulting systematic error can thus be regarded as insignificant compared to the overall precision of the determinations (ca. 10%).

During this study, it was observed that the apparent concentration of the monoalkyllead species increased when the extract was stored for several days or weeks in a refrigerator. It was also found that the butylated standards, and even a mixed working standard prepared from them, could be kept for months without showing any deterioration [3], so that the apparent increase remains unexplained as yet. The measurement system was checked carefully for a possible rearrangement reaction in the injection port of the gas chromatograph, as suggested by Harrison and Radojevic [4]. No rearrangement products were ever detected when the working standard was analyzed. Moreover, when monoalkyllead species were detected, their apparent concentration remained unaffected when the injection port temperature was varied. This possibility can therefore be excluded.

Conclusion

The data presented indicate that during the determination of ionic alkyllead compounds by a species-specific alkylation procedure based on Grignard derivatization, rearrangement products can be formed. In routine environmental applications, this process is likely to be of minor importance compared with the analytical characteristics of the method. However, the detection of monoalkyltributyllead species cannot be regarded as unambiguous evidence for the existence of monoalkyllead compounds in the environment.

R. Van Cleuvenbergen gratefully acknowledges a grant as research assistant from the National Fund for Scientific Research. This work was funded through FKFO grant 2.0091.85 and EC grant-768-B/RS.

REFERENCES

1 W. R. A. De Jonghe and F. C. Adams, Talanta, 29 (1982) 1057.
2 Y. K. Chau and P. T. S. Wong, in P. Granjean (Ed.), Biological Effects of Organolead Compounds, CRC Press, Boca Raton, FL 33431, U.S.A., 1984, p. 21.
3 D. Chakraborti, W. R. A. De Jonghe, W. E. Van Mol, R. J. A. Van Cleuvenbergen and F. C. Adams, Anal. Chem., 56 (1984) 2692.
4 R. M. Harrison and M. Radojevic, Environ. Technol. Lett., 6 (1985) 129.
5 R. J. A. Van Cleuvenbergen, D. Chakraborti and F. C. Adams, Environ. Sci. Technol., in press.
6 W. R. A. De Jonghe, D. Chakraborti and F. Adams, Environ. Sci. Technol., 15 (1981) 1217.
7 G. Calingaert, H. Shapiro, F. J. Dykstra and L. Hess, J. Am. Chem. Soc., 70 (1948) 3902.
8 D. De Vos and J. Wolters, Rev. Silicon, Germanium, Tin and Lead Compounds, 4 (1980) 209.
9 H. Shapiro and F. W. Frey, The Organic Compounds of Lead, Wiley, New York, 1968, pp. 93 and 293.

10 F. Huber, U. Schmidt and H. Kirchmann, in F. E. Brinckman and J. M. Bellama (Eds.), Organometals and Organometalloids, ACS Symposium Series 82, American Chemical Society, Washington D.C., 1978, p. 65.
11 F. Huber, J. Gmehling, H.-J. Haupt and H. Lindemann, Angew. Chem. Int. Ed. Engl., 10 (1971) 835.
12 J. M. Wood, in M. Branica and Z. Konrad (Eds.), Lead in the Marine Environment, Pergamon Press, Oxford, 1980, p. 299.
13 Y. K. Chau and P. T. S. Wong, in F. E. Brinckman and J. M. Bellama (Eds.), Organometals and Organometalloids, ACS Symposium Series 82, American Chemical Society, Washington D.C., 1978, p. 39.
14 G. Chobert and M. Devaud, J. Organometall. Chem., 153 (1978) C23.
15 G. Calingaert and H. A. Beatty, in H. Gilman (Ed.), Organic Chemistry, An Advanced Treatise, Vol. II, 2nd edn., Wiley, New York, 1943, p. 1806.
16 W. R. A. De Jonghe, W. E. Van Mol and F. C. Adams, Anal. Chem., 55 (1983) 1050.

Analytica Chimica Acta, 182 (1986) 245—250
Elsevier Science Publishers B.V., Amsterdam — Printed in The Netherlands

Short Communication

STUDIES ON 3,3′-DICHLORO-, 4,4′-DICHLORO- AND 5,5′-DICHLORO-2,2′-DIMETHYLDITHIZONE AND THEIR REACTIONS WITH METAL IONS

A. MAGEED KIWAN*, FATMA HAYDER and FATHY HASSAN
Department of Chemistry, University of Kuwait (Kuwait)
(Received 16th July 1985)

Summary. Three new dichlorodimethyl derivatives of dithizone are reported, with their electronic and i.r. spectra, acidity constants and partition coefficients between 0.5 M sodium perchlorate and chloroform or carbon tetrachloride. The extraction equilibria with Cd, Co(II), Hg(II), Ni, Pb, Tl(I), Zn and Bi and the spectrophotometric characteristics of the extractable metal chelates are described. Complete extraction of these complexes requires higher pH than that needed with dithizone itself. The 4,4′-dichloroisomer is more efficient than the 3,3′- and 5,5′-isomers, or dithizone itself, for the separation of cadmium from zinc or cobalt from nickel.

Dithizone (3-mercapto-1,5-diphenylformazan) is widely used as a very sensitive extraction photometric reagent for many metals [1]. The sensitivity and/or selectivity of the reagent are affected by introducing substituents on the phenyl rings. In a preceding paper [2], the effects of introducing four chlorine atoms into dithizone on the extraction parameters and spectral characteristics of six new tetrachlorodithizone isomers and their metal complexes were reported.

This communication describes the effects of introducing chlorine atoms and methyl groups into the phenyl rings of dithizone at the same time. The methyl groups were placed at C-2 in all cases while the chlorine atoms were introduced in three different positions. Thus the 3,3′-dichloro-, 4,4′-dichloro- and 5,5′-dichloro-2,2′-dimethyldithizone analogues were synthesized and their characteristics in the extraction-spectrophotometric determination of metal ions were evaluated.

Experimental

Reagents and chemicals. The 3,3′-dichloro-, 4,4′-dichloro- and 5,5′-dichloro-derivatives of 2,2′-dimethyldithizone were prepared from the corresponding arylamines by the nitroformazyl method [3]. The nitroformazan derivatives were converted to their dithizone analogues and purified as described before for other analogues [4]. The elemental data, melting points and some characteristic i.r. frequencies are shown in Table 1.

Deionized water and reagent-grade chemicals were used throughout, and the usual precautions were taken as with dithizone [1].

0003-2670/86/$03.50

TABLE 1

Elemental data and prominent i.r. bands of dichloro derivatives of 2,2′-dimethyldithizone analogues

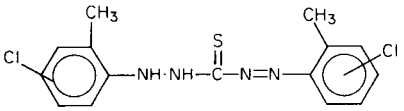

Compound	M.p. (°C)	Elemental data[a]			Main i.r. bands (KBr) (cm^{-1})
		C (%)	H (%)	S (%)	
3,3′-dichloro-	156	50.6	4.0	8.7	3060, 2090, 1580, 1490, 1460, 1430, 1390, 1280, 1260, 1185, 1160, 1130, 1015, 890, 785, 770, 700
4,4′-dichloro-	153	51.4	3.9	8.6	2095, 2085, 1590, 1490, 1460, 1425, 1390, 1280, 1265, 1245, 1220, 1190, 1150, 1015, 890, 790, 770, 700
5,5′-dichloro-	166	50.5	3.9	8.6	3180, 3120, 3060, 1595, 1580, 1490, 1405, 1385, 1290, 1265, 1250, 1220, 1190, 1150, 1070, 995, 920, 805, 745, 695

[a]Calculated values: 51.0% C, 4.0% H, and 9.1% S.

Procedures. The spectral characteristics (λ_{max} and ϵ_{max}) of substituted dithizone analogues, their partition coefficients and acidity constants were determined by the usual procedures [1]. The compositions of metal complexes, their spectral properties and extraction parameters were also determined in the usual manner.

The visible spectra of ligands and their complexes were recorded on a Unicam SP8000 spectrophotometer and the infrared spectra on a Unicam SP1000; a Radiometer PM64 pH-meter was used for pH measurements. The elemental analyses were done at the Alfred Bernhardt Microanalytisches Laboratorium, Elbach, F.R.G.

Results and discussion

Visible spectra of 3,3′-dichloro-, 4,4′-dichloro-, and 5,5′-dichloro-2,2′-dimethyldithizones. These reagents are black crystalline solids which resemble dithizone in appearance. They are insoluble in water but fairly soluble in organic solvents such as chloroform and carbon tetrachloride to give green solutions with two absorption bands in the visible region. The frequency and intensity of these bands were found to depend on the position of substituents as well as on the nature of solvent. Table 2 summarizes their spectral characteristics together with the corresponding data of some related compounds.

The introduction of a methyl group at C-2 or a chlorine atom at C-2, C-3 or C-4 of the phenyl rings of dithizone shifted both $\lambda_{max,1}$ and $\lambda_{max,2}$ to longer wavelengths. When both methyl and chlorine substituents were intro-

TABLE 2

Spectral characteristics of 3,3′-dichloro-2,2′-dimethyl-, 4,4′-dichloro-2,2′-dimethyl-, and 5,5′-dichloro-2,2′-dimethyl-dithizones and related compounds in chloroform and carbon tetrachloride

Derivative	Solvent	$\lambda_{max,1}$ (nm)	$\lambda_{max,2}$ (nm)	λ_{min} (nm)	$\epsilon_{max,1}$[a]	$\epsilon_{max,2}$[a]	ϵ_{min}[a]	R	ΔR[b]
Dithizone	$CHCl_3$	605	445	500	41.5	16.0	6.78	2.59	0.0
	CCl_4	620	450	—	34.6	20.3	—	1.70	0.0
3,3′-Cl_2-	$CHCl_3$	616	442	518	34.5	15.0	7.17	2.30	−0.29
2,2′-$(CH_3)_2$	CCl_4	632	460	522	34.2	18.1	6.48	1.89	+0.19
4,4′-Cl_2-	$CHCl_3$	628	462	524	47.7	14.7	10.34	3.25	+0.66
2,2′-$(CH_3)_2$	CCl_4	638	464	530	41.5	19.20	8.18	2.16	+0.46
5,5′-Cl_2-	$CHCl_3$	622	452	520	35.69	14.36	6.34	2.48	−0.11
2,2′-$(CH_3)_2$	CCl_4	634	450	528	33.50	18.32	7.33	1.83	+0.13
2,2′-$(CH_3)_2$	$CHCl_3$	615	455	512	43.20	12.50	7.95	3.30	+0.71
	CCl_4	628	460					2.44	+0.74
2,2′-Cl_2	$CHCl_3$	624	461	518	31.82	17.58	6.49	1.81	−0.78
	CCl_4	645	462		33.4	29.8		1.12	−0.58
3,3′-Cl_2	$CHCl_3$	610	445	508	32.04	17.96	6.31	2.00	−0.59
	CCl_4	624	451	516				1.27	−0.43
4,4′-Cl_2	$CHCl_3$	620	452	510	46.15	19.23	8.33	2.30	−0.29
	CCl_4	632	461					1.52	−0.18

[a]Molar absorptivity ($\times 10^3$ l mol^{-1} cm^{-1}). [b]$\Delta R = R_s - R_u$ where R_s and R_u are the peak ratios for the substituted and unsubstituted dithizone, respectively.

duced into the phenyl rings of dithizone, the former at C-2 and the latter at C-3, C-4 or C-5, the shifts in $\lambda_{max,1}$ were more significant than those in $\lambda_{max,2}$; the latter seem to depend primarily on chlorine.

The molar absorptivities of the substituted dithizones are also affected by the nature and position of substituents. Introduction of a chlorine atom at C-2 or C-3 of the phenyl rings lowered the $\epsilon_{max,1}$ but raised the $\epsilon_{max,2}$ value compared to dithizone, whereas both $\epsilon_{max,1}$ and $\epsilon_{max,2}$ for 4,4′-dichlorodithizone were higher than the corresponding values of the 2,2′-dichloro-, 3,3′-dichloro- or the unsubstituted dithizone (Table 2). The $\epsilon_{max,1}$ and $\epsilon_{max,2}$ of 3,3′-dichloro-2,2′-dimethyl-, 4,4′-dichloro-2,2′-dimethyl-, and 5,5′-dichloro-2,2′-dimethyldithizone seem to be mainly dominated by the effect of chlorine substituents.

The effect of substitution on the molar absorptivities of the dithizone analogues may be also gauged by the "peak ratio", R ($= \epsilon_{max,1}/\epsilon_{max,2}$), the value of which is believed to represent the relative concentrations of thiol and thione tautomers [1]. The finding that the peak ratios for all three isomeric dichlorodimethyl dithizone analogues in carbon tetrachloride are higher than that for dithizone itself may be taken as indicating some shift towards the thione tautomer. However, the peak ratios for 3,3′-dichloro-2,2′-dimethyl-, and 5,5′-dichloro-2,2′-dimethyl dithizones in chloroform are slightly lower

TABLE 3

Spectral characteristics and extraction data for metal complexes with dichlorodimethyldithizones and tetrachlorodithizones in chloroform[a]

Metal	Unsubs.		3,3'-Cl_2-2,2'-$(CH_3)_2$		4,4'-Cl_2-2,2'-$(CH_3)_2$		5,5'-Cl_2-2,2'-$(CH_3)_2$		2,2',3,3'-Cl_4[b]		2,2',4,4'-Cl_4[b]		2,2',5,5'-Cl_4[b]	
	λ_{max}	ϵ	λ_{max}	ϵ	λ_{max}	ϵ	λ_{max}	ϵ	λ_{max}	ϵ	λ_{max}	ϵ	λ_{max}	ϵ
Cd(II)	512	88.4	500	56.5	500	59.3	Insol.		524	63.7	532	77.3	524	71.9
Co(II)	540	68.3	550	37.0	540	36.4	545	43.2	534	42.5	554	47.4	542	41.1
Hg(II)	485	72.2	470	60.0	490	63.7	478	57.0	480	60.0	490	59.9	480	65.9
Ni(II)	490[c]	30.7	424[d]	24.5	430	31.5	428	25.7	490[d]	15.6	690	17.5	490	—
			506	22.1	566[d]	34.1	506[d]	24.6	—	—	—	—	—	—
	660	19.1	670	22.1	670	30.9	670	24.6	500[d]	29.3	560	19.8	670	—
Pb(II)	515	68.8	492	49.5	504	65.9	502	48.5	504	52.0	516	58.7	510	46.4
Tl(I)	506	34.8	500	25.1	510	28.2	506	23.8	Insol.		Insol.		Insol.	
Zn(II)	526	91.1	516	71.4	526	84.8	522	68.7	530	74.6	546	81.3	536	70.9
Bi(III)[c]	490	80.0	470	69.4	480	75.3	476	64.6	486	79.4	494	70.9	490	69.4
	log K_{ex}	$pH_{1/2}$[a]	log K_{ex}	$pH_{1/2}$	log K_{ex}	$pH_{1/2}$	log K_{ex}	$pH_{1/2}$	log K_{ex}	$pH_{1/2}$	log K_{ex}	$pH_{1/2}$	log K_{ex}	$pH_{1/2}$
Cd(II)	0.38	3.81	−3.30	5.65	−4.55	6.28	−3.57	5.79	0.55	3.73	0.32	3.84	1.45	3.27
Co(II)	−2.4	5.2	−5.52	6.76	−4.19	6.09	−5.20	6.6	−2.2	5.10	−2.37	5.19	−2.55	5.28
Cu(II)	7.3	0.35	—	—	2.15	2.93	2.45	2.78	3.56	2.22	5.07	1.46	5.62	1.19
Hg(II)	26.86	−9.43	22.33	−7.17	22.75	−7.38	22.34	−7.18	25.8	−8.9	26.15	−9.08	26.61	−9.61
Ni(II)	−4.17	6.09	−6.50	7.25	−6.23	7.12	−5.97	6.99	−4.43	6.22	−2.99	5.5	−3.38	5.69
Pb(II)	−0.56	4.28	−2.7	5.35	−4.6	6.3	−4.29	6.15	1.1	3.45	0.3	3.85	2.09	2.95
Tl(I)	−4.17	8.17	−4.48	8.48	−5.10	9.10	−4.35	8.35	Insol.		Insol.		Insol.	
Zn(II)	0.4	3.8	−3.58	5.79	−3.72	5.86	−4.05	6.03	−1.23	4.62	−0.81	4.41	1.10	3.45
Bi(III)[c]	9.89	0.70	9.16	0.95	7.88	1.37	8.98	1.00	11.48	0.17	10.71	0.43	10.25	0.58

[a]Wavelengths are given in nm and molar absorptivities (ϵ) in units of 10^3 l mol^{-1} cm^{-1}; $pH_{1/2}$ values are based on $[H_2RDz]_0 = 10^{-4}$ M. [b]Data from [2]. [c]In carbon tetrachloride. [d]Broad peak.

TABLE 4

Acidity constants, partition coefficients (P_r) and $pH_{1/2}$ values for the dichlorodimethyldithizones and some related compounds in carbon tetrachloride

Derivative	pK_a	log P_r	$pH_{1/2}$	Derivative	pK_a	log P_r	$pH_{1/2}$
3,3′-Cl_2-2,2′-$(CH_3)_2$-	5.49	5.4	10.95	2,2′,3,3′-Cl_4-[a]	4.87	5.05	9.92
4,4′-Cl_2-2,2′-$(CH_3)_2$-	5.87	5.22	11.20	2,2′,4,4′-Cl_4-[a]	5.8	4.3	10.10
5,5′-Cl_2-2,2′-$(CH_3)_2$-	5.2	5.29	10.72	2,2′,5,5′-Cl_4-[a]	5.08	4.82	9.9
				Unsubst.[b]	4.62	4.18	8.8[a], 8.63

[a]Data from [2]. [b]Data from [1].

than that of dithizone suggesting a shift in the equilibrium towards the thiol tautomer.

Table 3 summarizes the spectral data of metal complexes with the three isomers and with some related compounds. There seems to be no simple correlation between the molar absorptivities of the substituted and unsubstituted dithizone complexes. However, there is a general trend in the direction of shift of λ_{max} values of $M(HRDz)_n$ as a function of position of substituent R decreasing in the order: 4,4′-Cl_2-2,2′-$(CH_3)_2$- > 5,5′-Cl_2-2,2′-$(CH_3)_2$- > 3,3′-Cl_2-2,2′-$(CH_3)_2$-. Except for the nickel complexes, there is a definite decrease in the molar absorptivities of the metal complexes with the dichlorodimethyldithizones.

Extraction equilibria. The introduction of the methyl groups and chlorine atoms in the new derivatives affected the partition coefficients, acidity constants and the $pH_{1/2}$ values (Table 4). The extraction equilibria for metal M may be represented by $[n(CH_3)_2Cl_2H_2Dz]_o + M^{n+} \rightleftharpoons \{M[(CH_3)_2Cl_2HDz]_n\}_o + nH^+$, where subscript o indicates the organic phase. The metal extraction constant (K_{ex}) depends on K_a and P_r of the extractant as well as as on the thermodynamic stability and partition coefficient of the metal complex. Table 3 lists the extraction constants and the $pH_{1/2}$ values for metal complexes with the dichlorodimethyldithizones together with corresponding values for related compounds under the same conditions.

The following conclusions may be drawn. The extraction constants for the metal dichloro-2,2′-dimethyldithizonates are lower than those for the tetrachloro derivatives or dithizone itself under the same conditions. Thus complete extractions of cadmium, cobalt(II), copper(II), mercury(II), nickel, lead, thallium(I), zinc and bismuth with any of these dichlorodimethyldithizones are obtained only at higher pH's (Table 3) than with dithizone itself. The 4,4′-dichloro-2,2′-dimethyldithizone seems to be slightly more efficient than either the 3,3′- or 5,5′- isomer, or dithizone itself, for the separation of cadmium from zinc or cobalt from nickel.

The authors thank the Research Council of the University of Kuwait, for supporting this work.

REFERENCES

1 H. M. N. H. Irving, Dithizone, Analytical Sciences Monograph No. 5, The Chemical Society, London, 1977 and references therein.
2 A. M. Kiwan and G. A. Wanas, Anal. Chim. Acta, 144 (1982) 165.
3 D. M. Hubbard and E. W. Scott, J. Am. Chem. Soc., 65 (1943) 197.
4 A. M. Kiwan and A. Y. Kassim, Anal. Chim. Acta, 88 (1977) 177.

Analytica Chimica Acta, 182 (1986) 251—255
Elsevier Science Publishers B.V., Amsterdam — Printed in The Netherlands

Short Communication

DETERMINATION OF THE PURITY OF METHYL NITRITE

A. M. T. MAGALHÃES and P. M. CHALK*

School of Agriculture and Forestry, University of Melbourne, Parkville, Victoria 3052 (Australia)

(Received 27th June 1985)

Summary. The purity of methyl nitrite prepared by the esterification of methanol with aqueous nitrous acid was determined by absorbing gaseous samples in solutions of acidic potassium permanganate and hydriodic acid. Nitrate formed in the oxidation reaction was determined by steam distillation, and iodomethane formed in hydriodic acid was determined by gas-liquid chromatography. The method was used to evaluate purification procedures.

Methyl nitrite (CH_3ONO) has been used as a convenient source of methoxy and hydroxy radicals in studies concerned with free-radical reactions which lead to the formation of photochemical smog [1—4]. The radicals are generated as primary or secondary products of the photolysis [1—3] or pyrolysis [4] of methyl nitrite. Methyl nitrite has also been used as a low-pressure chemical ionization reagent [5]. There is increasing interest in sources of methyl nitrite in the environment, including formation in soil [6] and combustion processes such as vehicle emissions [7] and cigarette smoke [8]. In all studies concerned with the chemistry of methyl nitrite, synthesis and purification of the compound is required. Rook [9] claimed that preparation and purification procedures have not been very efficient.

Methyl nitrite is generally synthesized by the esterification of methanol by aqueous nitrous acid [1, 2, 5, 6, 10—13] or other nitrosating reagents such as dinitrogen tetroxide [7, 8] or nitrosylsulphuric acid [3, 9]. It has also been prepared by exchange between methanol and amyl nitrite [1, 4, 14]. Methyl nitrite (b.p., −12°C; m.p., −16°C) is usually condensed at −70 to −80°C by alcohol/dry ice mixtures, following passage through traps containing sodium hydroxide [2, 10, 12] or $KMnO_4/Na_2HPO_4/NaNO_3$ [6, 8, 11] to remove oxides of nitrogen, and through drying tubes containing anhydrous calcium chloride [2, 10, 12] or Drierite and anhydrous magnesium sulphate [8]. Final purification usually involves bulb-to-bulb distillations [1—4, 6—10, 12—14].

The purity of the end-product has been assessed by measurement of the vapour pressure (and hence boiling point) [14], and by identification of contaminants by gas chromatography [1, 4, 8], infrared spectroscopy [3, 9, 10]

0003-2670/86/$03.50

or mass spectrometry [10]. Qualitative or semi-quantitative estimates of purity are generally obtained by such indirect methods. The objective of this study was to develop a direct determination of the purity of methyl nitrite, based on the quantitative estimation of methoxy and nitrogen content, and to use the method to assess purification procedures.

Experimental

Synthesis of methyl nitrite. Methyl nitrite was prepared on a 1 M scale by the esterification of methanol by aqueous nitrous acid using the procedure described by Magalhães et al. [6]. The apparatus was darkened by exposure to γ-radiation to prevent photolysis of methyl nitrite. Four batches of methyl nitrite were prepared, two with a $KMnO_4/Na_2HPO_4/NaNO_3$ trap, and two without. Two bulb-to-bulb distillations were done on each batch [6]. The yield of methyl nitrite was determined gravimetrically. Duplicate samples (1.5 ± 0.015 ml, 25°C) were taken with a 2-ml gas-tight syringe (Precision Sampling, Series A-2) from each batch before and after each distillation for the determination of methoxy and nitrogen contents. The vessel containing the methyl nitrite was allowed to warm and the pressure was released five times before a sample was taken for analysis [6].

Determination of nitrogen. A sample of methyl nitrite was injected into a partially evacuated 100-ml amber flask (round bottom, long neck) stoppered with a No. 41 Suba-seal and containing 5 ml of 0.2 M potassium permanganate in 0.5 M sulphuric acid at 30°C. After 15 min, the nitrate content of the solution was determined by steam distillation [15]. In preliminary tests, the time required for complete absorption of methyl nitrite was established by measuring (every minute) the concentration of the gas in the flask atmosphere by gas chromatography [6].

Determination of methoxy content. A sample of methyl nitrite was injected into an amber 50-ml flask (round bottom, short neck) stoppered with a No. 41 Suba-seal and containing 1 ml of hydriodic acid (55% w/w). The flask had previously been placed in a freezer for 30 min and then immersed in an ice-bath, creating a negative pressure. After 3 min, 4 ml of hydriodic acid and 50 μl of 1-iodobutane internal standard solution [16] were added, and the flask was boiled under reflux for 30 min. The iodomethane formed was extracted with carbon tetrachloride and quantified by gas-liquid chromatography [16]. Again, the time requred for complete absorption of the gas was evaluated by gas chromatography [6].

Results and discussion

A gaseous sample of methyl nitrite (1.5 ml, 60.3 μmol N) was rapidly and quantitatively absorbed by 5 ml of acidic permanganate solution at 30°C (<15 min) and by 1 ml of hydriodic acid at 0°C (<3 min) (Fig. 1). The rates of absorption were first-order (Fig. 1), with the half-lives of methyl nitrite in the atmosphere being 68 s and 16 s for the acid permanganate and hydriodic acid absorbing solutions, respectively. Absorption of methyl nitrite in acidic

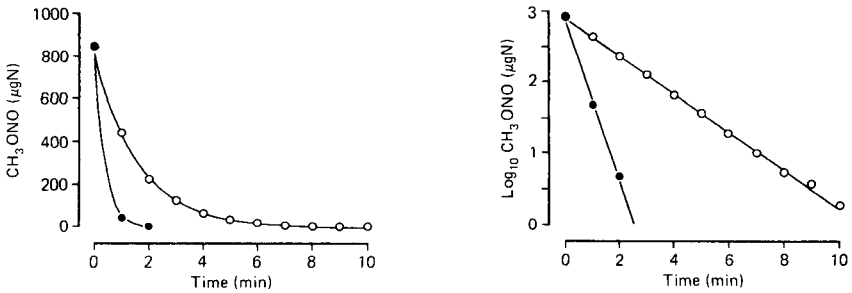

Fig. 1. Concentration of methyl nitrite in the atmosphere of flasks containing 5 ml of acidic permangante solution at 30°C (○), and 1 ml of hydriodic acid at 0°C (●). The linear-regression equation, correlation coefficient, standard error, standard error of the slope, standard error of the intercept, number of observations and rate constant, respectively, are: (○) $\log_{10} Y = 2.896 - 0.266 X$, 0.999, 0.047, 0.003, 0.019, 22, 0.613 min^{-1}; (●) $\log_{10} Y = 2.887 - 1.129 X$, 0.997, 0.090, 0.045, 0.058, 6, 2.600 min^{-1}.

permangante solution provided a convenient means for the determination of nitrogen by quantifying the nitrate formed in solution after steam distillation [15]. Similarly, absorption of methyl nitrite in hydriodic acid at 0°C provided a convenient means for the determination of methoxy content, by quantifying the iodomethane formed in the Zeisel reaction by gas chromatography [16]. The use of two absorbing solutions was found to be necessary to permit complete analysis of methyl nitrite, because methoxy is oxidized to carbon dioxide in acidic permanganate, and nitrogen could not be quantitatively recovered from the hydriodic acid.

The purity of methyl nitrite before bulb-to-bulb distillation was only marginally improved by the use of the $KMnO_4/Na_2HPO_4/NaNO_3$ solution trap (Table 1). However, two distillations were required to obtain a pure sample when the trap was not used, whereas only one distillation was necessary when the trap was included (Table 1). Stevenson and Kirkman [11] reported that methyl nitrite was slowly absorbed by the $KMnO_4/Na_2HPO_4/NaNO_3$ solution used to remove nitric oxide contamination. However, the yield of pure methyl nitrite prepared on a 1 M scale with the trap after one distillation (54.9 g, 89.9%) did not differ significantly from the yield obtained without the trap after two distillations (55.4 g, 90.7%), indicating that absorption of methyl nitrite in the trap was not important.

The principal impurities reported in methyl nitrite are methanol [1, 3, 4] and nitrogen oxides [12, 13]. The extent of contamination with methanol following bulb-to-bulb distillation has been reported as 0.3% [1], <1% [3] and traces of methanol with an unknown impurity of ≈0.2% [4]. Significant contamination with oxides of nitrogen is indicated by a green liquid [9, 12—14], possibly caused by the presence of dinitrogen trioxide (blue) in the pale-yellow pure liquid [12]. The green methyl nitrite obtained by Thompson and Purkis [14] had a boiling point of —18°C compared to the accepted value

TABLE 1

Effect of $KMnO_4/Na_2HPO_4/NaNO_3$ trap and bulb-to-bulb distillation on the recovery of nitrogen and methoxy in a 1.5-ml sample of methyl nitrite at 25°C

Number of distillations	Recovery[a] (μmol)			
	Without trap		With trap	
	N	$-OCH_3$	N	$-OCH_3$
0	54.4 ± 1.4 (90.1)	53.1 ± 1.9 (88.1)	56.2 ± 1.0 (93.1)	55.9 ± 0.9 (92.7)
1	59.3 ± 0.7 (98.4)	58.9 ± 0.4 (97.7)	60.2 ± 0.5 (99.8)	60.2 ± 0.2 (99.8)
2	60.2 ± 0.5 (99.8)	59.9 ± 0.6 (99.4)	60.2 ± 0.1 (99.8)	60.3 ± 0.3 (100.0)

[a]1.5 ml of pure sample contains 60.3 μmol N and $-OCH_3$. Data are means of 4 determinations with standard deviation, comprising 2 samples from each of 2 batches of CH_3ONO. Data in parentheses are mean % purities.

of −12°C for the pure compound. Significant contamination with nitrogen oxides appears to be caused by condensation at −196°C with liquid dinitrogen [9, 13, 14], or by the presence of oxygen during synthesis [12]. This contamination can be minimized by condensation in alcohol-dry ice mixtures and by the use of oxygen-free dinitrogen carrier gas during synthesis. The relative concentrations of nitrogen and methoxy in a sample can indicate contamination with oxides of nitrogen or methanol. However, as the nitrogen and methoxy concentrations did not differ significantly for any treatment (Table 1), it was not possible to ascertain the nature of the contamination.

We thank the Wheat Industry Research Council of Australia and the Conselho Nacional de Desenvolvimento Científico e Tecnológico-CNPq (Brasil) for financial support. Mr. A. A. Hendy provided technical assistance.

REFERENCES

1 R. A. Cox, R. G. Derwent, S. V. Kearsey, L. Batt and K. G. Patrick, J. Photochem., 13 (1980) 149.
2 R. Atkinson, W. P. L. Carter, A. M. Winer and J. M. Pitts, Jr., J. Air Pollut. Control Assoc., 31 (1981) 1090.
3 N. Sanders, J. E. Butler, L. R. Pasternak and J. R. McDonald, Chem. Phys., 48 (1980) 203.
4 L. Batt, R. D. McCulloch and R. T. Milne, Int. J. Chem. Kinet., 7 (1975) 441.
5 W. D. Reents, Jr., R. C. Burnier, R. B. Cody and B. S. Freiser, Anal. Chem., 54 (1982) 1245.
6 A. M. T. Magalhães, P. M. Chalk, A. B. Rudra and D. W. Nelson, Soil Sci. Soc. Am. J., 49 (1985) 623.
7 A. Jonsson and B. M. Bertilsson, Environ. Sci. Technol., 16 (1982) 106.
8 C. H. Sloan and B. J. Sublett, Tobacco Sci., 11 (1967) 21.

9 F. L. Rook, J. Chem. Eng. Data, 27 (1982) 72.
10 J. P. Gilman, T. Hseih and G. G. Meisels, J. Chem. Phys., 78 (1983) 1174.
11 F. J. Stevenson and M. A. Kirkman, Nature (London), 201 (1964) 107.
12 J. A. Gray and D. W. G. Style, Trans. Faraday Soc., 48 (1952) 1137.
13 J. A. Davidson and B. A. Thrush, United States National Technical Information Service, AD/A Report No. 003861/2GA, 1974, 22 pp.
14 H. W. Thompson and C. H. Purkis, Trans. Faraday Soc., 32 (1936) 674.
15 C. J. Smith and P. M. Chalk, Analyst (London), 104 (1979) 538.
16 A. M. T. Magalhães and P. M. Chalk, Analyst (London), 111 (1986) 77.

Analytica Chimica Acta, 182 (1986) 257—259
Elsevier Science Publishers B.V., Amsterdam — Printed in The Netherlands

Short Communication

X-RAY DIFFRACTION AND CHEMICAL ANALYSES OF MAGNESIUM ALUMINIUM FLUORIDE

K. W. RILEY* and A. HORNE

CSIRO Division of Fossil Fuels and CSIRO Division of Mineral Physics and Mineralogy, P.O. Box 136, North Ryde, NSW 2113 (Australia)

(Received 4th November 1985)

Summary. The preparation of magnesium aluminium fluoride by addition of hydrofluoric acid to a mixture of aluminium and magnesium nitrates is described. The x-ray diffraction pattern of the complex, identified by chemical and thermogravimetric analyses as $MgAlF_5 \cdot 2.2\ H_2O$, is reported.

In a study of precipitates formed during the decomposition of silicate rocks with hydrofluoric acid, Langmyhr and Kringstad [1] identified $MgAlF_5 \cdot 2.7\ H_2O$. Although they used x-ray diffraction (x.r.d.), x-ray diffraction data for this complex have not been published to date. It is important that the x.r.d. pattern be available for identification of any insoluble fluorides that may form during the commonly used hydrofluoric acid dissolution of silicate materials. This communication reports the results of x-ray diffraction and chemical analyses of $MgAlF_5 \cdot xH_2O$.

Experimental

Analytical reagent-grade chemicals and glass-distilled water were used in the preparation and subsequent analysis of the complex.

Preparation of $MgAlF_5 \cdot xH_2O$. Aluminium nitrate nonahydrate (3.75 g) and magnesium nitrate hexahydrate (2.56 g) were dissolved in 100 ml of water in a polyethylene beaker; 2 ml of 50% (w/w) hydrofluoric acid was added and the solution was allowed to stand overnight (ca. 16 h). The precipitate formed was filtered off (Whatman No.42 paper), washed with water, transferred to a platinum crucible and dried at 110°C in an air oven. This method differs from that used by Langmyhr and Kringstad [1], who added an excess of hydrofluoric acid directly to aluminium and magnesium oxides, heated the solution and filtered off the precipitate.

Chemical analysis. The Al, Mg and F contents of the dried complex were determined in triplicate. To determine the Al and Mg concentrations, subsamples (100 mg) of the complex were digested with 1.5 ml of 70% (w/w) perchloric acid in PTFE beakers. The perchloric acid was removed by evaporation, the residue was dissolved in nitric acid (2 ml) by warming, water was

0003-2670/86/$03.50

added and the volume was adjusted to 100 ml. Standards were prepared from Titrisol reagents by serial dilution in 2% (v/v) nitric acid. The concentrations of Al and Mg were determined with a Varian-Techtron AA5/IM6 instrument, under the conditions recommended by the manufacturer. Fluoride was determined by the method of Palmer [2]. Subsamples (150 mg) of the complex were fused with 4 g of sodium hydroxide in a nickel crucible by heating gently over a Meker burner. The cooled melt was leached with water and the volume was adjusted to 100 ml. Aliquots (5 ml) were added to 25 ml of 0.4 M ammonium sulphosalicylate (pH 9.5) in a 50-ml volumetric flask and the volume was adjusted with water. The potentials of the solutions were measured with an Orion 701A meter equipped with a fluoride electrode and single-junction reference. Varying amounts of sodium fluoride ("Baker Analyzed" reagent) were subjected to the same procedure and used as standards. Results of the chemical analysis are given in Table 1.

Thermogravimetric analysis. The water content was estimated from the loss of mass on heating the complex in a stream of nitrogen. The complex (ca. 10 mg) was heated to 900°C from ambient temperature at 20°C min^{-1}, with a Dupont Model 951/990 thermogravimetric/thermal analyzer. The plot of temperature versus mass is shown in Fig. 1. By 400°C, there is a discrete loss of 21.5 ± 0.5% (w/w). This agrees well with the estimate by difference of 21.2% (w/w) H_2O. At temperatures greater than 500°C, the complex gradually decomposes.

X-ray diffraction analysis. X-ray diffraction data were obtained with a Philips instrument. The PW1030 generator was run at 45 kV and 45 mA; the divergence and receiving slits were set at 1/2°; the scan rate of the vertical goniometer (graphite monochromator) was 1/8 (2θ) min^{-1} from 4° to 100° (2θ); the radiation source was CuK_α (1.5418 Å); silicon was used as an internal standard. The x.r.d. pattern is shown in Fig. 2, and the relative intensities and calculated *d* spacings are given in Table 2.

Discussion

The data given in Table 2 and Fig. 2 should be of assistance in identifying complex fluorides that can form during the routine digestion of silicate materials with hydrofluoric acid.

TABLE 1

Chemical analysis of magnesium aluminium fluoride

	Determined (% w/w)	Average (% w/w)	Stoichiometric ratio
Al	14.6, 14.6, 14.5	14.6	1.00
Mg	12.9, 12.9, 12.9	12.9	0.98
F	51.2, 51.0, 51.6	51.3	4.99
H_2O	Balance	21.2	2.17

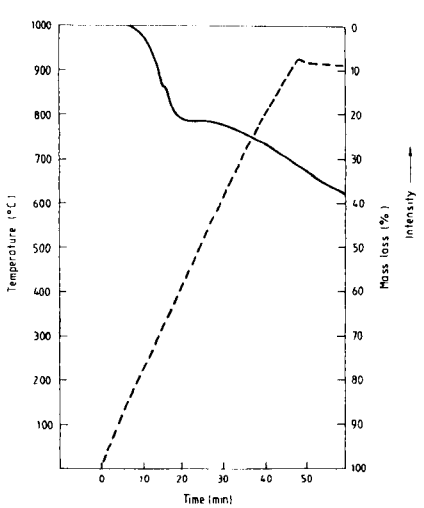

Fig. 1. Thermogravimetric analysis of $MgAlF_5 \cdot xH_2O$: (---) temperature; (—) mass loss.

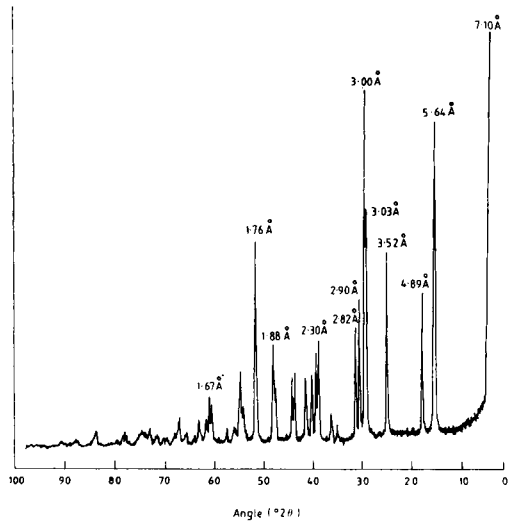

Fig. 2. X.r.d. trace of $MgAlF_5 \cdot xH_2O$ (CuK_α, 1.5418 Å).

TABLE 2

X.r.d. pattern of $MgAlF_5 \cdot xH_2O$ (radiation: CuK_α, 1.5418 Å)

d (Å)	I/I_1 (%)	d (Å)	I/I_1 (%)	d (Å)	I/I_1 (%)	d (Å)	I/I_1 (%)
7.10	4	2.82	28	2.03	16	1.53	9
5.64	88	2.53	3	2.01	4	1.51	11
4.89	46	2.45	6	1.90	15	1.50	7
3.52	53	2.30	27	1.88	26	1.47	5
3.28	3	2.27	25	1.76	45	1.41	3
3.03	63	2.22	16	1.69	11	1.39	7
3.00	100	2.16	16	1.67	20	1.22	3
2.90	37	2.06	18	1.60	3		

The water content of the complex is still somewhat uncertain. This work indicates that the composition is $MgAlF_5 \cdot 2.2\ H_2O$ (Table 1), whereas Langmyhr and Kringstad [1], using gravimetric techniques to determine Al, Mg and F, identified the complex as $MgAlF_5 \cdot 2.7\ H_2O$. Unfortunately, in both cases the water content was determined by difference, although in this work, the result was checked by thermogravimetric analysis. The variation in the analytical results is not surprising, considering the difference in the analytical techniques used.

REFERENCES

1 F. J. Langmyhr and K. Kringstad, Anal. Chim. Acta, 35 (1966) 131.
2 T. A. Palmer, Talanta, 19 (1972) 1141.

Analytica Chimica Acta, 182 (1986) 261—265
Elsevier Science Publishers B.V., Amsterdam — Printed in The Netherlands

Short Communication

DETERMINATION OF LEAD IN SOLUTION WITH A PIEZOELECTRIC QUARTZ CRYSTAL COATED WITH COPPER OLEATE

T. NOMURA*, T. OKUHARA and T. HASEGAWA

Department of Chemistry, Faculty of Science, Shinshu University, Asahi, Matsumoto 390 (Japan)

(Received 17th June 1985)

Summary. Copper(II) oleate was coated on a piezoelectric quartz crystal, and the copper removed by passing EDTA solution. The remaining coating reacted with aluminium, copper(II), iron(III) and lead ions in a flowing acidic solution, to form absorbed compounds which changed the frequency of the crystal. Lead (3—40 μM) could be determined at pH 5.5—5.8 with good reproducibility. Interfering metal ions (Al^{3+}, Cu^{2+}, Fe^{3+}) were masked with acetylacetone.

Piezoelectric quartz crystals have been used for the determination of ions in solution on the basis of the frequency change that resulted from the reaction of the ions at the electrodes of the crystal [1]. When the crystal is connected to the transistorized oscillator, there is a potential difference between the electrodes and many metal ions electrodeposit on the electrode, so that any frequency change caused by the reaction of ions with the electrodes other than by electrodeposition could not be detected. A crystal connected to an integrated circuit (i.c.) oscillator had so little potential difference between the electrodes that only mercury(II) and silver electrodeposited [2].

To determine metal ions by means of an organic reagent coated on the electrodes, the organic reagent should be insoluble in aqueous solution, and produce insoluble compounds with the metal ions which can be removed by dissolution before the next determination. The reagent should be selective for the metal ion, and be of small molecular weight so that there is a large weight change on combination with the metal ion. A suitable solvent must be available to dissolve the coating. Of the many reagents used in spectrophotometry and gravimetry, copper(II) oleate had the required properties, other than high selectivity, and was used in this investigation to determine lead.

Experimental

Apparatus and reagents. The piezoelectric quartz crystal used was a 9-MHz, AT-cut crystal (Toyo Craft) having a gold electrode (5-mm diameter) on

0003-2670/86/$03.50

each side. The crystal was immersed in ca. 1% (w/v) copper(II) oleate (Wako Pure Chemicals) in diethyl ether solution, and dried in air. The amount of substrate deposited gave a 3—6 kHz frequency change. The crystal was set up in a flow cell[3] and directly connected to an i.c. oscillator supplied with 5 V by a variable transformer. The same apparatus as used previously [1] was used to measure the frequency change resulting from lead binding. Copper was removed from the coating by passing 1 mM disodium EDTA solution until the frequency became constant, followed by 0.01 M acetate buffer (pH 5.6). The crystal was then ready for use.

Lead(II) stock solution (0.01 M) was prepared by dissolving the nitrate in water and standardizing with 0.01 M EDTA solution.

Procedure. Transfer the sample or standard solution, in 0.01 M acetate buffer (pH 5.6), and the reagent blank solution to their respective containers. Pass the reagent blank solution through the cell at 6.1 ml min^{-1}. When the crystal frequency has become constant (F_1), pass the sample solution for exactly 5 min and then the reagent blank solution until the frequency is constant (F_2). The frequency change, $\Delta F = F_1 - F_2$, is proportional to the concentration of lead, and a calibration graph may be constructed on this basis. After the experiment, pass 1 mM EDTA solution through the cell for ca. 5 min to remove metal ions in preparation for the next determination.

When the frequency obtained after the absorption of lead increases gradually as buffer solution flows through the cell (i.e., lead absorbed on the electrodes is gradually removed by the buffer solution which occurs after ca. 50 experiments), the substrate is removed by immersing the crystal in 1 M sodium hydroxide for several seconds, washing with water and then acetone, and drying in air. The crystal is then recoated with copper(II) oleate as described above.

Results and discussion

Reaction of an oleate coating with metal ions. Copper(II) oleate deposited on the crystal gradually dissolved on passing pH 9.4 solution, so that the crystal frequency increased. Copper(II) oleate was not dissolved by 5 mM phosphate solution (pH 6.7) but copper(II) was easily removed from the oleate by passing 1 mM EDTA, leaving oleic acid on the crystal. Common metal ions (50 μM) were passed through the cell to test for reaction with the oleic acid. (When oleic acid was coated directly on the crystal, it did not give frequency changes with metal ions.) At pH 6.7, Ca^{2+}, Sr^{2+}, Ba^{2+}, Cd^{2+}, Co^{2+}, Mn^{2+}, Ni^{2+} and Zn^{2+} were held, giving the frequency changes shown in Fig. 1A; Mg^{2+} and Cr^{3+} did not adsorb, and Al^{3+}, Cu^{2+}, Fe^{3+} and Pb^{2+}, which form phosphate precipitates, were not investigated. Metal ions held on the crystal could be removed with 1 mM EDTA.

In 0.01 M acetate buffer (pH 5.8), copper(II) oleate was not dissolved from the crystal, but copper(II) could easily be removed by 1 mM EDTA. Aluminium, Cu^{2+}, Fe^{3+} and Pb^{2+} were held on the resulting substrate (Fig. 1B).

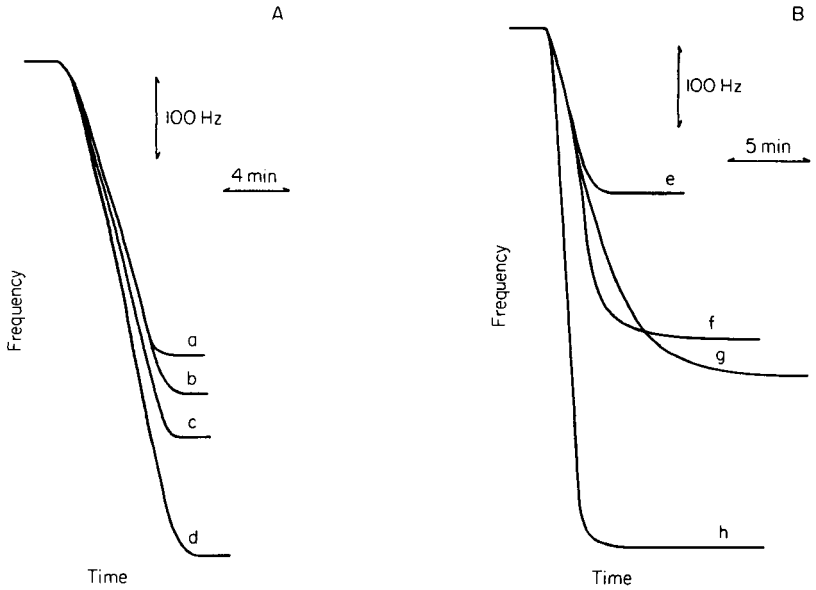

Fig. 1. Frequency change of the crystal coated with oleate caused by absorption of metal ions: (A) 0.05 mM metal, at pH 6.7; (B) 0.1 mM metal at pH 5.8. Metal ions were passed through the cell at 8.1 ml min^{-1}, for 3 min: (a) Mn^{2+}; (b) Co^{2+}, Zn^{2+}, Cd^{2+}; (c) Ni^{2+}; (d) Ca^{2+}, Sr^{2+}, Ba^{2+}; (e) Fe^{3+}; (f) Al^{3+}; (g) Cu^{2+}; (h) Pb^{2+}.

Of these metal ions, Cu^{2+} and Pb^{2+} could be removed from the substrate with 1 mM EDTA, but dissolution of Al^{3+} and Fe^{3+} with EDTA, citrate or oxalate was not complete. These four metal ions were also absorbed by the substrate when the applied voltage to the oscillator was cut off. It was supposed that the metal ions reacted with the substrate to form oleates.

The dependence on pH of the frequency change brought about by the absorption of these metal ions is shown in Fig. 2. Figure 3 shows the detailed effect of pH on the frequency/time dependence for lead. There was no absorption at pH $\leqslant$ 4.2, but the absorption gradually increased with increasing pH above this value. At lower pH values, absorbed lead gradually dissolved when the reagent blank solution was passed through the cell, and complete absorption required a long time in the higher pH region (Fig. 3). Other metal ions reacted with the substrate in a similar way to lead except for differences in the pH values.

The metal ions absorbed on the crystal could be removed by passing 1 mM EDTA solution (Cu^{2+} and Pb^{2+}) through the cell containing the crystal for ca. 5 min, 0.01 M citric acid for ca. 5 min (Al^{3+}) or 0.02 M acetylacetone for ca. 7 min (Fe^{3+}). These solutions did not dissolve the substrate from the crystal. Of these metal ions, the behaviour of lead was investigated in detail because it had the largest and most reproducible frequency change at pH 5.6.

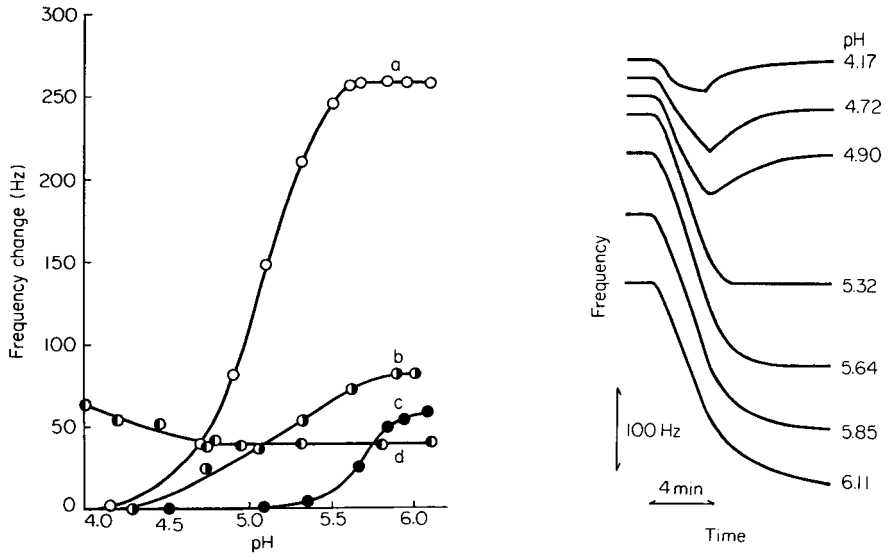

Fig. 2. Dependence of frequency change on pH for 30 μM metal ions flowing at 6.1 ml min^{-1} for 3 min: (a) Pb^{2+}; (b) Al^{3+}; (c) Cu^{2+}; (d) Fe^{3+}.

Fig. 3. Frequency/time dependence for the absorption of lead (30 μM) at various pH values. Lead solution was passed through the cell at 6.1 ml min^{-1} for 3 min.

Effect of the flow rate and reaction time. Absorption of lead increased with the increasing flow rate of the lead solution (Fig. 4A) but the increase was not in proportion to the increased flow rate because the lead absorbed on the crystal was slowly removed at the faster flow. In addition, the frequency changes at the faster flow rates, especially above 12 ml min^{-1}, had poor reproducibility. A flow rate of 6.1 ml min^{-1} is recommended, to achieve a compromise between good sensitivity, reproducibility and economy of buffer solution.

The frequency change caused by the absorption of lead was proportional to the reaction time (the period of the time allowed for the lead solution to pass through the cell), as shown in Fig. 4B. The graph deviated from linearity at >6 min because the substrate was becoming saturated with lead. Thus the lead sample solution was usually passed for 3 min. A longer reaction time, however, could be used for samples of lower lead concentration. The frequency change caused by a given amount of lead was independent of the amount of substrate on the crystal over the range 3 to 6 kHz. Each new coating, however, should be recalibrated.

Calibration graph and reproducibility. The calibration graph of frequency change against the concentration of lead is shown in Fig. 4C. It is not linear, but was reproducible over the range 3—40 μM. The standard deviation was 4.67 Hz (2.67%) for 6 determinations of 20 μM lead.

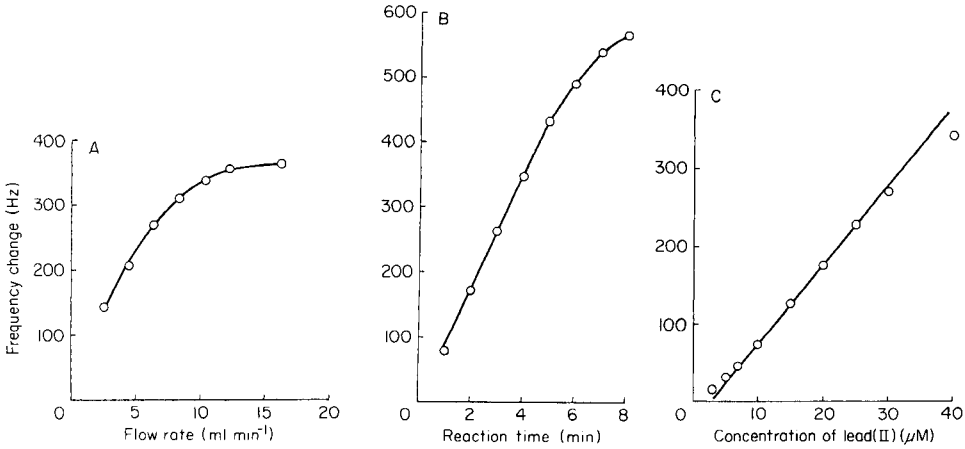

Fig. 4. Dependence of frequency change on different variables: (A) the flow rate of 30 μM lead in 0.01 M acetate buffer (pH 5.64), with a reaction time of 3 min; (B) the reaction time for 30 μM lead (pH 5.64) flowing at 6.1 ml min^{-1}; (C) the concentration of lead ions (pH 5.64) flowing at 6.1 ml min^{-1} for 3 min.

Effect of other ions. The effect of various ions on the determination of 20 μM lead was investigated; changes in frequency of more than ±6% (i.e., twice the standard deviation) were considered to result from interferences. As mentioned above, Cu^{2+}, Al^{3+} and Fe^{3+} interfered at pH 5.64, but Cu^{2+} did not interfere at pH 5.0. Mercury(II) and Ag^{+} also interfered by electrodeposition on the crystal [2]. Sulphide (0.1 mole ratio), phosphate and chromate (equal mole ratio) and ⩾100-fold molar amounts of perchlorate, sulphate, thiosulphate, carbonate and cyanide interfered by forming precipitates or complexes.

The effects of interfering cations (up to 10-fold amounts), such as Cu^{2+}, Al^{3+} and Fe^{3+}, could be eliminated by the addition of acetylacetone to the sample solution to give a final concentration of 0.01 M. Much larger amounts of these cations could be eliminated by extraction with 10 ml of 0.1 M acetylacetone in benzene solution from a sample solution adjusted to pH 5.6 with acetate buffer. The effects of Hg^{2+} and Ag^{+} (up to 10-fold and equivalent amounts, respectively) could be eliminated by switching off the power to the oscillator while the sample solution containing acetylacetone was passing through the cell.

REFERENCES

1 T. Nomura, M. Watanabe and T. S. West, Anal. Chim. Acta, 175 (1985) 107.
2 T. Nomura and M. Ando, Anal. Chim. Acta, 172 (1985) 353.
3 T. Nomura and K. Tsuge, Anal. Chim. Acta, 169 (1985) 257.

Analytica Chimica Acta, 182 (1986) 267—270
Elsevier Science Publishers B.V., Amsterdam — Printed in The Netherlands

Short Communication

ELECTROLYTIC DETERMINATION OF MERCURY(II) IN WATER WITH A PIEZOELECTRIC QUARTZ CRYSTAL

T. NOMURA* and M. FUJISAWA

Department of Chemistry, Faculty of Science, Shinshu University, Asahi, Matsumoto 390 (Japan)

(Received 9th August 1985)

Summary. Mercury(II) is deposited on the gold electrodes of a piezoelectric quartz crystal and the change in weight causes a frequency change proportional to the mercury(II) concentration in the range 2—30 μM. Of the cations tested in 10-fold molar amounts, only silver(I) interfered.

A piezoelectric quartz crystal for the determination of mercury was reported by Ho and Guilbault [1]. Mercury(II) was reduced to the element, which was transferred by nitrogen to a cell containing the crystal where it amalgamated with the gold electrodes of the crystal. The increased weight of the electrodes and, therefore, the frequency change, was proportional to the concentration of mercury(II) in the solution. To remove the mercury from the electrodes for the next experiment, the crystal was heated to 170° C and hot purified air or nitrogen was passed through for several minutes. This method, which could determine 5—100 ng of mercury(II), was time-consuming and had poor reproducibility.

A piezoelectric quartz crystal connected to the transistorized oscillator is able to oscillate in solution. When a potential of ca. 0.4 V was applied between the electrodes, many metal ions electrodeposited on the electrode. In comparison, when the crystal was connected to an integrated circuit (i.c.) oscillator, with ca. 0.1 V between the electrodes only mercury and silver were deposited [2]. In this communication, mercury(II) was amalgamated directly onto a gold electrode of the crystal and determined by the frequency change resulting from the increasing weight.

Experimental

Apparatus and reagents. The piezoelectric quartz crystal was AT-cut, 9 MHz with gold electrodes (diameter 5 mm, Toyo Craft), connected to an i.c. oscillator (Normal-TTL) [2], which oscillated when 5 V was applied from a Metronix 521C power supply. The frequency was measured with a frequency counter (Takeda Riken TR-5142) or a chart recorder (Toa Electronics, FBR-252A). The crystal was held in a cell [3] which was connected

0003-2670/86/$03.50

to a thermostatted water bath (Taiyo Kagaku C-650) at 20 ± 0.05° C. Solutions were passed through the cell at a constant rate by a peristaltic pump (Tokyo Rikakikai MP-3).

A stock solution of mercury(II) (0.01 M) was prepared by dissolving the analytical-grade nitrate (Wako Pure Chemical Industries) in 0.5 ml of concentrated nitric acid and 100 ml of water and diluting to the appropriate concentration after standardization with 0.01 M EDTA. All other reagents were of analytical grade and were used as received.

Procedure. Pass 0.01 M acetate buffer (pH 4.6; reagent blank) through the cell containing the crystal at 7.6 ml min^{-1} until the frequency is constant (F_1). Replace the buffer by a mercury(II) sample solution for exactly 3 min and then restore the buffer flow until the frequency is again constant (F_2). Use the frequency change, $\Delta F = F_1 - F_2$, to give the mercury(II) concentration from a calibration graph prepared from the results for standard mercury(II) solutions using the procedure described above.

Remove mercury from the electrode by passing a 5 mM ammonium peroxydisulfate/5 mM nitric acid solution through the cell for 5 min with no electrolytic current, i.e., by switching off the connection between the crystal and the oscillator.

Results and discussion

Removal of mercury from the electrode. As there was a potential of ca. 0.1 V between the electrodes of the crystal connected to the i.c. oscillator, mercury(II) and silver electrodeposited on an electrode, thus changing its weight and resulting in a frequency change. If the crystal was disconnected from the oscillator during the period when the mercury(II) was in contact with the gold electrodes (and the crystal was made to oscillate only in the buffer), mercury again deposited on an electrode. However, the frequency change in the former case was larger and more reproducible than in the latter, under otherwise the same conditions; therefore, the former conditions were preferred for this work. Additional depositions produced a gradually decreasing frequency change after about 10 experiments, and oscillation ceased after 50—70 experiments. Mercury amalgamated on the electrode should therefore be removed frequently. Passing 2 M nitric acid for 5 min with no electrolytic current removed very little mercury. Immersion of the crystal (removed from the cell) in 5 M nitric acid for 10 s did not remove the mercury completely. However, a 1:1 mixture of 0.01 M ammonium peroxydisulfate and 0.01 M nitric acid removed the mercury in 5 min with no electrolytic current, without dissolving the gold electrodes.

Selection of buffer solution. As some metal ions form hydroxide precipitates and adhere to the electrodes of the crystal in neutral or alkaline solution, the frequency change resulting from mercury deposition could not be detected under such conditions. However, amalgamation also occurs in acidic solutions, as is recommended. Strongly acidic solutions could not be used for the reagent blank because the specific gravity, specific conductivity and

viscosity of the solution must be held at low and constant values for the frequency measurements [2]. Amalgamation from acetate buffer showed a constant frequency change in the pH range 3.5—6.0. Below pH 3.5 (citrate/hydrochloric acid buffer), the frequency change was slightly higher, but less reproducible. Therefore pH 4.6 acetate buffer is recommended.

Dependence of frequency change on the other conditions. It was supposed that a faster flow rate would give a greater frequency change. The frequency change, however, was almost constant above 5 ml min^{-1}, and only slightly lower below this flow rate; for example, with a solution of 1×10^{-5} M mercury(II) at pH 4.6 the frequency change was ca. 50 Hz at flow rates of 5—9 ml min^{-1}, but ca. 40 Hz at a flow rate of 2 ml min^{-1}. This indicates that the amalgamation rate was fairly slow. On the basis of these results, a flow rate of 7.6 ml min^{-1} was used in further experiments.

The period of time for passing the sample solution through the cell was exactly proportional to the frequency change. Reproducibility decreased at >5 min deposition time, so 3 min was used in this work although a longer time could give greater sensitivity.

Calibration and reproducibility. The calibration graph of frequency change (ΔF) against mercury(II) concentration was linear over the range 2—30 μM, and is described by the equation [Hg(II)] = $\Delta F/5.40$ μM, where ΔF is measured in Hz. The standard deviation was 1.41 Hz (2.6%) for five determinations of 10 μM mercury(II). The crystal positioned in the cell could be used for about 100 measurements, but with gradually decreasing sensitivity, so that frequent recalibration is recommended.

Effect of other ions. The effect of various ions on the determination of 10 μM mercury(II) was investigated. Changes in frequency of more than 5% (2σ) were considered to result from interferences. Ten-fold molar amounts of all cations except silver did not interfere. Silver interfered with the deposition on the crystal. A 100-fold molar amount of carbonate, perchlorate, sulfate, phosphate or chloride did not interfere. Equal concentrations of cyanide could be tolerated, as could ten-fold amounts of bromide, iodide, chromate or thiocyanate, all of which form stable complexes with mercury(II). Thiosulfate interfered when its amount was a tenth that of mercury.

The interference of silver presumably resulted from its electrodeposition onto the electrode, so that there would be no interference from silver when no potential was applied. However, silver under these conditions gave an increasing frequency change, but with poor reproducibility. The reason for this is not clear. When a citrate/hydrochloric acid buffer (0.01 M, pH 3.5) was used to precipitate silver chloride, equivalent amounts of silver could be tolerated but a 10-fold amount interfered (+23% error). As mercury(II) deposited when no voltage was applied to the transistorized oscillator but silver did not [3], the mercury(II) could be determined without interference from silver, but with less reproducibility. Interfering cyanide and thiosulfate must be eliminated with hydrogen peroxide as in the preceding paper [4].

REFERENCES

1 M. H. Ho and G. G. Guilbault, Anal. Chim. Acta, 130 (1981) 141.
2 T. Nomura, M. Watanabe and T. S. West, Anal. Chim. Acta, 175 (1985) 107.
3 T. Nomura and K. Tsuge, Anal. Chim. Acta, 169 (1985) 257.
4 T. Nomura and M. Iijima, Anal. Chim. Acta, 131 (1981) 97.

Analytica Chimica Acta, 182 (1986) 271—274
Elsevier Science Publishers B.V., Amsterdam — Printed in The Netherlands

Short Communication

PHOSPHORIMETRIC MICROASSAY FOR SUCCINYLTRIALANYL-*p*-NITROANILIDE-HYDROLYZING ENZYME ACTIVITY IN HUMAN SERUM

NAOTAKA KURODA, KIYOSHI ZAITSU and YOSUKE OHKURA*

Faculty of Pharmaceutical Sciences, Kyushu University 62, Maidashi, Higashi-ku, Fukuoka 812 (Japan)

(Received 12th November 1985)

Summary. A phosphorimetric assay of succinyltrialanyl-*p*-nitroanilide-hydrolyzing enzyme activity in human serum is described. *p*-Nitroaniline formed enzymatically is extracted with ether and determined phosphorimetrically in an ether/ethanol glass. The method is precise and very sensitive, requiring as little as 5 μl of human serum. The limit of detection is 10 pmol.

Succinyltrialanyl-*p*-nitroanilide (*N*-succinyl-Ala-Ala-Ala-*p*-nitroanilide; Suc-$(Ala)_3$-*p*NA) was first synthesized as a chromogenic substrate for pancreatic elastase [1]. Components of human serum [2, 3], bile [4], rheumatoid synovial fluid [5] and rat kidney [6] have been found to hydrolyze this substrate. It has been reported that the enzyme activity in human serum increases in patients with chronic active hepatitis, alcoholic hepatitis and choleodocholithiasis [2]. However, the clinical significance and physiological function of the enzyme are not fully understood. The activity in human serum has been assayed spectrophotometrically [2]. This method requires a relatively large amount of serum (200 μl) because of the low activity.

p-Nitroaniline has been shown to phosphoresce very intensely in a mixture of ether and ethanol at 77 K, and this finding has been applied to ultramicroassays for γ-glutamyltranspeptidase and leucine aminopeptidase in biological materials, based on the phosphorimetric determination of *p*-nitroaniline formed enzymatically [7, 8]. This communication describes a phosphorimetric microassay of the Suc-$(Ala)_3$-*p*NA-hydrolyzing activity in human serum.

Experimental

Reagents and apparatus. All chemicals and solvents were of analytical-reagent grade, unless otherwise stated. Double-distilled water was used. *p*-Nitroaniline (Wako, Osaka) was purified by recrystallization from water. The substrate solution was prepared by dissolving Suc-$(Ala)_3$-*p*NA (Protein Research Foundation, Osaka) in 30 mM Tris-hydrochloric acid buffer

0003-2670/86/$03.50

(pH 8.1) to give an 8.8 mM solution. The solution was stable for at least a month when stored at 4°C.

Uncorrected phosphorescence spectra and intensities of the sample solution in ether/ethanol were measured on the glassy solid at 77 K (liquid nitrogen) with a Hitachi MPF-3 spectrofluorimeter equipped with a Hitachi phosphoroscope attachment and quartz sample tubes (4.0 mm i.d., 5.0 mm o.d., 200 mm long; sample volume, ca. 150 μl). The spectral bandwidths of the excitation and emission monochromators were both 10 nm. The phosphorescence lifetimes were measured on a Hitachi V-550 synchroscope.

Sera were obtained from normal men (22—54 years of age) and nonpregnant women (21—22 years of age) in this laboratory. The sera were diluted 4 times with the Tris buffer (pH 8.1).

Assay procedure. The substrate solution (200 μl) was pre-incubated at 37°C for 2 min, and again incubated at 37°C for 90 min after addition of 20 μl of diluted serum. The reaction was stopped by the addition of 20 μl of 8.3 M acetic acid. The *p*-nitroaniline formed was extracted into 2.0 ml of ether by shaking on an Iwaki KM shaker (amplitude, 5 cm; ca. 250 rpm) for about 5 min. After brief centrifugation, the ether layer (1.4 ml) was diluted with 0.35 ml of ethanol. For the blank, the same procedure was used except that the diluted serum was replaced by the Tris buffer. For calibration, the substrate solution was replaced by solutions containing *p*-nitroaniline (0.05—50 nmol/200 μl). Phosphorescence intensities were measured at 510 nm with an excitation wavelength of 380 nm.

For the examination of the effect of various compounds on the Suc-$(Ala)_3$-*p*NA-hydrolyzing activity, diluted serum (20 μl) was pre-incubated with the compound to be tested, which was dissolved in the Tris buffer (50 μl), at 25°C for 30 min. A substrate solution (11.7 mM Suc-$(Ala)_3$-*p*NA, 150 μl) was added and again incubated at 37°C for 90 min. The incubated mixture was taken through the above procedure.

Results and discussion

The Suc-$(Ala)_3$-*p*NA-hydrolyzing enzyme in human serum was most active at pH 8.0—8.2 in the 30 mM Tris buffer. Tris gave a maximum and constant activity in a concentration range 20—30 mM; 30 mM (pH 8.1) was used in further experiments. Almost maximum and constant activity was obtained in the presence of 6.0—9.0 mM Suc-$(Ala)_3$-*p*NA, with an observed Michaelis constant value at 4.44 mM. Inhibition occurred at >9.9 mM (Fig. 1); 8.0 mM in the incubation mixture was used in the present procedure.

The reaction rate was constant for at least the first 180 min with incubation at 37°C. The amount of *p*-nitroaniline formed during an incubation time of 90 min was proportional to the human serum sample size up to at least 12.5 μl; 5.0 μl was used in the recommended procedure.

Inhibition of the Suc-$(Ala)_3$-*p*NA-hydrolyzing enzyme by various compounds is shown in Table 1. The enzyme activity was not affected by the serine protease inhibitor, phenylmethanesulfonyl fluoride. However, it was

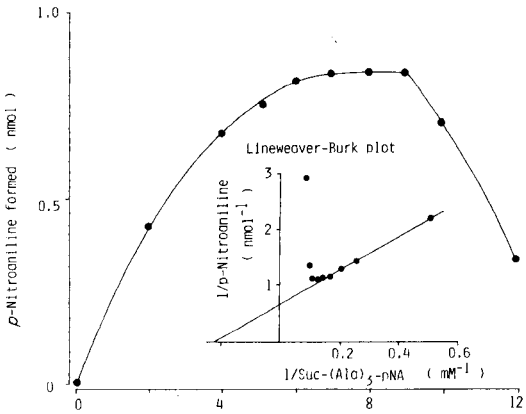

Fig. 1. Effect of the Suc-$(Ala)_3$-*p*NA concentration in the incubation mixture on the amount of *p*-nitroaniline formed. Portions (20 μl) of 4-times diluted serum containing various concentrations of Suc-$(Ala)_3$-*p*NA were treated as in the recommended procedure. The serum activity was 2.01 nmol min^{-1} ml^{-1}.

TABLE 1

Effect of various compounds on Suc-$(Ala)_3$-*p*NA-hydrolyzing activity in human serum

Compound	Concentration in pre-incubation mixture (mM)	Activity (%)
None	—	100.0
Phenylmethanesulfonyl fluoride	1.0	101.0
p-Chloromercuribenzoic acid	1.0	96.3
EDTA	5.0	27.8
	10.0	9.4
L-Cysteine	10.0	33.3
Zinc chloride	1.0	13.1
Magnesium chloride	1.0	99.0
Calcium chloride	1.0	99.5

strongly inhibited by EDTA. These results suggest that the activity is metal-dependent and not due to elastase, a serine protease. In addition, the activity was not inhibited by the thiol-blocking agent, *p*-chloromercuribenzoic acid, but was inhibited by L-cysteine or zinc chloride. These characteristics are similar to those observed by other workers [3—5].

p-Nitroaniline formed enzymatically was effectively extracted with ether from the acidified incubation mixture. The extract (1.4 ml) readily formed a clear solid at 77 K after mixing with 0.2—0.6 ml of ethanol; 0.35 ml of ethanol was used. The recovery of 1 nmol of *p*-nitroaniline added to the enzyme reaction mixture blank in the assay procedure was 96 ± 1% (mean

and standard deviation, n = 10). The calibration graph was linear up to 50 nmol of *p*-nitroaniline.

The phosphorescence excitation (maximum 380 nm) and emission (maximum, 510 nm) spectra, and lifetime (0.47 s) for the final solution were identical with those of *p*-nitroaniline dissolved in the same solvent.

The limit of detection for *p*-nitroaniline was 10 pmol (phosphorescence intensity of twice the blank). This is much better than that of the spectrophotometric method [2], and may permit the assay of the enzyme activity in only 0.5 μl of serum. The within-day precision of the present method was examined using serum with a mean activity of 1.87 nmol min^{-1} ml^{-1}. The coefficient of variation was 1.3% (n = 10).

The activity of the Suc-$(Ala)_3$-*p*NA-hydrolyzing enzyme in sera from normal subjects (21—54 years of age, n = 14) assayed by the present method was 2.02 ± 0.37 nmol min^{-1} ml^{-1} (mean and standard deviation). The values are similar to those obtained by other workers [2].

REFERENCES

1 J. Bieth, B. Spiess and C. G. Wermuth, Biochem. Med., 11 (1974) 350.
2 K. Katagiri, K. Ito, M. Miyaji, T. Takeuchi, T. Yoshikane and M. Saki, Clin. Chim. Acta, 95 (1979) 401.
3 M. P. Jacob, G. Bellon, L. Robert, W. Hornebeck, M. Ayrault-Jarrier, J. Burdin and J. Polonouski, Biochem. Biophys. Res. Commun., 103 (1981) 311.
4 M. Ogawa, G. Kosaki, S. Tanaka, K. Iwaki and M. Nomoto, Clin. Chim. Acta, 93 (1979) 235.
5 J. Saklatvala, J. Clin. Invest., 59 (1977) 794.
6 K. Katayama and M. Kuwada, Biochim. Biophys. Acta, 787 (1984) 138.
7 M. Yamaguchi, N. Kuroda, K. Zaitsu and Y. Ohkura, Anal. Chim. Acta, 135 (1982) 313.
8 N. Kuroda, M. Yamaguchi, J. Ishida and Y. Ohkura, Chem. Pharm. Bull., 31 (1983) 2913.

Analytica Chimica Acta, 182 (1986) 275—280
Elsevier Science Publishers B.V., Amsterdam — Printed in The Netherlands

Short Communication

LITHIUM-SELECTIVE ELECTRODES BASED ON NON-CYCLIC POLYETHER DIAMIDE CARRIERS IN CONJUNCTION WITH ORGANOPHOSPHORUS SOLVENT MEDIATORS

H. SUGIHARA, T. OKADA* and K. HIRATANI
Industrial Products Research Institute, M.I.T.I., Yatabe, Tsukuba, Ibaraki 305 (Japan)
(Received 12th July 1985)

Summary. Series of non-cyclic polyether amides were synthesized as derivatives of pyrocatechol. Poly(vinyl chloride) membrane electrodes based on some of these carriers exhibited lithium selectivities over other alkali or alkaline-earth metal ions when dioctyl phenylphosphonate alone or mixed with *o*-nitrophenyl octyl ether served as plasticizer. Selectivity coefficients for lithium over sodium were up to 2.1×10^1, over potassium up to 1.4×10^2 and over alkaline-earth metals up to 1.5×10^2. The detection limit for lithium was 5.0×10^{-5} mol dm^{-3}.

Polymeric-membrane ion-selective electrodes based on neutral carriers have been studied extensively in recent years [1—3]. Some of these electrodes exhibit superior selectivities towards alkali and alkaline-earth metal ions compared with other types of electrodes, and are used quite widely for clinical and analytical applications. The neutral carriers utilized are of several types, including antibiotics (e.g., valinomycin [2, 4]), crown compounds [5, 6], bis-crown compounds which form sandwich-type structure with ions [7—9], non-cyclic polyethers [10, 11] and cryptands [3, 12]. Various requirements must be met if the neutral carriers are to be successful: the carriers must possess good coordination sites (cavities) which fit the sizes of particular ions [13], but their structures should also be flexible enough to react reversibly at the ion-sensitive membrane/solution interface; obviously, the carriers must be sufficiently lipophilic to be soluble and/or mobile in the membrane. From these points of view, non-cyclic or sandwich-type polyether derivatives would be expected to have advantages over other types of carriers, apart from a few valuable crown ethers.

During a study of ion transport through water/chloroform interfaces, some non-cyclic polyether compounds were synthesized and shown to have excellent properties in selective ion transport [14, 15]. In the present study, non-cyclic polyether amides were synthesized and examined as carriers in poly(vinyl chloride) (PVC) ion-selective electrodes. Some of these compounds are shown to provide lithium ion-selective electrodes which might be useful for clinical applications.

0003-2670/86/$03.50

Experimental

Synthesis of carriers. 1,2-Bis-(2-chloroethoxy)-4-t-butyl benzene and 1,2-bis-(3-chloropropoxy)-4-t-butyl benzene were prepared as reported previously [15]. The diamines were prepared by the Gabriel reaction of the respective dichlorides with potassium phthalimide and hydrazine hydrate [16]. From these diamines, the diamides were prepared by acylation with 2 equivalents of acid chloride. To an ethereal solution (100 ml) of 10 mmol of 1,2-bis-(2-chloroethoxy)-4-t-butyl benzene or 1,2-bis-(3-chloropropoxy)-4-t-butyl benzene and 22 mmol of triethylamine was added 10 ml of diethyl ether containing 22 mmol of the relevant acid chloride, in a salt/ice bath and the mixture was stirred for 1 h. The mixture was then allowed to reach room temperature. Water was added, and the organic layer was washed with water, separated and dried over sodium sulfate. After removal of the solvent, the crude product was obtained; it was then purified by passage through a column of silica gel. The carriers synthesized were as follows:

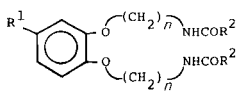

R^1		n	R^2
t-Bu	H		
1a	**2a**	3	$n\text{-}C_{15}H_{31}$
1b	**2b**	3	$n\text{-}C_{11}H_{23}$
1c	**2c**	3	$n\text{-}C_7H_{15}$
1d	**2d**	3	$n\text{-}C_3H_7$
3a	**4a**	2	$n\text{-}C_{15}H_{31}$
3b	**4b**	2	$n\text{-}C_7H_{15}$
3c	**4c**	2	$n\text{-}C_3H_7$

The numbers listed (**1a**—**4c**) are used to indicate the compounds in the later text.

Preparation of electrodes. The carrier (5—10 mg), plasticizer (250 mg), PVC (100 mg) and potassium tetrakis-(*p*-chlorophenyl)borate (KTCPB) (3 mg) were dissolved in 4 ml of tetrahydrofuran (THF). Plasticizers used were *o*-nitrophenyl octyl ether (NPOE), di-n-octylphenyl phosphate (DOPP), bis-(2-ethylhexyl) sebacate (DOS) and trioctyl phosphate (TOP). The mixture was poured into a Petri dish (42-mm diameter) which was kept horizontally on a mercury pool, and the THF was allowed to evaporate slowly at room temperature. A semi-transparent homogeneous membrane (ca. 0.2 mm thick) was obtained. A disk (5-mm diameter) was cut from the cast membrane and mounted on an ORION model 92 electrode body for e.m.f. measurements. The cell assembly for the electrode was as follows: $Ag/AgCl/10^{-2}$ mol dm^{-3} LiCl//membrane//test solution/10^{-1} mol dm^{-3} NH_4NO_3/sat. KCl/AgCl/Ag, where the silver/silver chloride electrode was used as the external reference electrode, connected by a salt bridge.

Measurements. Test solutions were prepared from analytical-grade chlorides of alkali and alkaline-earth metals and deionized water (specific conductivity $< 5 \times 10^{-7}\ \Omega^{-1}\ cm^{-1}$). The e.m.f. of quiescent solutions at 25°C was measured with an ORION model 701A digital Ionalyzer (input impedance

$>10^{13}$ Ω) and was recorded with a strip-chart recorder and a printer. The time for the electrode to attain a constant potential (within ±1 mV) for a period of 30 s is referred to as the response time. The potentiometric selectivity coefficient $k_{i,j}^{pot}$ of ion i over ion j was evaluated by the separate solutions method [17].

Results and discussion

The calibration curves obtained for carrier **1a** with NPOE as plasticizer are shown in Fig. 1. Changing the carrier content from 1.4% to 2.8%, with the other components of the membrane at the same amounts, produced a shift of the e.m.f. in the negative direction by 10—15 mV, but the relative potential responses amongst different ions remained almost unchanged. Changing the NPOE from 68.9% to 75.6% had no significant effect on the response. From these results, it can be concluded that the carrier content in the membrane did not significantly affect the selectivity of the electrode.

Figures 2 and 3 show the potentiometric selectivity coefficients for the carriers **1a—1d**, **2a—2d**, **3a—3c** and **4a—4c** in the PVC membranes with NPOE as plasticizer. The detection limits for monovalent cations ranged from 2.0×10^{-5} mol dm^{-3} for K^+ to 3.0×10^{-5}—1.0×10^{-3} mol dm^{-3} for Li^+. The

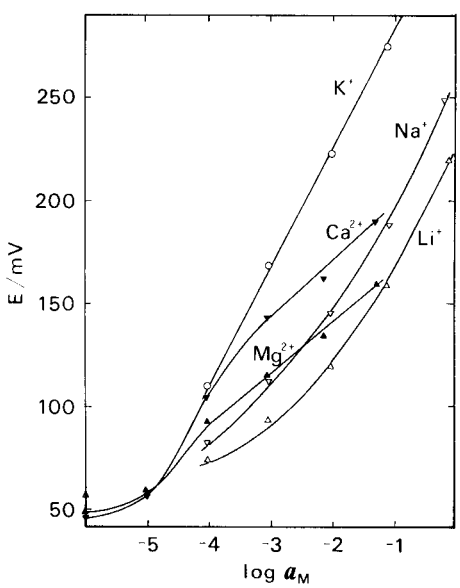

Fig. 1. Calibration curves for the electrode based on carrier **1a** with NPOE as plasticizer.

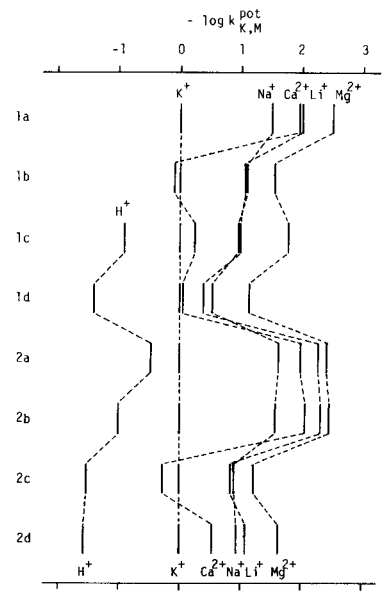

Fig. 2. Logarithmic potentiometric selectivity coefficients for K^+ over alkali and alkaline-earth metal ions measured for electrodes based on carriers **1a**, **1b**, **1c**, **1d**, **2a**, **2b**, **2c** and **2d** with NPOE as plasticizer.

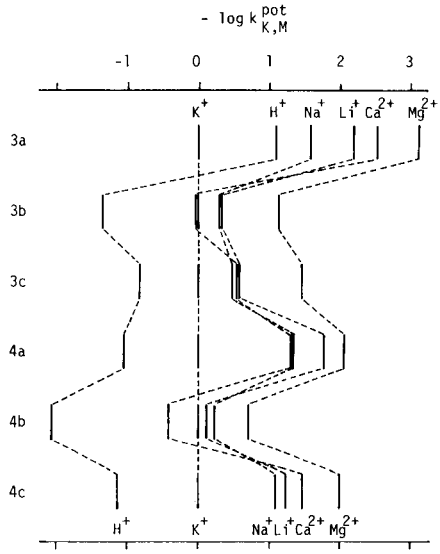

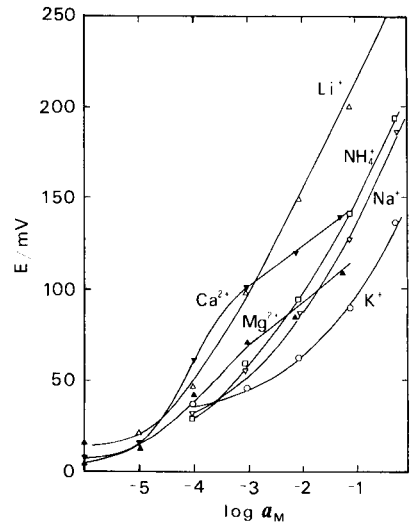

Fig. 3. Logarithmic potentiometric selectivity coefficients for K^+ over alkali and alkaline-earth metal ions measured for electrodes based on carriers **3a**, **3b**, **3c**, **4a**, **4b**, and **4c** with NPOE as plasticizer.

Fig. 4. Calibration curves for the electrode based on carrier **3b** with DOPP as plasticizer.

response times were 1.5—2 min in all cases. It has been reported that NPOE itself shows some selectivity for potassium ion [18]. A comparison of results obtained with and without a carrier indicated that the effects on selectivity were small when the carrier had end groups with relatively long chains. However, as the chain became short, as in compounds **1c**, **1d**, **3b** and **3c**, selectivity for K^+ over Li^+, Na^+ or divalent cations decreased. It appears that the chain length of the end group of the carrier has a larger effect than the length of the coordination chains, in complexing small ions such as Li^+. These results suggested the possibility that membranes with good selectivity toward Li^+ might be achieved if an appropriate plasticizer could be found.

The calibration curves obtained for the carrier **3b** with DOPP as plasticizer are shown in Fig. 4. Near-Nernstian response with 55 mV/decade was obtained for Li^+ and the detection limit for Li^+ was 5.0×10^{-5} mol dm^{-3}. The response time ranged from 1 to 3 min. Figures 5 and 6 show the selectivity coefficients for PVC membranes with carriers **1a—1d**, **2a—2d**, **3a—3c**, **4b** and **4c** with DOPP as plasticizer. It was shown in comparative tests that DOPP had some selectivity for lithium ion, and so it was expected that this plasticizer would help to improve the selectivity of these membranes towards Li^+. In the series of carriers, good Li^+ selectivity was obtained for carriers which had intermediate (e.g., **3b** with $R^2 = n\text{-}C_7H_{15}$) chain length of substituted groups.

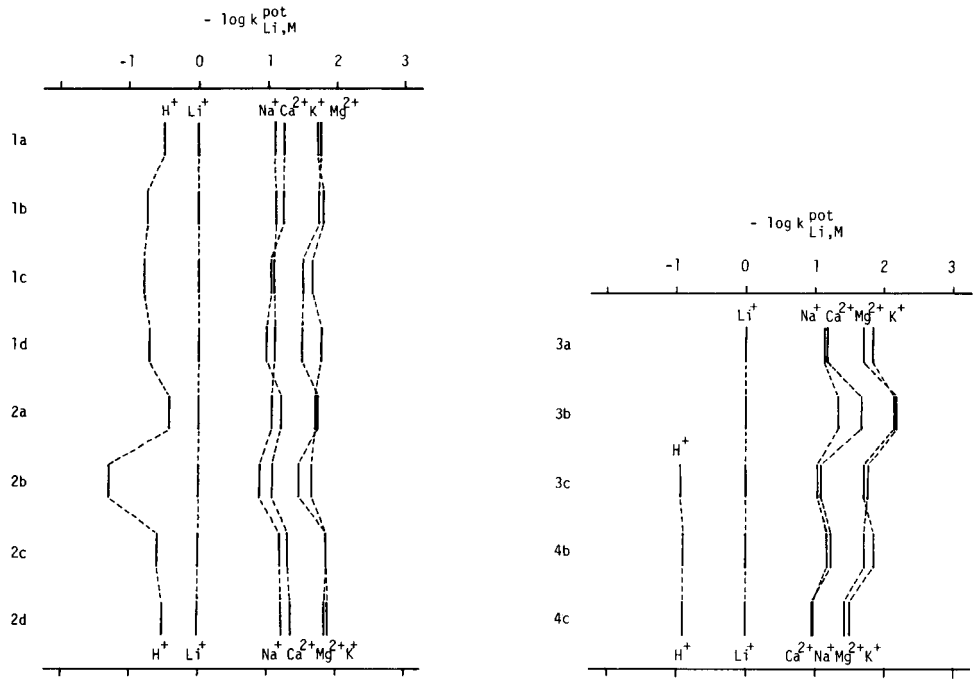

Fig. 5. Logarithmic potentiometric selectivity coefficients for Li^+ over alkali and alkaline-earth metal ions measured for electrodes based on carriers **1a**, **1b**, **1c**, **1d**, **2a**, **2b**, **2c** and **2d** with DOPP as plasticizer.

Fig. 6. Logarithmic potentiometric selectivity coefficients for Li^+ over alkali and alkaline-earth metal ions measured for electrodes based on carriers **3a**, **3b**, **3c**, **4b** and **4c** with DOPP as plasticizer.

Detaching the t-butyl group from the benzene ring appeared to increase Li^+ selectivity slightly (Fig. 5). The lipophilic additives KTCPB greatly contributed to improve Nernstian response of the electrode.

Carrier **1a** was incorporated into a PVC membrane, with a mixed (3/2) NPOE/DOPP plasticizer (Table 1). In this case, Li^+ selectivity over divalent cations was somewhat improved, which would be preferable for clinical applications.

When DOS was used as the plasticizer, no significant difference was observed in selectivity between monovalent cations. Instead, selectivities towards divalent cations increased in comparison with monovalent cations as the chain length of the substituted groups became longer. In the case of TOP, Li^+ selectivity appeared for the carriers with short substituted groups, but the membrane was also sensitive to divalent cations.

Carriers used in these experiments exhibited ion selectivities which also depended on the membrane composition, and good Li^+-selective electrodes were obtained with phosphorus plasticizers such as DOPP or TOP. The selec-

TABLE 1

Comparison of ion selectivities of Li^+-selective electrodes

Membrane components		log $k^{pot}_{Li,M}$					
Carrier	Plasticizer	H^+	Na^+	K^+	NH_4^+	Ca^{2+}	Mg^{2+}
1a	DOPP/NPOE = 3/2	0.57	−1.2	−2.0	—	−1.2	−1.9
3b	DOPP	0.70	−1.3	−2.2	−1.1	−1.7	−2.2
1c	TOP	0.93	−1.0	−2.1	—	−2.0	−2.2
Fluka 62559 [19]	TEHP	−0.1	−1.3	−2.2	−1.4	−3.3	−3.8
Crown ether [20]	NPOE	−3.4	−2.2	−2.0	−3.0	−4.3	−4.6
Crown ether [21]	NPOE	−3.5	−1.0	−0.84	−2.0	−4.0	−3.7
Crown ether [22]	TEHP	0.67	−1.0	−1.7	−0.47	−2.9	−2.8

tivity coefficients of the best electrodes found here are compared with those of other reported Li^+-selective electrodes in Table 1. Further work on improving selectivity by combining suitable plasticizers and carriers is in progress.

The authors express their great appreciation to Prof. T. Shono and Dr. K. Kimura of Osaka University for helpful discussions.

REFERENCES

1 D. Ammann, W. E. Morf, P. Anker, P. C. Meier, E. Pretsch and W. Simon, Ion-Selective Electrode Rev., 5 (1983) 3.
2 H. Freiser (Ed.), Ion-Selective Electrodes in Analytical Chemistry, Vol. 1, Plenum Press, New York, 1981, Chaps. 3 and 4.
3 S. J. Pace, Sensors and Actuators, 1 (1981) 475.
4 L. Stefanak and W. Simon, Microchem. J., 12 (1967) 125.
5 G. A. Rechnitz and E. Eyal, Anal. Chem., 44 (1972) 370.
6 O. Ryba, E. Knizàkovà and J. Petrànek, Collect. Czech. Chem. Commun., 38 (1973) 497.
7 K. Kimura, T. Maeda, H. Tamura and T. Shono, J. Electroanal. Chem., 95 (1979) 91.
8 K. Kimura, H. Tamura and T. Shono, J. Electroanal. Chem., 105 (1979) 335.
9 H. Tamura, K. Kumami, K. Kimura and T. Shono, Mikrochimica Acta, II (1983) 287.
10 M. Güggi, M. Oehme, E. Pretsch and W. Simon, Helv. Chim. Acta, 58 (1976) 2417.
11 R. A. Steiner, M. Oehme, D. Ammann and W. Simon, Anal. Chem., 51 (1979) 351.
12 J. Gajowski, B. Rieckemann and F. Umland, Fresenius Z. Anal. Chem., 309 (1981) 343.
13 J. M. Lehn, in J. D. Dunitz (Ed.), Structure and Bonding, Vol. 16, Springer-Verlag, Heidelberg, 1973, pp. 1—69.
14 K. Hiratani, K. Taguchi, H. Suguhara and K. Iio, Bull. Chem. Soc. Jpn., 57 (1984) 1967.
15 K. Hiratani, H. Sugihara, K. Taguchi and K. Iio, Chemistry Letters, Chem. Soc. Jpn., (1983) 1657.
16 S. R. Sandler and W. Karo, Organic Fundamental Group Preparations, Vol. 1, Academic Press, New York, 1968, pp. 331.
17 K. Srinivasan and G. A. Rechnitz, Anal. Chem., 41 (1969) 1203.
18 R. Bissig, E. Pretsch, W. E. Morf and W. Simon, Helv. Chim. Acta, 61 (1978) 1520.
19 M. Güggi, U. Fiedler, E. Pretsch and W. Simon, Anal. Lett., 8 (1975) 857.
20 S. Kitazawa, K. Kimura, H. Yano and T. Shono, J. Am. Chem. Soc., 106 (1984) 6978.
21 U. Olsher, J. Am. Chem. Soc., 104 (1982) 4006.
22 K. M. Aalmo and J. Krane, Acta Chem. Scand., Ser. A: 36 (1982) 227.

Analytica Chimica Acta, 182 (1986) 281—284
Elsevier Science Publishers B.V. Amsterdam — Printed in The Netherlands

Short Communication

A POTENTIOMETRIC DETECTOR FOR FOLLOWING pH SHIFTS IN LIQUID CHROMATOGRAPHY

JOSEPH GEORGES* and MOHAMED KHALIL

Laboratoire de Chimie Analytique 3-UA 04 0435, Université Claude Bernard, Lyon I, 69622 Villeurbanne Cedex (France)

(Received 26th July 1985)

Summary. A potentiometric detector suitable for measurement of pH shifts caused by cation-exchange phenomena in reverse-phase liquid chromatography is described. A capillary flow-through glass pH electrode and a small reference electrode are included in a design that produces reliable results in the acid pH range. The detector is calibrated in the steady-state and dynamic modes with pH reference solutions in water and water-methanol mixtures.

In order to measure pH shifts of eluents in reverse-phase liquid chromatography, in relation to cation-exchange phenomena [1—3], it was necessary to set up a flow-through detector with a glass pH electrode and a reference electrode. Such a detector needs to have a fast reproducible response, and the slope of the signal vs. pH plot should be as near Nernstian as possible over a wide dynamic range; further, the active part of the electrode should have the smallest possible dead volume. To fulfil such requirements, it is necessary to use a miniaturized detector capable of reaching a steady-state potential within about a second, which means that wetting of the sensing area by the solution must be rapid and complete [4]. Recent developments in flow injection analysis have led to the use of tubular flow-through cells incorporating a flat membrane electrode [5, 6] or in some cases capillary flow-through pH electrodes [7, 8].

The detector proposed here is of the capillary flow-through type and the reference electrode is mounted in such a way that it should satisfy the requirements for a chromatographic detector. The response of the system is checked first in the static mode and then in the dynamic mode with the detector connected to a capillary tube.

Experimental

Reagents. The pH reference solutions used for testing the detector in aqueous eluent were standardized solutions of perchloric acid (10^{-1}, 10^{-2}, 10^{-3} and 10^{-4} M) and standard buffers; potassium hydrogen tartrate (sat.; pH 3.56), phosphate (0.05 M, pH 7.0) and sodium tetraborate (0.01 M; pH 9.2) were used. For studies in water/methanol mixtures in which perchloric

0003-2670/86/$03.50

acid is completely dissociated (strong acid), the standard solutions of the acid were also convenient pH reference solutions. Another reference solution was obtained by buffering the water/methanol mixture with benzoic acid (0.1 M); the pH is 4.70 and 6.21 when the mixture contains 25% and 75% of methanol, respectively [9]. Except for these last buffers, the pH of the reference solutions was checked with a laboratory pH meter before use.

All reagents (analytical grade) were used as supplied. Water was distilled in glass after deionization. Because of the conditions of further utilization of the detector [3], no buffering agent was added to the carrier stream.

Apparatus. The flow system consisted of a Chromatem 380 pump (Touzart et Matignon) fitted with a pulse-damping system and connected to an injection valve with a 200-μl sample loop.

Capillary tubing (300 cm long, 0.25 mm i.d.) connected the valve to the detector. Potentials were recorded with a EPL-2 potentiometric recorder (Solea-Tacussel) fitted with a very high input impedance differential voltage plug-in (type TD-11-G; Solea-Tacussel).

Detector. The pH electrode was a capillary glass electrode (Ingold). The inner diameter of the capillary was about 0.8 mm and the dead volume corresponding to the active part of the capillary was less than 10 μl. The solution passed through the capillary into a jacket surrounding the electrode (Fig. 1) in which a miniature reference electrode was placed. The jacket had an outlet for the overflow of carrier stream. The reference electrode was a Ag/AgCl/saturated KCl electrode housed in a PTFE stem (Solea-Tacussel);

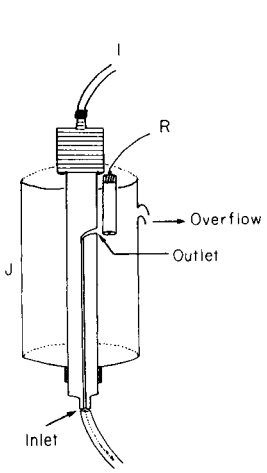

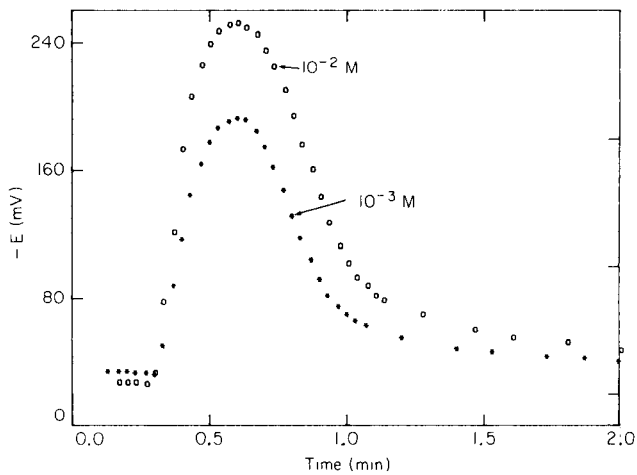

Fig. 1. The potentiometric cell: I, capillary glass flow-through Ingold electrode; R, miniature reference electrode Ag/AgCl/saturated KCl; J, jacket around the electrodes, filled with 1 M sodium chloride solution.

Fig. 2. Response curves in the dynamic mode obtained by injecting 200-μl samples into water: (○) 10^{-2} M; (*) 10^{-3} M. Flow rate 1 ml min^{-1}; chart speed 150 mm min^{-1}.

the porous ceramic junction was placed close to the outlet of the capillary electrode in order to decrease the resistance between the electrodes. In addition, the solution in the jacket surrounding the pH electrode was made conductive by addition of sodium chloride (to give a ca. 1 M solution) to prevent variations of the liquid-junction potential between the reference electrode and the solution. When necessary, the solution in the jacket was earthed to the potentiometer in order to avoid electrical noise and instability of the signal.

Results

The pH detector was tested under steady-state and dynamic or flow-injection conditions.

The detector response was first calibrated in the steady-state mode by injecting the pH reference solution directly into the inlet of the electrode from a syringe until a steady signal was reached. Then another solution was injected and the process was repeated until the investigated pH range (1—9) had been covered stepwise. The plots of potential vs. pH were linear over the whole pH range studied (pH 1—9.2). The slope of the response was 57 mV with water, 54 mV with 1:3 methanol/water and 52 mV with 3:1 methanol/water.

In the dynamic mode, a chromatographic column was not included, so as to avoid any cation-exchange phenomena which could change the amount of H^+ ions in the flow stream. Water was pumped continuously at a flow rate of 1 ml min^{-1} and the pH reference solutions were injected. In order to obtain easily manageable signals, 200-μl samples were injected and the signals were recorded at a fast chart speed. Typical response curves are shown in Fig. 2. Generally, the maximum potentials were lower than those obtained by the steady-state mode because of the influence of sample dispersion. Larger sample volumes would be necessary to obtain a potential plateau corresponding to the steady-state signals. The goal here was, however, to work as closely as possible to chromatographic conditions and to check if the amount of hydrogen ion measured by the detector corresponded to the amount injected. This was done by integrating the peak area after the potentials had been converted to pH by means of the calibration plots obtained from the steady-state data. The pH at any point of the response curve is given by the relation $pH = -E/a + b$, where E is the actual potential measured at this point, a is the slope of the calibration plot and b the pH at $E = 0$. The hydrogen ion concentration originating from the sample is given by 10^{-pH} minus the hydrogen-ion concentration in the carrier stream corresponding to the baseline of the response curve. Figure 2 shows only the parts of the response curves that were integrated. The baseline was regained after 3—4 min, but the difference in pH between the responses at 2 min and at 4 min was negligible, given that the pH of the water carrier stream was 5.5. About 20 points were sampled on each curve and calculations were done by a computer.

The results (Table 1) show good agreement, considering the poor precision attainable with logarithmic responses. The slope of the electrode response in

TABLE 1

Comparison between the quantity of hydrogen ion injected and the quantity detected in the dynamic mode. Samples were standardized perchloric acid solutions; the volume injected was 200 μl

Sample (M)	10^{-1}	10^{-2}	10^{-3}
H^+ injected (μmol)	20	2	0.2
H^+ detected (μmol)	19 ± 2	2 ± 0.2	0.18 ± 0.02

the dynamic mode can differ slightly from that based on steady-state calibration and the error in determining hydrogen ion concentration from Eqn. 1 will then be significant. Thus careful calibration under dynamic conditions is needed for best results. However, the design of the detection system appears to be very suitable for measurement of pH shifts in liquid chromatography [3].

REFERENCES

1 O. A. G. J. Van Der Houwen, R. H. A. Sorel, A. Hulshoff, J. Teeuwsen and A. W. M. Indemans, J. Chromatogr., 209 (1981) 393.
2 S. G. Weber and W. G. Tramposch, Anal. Chem., 55 (1983) 1771.
3 M. Khalil and C. Gonnet, Presented at the 9th International Symposium on Column Liquid Chromatography, Edinburgh, July 1985.
4 C. Hongbo, E. H. Hansen and J. Růžička, Anal. Chim. Acta, 169 (1985) 209.
5 J. Růžička and E. H. Hansen, Anal. Chim. Acta, 161 (1984) 1.
6 M. E. Meyerhoff and P. M. Kovach, J. Chem. Educ., 60 (1983) 766.
7 J. Růžička, E. H. Hansen and A. K. Ghose, Anal. Chem., 51 (1979) 199.
8 T. E. Edmonds and G. Coutts, Analyst (London), 108 (1983) 1013.
9 J. Juillard, Thesis, Université de Clermont Ferrand, France, 1968.

Analytica Chimica Acta, 182 (1986) 285—291
Elsevier Science Publishers B.V., Amsterdam — Printed in The Netherlands

Short Communication

THE INVESTIGATION OF COATING MATERIALS FOR THE DETECTION OF NITROBENZENE WITH COATED QUARTZ PIEZOELECTRIC CRYSTALS

J. A. O. SANCHEZ-PEDRENO[a], P. K. P. DREW and J. F. ALDER*

Department of Instrumentation and Analytical Science, University of Manchester Institute of Science and Technology, P.O. Box 88, Manchester M60 1QD (Great Britain)

(Received 18th July 1985)

Summary. Powdered activated charcoal, quadrol tetrabase and polyethylene glycol (PEG)-400 and -750 are used as coatings on 15-MHz quartz piezoelectric crystals for the detection of nitrobenzene in air. The response to nitrobenzene over the range 2—10 ppm (2—10 × 10^{-6} mol mol^{-1}) was almost linear for all the coatings except charcoal which exhibited marked non-linearity, as well as greater sensitivity than the other coatings. The charcoal response was linear over the range 0.7—7.6 ppm nitrobenzene. For the other coatings, sensitivity increased in the order tetrabase < quadrol < PEG-400 < PEG-750.

Nitrobenzene is widely used in industry as a solvent and in certain manufacturing processes. It is a moderately toxic compound and the currently accepted threshold limit value is 1 ppm (10^{-6} mol mol^{-1}, where 1 "mole" of air implies 22.4 l at 0°C and 1 atm). Coated piezoelectric-crystal detectors have been investigated for many compounds at such ppm concentrations and the application of these devices has been reviewed [1]. The mode of operation is that the analyte gas is selectively adsorbed onto a layer of substrate coated onto the electrodes of a quartz piezoelectric crystal. The adsorption is manifested as a frequency change if the crystal is made part of a resonant oscillator circuit. Although such detectors have not been applied specifically to nitrobenzene, they have been investigated for *o*-nitrotoluene [2] with a Carbowax (polyethylene glycol)-1000 coating and a flow-injection system.

Diphenylamine and 4,4′-methylene-bis(*N*,*N*-dimethylaniline) have been used [3] as selective spot-test reagents for nitro compounds and were considered as crystal coatings in this work. A number of chromatographic coatings were also tested and the use of activated charcoal powder was considered.

Experimental

Apparatus. The cell used in all experiments was constructed from a B34/35 glass socket. Figure 1 shows a line diagram of the flow rig and the inset shows the cell. The inlet and outlet tubes to the cell were arranged in such a way

[a]Permanent address: Department of Chemistry, University of Murcia, Murcia, Spain.

0003-2670/86/$03.50

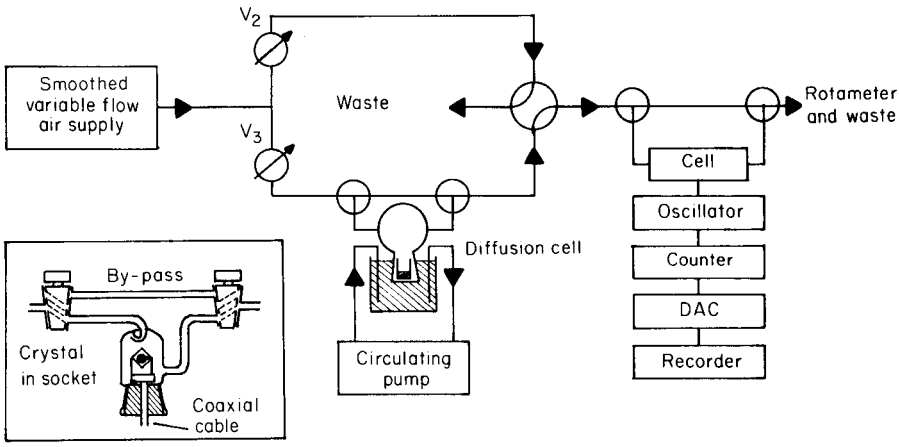

Fig. 1. Line diagram of flow rig. DAC = digital-to-analog converter. The inset shows the cell construction.

that the flow did not impinge directly onto the crystal surface, thus minimizing any flow dependence of the response. The crystal was inserted into a socket attached by a 50-ohm coaxial cable, through a rubber bung, to a Pierce crystal oscillator.

The rig permitted the control of nitrobenzene concentration through control of the flow rate across a diffusion tube. Air from a pump (A85-C; Charles Austen, West Byfleet, Surrey) was filtered and most of it was bled off to leave a flow which was controlled by a needle valve. Pump pulses were damped by means of two large vessels. The air was split into two flows and needle valves (V_2, V_3) were used to balance the two flows. One path led to a 50-ml flask in the base of which was held a hollow glass stopper into which the diffusion tube was placed (see below). The stopper was immersed in a 400-ml beaker, the water in which was circulated and maintained at a constant 25° C by means of a Churchill thermostat circulating pump (Churchill, Perivale, Middlesex). Both clean and "loaded" flows were passed to a 2-way 4-port tap. This enabled the flow over the diffusion tube and the cell to be continuous while allowing the alternation of clean and loaded air over the detector crystal.

The crystals used were 14.9-MHz AT-cut quartz units with gold electrodes in HC-25 mounts (Quartz Crystal Co., New Malden, Surrey). The oscillator used was a buffered Pierce-type oscillator built in-house connected to a regulated power supply. The frequency counter was a Philips PM6671 120-MHz device fitted with an internal digital-to-analog converter (PM9695) which converted any three successive digits from the display to an output of 0—1 V fed to a chart recorder (Tarkan 600, Kontron Instruments).

Atmospheric generation. A cylindrical glass sample tube (5.5 mm i.d. and 37 mm long) was used as a diffusion tube for the preparation of atmospheres

of nitrobenzene. The diffusion rate (Q) from such a tube has been calculated [4] to be $Q = (DMPA/LRT) \ln [P/(P-p)]$, where D is the diffusion coefficient of nitrobenzene, M is the molecular weight of nitrobenzene, P is the pressure within the diffusion tube, A is the cross-sectional area of the tube, R is the molar gas constant, T is the absolute temperature, L is the diffusion length of the tube and p is the partial pressure of nitrobenzene. The experimental diffusion rate was determined by measuring the weight loss over 8-h periods to within 10 μg. The experimental diffusion rate was found to be 6.54×10^{-8} g s^{-1} which compared well with a calculated release rate of 8.2×10^{-8} g s^{-1}. Responses of the coated crystals became constant within 15 min of rig switch-on.

Methods of coating. All materials except polyethylenimine (PEI) and charcoal were dissolved in chloroform and the resulting solutions were applied over the entire surface of one gold electrode using a cotton swab, as uniformly as possible. The amount of coating in each case corresponded to a decrease of 8.9 kHz (the theoretical mass sensitivity of the crystal is ca. 1 Hz ng^{-1}). The PEI, which was supplied as a 1:1 aqueous mixture, was further diluted with ethanol before application.

The charcoal used was initially passed through a 212-μm test sieve to remove the largest particles. The charcoal was placed in an applicator (Fig.2) and the slowest possible stream of air was passed that could be observed to deposit a fine black film on a piece of filter paper, to carry off only the finest particles. This stream was directed at the electrode from a distance of ca. 5 mm and moved about to generate a more uniform coating. Only a 0.57-kHz decrease in frequency was applied because the amount of charcoal corresponding to 0.75 kHz was found to stop oscillation of the crystal.

It is essential that only the very finest particles of charcoal be deposited on the crystal, as experiments showed that larger particle sizes were much less efficient for adsorbing nitrobenzene. An attempt was made to generate finer particles by grinding in a ball-mill. However these particles of charcoal agglomerated and resisted projection.

Reagents. All reagents were of the purest form available, unless otherwise stated. Quadrol (N,N,N',N'-tetrakis-2-hydroxypropyl-1,2-diaminoethane), Carbowax (PEG)-750, Carbowax (PEG)-1000, polyvinylpyrollidone and phenyldiethanolamine succinate were from Phase Separations, Queensferry, Clwyd. Tetrabase (4,4'-methylene-bis[N,N-dimethylaniline), nitrobenzene (99%), tri-n-octylamine, diphenylamine and polyethylenimine (50% solution in water) were obtained from Aldrich. PEG-400 and -1540 (for GLC use) and charcoal (decolourizing powder, activated) were from BDH.

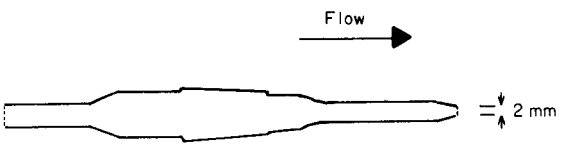

Fig. 2. Applicator used for coating with charcoal.

Results and discussion

Eight coating materials were investigated on crystals exposed to 7 ppm nitrobenzene. The data collected are shown in Table 1. Charcoal showed the highest sensitivity; PEG-750 was the most sensitive of the polyethylene glycols. An uncoated crystal showed little response to nitrobenzene.

Adsorption or desorption times shown relate to 100% completion, i.e., until the frequency of the crystal becomes constant or, for volatile coatings, parallel to the baseline. All the coated crystals showed a completely reversible response at the small weight of coating used. The adsorption and desorption times increased with the sensitivity of the coating and the rates of frequency change were generally greatest for the most sensitive coatings.

The reproducibility of response of each coating to 7 ppm nitrobenzene was found by exposing the crystals to a series of six adsorption/desorption cycles each comprising a 6-min exposure followed by 4 min in clean air or, for charcoal, 8 min because of its longer desorption time. Table 2 shows the amount of adsorption after 4 min as a fraction of the total, and the reproducibility of the response. Charcoal gave the most reproducible results of the coatings tested.

A frequency decrease was found generally for all coatings when the flow was completely stopped. For triethanolamine and quadrol this was presumably partly due to water adsorption, but in each case it could be that nitrobenzene previously adsorbed on other parts of the apparatus desorbed to be adsorbed preferentially onto the coating.

Other coatings were investigated and rejected because of their rapid evaporation (bleeding) from the crystals. Dicyclohexylamine (b.p. 119°C) could be observed to vaporize rapidly. Diphenylamine (b.p. 302°C, m.p. 53°C) lost 0.25% of the mass of coating per minute and tri-n-octylamine (b.p. 365°C) lost 0.8% min^{-1} over the first few minutes.

The baseline stabilities of charcoal and tetrabase were very good but that of triethanolamine was too erratic, in view of its low sensitivity, to give a

TABLE 1

Response of several coatings to 7 ppm nitrobenzene in dry air at a flow rate of 94 ml min^{-1}

	Amount coating (kHz)	Response ΔF (Hz)	Response times (min)		Rate of adsorption (Hz min^{-1})
			Adsorption	Desorption	
Charcoal	0.57	−136	16	13.2	−8.5
PEG-400	8.8	−53	7	3.2	−7.6
PEG-750	8.9	−86	10	4.4	−8.6
PEG-1000	8.9	−24	4.8	2.6	−5.0
PEG-1540	8.9	−14	2.8	2.4	−5.0
Quadrol	8.9	−48	8	5	−6.0
Tetrabase	8.9	−31	6	2.8	−5.2
Triethanolamine	8.8	−18	4	2.8	−4.5
Uncoated (blank)	0.0	−13	3.5	2.4	−3.7

TABLE 2

Reproducibility of responses to a series of six adsorption/desorption cycles[a]

	R.s.d. (%)	% Total adsorption
Charcoal	1.3	91
PEG-400	2.5	97
PEG-750	3.5	94
Quadrol	4.4	98
Tetrabase	2.4	100

[a]Each cycle involved exposure to 7 ppm nitrobenzene for 6 min and to clean air for 4 min (8 min for charcoal).

useful signal-to-noise level. The other coatings were intermediate in performance. When the inflowing air was dried with silica gel, the baseline for triethanolamine could be stabilised and it is therefore presumed that baseline wandering is due to short-term variations in laboratory humidity. On passage of dry air, a triethanolamine coating reversibly lost 19% of its mass, presumably as water.

Several calibration graphs of response to nitrobenzene for different coatings are shown in Fig. 3. Analytical performance data are given in Table 3. Linear ranges up to 10 ppm were obtained for PEG-400, PEG-750 and quadrol and up to 7 ppm for tetrabase, above which concentrations negative curvature occurred. The response for charcoal (Fig.4) is linear from 0.7 to 7.6 ppm, but above this attains a plateau, and at very low concentrations appears to have higher sensitivity. An explanation for this effect may be that saturation coverage occurs and adsorption of further molecular layers may be thermodynamically unfavourable. For charcoal, the adsorption is almost certainly pure physisorption. The calculated frequency change for adsorption of one monolayer at the mass loadings on the crystals is ca. 9 Hz. The saturation weight change for charcoal (150 Hz change) is 24% of the charcoal mass (570 Hz change) which corresponds reasonably to a supposed pore volume fraction of 20—30%. The nature of the adsorption on the other coatings is less certain and it would be unwise to extrapolate this argument to them at present.

Conclusions

Several coatings were found useful for nitrobenzene at ppm levels in laboratory air at room temperature: PEG-400, PEG-750, quadrol, tetrabase and activated charcoal. The most sensitive was charcoal, which allowed detection below 1 ppm. Further investigation of the effect of charcoal particle size would be interesting. Interference from other organic gases has not been investigated, and charcoal is well known for its inselective adsorption. The air used to generate the nitrobenzene-contaminated atmosphere was direct

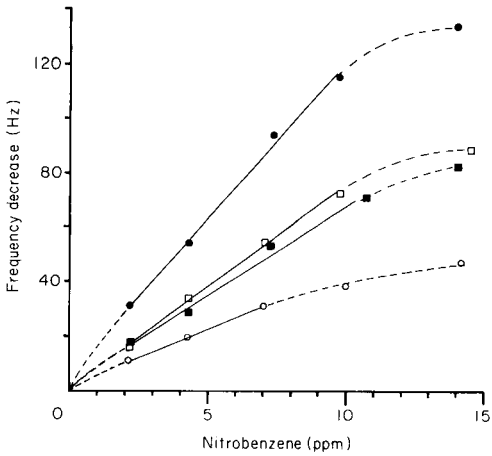

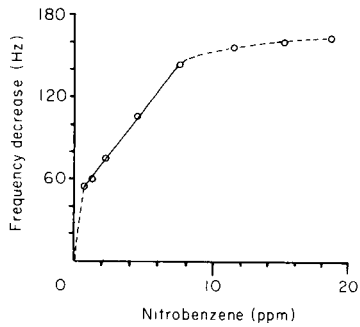

Fig. 3. Responses of various coatings to nitrobenzene: (□) PEG-400; (●) PEG-750; (○) tetrabase; (■) quadrol.

Fig. 4. Response of charcoal-coated crystal to nitrobenzene.

TABLE 3

Analytical performance data for various coatings used to adsorb nitrobenzene

	Amount of coating (kHz)	Linear range (ppm)	No. of points	Least-squares regression		Correlation coefficient
				Slope (Hz ppm^{-1})	Intercept (Hz)	
Charcoal	0.57	0.73—7.6	5	—13.1 ± 0.3	44 ± 1	0.999
PEG-400	8.8	2.1—9.7	4	—7.3 ± 0.3	2 ± 2	0.999
PEG-750	8.9	2.2—9.7	4	—11.4 ± 0.5	6 ± 4	0.998
Quadrol	8.9	2.2—10.7	4	—6.4 ± 0.4	3 ± 3	0.996
Tetrabase	8.9	2.2—7.0	3	—4.1 ± 0.0	2 ± 0	1.000

[a] ± Standard deviation.

from the laboratory at 35—55% relative humidity (22—25°C), and had little effect on the response of the charcoal-coated crystals; the effect of relative humidity was not studied.

It is clear that the application of a charcoal-coated crystal to monitoring nitrobenzene vapour can be considered only for well-defined situations. In a practical application, the charcoal-coated crystal would have to be preceded by a separation stage to ensure that the response arose only from the analyte, as indeed would a PEG-750-coated crystal which is known to adsorb a wide range of compounds, including water. As the adsorption process from charcoal is almost entirely physical, the coating would selectively adsorb vapours of lower vapour pressure in preference to volatile gases and a degree of

discrimination is implicit in this process. The fact that charcoal is so inselective in adsorbing organic vapours can of course be used to advantage in a general-purpose organic vapour sensor based on a coated piezoelectric crystal.

REFERENCES

1 J. F. Alder and J. J. McCallum, Analyst (London), 108 (1983) 1169.
2 Y. Tomita, M. H. Ho and G. G. Guilbault, Anal. Chem., 51 (1979) 1475.
3 F. Feigl, Spot Tests in Organic Analysis, Elsevier, Amsterdam, 1960, p. 172.
4 G. O. Nelson, Controlled Test Atmospheres, Ann Arbor Press, Ann Arbor, MI, 1972, p. 131.

Analytica Chimica Acta, 182 (1986) 293—298
Elsevier Science Publishers B.V., Amsterdam — Printed in The Netherlands

Short Communication

CHROMATOGRAPHIC PURIFICATION AND RADIO-IMMUNOASSAY OF DIETHYLSTILBESTROL RESIDUES IN MEAT

C. H. VAN PETEGHEM* and G. M. VAN HAVER

Laboratory of Food Analysis, State University of Ghent, Harelbekestraat 72, B-9000 Ghent (Belgium)

(Received 10th July 1985)

Summary. A rapid, reliable and sensitive method is reported for the detection of residues of diethylstilbestrol (DES) in meat samples. Enzymatic digestion of the muscle tissue followed by ether extract yields a raw extract which, depending on its fat content, can be partitioned in an alkali/chloroform mixture or passed through a Sephadex LH-20 column. To avoid false positive results in the radio-immunoassay, this extract is purified further by high-performance liquid chromatography on an RP-18 column. The detection limit is 0.07 ng g^{-1}.

The synthetic estrogen diethylstilbestrol (DES) has been used extensively as a growth-promoting agent in livestock breeding. Scientific interest in its toxicological properties arose from the observation of an increased incidence of cervical and vaginal cancer in mice treated with DES [1, 2]; DES, like all other natural or synthetic anabolics, has been banned in Belgium for fattening cattle. To achieve early detection of contraventions of the regulations, most analytical methods are directed to urine and faeces [3—8]. Existing methods for tissue samples tend to be laborious and time-consuming, which limits the number of analyses that can be done. Because of their sensitivity, immunochemical methods have become important [9—11]. Their sensitivity can only be equalled by gas chromatography/mass spectrometry (g.c./m.s.) [6, 12, 13], which is also useful for confirmation of identity [14].

Immunochemical methods usually have to be preceded by extensive purification of the sample extract to ensure selectivity [15]. In this communication, a method is presented which combines a simplified sample work-up with a sensitive and reliable detection system. Its usefulness for screening purposes is confirmed by g.c./m.s. of the samples which proved positive by the radio-immunoassay (r.i.a.).

Experimental

Chemicals. All solvents were of analytical-reagent grade. *Trans*-diethylstilbestrol (Serva, Heidelberg, F.R.G.) was shown by high-performance liquid chromatography (h.p.l.c.) with u.v. detection to contain 5% of *cis*-diethylstilbestrol. Subtilisin A (dialyzed and lyophilized, 29.3 Anson units/g) was from

0003-2670/86/$03.50

Novo Industri (Denmark). Sephadex LH-20 was from Pharmacia Fine Chemicals (Sweden). The tracer ^{3}H-diethylstilbestrol (Amersham) had a specific activity of 70—120 Ci mmol^{-1} (2.6—4.4 TBq mmol^{-1}); as decomposition is fairly quick, the stock solution obtained from the supplier was renewed every 6 months. The DES antiserum was obtained from Laboratoire d'Hormonologie, Marloie (Belgium).

Chromatographic equipment. For h.p.l.c., the components were a Rheodyne injection system with a 50-μl sample loop, a pump (Pye-Unicam PU-4011), controlled by a system controller (PU-4030) and a u.v. detector (PU-4020) operated at 240 nm. The column (250 × 4.6 mm) was packed with Lichrosorb RP-18 (5 μm, Merck) and was protected by a guard column (75 × 2.1 mm, Chrompak); it was operated at ambient room temperature. The eluant was methanol/water (65/35, v/v) at 0.9 ml min^{-1}. Retention times of *trans*- and *cis*-DES were ca. 9.0 and 17.0 min, respectively. After every 10 injections, the column system was rinsed for 25 min with pure methanol. It was ready for re-use after another 30 min.

All glassware was carefully rinsed with twice-distilled water. No further attention was paid to silylation or siliconizing.

Isolation of DES from tissue samples. A 1.0-g sample of minced meat is deproteinated enzymatically with 1 mg of Subtilisin A in 4 ml of 0.1 M Tris solution (pH 9.5) for at least 2 h at 60°C in a water bath. Overnight digestion does not affect the quality of the digestate. The liquid suspension is chilled to room temperature and extracted twice with 5-ml portions of diethyl ether. The combined layers are evaporated to dryness in a stream of nitrogen at 35°C, yielding the crude extract.

Purification of the crude extract. The amount of residue, which determines the selection of the first clean-up step, is estimated visually. When lean meat samples are extracted, only a very thin film is left on the wall of the glass tube. In those cases, the crude extract is taken up in 0.2 ml of a dichloromethane/methanol (94/6, v/v) mixture and applied on top of a small glass column (145 × 6 mm), plugged at the bottom with glass wool and filled with 4 cm of Sephadex, swollen and conditioned with the same solvent. The extraction tube is rinsed with another two 0.2-ml portions of the solvent. The column is then eluted with the same solution. The first 3 ml are discarded; the next 3.5 ml are collected and evaporated to dryness at 35°C in a stream of nitrogen. The residue is taken up in 70 μl of methanol/water (65/35, v/v) of which 50 μl is injected for h.p.l.c. The fraction between 8.0 and 10.0 min, corresponding to the *trans*-DES window, is collected and evaporated to dryness at 35°C in a stream of nitrogen.

When fatty meat or sausage meat is extracted, many lipids are present in the crude extract. In such cases, the residue is taken up in 1 ml of chloroform and extracted with 3 ml of 1 M sodium hydroxide. After separation of the layers by centrifugation, the aqueous phase is neutralized by addition of 3 ml of 1 M hydrochloric acid and back-extracted with two 5-ml portions of diethyl ether. After evaporation of the solvent, the residue is subjected to the h.p.l.c. clean-up as already described.

Assay procedure. The dry residue is taken up in 1.5 ml of phosphate/gelatine buffer. The r.i.a. method prescribed by the E.E.C. working party is applied with slight modifications [16]. The calibration curve, established by means of standard DES solutions in methanol, covers the range 10—1000 pg.

Results and discussion

A typical chromatogram as obtained from both purification systems is shown in Fig. 1. The concentrations normally encountered do not permit visual detection of the *trans*-DES peak, the elution time of which is indicated by the arrow. However, with a view to partial automation of the purification procedure, the Sephadex method is to be preferred, whenever possible, to the chloroform/alkali partitioning system because with the latter, after a few injections, slowly eluting compounds actually interfere with the final r.i.a.

Although washing and elution of the analyte from the column are done with the same solution, the DES-containing fraction can be collected accurately and precisely. A typical elution pattern, obtained from a blank crude extract spiked with radiolabelled tracer, is shown in Fig. 2. When blank crude extracts were spiked with natural DES (100 ng ml^{-1}) and subjected to the Sephadex purification step, the recovery was 85% with a relative standard deviation (RSD) of 4% (n = 6). In the procedure, h.p.l.c. was used with u.v. detection at 240 nm. As can be seen from Table 1, the overall recoveries from samples spiked at different levels were reasonably satisfactory. The RSD is higher than the RSD for the Sephadex elution, so that it can be assumed that the imprecision is mainly due to the extraction itself and to the r.i.a. Spiking levels are obviously different but it is the only way to check the

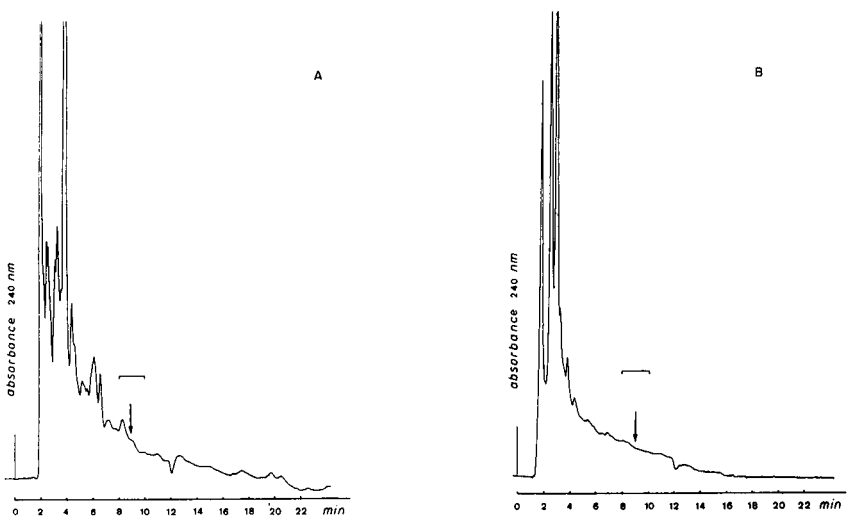

Fig. 1. Chromatograms of a sample extract: (A) after Sephadex LH-20 purification; (B) after chloroform/alkali partitioning. The retention time of *trans*-DES is indicated by an arrow, and the collection window by a bracket.

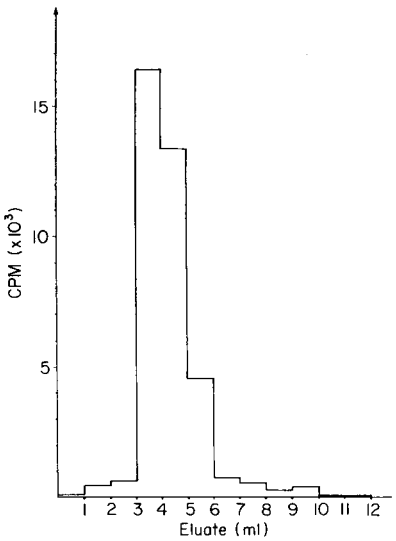

Fig. 2. Elution pattern from a Sephadex LH-20 column of a blank extract spiked with ^{3}H-DES (37 000 cpm).

TABLE 1

Recovery of DES added to 1 g of muscle tissue digested in 4 ml of 0.1 M Tris

Spiking level (ng g^{-1})	Recovery[a] (%)			
	Sephadex LH-20		Partitioning	
	$\bar{x}$	s	$\bar{x}$	s
0.1	115	55	138	41
0.5	64	14	62	8
1.0	67	7	—[b]	—[b]

[a]Mean and relative standard deviation for six determinations at each level. [b]Not determined.

precision of the Sephadex clean-up. The use of ^{3}H-DES as an internal standard is problematic, given the significant difference in recovery between ^{3}H-DES determined by liquid scintillation counting and DES determined by r.i.a. [11].

The Sephadex clean-up step, which yields cleaner chromatograms by h.p.l.c., is seriously impeded if too much fatty material is extracted from the meat samples. The chloroform/alkali partitioning method offers a valuable alternative. Overall recoveries are shown in Table 1.

Enzymatic digestion or deproteination of tissue samples was reported to be successful in toxicological analyses for benzodiazepines, barbiturates, salicylic acid and other acidic compounds [17, 18]. This approach yielded far higher recoveries than conventional extraction methods and the subsequent

chromatographic analysis allowed rapid separation and detection of nanogram quantities of drugs without elaborate preliminary purification [17, 18]. At present, two facts preclude reliable extension of these conclusions to analysis for DES. First, anabolic drug residues generally occur at the pg g^{-1} level which is much lower than the levels found in human poisoning cases with therapeutic drugs. Secondly, final detection and/or quantitation is done by r.i.a., which is more sensitive than chromatography but less selective, so that more care is needed in purification of the extracts. Yet the enzymatic deproteination and extraction offers the considerable advantage that a large number of samples can be left to digest overnight. To prove that extraction efficiencies are higher would require analysis of naturally contaminated tissues, but these were not available.

It was checked that Subtilisin affects neither DES nor the *cis/trans* isomerization. The latter is known to occur during metabolization in the organism, during extraction of samples, especially under acidic conditions, and during derivatization prior to gas chromatography. The *cis/trans* ratio of a methanolic solution of the DES standards, which was 5/95, was not significantly altered by the overall procedure recommended under Experimental at spiking levels which were detectable by monitoring at 240 nm (i.e., 100 ng g^{-1} of meat).

Hexestrol and dienestrol cross-react with the commercial DES antiserum; the cross-reactivities were found to be 3.3 and 1%, respectively, relative to DES (100%). The cross-reactivities of 17-β-estradiol, estrone, estriol, progesterone, testosterone, trenbolone and zeranol were all <0.001%. The quantitative results will hardly be affected by this, particularly as hexestrol and dienestrol are well resolved in the h.p.l.c. system, even with the wide window used to ensure that the DES peak is not missed because of slight changes in chromatographic conditions. It can be assumed that the antiserum was raised against *trans*-diethylstilbestrol, the biologically active form. The *cis*-isomer is not commercially available and attempts to isolate it by the method of White and Ludwig [19] failed. However, *cis*-DES is well resolved from *trans*-DES by h.p.l.c. and is not included in the *trans* window. With the recommended method, no significant increase of the *cis* content is caused by sample handling but if biological isomerization has taken place, the natural *cis*-content of the sample will not be assayed.

No difference in r.i.a. response was observed whether common glassware, silylated glassware, siliconized glassware, polyethylene or polypropylene was used.

Despite the clean-up procedure there is still a background of DES-like activity in the extracts. The r.i.a. response is situated somewhere between the 0 and the 20 pg standard of the calibration curve; this corresponds to 0.05 ng g^{-1} DES with a standard deviation of 0.01 ng g^{-1} (n = 21). The lower detection limit of the method is set at 0.07 ng g^{-1}, calculated from twice the standard deviation of the background. This value is in fairly good agreement with other values in the literature: 0.03 ng g^{-1} [10], 0.06 ng g^{-1} [9] and 0.09 ng g^{-1} [11].

All samples which were found to contain >0.1 ng g^{-1} DES after correction for the background (0.05 ng g^{-1}) were also analyzed by quantitative g.c./m.s. All the results were confirmed quantitatively. Several DES-negative samples were also examined by g.c./m.s.; none showed the presence of DES.

The method allows a considerable reduction in working time if the digestion is done overnight. One operator can get through 16 samples in 1.5 days; this output would be increased if the h.p.l.c. were fully automated.

REFERENCES

1 T. B. Dunn and A. W. Green, J. Nat. Cancer Inst., 31 (1963) 425.
2 W. U. Gardner, Ann. NY Acad. Sci., 75 (1959) 543.
3 P. L. Schuller, J. Chromatogr., 31 (1967) 237.
4 K. Vogt, Arch. Lebensmittelhyg., 29 (1978) 178.
5 A. E. Tirpenou, S. D. Kilikidis and A. P. Kamarianos, J. Assoc. Off. Anal. Chem., 66 (1983) 1230.
6 H. J. G. M. Derks, J. Freudenthal, J. L. M. Litjens, R. Klaassen, L. G. Gramberg and V. Borrias-Van Tongeren, Biomed. Mass Spectrom., 10 (1983) 209.
7 E. H. J. M. Jansen, R. Both-Miedema, H. Van Blitterswijk and R. W. Stephany, J. Chromatogr., 299 (1984) 450.
8 E. H. J. M. Jansen, R. H. Van Den Berg, H. Van Blitterswijk, R. Both-Miedema and R. W. Stephany, Vet. Quarterly, 6 (1984) 5.
9 B. Hoffmann and W. Laschutza, Arch. Lebensmittelhyg., 31 (1980) 105.
10 K. Vogt, Arch. Lebensmittelhyg., 31 (1980) 138.
11 J. C. Gridley, E. H. Allen and W. Shimoda, J. Agr. Food Chem., 31 (1983) 292.
12 H. J. Stan and B. Abraham, J. Chromatogr., 195 (1980) 231.
13 H. W. Dürbeck and I. Büker, Fresenius Z. Anal. Chem., 315 (1983) 479.
14 E. W. Day, L. E. Vanatta and R. F. Sieck, J. Assoc. Off. Anal. Chem., 58 (1975) 520.
15 Th. J. Benraad, R. W. Stephany, F. M. A. Rosmalen, J. A. Hofman, J. G. Loeber and L. H. Elvers, Vet. Quarterly, 3 (1981) 153.
16 Commission of the European Communities, Directorate-General for Agriculture, Working Document No. 4694/VI/81-EN File No. 67.1.
17 M. D. Osselton, M. D. Hammond and P. J. Twitchett, J. Pharm. Pharmacol., 29 (1977) 460.
18 M. D. Osselton, I. C. Shaw and H. M. Stevens, Analyst (London), 103 (1978) 1160.
19 W. A. White and N. H. Ludwig, J. Agr. Food Chem., 12 (1971) 390.

Analytica Chimica Acta, 182 (1986) 299—302
Elsevier Science Publishers B.V., Amsterdam — Printed in The Netherlands

Short Communication

COMPARISON OF RECOVERIES OF TRICHLOROETHYLENE FROM CHARCOAL TUBES AND THERMALLY-DESORBABLE PERSONAL MONITORS

JOHN M. THOMPSON* and WILLIAM I. STEPHEN

Department of Chemistry, University of Birmingham, Edgbaston, Birmingham B15 2TT (Great Britain)

RADJADURAI SITHAMPARANADARAJAH[a]

Dutom Meditech, 79 Warwick Street, Birmingham B12 0NH (Great Britain)

(Received 23rd July 1985)

Summary. Solvent-extractable NIOSH charcoal tubes and thermally-desorbable Simtec Adsorba porous polymer monitors for trichloroethylene are compared for recovery efficiencies. The latter monitors are shown to have better recovery efficiencies with less variability than the charcoal monitors. Methods of distribution-free statistical evaluation are outlined for comparing monitors so that reliable conclusions can be drawn.

The adsorptive trapping of solvent vapours on activated charcoal, followed by liquid-liquid extraction with carbon disulphide and gas chromatography, has been a standard approach [1]. The use of porous polymers to trap such vapours, with thermal desorption for recovery, has been the subject of more recent work [2—4]. The work described below illustrates the behaviour of the two types of monitoring and also some appropriate statistical techniques for comparing such data.

Experimental

Standard atmospheres of trichloroethylene (1000 mg m^{-3}) were generated by means of a diffusion dilution cell as described by Barratt et al. [5]. Charcoal tubes (U.S. National Institute of Occupational Safety and Health) and Simtec Adsorba tubes [6] packed with Porapak-Q (from Thorn-EMI Electronics, Simtec Division, Nottingham) were exposed for 25 min with the sample flowing at 2 ml min^{-1}.

Charcoal in the front section of each charcoal tube was emptied into a vial containing 0.50 ± 0.01 ml of carbon disulphide; the vial was capped immediately and shaken. A 1-μl aliquot of the extract was injected into the gas chromatograph. Porapak-Q tubes were heated at 180°C whilst connected

[a]Present address: Institute of Naval Medicine, Alverstoke, Gosport, Hampshire, Great Britain.

0003-2670/86/$03.50

to a sample loop on a six-port sample valve. After desorption at 180°C for 5 min, the sample valve was turned to elute the desorbed material into the gas chromatograph. In both cases, the gas chromatographic conditions were as follows: carrier gas, oxygen-free nitrogen at 60 ml min^{-1}; column oven at 80°C; injection port at 110°C; detector oven at 200°C; flame ionization detector; column, 3.04-m coil of 4-mm bore Pyrex glass filled with 10% (w/w) DC-560 silicone oil coated on Universal Support-B (80—100 mesh).

Additionally, a series of Porapak-Q tubes was exposed to standard atmospheres of trichloroethylene to produce loadings ranging from 10 to 500 μg, in order to evaluate recovery efficiency as a function of loading.

Results and discussion

The recoveries of different amounts of trichloroethylene are shown in Table 1. The experimental data (Table 2) comparing the charcoal and Porapak-Q tubes are illustrated in Figs. 1 and 2. The data in Table 1 show clearly that recovery efficiency varies little over the 50-fold range in adsor-

TABLE 1

Recovery of different amounts of trichloroethylene from Porapak-Q (50—80 mesh)

Amount adsorbed (μg)	Mean recovery (%)	Number of observations	R.s.d. (%)
10	97.9	10	2.2
50	98.9	10	3.1
100	99.1	10	2.3
200	99.4	5	1.2
500	99.0	5	2.7
Overall recovery	98.6	40	2.4

TABLE 2

Comparison of the distribution of recoveries of trichloroethylene from Porapak-Q Adsorba tubes and NIOSH-type charcoal tubes

Recovery (%)	Number in class		Cumulative frequency	
	Porapak-Q	Charcoal	Porapak-Q	Charcoal
<90	0	16	0	0.276
90—91	0	3	0	0.328
92—93	0	3	0	0.378
94—95	2	8	0.037	0.517
96—97	14	3	0.296	0.569
98—99	17	5	0.611	0.655
100—101	13	7	0.852	0.776
>101	8	13	1.000	1.000

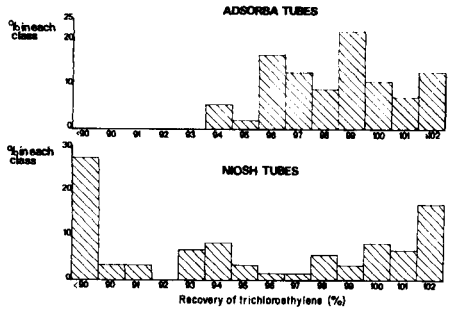

Fig. 1. Frequency histograms showing the recoveries of trichloroethylene from the thermally-desorbed Adsorba tubes and the solvent-desorbed charcoal tubes.

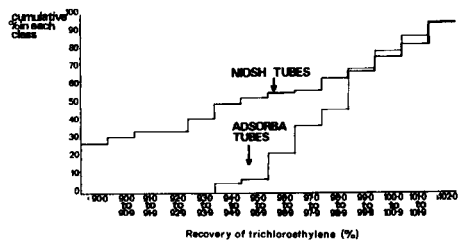

Fig. 2. Cumulative frequency histograms showing the recoveries of trichloroethylene from the Adsorba tubes and the charcoal tubes.

bent loadings which were tested. Thus Porapak-Q monitors of this type should be suitable for monitoring both the 8-h TWA (long-term exposure limit) and the 10-min TWA (short-term exposure limit) announced in the U.K. Health and Safety Executive's Guidance EH40.

As can be seen from Fig. 1, not only do the histograms for recoveries of trichloroethylene from the two types of monitors both show abnormal distributions, but the distributions look substantially different in shape. Both distributions are necessarily truncated at 100% recovery, apart from a minor slippage caused by experimental measurement errors. Comparison of such distributions by means of the unpaired Student's t-test would be inappropriate for two reasons: first, the variances are obviously very different, and secondly neither distribution is normal. Thus, the statistical technique used must allow a general comparison between the two distributions and must not depend for its validity on the distributions being of any particular kind. The Kolomogorov-Smirnov Two-Sample test is useful for the general null hypothesis of two identical populations [7]. The median test and the Mann-Whitney-Wilcoxon test may be used to detect differences in medians but these tests may not be sensitive to differences in variances, etc. The advantage of the Kolmogorov-Smirnov Two-Sample test is that it is consistent against all types of differences that may be present between the two distribution functions [8]. The test statistic for the Kolmogorov-Smirnov Two-Sample Test is calculated as $D = \max|S_{\mathrm{NIOSH}} - S_{\mathrm{Adsorba}}|$, where S_{NIOSH} and S_{Adsorba} are the cumulative frequency distribution functions. For the sets of data given above, the test statistic is 0.480, which is greatly in excess of what would be expected were there no significant differences between the two distributions. The level of significance of the difference is at $p \ll 0.01$ for the two-sided hypothesis and at $p \ll 0.005$ for the one-sided hypothesis.

There is obviously also value in conducting tests to demonstrate not only

such general differences, but also differences in location or in spread of the distributions. The Mann-Whitney-Wilcoxon test is useful for testing differences in location of distribution; it is robust against variations in the shape of the distribution and is a much safer test to use than the unpaired t-test [8]. The test statistic, corrected for the tied data, was 2.905, demonstrating a highly significant difference in recovery efficiencies in favour of the thermally-desorbable monitors ($0.002 > p > 0.001$).

Whilst it is important to characterize recovery efficiency in terms of medians or means, it is also essential to characterize the behaviour of such environmental monitors for their variability. A test of equality of spread or variance for use with such non-gaussian data is the squared-ranks test [8], in which the absolute differences of each observation from the mean of the data set are calculated. The differences for the two data sets are pooled and ranked. The ranks are squared and the sum of the squares of ranks for one of the sample data sets is calculated and corrected for tied data. The corrected statistic is compared with values from the standardized normal distribution. In the two-sided test, a value of the statistic comparable in size to values in the tails of the standardized normal distribution indicates significant differences in the variances. For the two monitors compared here, the corrected test statistic had a value of 11.45, demonstrating a highly significant difference in the variability of the recovery efficiencies of these two monitors in favour of the thermally-desorbable monitor ($p \ll 0.001$).

Thus, in all aspects the thermally-desorbable monitor is demonstrably superior in recovery efficiency to the solvent-extractable one.

The support of the Medical Research Council for R.S. during this work is gratefully acknowledged.

REFERENCES

1 NIOSH Manual of Analytical Methods, Vol. 1, 2nd edn., Dept. of Health, Education and Welfare, Cincinnati, 1977, p. 127.
2 J. Gelbičová-Ružičková, J. Novák and J. Janák, J. Chromatogr., 64 (1972) 15.
3 J. W. Russell and L. A. Shadoff, J. Chromatogr., 134 (1977) 375.
4 R. H. Brown and C. J. Purnell, J. Chromatogr., 178 (1979) 79.
5 R. S. Barratt, R. L. Jones and J. M. Thompson, Br. J. Anaesth., 47 (1975) 1177.
6 J. M. Thompson, R. Sithamparanadarajah and W. I. Stephen, U.K. Patent No. GB2078128B, 1984.
7 J. D. Gibbons, Nonparametric Methods for Qualitative Analysis, Holt, Rinehard and Winston, New York, 1976, p. 250.
8 W. J. Conover, Practical Nonparametric Statistics, 2nd edn., Wiley, New York, 1980, pp. 216, 239 and 368.

Analytica Chimica Acta, 182 (1986) 303
Elsevier Science Publishers B.V., Amsterdam — Printed in the Netherlands

Software Review

S. M. Deming and S. L. Morgan, INSTRUMENTUNE-UP, Elsevier Scientific Software, Amsterdam, 1984. (Order ref. no. ISBN 0-444-42329-X or 0-444-42330-3) Price US$ 150, £125, Dfl. 495; manual only US$ 27.50, £23, Dfl. 90.

Computer	Apple II, II+, IIe, IIc	IBM-PC, -XT, -AT
Operating system	DOS 3.3	PC-DOS 2.0
Language	Applesoft BASIC	PC-BASIC
Required peripherals	140K 5¼-in. disk drive	180K/360K 5¼-in. disk drive
Minimum memory	48K RAM	64K RAM
Storage medium	5¼ in.-diskette	5¼ in.-diskette

The INSTRUMENTUNE-UP program is designed to improve the performance of common laboratory instruments. The program was used here for the optimization of the homogeneity of a superconducting n.m.r. magnet. The problem involves four variables (dial settings); 10% of the variable range was used as the step size. In the fixed as well as in the variable step-size mode, rather slow convergence was observed. Starting with an experiment rating of 540 (arbitrary units), a minimum of 350 was obtained after 60 experiments in the fixed mode, and a minimum of 380 after 50 experiments in the variable mode. The best minimum obtained by hand is 210. The time needed to reach the minimum with the program seems to be about equal to the time needed for the manual search, if no prior knowledge is available. In all other cases, the simplex seems to be much slower. A further improvement of the minimum at 210 starting the simplex at this setting failed.

Some simulations with two-dimensional problems indicated that the algorithm is very sensitive to noise. An attempt to minimize a least-squares problem (multicomponent analysis) failed completely for this reason. The presentation form of the program and the well organized manual look attractive and this makes starting with the program a real pleasure. The program itself is documented with adequate notes. However, the program itself is rather badly structured; the large number of "goto's" and the numerous separate statements used for screen editing make it difficult to follow the program flow.

A final remark concerns the price of this software. In the reviewer's opinion, the price for such a small program, the algorithms of which can be found in any statistical or mathematical software package, seems far too high.

E. J. Spruit

ANALYTICA CHIMICA ACTA, VOL. 182 (1986)

AUTHOR INDEX

ntinued from outside back cover)

CONTENTS

(Abstracted, Indexed in: Anal. Abstr.; Biol. Abstr.; Chem. Abstr.; Curr. Contents Phys. Chem. Earth Sci.; Life Sci.; Index Med.; Mass Spectrom. Bull.; Sci. Citation Index; Excerpta Med.)

(continued on inside back cover)